Northeast Fisheries Science Center Reference Document 20-07

Final Report of Red Hake Stock Structure Working Group

by the Northeast Fisheries Science Center

August 2020

Northeast Fisheries Science Center Reference Document 20-07

Final Report of Red Hake Stock Structure Working Group

by the Northeast Fisheries Science Center

NOAA Fisheries Service, Northeast Fisheries Science Center, 166 Water Street,
Woods Hole, Massachusetts 02543, USA

US DEPARTMENT OF COMMERCE
National Oceanic and Atmospheric Administration
National Marine Fisheries Service
Northeast Fisheries Science Center
Woods Hole, Massachusetts

August 2020

Northeast Fisheries Science Center Reference Documents

This series is a secondary scientific series designed to assure the long-term documentation and to enable the timely transmission of research results by Center and/or non-Center researchers, where such results bear upon the research mission of the Center (see the outside back cover for the mission statement). These documents receive internal scientific review, and most receive copy editing. The National Marine Fisheries Service does not endorse any proprietary material, process, or product mentioned in these documents.

Editorial Treatment: To distribute this report quickly, it has not undergone the normal technical and copy editing by the Northeast Fisheries Science Center's (NEFSC's) Editorial Office as have most other issues in the NOAA Center Reference Document NMFS-NE series. Other than the covers and preliminary pages, all writing and editing have been performed by – and all credit for such writing and editing rightfully belongs to – those so listed on the title page.

If you do not have Internet access, you may obtain a paper copy of a document by contacting the senior Center author of the desired document. Refer to the title page of the document for the senior Center author's name and mailing address. If there is no Center author, or if there is corporate (*i.e.*, nonindividualized) authorship, then contact the Center's Woods Hole Laboratory Library (166 Water St., Woods Hole, MA 02543-1026).

Information Quality Act Compliance: In accordance with section 515 of Public Law 106-554, the Northeast Fisheries Science Center completed both technical and policy reviews for this report. These predissemination reviews are on file at the NEFSC Editorial Office.

This document may be cited as:

> Northeast Fisheries Science Center. 2020. Final report of red hake stock structure working group. US Dept Commer, Northeast Fish Sci Cent Ref Doc. 20-07; 185 p. Available from: https://www.fisheries.noaa.gov/new-england-mid-atlantic/northeast-center-reference-document-series

Table of Contents

List of Attendees of Working Group meetings and webinars

NAME	AFFILIATION	E-MAIL
David Richardson*	NEFSC	David.Richardson@noaa.gov
Toni Chute*	NEFSC	Toni.Chute@noaa.gov
Larry Alade*	NEFSC	Larry.Alade@noaa.gov
Steve Cadrin*	SMAST	scadrin@umassd.edu
Jonathan Grabowski*	Northeastern University	J.Grabowski@northeastern.edu
Nicole Lengyel*	RI DEM	nicole.lengyel@dem.ri.gov
Katey Marancik*	NEFSC/Integrated Statistics	Katey.Marancik@noaa.gov
Rich McBride *	NEFSC	Richard.McBride@noaa.gov
Zachary Whitener*	GMRI	zwhitener@gmri.org
Isaac Wirgin*	NYU	Isaac.Wirgin@nyulangone.org
Timothy Miller	NEFSC	Timothy.J.Miller@noaa.gov
Kathy Sosebee	NEFSC	Katerine.Sosebee@noaa.gov
Michele Traver	NEFSC	michele.traver@noaa.gov
Andrew Jones	NEFSC/Integrated Statistics	andrew.jones@noaa.gov
Harvey Walsh	NEFSC	harvey.walsh@noaa.gov
Deborah Hart	NEFSC	deborah.hart@noaa.gov
Andrew J. Applegate	NEFMC	AApplegate@nefmc.org
Mark Wuenschel	NEFSC	Mark.Wuenschel@noaa.gov
Anna Mercer	NEFSC	anna.mercer@noaa.gov
Alison Frey	SMAST	afrey@umassd.edu
Katie Almeida	Town Dock, RI	kalmeida@towndock.com
Tyler Pavlowich	NEFSC/Integrated Statistics	tyler.pavlowich@noaa.gov
Eric Robillard	NEFSC	eric.robillard@noaa.gov
Wendy Gabriel	NEFSC	wendy.gabriel@noaa.gov
James Churchill	WHOI	jchurchill@whoi.edu
Jennifer Couture	NEFMC	jcouture@nefmc.org
Kevin Friedland	NEFSC	Kevin.Friedland@noaa.gov
Jessica Blaylock	NEFSC/Integrated Statistics	Jessica.Blaylock@noaa.gov
Russ Brown	NEFSC	Russell.Brown@noaa.gov

*Working group members

EXECUTIVE SUMMARY

TOR1: Review and summarize all relevant literature on the existing stock structure of red hake in the northwest Atlantic.

Two different stock structures have been applied to red hake since the start of formal assessments in the late 1960s. During the 1960s and 1970s, red hake in the western Atlantic were divided into southern New England, Georges Bank, Gulf of Maine and Scotian Shelf stocks, based on meristics, survey distributions, length-at-age, the dynamics of the fisheries and practical considerations with respect to conducting the assessment. In 1985 the U.S. switched to assessing two stocks, a southern stock encompassing southern New England and southern Georges Bank and a northern stock in the Gulf of Maine and northern Georges Bank; the Scotian Shelf was not evaluated by the U.S.. This change was made in part due to similarity to silver hake, a species with substantial overlap in the small mesh fishery, but also due to survey distribution, otolith banding patterns and growth differences. A review of stock structure information on red hake revealed that no attempt has been made to tag individuals, nor has there been a genetic study, thus many of the traditional datasets used for stock identification are not available.

TOR2: Identify and evaluate any new and/or existing data relevant to the stock structure of red hake including but not limited to the species' life history (i.e. spawning, distribution, abundance, growth, maturity and natural mortality), morphometrics, and genetics.

The distribution of red hake on the fall and spring trawl surveys, as well as the distribution of red hake catch in the fishery, is discontinuous, with low abundances across the shallow areas of Georges Bank. An evaluation of length-at-age data shows persistent differences in growth across the region, with two identifiable clusters corresponding to the existing stock boundaries. Similarly, the application of the management unit estimator, which evaluates spatial coherence in time series of abundance, also provided meaningful support for the existing stock structure. In contrast data on early life history and spawning does not provide clear support for two stocks. Since the 1970s there has been a prominent shift in the abundance of red hake adults from southern New England and the Georges Bank to the Gulf of Maine during the spring and

fall trawl surveys. During this same period summertime larval distributions and the distribution of Age-0 fish (1-10cm) have remained relatively consistent, with a majority located on Georges Bank. Ontogenetic and seasonal spawning movements across the existing stock boundary may explain the data on early life stage distributions.

TOR3: Recommend the most likely biological stock structure among a set of alternatives from TOR2. Consider the current management unit as the null hypothesis.

The working group considered the information available insufficient to reject the null hypothesis of two stocks. Specifically, we recommend two stocks, a northern stock that encompasses northern Georges Bank and the Gulf of Maine and a southern stock that encompasses southern New England and southern Georges Bank. The clear evidence of two phenotypic stocks, with coherent trends in abundance, and unique fisheries provided the basis for the decision to maintain two stocks. This evidence was weighed against the possibility of spawning migrations across the stock boundary and mixing of the two stocks during spawning and recruitment. The working group decided that the lack of secondary confirmation of the possible cross boundary migrations, beyond early life stage distribution data, did not provide a sufficient basis to reject the hypothesis of two stocks.

TOR4: Evaluate existing experimental data on survey catchability of red hake. Examine the sufficiency of catchability data and, if appropriate, incorporate the catchability estimates into the assessment.

A paired gear study using a twin trawl rig indicated that the standard trawl gear used on the NEFSC trawl survey, and in particular the rockhopper sweep, is ~23% efficient in catching red hake. Comparisons of red hake densities from the HabCam imaging system and the trawl survey further supported these results. The working group accepted the applicability of the twin trawl study design and analysis for estimating red hake catchability. The working group recommended these results be included in the assessment. The working group also evaluated an experiment designed to test how differences in wing spread affect the catchability of red hake in the survey gear. No evidence was found for changes in gear efficiency across the measured wingspreads. However the differences in area swept at different wingspreads were considered important in calculating swept area biomass and abundance estimates, and the working group recommended further work be pursued in making these calculations.

TOR5: Apply the existing assessment model framework to the stock structure based on TOR 3 and 4 to ensure its utility in subsequent management track assessments. Evaluate existing reference points.

Updated assessment models using AIM (An Index Method) were run for the northern and southern stocks of red hake and were found to be not significant. Based on the catchability data (TOR4), these models also estimated very low exploitation rates (<1%) at a replacement ratio of 1 (population stability). The working group determined the existing model framework using AIM was inappropriate for developing future catch advice, due to the lack of significance of the models and the results from the catchability study.

An alternative empirical approach to developing reference points for both stocks of red hake was developed. This approach directly incorporated estimates of stock biomass and recruitment from the catchability study, and calculates an F_{40} and SSB_{40} using maturity and growth data and assumed values for natural mortality and fisheries selectivity. For both stocks of red hake, fishing mortality over the past decade has been well below F_{40} and spawning stock biomass has been above SSB_{40}. Both stocks are thus considered to be not overfished with overfishing not occurring.

TOR6: Identify gaps in the existing research with respect to red hake stock structure. Develop a prioritized list of research recommendations to address these gaps. Comment on the feasibility and time horizon of the proposed research recommendations.

Research recommendations included a population genetics study for red hake and the testing of the hypothesized spawning migration, among other studies. The working group also presented more general recommendations, recognizing that stock structure questions will continue to emerge in the Northeast. In particular, the group recommended developing prioritized lists of species in need of additional reviews of stock structure and additional research on stock structure. Finally, the working group recommended continuing long-term monitoring efforts (e.g. ichthyoplankton, aging), and noted the uncertainties that emerge when there are gaps in these efforts.

WORKING GROUP PROCESS

The working group held an initial data scoping meeting via a webinar on 4 November 2019. The purpose of this meeting was to evaluate the data available to address the Terms of Reference and

to coordinate analyses to ensure that topics were not missed and there was not a duplication of effort. The stock structure workshop was held 6-8 January 2020 at the University of Massachusetts at Dartmouth School for Marine Science & Technology in New Bedford with individuals participating in person and via webinar. A final webinar was held 5 February 2020 in order to discuss and finalize the details of an alternative assessment model for both stocks of red hake.

INTRODUCTION

Red hake identification and basic biology

Red hake (*Urophycis chuss*; family Phycidae; order Gadiformes) is a medium size benthic fish (Figure 1.1) that is distributed typically in soft-sand and mud habitats from Cape Hatteras, North Carolina (U.S.A.) to the Gulf of St. Lawrence (Canada) (Figure 1.2). This species is one of eight in the genus *Urophycis*, all of which occur in the western Atlantic Ocean. Four of these species occur north of the equator, three occur south of the equator, and one straddles the equator. On the northeast U.S. continental shelf, three *Urophycis* species are common, red hake, spotted hake (*U. regia*), and white hake (*U. tenuis*). Spotted hake has a more southerly distribution than red hake, though the northern portion of the spotted hake range overlaps with the southern portion of the red hake range (Figure 1.3). The prominent spots on spotted hake readily distinguish them from red hake. White hake have a more northerly distribution than red hake, though there is substantial overlap of the two species in the Gulf of Maine north through the Scotian Shelf. White hake grow larger than red hake (130 cm vs 55 cm maximum), though characters to reliably distinguish small white hake from red hake tend to be subtle (e.g. 2 vs 3 gill rakers on upper arch) (Figure 1.1). Misidentifications of red hake as white hake and *vice-versa* is thus common, particularly in fisheries-dependent datasets, but also in some fisheries-independent surveys (NEFSC 2011).

Red hake spawn pelagic eggs, which hatch into larvae after 5-7 days. Larval red hake undergo flexion (posterior end of the vertebral column bending upwards) at approximately 5 mm, and then transition to a pelagic juvenile stage at approximately 10 mm. This pelagic juvenile stage ends when an individual is approximately 40 mm (≈60 days), at which time individuals settle to the benthos. Scallop beds are one type of settlement habitat for juvenile red hake, and individuals up to about 11 cm commonly are found within live scallop shells. Notably, experimental studies do not suggest this is an obligate association, but rather that the inhabitation of scallops is one manifestation of a strong preference for shelter by red hake juveniles (Steiner et al. 1982).

The early life stages of *Urophycis* species in the western North Atlantic have historically been challenging to impossible to identify to species. Red hake eggs are small (0.63-0.83 mm)

with pigment forming late in development. No morphological characters are known to separate species of *Urophycis* eggs (Berrien and Sibunka 2006), rather genetic identification is required (Lewis et al. 2016). Additionally, some misidentification of eggs of other taxa as *Urophycis* and *vice versa* is likely common. Historically *Urophycis* larval identifications were also unreliable at the species level due to the lack of verified diagnostic characters to separate among species. However, Marancik et al. (in press) used a set of genetically identified larvae (n=88) to determine a set of characters that separate species (Figure 1.4). These characters were then applied to a new set of 189 *Urophycis* larvae as a test of the approach. Genetic identification of this second set of larvae demonstrated the reliability of this set of characters for larval identification.

Fishery description

The following description of the fishery is based on available documents and regulations, fisheries-dependent data, and informal discussions with six fishermen in preparation for the red hake stock structure workshop. The industry discussions focused on the dynamics of the red hake fishery, the ecology and movements of red hake, and the efficiency of different types of trawl nets for red hake. We talked with fishermen that work in the Gulf of Maine (n=2) and on Georges Bank and off southern New England (n=4). These discussions should not be considered to provide a comprehensive accounting of the interactions of fishermen with red hake, though do provide many important insights.

The dynamics of the red hake fishery through time can be attributed in part to the low desirability and utility of red hake as a food fish once frozen. This attribute was characterized in numerous studies in the 1970s and 1980s that sought to develop further marketable products for this species (e.g. Gill et al. 1979; Lliciardello et al 1982). In particular, red hake flesh was characterized as having a “cottony-spongy” texture once frozen that was attributable to the breakdown of trimethylamine oxide to dimethylamine and formaldehyde (Fey and Regenstein 1982). This rapid toughening of red hake muscle, rather than measures of rancidity or poor taste, were identified as underlying the difficulty in developing a broad market for red hake beyond the fresh market (Licciaredello et al. 1982). Attempts to address this quality issue in the early 1980s

in order to broaden the market for red hake (e.g. develop breaded products) appear not to have been successful. The market for red hake has thus generally been for uses other than food or as a fresh product, which is reported to be of reasonable taste and consistency.

Trash fishery (late 1940s-1970s)— The trash fishery off New England was a fishery for species of low value as food fish, that could instead be turned into either fish meal or other products. This fishery was largely indiscriminate, but did rely heavily on red hake. In 1948 a limited trash fishery existed with the primary end users being fur-farm operators. In 1949 the trash fishery started supplying reduction plants that produced fish meal to add to animal feeds. Due to the development of demand by the reduction plants, landings of trash fish in New Bedford, one of the main ports, increased 10-fold year-over-year from 1948 to 1949 (Snow 1950). After that initial jump, landings continued to increase coastwide from 22,000 mt in 1949 to 66,000 mt in 1956 (Edwards and Lux 1958). Reports note that the landings then started to drop off as competitive fish meal products were developed at a lower price point, though reports from fishermen noted that the trash fishery did not end until the 1970s.

While all fish were landed by the trash fishery, red hake consistently were listed as the highest proportion of landings (Snow 1950, Edwards and Lux 1958). One fisherman noted a targeting of red hake offshore of Muskeget Channel (between Martha's Vineyard and Nantucket) in the spring by the trash fishery. Published reports from the 1950s substantiate this (Snow 1950; Figure 1.5). Specifically, red hake were fished in a region offshore of Muskeget Channel named the No Man's Fishing Ground from April to October, with red hake comprising 67% of landings by weight (Edwards and Lux 1958). This fishery was noted a few times in conversations as the most prominent targeting of red hake off southern New England.

Distant-water fleets (1962-1976)—In the early 1960s factory trawlers from Eastern European nations arrived in the waters of the Scotian Shelf, Georges Bank and off southern New England. Many species were targeted by this fleet and experienced historically high catches. Red hake was no exception. The catch of red hake by the foreign fleet rapidly increased from about 4,000 mt in 1962 to >100,000 mt in 1966, before declining to 7,000 mt in 1970, and then increasing to a second peak of 60,000 mt in 1973 (NEFSC 2011). The foreign fleet targeting red hake primarily operated in southern New England and on Georges Bank, with notable changes

across time in relative catches from these areas. In 1976, the 200-mile limit was established, essentially stopping the foreign fleets from catching red hake.

Recent fishery (1980s-present)—Red hake are currently not a primary target species, but rather are caught and either landed or discarded when fishing for other species. Most notably red hake are caught in the whiting (silver hake) fishery which uses small mesh nets; the larger mesh nets of the groundfish fishery typically extrude most red hake (Pol et al. 2016). In the Gulf of Maine, the whiting fishery is highly restricted in space and time in order to minimize the bycatch of juvenile groundfish. This fishery is managed through the use of four small mesh exemption areas, each of which is open during a particular time period (Figure 1.6). In addition, three of these exemption areas require the use of a raised footrope trawl, which is effective for catching silver hake but reduces the catch of red hake and flatfish species. The distribution of red hake catch in space and time reflect these regulations (Figure 1.7 and Figure 1.8). Additionally, the degree that red hake overlap with whiting in any one year was identified as another driver of interannual and spatial patterns in catch.

The southern fishery operates in a number of different areas, and in this region red hake is caught in both the whiting fishery and in the squid fishery. Catches occur along the southeastern edge of Georges Bank, along the shelf break south of Long Island and closer to shore along southern New England(Figure 1.7, 1.8, 1.9). Multiple fishermen noted active means to avoid red hake in the whiting fishery. One noted moving the location of subsequent tows if red hake catch was too high when fishing for whiting. The rationale for moving locations was to minimize the time required to pick out red hake. Another mentioned gear changes in fishery on the eastern edge of Georges Bank in order to reduce the catch of red hake and flatfish while targeting whiting and squid. The general view was that the market for red hake can handle very little product, and that once saturated it is not worthwhile to land more. The market dynamics were thus described as eliminating the targeting of red hake, and in some case the development active approaches to reduce catch.

Future prospects-bait market—One recent event that may affect the red hake fishery going forward is tied to the severe reduction in Atlantic herring landings starting in 2019. The American lobster fishery historically has been heavily dependent on Atlantic herring for bait.

From 2002-2015, Atlantic herring landings were 80,000-115,000 mt with estimates that 70% of those landings were used as lobster bait (Grabowski et al 2010). In 2019, Atlantic herring landings dropped to <15,000 mt, and bait prices in the lobster fishery increased. A couple of fishermen noted this dynamic as potentially relevant for the red hake fishery. As Atlantic herring catch has declined, prices for alternate bait sources have increased, including for species that may be of lower quality as bait, such as red hake. It was noted that bait prices have not reached the level that red hake would be targeted, but rather that fish that are currently discarded due to regulations in the northern stock area now had an increased market as lobster bait. Fishermen in the southern stock area did not indicate that red hake were sold into the lobster bait market. This was attributed to transport costs combined with the low volume of landings.

TOR1: Review and summarize all relevant literature on the existing stock structure of red hake in the northwest Atlantic.

Here we: 1) review previously published or documented information of stock identity of red hake, 2) provide a summary of the technical basis for defining previous and current spatial management units in their primary range of abundance, and 3) identify putative spatial groups that will be further evaluated with new data. Information is presented in chronological order, describing two periods that adopted different stock definitions for red hake. This review is intended to help understand the historical development of information and perceptions of stock identity.

ICNAF Stock Definitions

The International Convention for the Northwest Atlantic Fisheries (ICNAF) was formed in 1949 to provide for the assessment and management of fisheries in the Northwest Atlantic. After the extension of national jurisdictions in the late-1970s, ICNAF was replaced by domestic management systems for U.S. and Canadian fisheries and the Northwest Atlantic

Fisheries Organization (NAFO) for fisheries in international waters (Anderson 1998). After preliminary investigation of geographic patterns in meristics, otolith size, fishing patterns, survey patterns and age composition and consideration of practicalities for assessment and fishery management, ICNAF defined four stocks of red hake: Scotian Shelf, Gulf of Maine, Georges Bank, and southern New England-Mid Atlantic Bight (Richter 1968, Anderson 1974b).

Richter (1968) sampled red hake fishery catches in 1965-1966 from the Scotian Shelf to the Mid Atlantic Bight (Figure 1.10) and found differences in size-at-age, age composition and morphology. Size-at-age was largest on northern Georges Bank, smallest from the southern Georges-southern New England slope, and intermediate on the Scotian Shelf and the Mid Atlantic slope. Meristic characters were significantly different between northern Georges Bank and southern Georges-southern New England Slope and between the Scotian Shelf and the southern Georges-southern New England Slope (Table 1.1). These meristic differences are similar to the observation that the number of scale rows is greater on the Scotian Shelf than in the Gulf of Saint Lawrence (Bigelow & Schroeder 1953). Such significant differences in meristics often indicate different larval environments (Lindsey 1988). Otolith weight-at-size was significantly different between northern Georges Bank and the southern Georges-southern New England slope and between the southern Georges-southern New England Slope and the Mid Atlantic slope (Table 1.1). Richter (1970) expanded the study with 1965-1968 samples of size-at-age (n=3,790) from Georges Bank to the Mid Atlantic Bight. He found larger size-at-age in the Georges Bank-southern New England area, and concluded that there were different stocks on the southern shelf of Georges Bank to southern New England, and from southern New England to the Mid-Atlantic Bight, with some overlap off southern New England (Figure 1.11). The southern New England fishery (5Zw, Figure 1.3) was sampled from 1967 to 1971 and was considered a separate stock for population dynamics analyses (Rikter 1973, 1974).

Anderson (1974b) reviewed the information provided by Richter (1968, 1970) as well as patterns in survey data. Survey data suggested seasonal distributions and movements to shallower habitats in spring-early summer and to deeper habitats in fall-early winter, such that winter distributions are discontinuous (with no catches on the central portion of Georges Bank). A more continuous distribution across Georges Bank occurred in the summer (Figure 1.12). Anderson (1974b) concluded that information was insufficient to definitively determine stock structure for red hake, and assessing northern and southern Georges Bank as separate stocks

would be problematic for assessment and fishery management. Therefore, he proposed three stocks off the U.S.: Georges Bank, southern New England-Mid Atlantic Bight, and Gulf of Maine. Gulf of Maine landings were considered too little to justify an assessment for that stock. These stock definitions were adopted by ICNAF, but some spatial overlap of red hake from Georges Bank and southern New England was recognized (Brown 1974). Anderson (1974a) developed separate stock assessments for Georges Bank and southern New England-Mid Atlantic Bight. The assessment was updated and revised in the post-ICNAF period by Almeida & Anderson (1981), and assessment updates were reported in the "Status of the Fishery Resources off the Northeastern United States" series in 1980, 1982, 1983, and 1984 (e.g., Anderson 1984). The stock areas defined by ICNAF for red hake (Scotian Shelf, Gulf of Maine, Georges Bank, and southern New England-Mid Atlantic Bight) were also recognized by Canada in the post-ICNAF period (e.g., Showell 1987)

Northeast Stock Assessment Workshop and Fishery Management Plan Stock Definitions

In 1985, stock definitions for red hake in U.S. waters were revised to the current management units (Figure 1.13): a northern stock (including northern Georges Bank and the Gulf of Maine) and a southern stock (including southern Georges Bank, southern New England and the Mid Atlantic Bight). These stock definitions were based in part on survey distributions and similarity to silver hake (NEFC 1985). The revised definitions were adopted in all subsequent stock assessments and are supported by some subsequent investigations (Derry 1988, Steimle et al. 1999). The second NEFC Stock Assessment Workshop included detailed stock assessments of the revised spatial units and stated that the previous stock definitions '*are currently thought to be incorrect*' (NEFC 1986).

The Fishery Management Plan for the Northeast Multispecies Fishery was amended in 1990 to include red hake and these northern and southern stock definitions (NEFMC 1990). The 1990 benchmark assessment of red hake adopted these spatial units, reporting that two stocks tentatively have been identified, a Gulf of Maine-northern Georges Bank and a southern Georges Bank-Middle Atlantic stock (NEFC 1989). The most recent benchmark assessment of red hake updated assessments of the northern and southern stocks and stated '*Red hake are separated into*

northern and southern stocks for management purposes' (NEFSC 2011). In addition to survey distributions, the 2010 assessment documented the difference in size at ages>3 years between the northern and southern stock for both female and male red hake during both the spring and fall trawl survey over the 1975-1985 period (NEFSC 2011; Figure 1.14). The 2010 assessment also contained a recommendation for further stock structure work.

Derry (1988) reported differences in spawning seasons, seasonality of otolith annulus formation, and growth patterns between the northern and southern stocks of red hake. Early reports of the seasonal distributions of red hake eggs and larvae, indicated spawning occurs May-November in southern waters (Georges Bank to the mid Atlantic Bight) but may not begin until June in the Gulf of Maine, though characters used to identify red hake early life stages in these reports were not diagnostic. Otolith banding patterns suggested that annuli form by April-May for the southern stock, but annuli were not completely formed until early summer for the northern stock, and otolith growth patterns were more variable for the northern stock. In the northern stock, red hake otoliths are more similar in shape to those from white hake.

Steimle et al. (1999) reported that red hake spawning seasons, seasonal habitats and movement patterns are delayed in the northern stock relative to the southern stock. Based on gonad staging and egg distributions, red hake in the southern stock spawn April-October (peaking May-June), and red hake in the northern stock spawn May-November (peaking July-August). The larval period for the southern stock is May-November (peaking August-September), and the larval period for the northern stock is May-December (peaking September-October). As with earlier reports, species-level larval identification used in these analyses were uncertain. Red hake in the southern stock move inshore in spring-fall and offshore in summer and winter, whereas those in the northern stock move offshore in the winter and inshore in the summer.

Summary of Previous Information

Although ICNAF previously assumed different stock boundaries for practical reasons (i.e., difficulty separating catches from northern and southern Georges Bank), information reviewed for stock identification of red hake generally supports the current management units and offers preliminary results for further analysis. It appears that the colder waters of the Gulf of

Maine and northern Georges Bank affect the phenology, growth and morphology of red hake relative to the warmer water of southern Georges Bank and southern New England. Therefore, the current management units may be phenotypic stocks (Booke 1981).

The information reviewed was not definitive, but it was useful for defining putative stocks for further exploration and confirmatory analyses:

1. ***Scotian Shelf*–**significant differences in meristics compared to those from more southern areas (Richter 1968).

2. ***Gulf of Maine-northern Georges Bank***–significant differences in spawning season (Derry 1988, Steimle et al. 1999), growth (Derry 1988), and meristics (Richter 1968) compared to those from more southern areas (southern Georges Bank to Mid Atlantic Bight). Significant differences in meristics compared to those from the Scotian Shelf (Richter 1968). There are no comparisons of these traits between the Gulf of Maine and northern Georges Bank.

3. **Southern Georges Bank–**significant differences in spawning season (Derry 1988, Steimle et al. 1999), growth (Derry 1988) and meristics (Richter 1968) compared to those from more northern areas (northern Georges Bank, Gulf of Maine and Scotian Shelf); and based on difference in relative otolith size compared to those in southern New England Mid-Atlantic(Richter 1968).

4. **Southern New England-Mid Atlantic**-significant differences in spawning season (Derry 1988, Steimle et al. 1999), growth (Derry 1988) and meristics (Richter 1968) compared to those from more northern areas (northern Georges Bank, Gulf of Maine and Scotian Shelf); and based on difference in relative otolith size compared to those on southern Georges Bank (Richter 1968).

Considering the apparent influence of temperature on red hake populations, the regional warming in recent decades, and associated shifting distributions of red hake (Nye et al. 2009, Pinsky & Fogarty 2012, Walsh et al.2015, Kleisner et al. 2016), the review of previous data indicated that geographic variation should consider temporal stability of differences and relevance to current and future conditions in the region.

Summary of recent assessments

The last benchmark assessment for red hake occurred at the Northeast Stock Assessment Workshop 51 (SAW 51) in 2010, with subsequent management advice provided by updates to that assessment. During this assessment extensive work was put into developing an accurate time series of catch due to issues with the misidentification of red hake and white hake and the high levels of discards. Even with these efforts, catch data remained a significant source of uncertainty due to the issues with the underlying data. Additionally, at the 2010 assessment estimates were made of the consumption of red hake by a suite of predatory fishes and this was considered as a direct input into the assessment model. The stomach content data from the NEFSC trawl survey and estimates of predator biomass formed the basis of these consumption estimates. Ratios of consumption to catch ranged from less than 1 prior to 1992 to around 6 from 2000-2010.

During SAW 51, statistical catch-at-age models (SCALE and SS3) were attempted, but the diagnostics were not considered adequate for stock status determination or fishery management. Among the underlying challenges that faced the implementation of these models was the lack of recent age data. Ultimately the assessment moved forward with An Index Method (AIM) analyses for the northern and southern stocks. These analyses used catch and the spring trawl survey data from 1980-2009 as the basis for proposed biological reference points. Attempts were made to use a longer time series, but the results suggested non-stationarity in the relationship between relative fishing mortality and index trends. Additionally, the use of the fall survey data as the input index to this approach led to a worse model fit.

A full description of the AIM methodology is provided in the red hake assessment (NEFSC 2011) and Anon (2002). Briefly, this methodology requires only a catch and index time series to implement. The underlying approach evaluates the relationship between relative fishing mortality rates and the trend in the stocks, as characterized by a replacement ratio (i.e. replacement ratios >1 equal population growth; ratios <1 equal population decline). The relative fishing mortality at a replacement ratio of 1 is then used to guide management advice. To evaluate the model, a significance test is run to test the hypothesis that relative fishing mortality is driving trends in the stock. For red hake at the 2010 assessment the models were found to not be significant, but were considered to be the best option available for providing management

advice by the working group and review committee, with further recommendations provided by both groups on how to improve future assessments (SARC 2011).

TOR2: Identify and evaluate any new and/or existing data relevant to the stock structure of red hake including but not limited to the species' life history (i.e. spawning, distribution, abundance, growth, maturity and natural mortality), morphometrics, and genetics.

The working group followed the interdisciplinary approach to stock identification outlined in Cadrin et al. (2014). This approach has been used numerous times with other species and in different regions (ICES 2009, SEDAR 2018, McBride and Smedbol in press). Notably, red hake lack many of the data sources that are often available for other species. In particular, a population genetics study has not been done on red hake, nor has there been any effort to tag them. Additionally, red hake aging from survey samples has been sporadic, which limits the evaluation of age-based patterns in distribution through time and regional patterns in year class strength.

The evaluation of red hake stock structure was data poor in many respects, but was supported by a high quality and long-time series of survey observations. Sampling during the NEFSC trawl and plankton surveys thus formed the basis for many analyses. In evaluating survey data the working group decided on the establishment of four regions for analysis based on the defined stock boundaries (see TOR1) from the 1970s. These four regions were the Scotian Shelf (entirely in Canadian waters), the Gulf of Maine, Georges Bank, and southern New England. Each of these regions was further divided into 2-4 sub-regions that were used in analyses that required higher resolution spatial data and to evaluate the location of stock boundaries (Figure 2.1). The working group also decided to use the survey strata in defining stock boundaries, regions and sub-regions.

Fishery-Dependent Data

General spatial patterns of catch

Spatial patterns in the catch were evaluated using observer data. Observer data allows for the evaluation of fine-scale spatial patterns in catch with the associated tradeoff that only a portion of tows are observed. Details of the observer program as it applies to red hake are available in NEFSC (2011) and more generally in Hogan et al. (2019). All observer data are presented at a resolution of $1/6^{th}$ of a degree latitude and longitude, with the exception of a

couple of general plots for the entire 1994-2018 dataset that are presented at 1/20th degree resolution to show the fine-scale patterns of fishing practices. In all plots, grid cells with less than three vessels operating over the time series are excluded.

Across all observed vessels and all years, regardless of the targeted fishery, red hake was caught across a broad, but discontinuous range of the northeast shelf (Figure 1.7A). Areas that are notable include 1) the shelf break south of Long Island, 2) nearshore areas of southern New England, 3) the southeastern edge of Georges Bank, 4) the northern edge of Georges Bank, 5) shallow waters surrounding Cape Cod, and 6) waters north of Cape Anne. Red hake was rarely listed as a primary target species. The distribution of those tows are not presented as only 5 grid cells contained at least 3 vessels reporting targeting red hake. Catch within the targeted whiting (silver hake) fishery occurred in relatively restricted areas, but included most of the general areas in the full dataset (Figure 1.7B). As expected, within the Gulf of Maine, catch in the whiting fishery is restricted to the small mesh exempted areas. Catch within the targeted squid fishery was restricted to the areas within southern Georges Bank and southern New England (Figure 1.7C). For the remainder of the targeted fisheries, catch of red hake was widespread (Figure 1.7D).

Seasonally, the effects of regulations and fish migrations are evident in the distribution of the observed catch (Figure 1.8). For the January-March period red hake are primarily caught in southern New England along the shelf break. Red hake are typically offshore during this season. Within the Gulf of Maine, only one small mesh exempted areas is open for fishing January through March. During April-June the fishery extends inshore in southern New England and catch expands into the Gulf of Maine as areas open to fishing. July-September encompasses the spawning season for red hake and catch is mostly inshore in the Gulf of Maine and southern New England, with secondary concentrations on the northern and southern edges of Georges Bank. Finally, for the October-December time period catch again picks up along the shelf edge and is more concentrated in the southern stock area.

In general, catch of red hake occurs in numerous discontinuous areas. The most notable area of little to no catch occurs across the shallow areas of Georges Bank, which encompasses the existing stock boundary. Importantly, red hake is not being targeted. Rather, red hake is caught in small mesh fisheries with other target species, and in some cases with restricted areas

open to fishing. The distribution of catch should thus not be interpreted as the distribution of the species. The distribution of the number of tows combined in the whiting, squid and butterfish targeted fisheries, which use small mesh nets, shows how patchy these fisheries are (Figure 1.9).

Clustering of vessels catching red hake

Catch data from the Greater Atlantic Regional Fisheries Office (GARFO) Data Matching and Imputation System (DMIS) were used to cluster vessels into groups and explore the composition of the catch. Further information on these data are available in Appendix 1. We were most interested in whether vessels consistently fished both of the currently designated stock areas. To cluster vessels we used a standard hierarchical clustering technique and distance metric (euclidean distance) implemented in the hclust package (Maechler et al. 2019). Data used for this analysis was the summed proportion of landing for each stock from 2010 to 2018. Because of the low dimensionality of the data set (only catch of hake stocks are input), the results represent the natural groupings in the data based on the proportions of landing from each stock. To further explore these groupings, clustering was also repeated using a range of weight thresholds to explore how total catch by a vessel impacted cluster membership.

More than 750 vessels reported landings of red hake between 2010 and 2018 in the DMIS data set. Many of these vessels reported a small total weight during this period. Filtering the data to vessels reporting > 1000 lbs over that time period reduced the number of permits to ~200 vessels, and at > 10000 lbs the number of vessels drops to ~120 vessels. Clustering based on the landings of the current red hake stocks alone indicated two larger groups of vessels (Figure 2.2). This pattern became more striking when the clustering was restricted to just vessels with higher levels of landings. Inspection of the catch composition of these vessels indicated that generally, vessels that caught larger weights of the current southern stock landed that stock exclusively. Conversely, vessels that landed the current northern stock tended to land smaller quantities and also landed similar quantities of the southern stock as well (Figure 2.3). Taking a closer look, 152 vessels only fished the southern stock area (3454 mt landings), 17 only the northern stock area (113 mt total landings), and 36 fished both (1068 mt southern and 595 mt northern red hake landings).

Time series in catch and catch-per-unit-effort

An analysis of time series of catch and catch-per-unit-effort using two different fisheries-dependent data sources were evaluated. Full details of the methods used in this analysis and the comparative model results are available in Appendix 1. Briefly, this analysis used Multivariate Auto-Regressive State-Space (MARSS) models to evaluate coherence in trends in catch data across different fishing statistical areas. Generally, a two stock model was found to have the most support with the two stock areas most often consistent with the current boundaries of the stock.

Trawl Survey Distributions

The Northeast Fisheries Science Center (NEFSC) trawl survey covers the continental shelf from Cape Hatteras, North Carolina to the western Scotian Shelf (Azarovitz 1981). Fall coverage started in 1963 but was restricted to Hudson Canyon north until 1968. Spring coverage started in 1968. Sampling was expanded to inshore strata <27 m depth in 1973. In 2009, the vessel used for the survey switched from *NOAA Ship Albatross IV* (hereafter *Albatross*) to the *NOAA Ship Henry B. Bigelow* (hereafter *Bigelow*). Concurrent with this change in vessel there was a change to a more efficient survey gear and the elimination of strata <20 m from sampling. A calibration study accompanied this change in vessel and gear (Miller et al. 2010), with separate length-based calibration factors developed for red hake for the spring and fall surveys (NEFSC 2011). To calibrate biomass-per-tow, length-based calibration factors were used, and a length-weight relationship was used to convert abundance-at-length to weight.

The Canadian Department of Fisheries and Oceans (DFO) trawl survey has sampled from the Bay of Fundy to the eastern Scotian Shelf from 1980 to the present in the summer. This survey uses a stratified sampling design. Importantly, the gear used on the Canadian DFO survey is different and the scale of index values should not be compared with those of the NEFSC trawl survey.

Indices of Abundance

Stratified mean biomass was calculated for the spring and fall NEFSC trawl survey for each subregion, region, and across the entire northeast U.S. continental shelf (Figures 2.4, 2.5). Strata sets used in the calculations are listed in Figure 2.1, and index values are presented in *Albatross* units. Similar calculations were made for the Scotian Shelf summer survey. In general there has been a decline in survey indices for southern New England and a general increase in survey indices for the Gulf of Maine. In most sub-regions there is a general agreement between the spring and fall indices. Across the northeast U.S. shelf, the spring index declined from highs in the 1970s to now be at moderate index values, whereas the fall index has remained relatively stable (Figure 2.5).

Adult Distribution

Distribution of red hake on the trawl survey was typically mapped using a 3-dimensional inverse distance weighted interpolation procedure (Richardson et al. 2014). This procedure uses depth differences between sampled points and interpolated points as a third measure of distance. The conversion factor between depth and horizontal distance is based on a leave one out optimization procedure using bottom temperature. All interpolated distribution maps only included the area within trawl strata that were sampled during that survey.

In the spring, red hake off of southern New England and Georges Bank are typically distributed in the deeper (around 100 m) and warmer waters near to the continental shelf edge (Figure 2.6). Red hake in the Gulf of Maine area also distributed in deep waters, with a higher proportion in the deep areas of the western Gulf of Maine. Few individuals occur in the areas of Georges Bank and the Great South Channel that separate these two centers of distribution. In the fall, fish are in shallower waters, with centers of abundance off southern New England, the southern flank of Georges Bank, deep waters off the northern edge of Georges Bank and the western Gulf of Maine (Figure 2.6).

A summer NEFSC trawl survey occurred from 1977-1983, though strata in the eastern Gulf of Maine and along the continental shelf edge were not sampled. During those years in the summer, fish were distributed in even shallower waters than spring and fall along southern New

England, the southern flank of Georges Bank, and in the western Gulf of Maine (Figure 2.6). A winter survey occurred from 1992-2007, but excluded the Gulf of Maine. Red hake distributions in the winter were similar to the spring distributions for southern New England and Georges Bank (Figure 2.6).

Changes in distribution

Maps of red hake distribution in four-year blocks are presented for the spring and fall (Figure 2.7, 2.8). A prominent northeastward shift is evident in these maps. The center of the highest abundance occurred off southern New England in the late 1960s and shifted to the Gulf of Maine throughout the 2000s, a pattern also documented elsewhere (Nye et al. 2009; Pinsky and Fogarty 2012; Walsh et al. 2015).

For each survey and each year the weighted-average latitude, longitude, depth and bottom temperature were calculated (Richardson et al. 2010). Weighting factors were applied to account for both the biomass per tow and the stratified sampling design (strata area divided by the number of tows sampled in that strata). Red hake have shifted northward, eastward and to deeper waters over the 1968-2018 period based on sampling on both the spring and fall NEFSC trawl survey (Figure 2.9). During both seasons, the center of biomass shifted approximately 270 km over the 50 year period from 1968 to 2018.

The biomass-weighted average depth of red hake across the northeast U.S. continental shelf in the spring has deepened from approximately 125 m in the early 1970s to 175 m in the 2010s. In the fall the biomass weighted average depth has deepened from 75 m in the early 1970s to 150 m in the 2010s (Figure 2.9). At a subregional scale, the weighted average depth has been much more stable, with fish typically centered in shallower waters in southern New England and deeper waters in the Gulf of Maine (Figure 2.10). The shelfwide shift in depth is thus largely driven by a shift of fish from subregions where they have always occurred at shallower depths to those subregions where they occur at deeper depths.

In comparison to latitude, longitude and depth, average biomass-weighted bottom temperature for red hake collections has remained relatively stable for the fall and spring bottom trawl surveys (Figure 2.11). In the spring there was an initial decline in average temperature from 8 °C in the early 1970s to 6 °C around 1980 followed by an increase to about 7 °C in the

2010s. In the fall there was a decline in average temperature from about 10 °C in the early 1970s to 8.5 °C in the early 2000s, followed by a slight increase through the 2010s. The biomass weighted average temperature of red hake at a sub-regional scale have generally increased across both seasons and in all subregions. In general red hake in southern New England and Georges Bank occur at warmer temperature than red hake in the Gulf of Maine. The biomass-weighted average temperature across the entire shelf thus integrates two opposing processes, a distribution shift from warmer sub-regions to colder sub-regions, and a general warming in all sub-regions.

Length specific patterns

For each length class, the proportion of shelf wide abundance was calculated for each year (Figure 2.12-2.15). In the fall, for the 1-10 cm size class, the majority of individuals have been collected in GB-A and GOM-D for nearly the whole time series, though there has been an increase in the proportion of red hake in GOM-A (northern Gulf of Maine) since 2013. For the other size classes, the general shift from southern New England to the Gulf of Maine is evident, with larger fish consistently occurring in higher proportions in the Gulf of Maine. For the spring 1-10 cm fish are typically found in southern New England. The relative abundance patterns for larger fish in the spring generally follow the patterns seen in the fall. Length frequency distributions, show a mode of small fish (3-12 cm) in the fall, but a less prominent of a mode in the spring (Figure 2.13, 2.14), and the general pattern of larger fish occurring in more northerly latitudes.

Length truncation

A prominent and coherent truncation in length structure across the time series was evident in each of the 9 sub-regions in the fall (Figure 2.16). For this analysis only ≥1 year old fish were considered. This was accomplished by excluding the <17 cm fish which have high variability in abundance. At the start of the time series ~10% of Gulf of Maine fish on the fall trawl survey were >45-47 cm. By the end of the time-series ~10% of the Gulf of Maine fish were >37-39 cm. The top decile of length also dropped substantially in southern New England. Notably in the fall, the length of the top decile of GOM-D fish more closely matched those of GB-A than the other Gulf of Maine regions; these two regions were intermediate to the southern New England and Gulf of Maine regions.

Spatial Coherence in Time-Series Abundance

One data limited approach to stock identification was developed by Cope and Punt (2009) and is referred to as the management unit estimator. This approach utilizes spatially resolved standardized relative measures of abundance and a two-step clustering process to look for synchronies across space in time-series of abundance. The goal of this methodology is to combine spatial units with similar population trends, under the assumption that areas that are clustered together behave as a single stock with the same population dynamics. The full details outlining the implementation of the management unit estimator and the results are presented in Appendix 2. An abbreviated summary of the approach and results are presented here

Methods

The management unit estimator involves multiple steps (Figure 2.17). First, spatial units are defined, which in the case of a fisheries-independent survey involves defining groups of strata (Figure 2.1). Second, for each spatial unit an index (Figure 2.4) and the uncertainty of that index are calculated. Third, a sample index for each spatial unit is calculated, accounting for the uncertainty in that index; these sample indices are then normalized. Fourth, the resulting normalized sample indices for each spatial unit are clustered using the k-mediods method across a range of *a priori* cluster numbers referred to as k. Fifth, the best k for that sample of indices is determined using cluster diagnostics and the results of that clustering are recorded. Sixth, steps 3-5 are repeated a pre-determined number of times (e.g. 1000). Seventh, the resulting clustering of spatial units is subject to a second-stage of k-mediods clustering, the best k-value is determined with cluster diagnostics, and the results for that k-value are presented (Figure 2.18).

We evaluated the Management Unit Estimator using1968 to 2018 fall only data, spring only data, and fall plus spring data. We also evaluated other iterations of the approach that included Scotian shelf summertime survey data and an associated truncation in the time series to 1980, but do not consider these results here for brevity (but see Appendix 2).

Cope and Punt (2009) provide guidelines for the evaluation of the management unit estimator using a measure called the silhouette value, which quantifies how closely an area

matches other areas within its cluster versus areas in other clusters. Silhouette values of 1 indicate a perfect match, 0 no match, and negative values a better match to other clusters. The average silhouette value (with unitary clusters assigned a value of 0) provides a measure of overall support for the designated stock structure, with values of <0.25 providing no support for the resulting management units, 0.25-0.50 provide weak but possibly meaningful support, and >0.5 indicate a strong management unit distinction. One final factor to consider in the evaluation of results is how evenly the silhouette values are for each cluster; ideally there is little difference in silhouette values among and within defined clusters.

Results of management unit estimator

The results of the clustering when the spring and fall survey data were both included is shown in Figure 2.18. For k=2, the currently defined northern and southern stocks were the best supported clusters. For k=3, GOM-D (northern edge of Georges Bank) and GOM-B (the western Gulf of Maine) broke out as a third cluster. Finally, for k=4, GB-A (southern Georges Bank) formed a unitary fourth cluster. The average overall silhouette value was highest for four region clustering. However, the differences in average silhouette values among k=2, k=3 and k=4 were moderate. Additionally, with the k=3 and k=4 clustering some clusters were highly supported, such as the two deep areas of the Gulf of Maine and the three Southern New England regions, whereas others were less supported. In contrast, the average silhouette value was less variable among regions and within regions for k=2, though those regions at the middle of the range typically had the lowest silhouette values. Overall, the average silhouette values were between 0.47 and 0.58, indicating moderate to meaningful distinctions among units.

The results of the clustering including only the spring trawl survey data are shown in Figure 2.19. For a k=2, the currently defined northern and southern stocks were the best supported clusters. For k=3, GOM-D (northern edge of Georges Bank) and GOM-B (the western Gulf of Maine) from the northern management unit joined GB-A and GB-B in a third cluster. Finally, for k=4, GB-A (southern Georges Bank) formed a unitary fourth cluster. The average silhouette value for the two region clustering was low (mean S=0.232) but increased to moderate levels for k=3 (means S=0.423) and k=4 (mean S=0.455). As with the model including both spring and fall data, the deep areas of the Gulf of Maine and the southern New England strata typically had higher silhouette values than the regions at the intermediate portions of the

range.

The results of the clustering including only the fall trawl survey data are shown in Figure 2.20. For k=2, the currently defined northern and southern stocks were the best supported clusters. For k=3, GB-A (southern Georges Bank) was designated out as a unitary third cluster, and for k=4, GOM-B was designated as a unitary fourth cluster. The average silhouette value for the two region clustering was the highest (mean S=0.559) with levels indicating meaningful support for that clustering. The three and four region clustering were not as well supported.

Overall, the management unit estimator to red hake provided a number of consistent findings. First, when the approach was restricted to two management units for U.S. waters, the current stock boundaries were identified as the most appropriate, regardless of whether spring, fall or both datasets were used. Support for this two stock clustering ranged from moderate to meaningful. Second, all three southern New England regions at the southern extreme grouped together in all analyses, as did the two deeper and northernmost regions of the Gulf of Maine. Regions in between these two often grouped independently or with either of the other regions, depending on the number of clusters. Finally, adding the Scotian Shelf data, with the necessary tradeoff of shortening the time series, provided results that were difficult to interpret (Appendix 2).

Habitat Analysis

Friedland et al. (2020) described the development of species distribution models for species on the northeast U.S. continental shelf using random forest classification and regression trees. In general the results of this work pointed to an ongoing transition on the northeast U.S. continental shelf from a dominance by cold boreal species to species associated with warm temperate environments. We evaluated the results of the regression tree models for red hake across the shelf and at a sub-regional scale. For the spring and fall, bottom depth, satellite measures of chlorophyll, bottom sediment and measures of temperature were important variables in the models (Figure 2.22, 2.23). For both seasons there was a decline in suitable habitat in the Mid-Atlantic and an increase in habitat in the Gulf of Maine and on Georges Bank as indicated by both the maps of changes in habitat over the time series and the sub-regional trends.

Life History

Otolith appearance

Past evaluations have indicated notable differences in the appearance of otoliths from the currently defined northern stock and southern stocks (Derry 1988). In that publication, differences were found to be stable year-to-year and across cohorts. Differences included factors that affect the readability and interpretation of the otoliths. In particular, red hake otoliths from southern areas are typically easy to interpret with relatively clearly defined annuli. In contrast, many otoliths from the northern areas are anomalous and more difficult to read. No quantitative data was available to the working group to re-evaluate these differences. However, a descriptive presentation of recent efforts to age red hake otoliths confirmed that these same patterns persist in samples collected over the past decade. That is, differences in otolith appearance between southern new England/southern Georges Bank versus the Gulf of Maine have persisted in the 30 years since the differences were first described. As with earlier interpretations of these patterns (Derry 1988), these patterns provide support for the existing two-stock structure.

Age and Growth

Age data for red hake on the NEFSC survey was available from two periods of time. Approximately 20,000 fish were aged from 1970-1985. An analysis of the length-at-age from these fish had been done previously, and had shown clear differences in growth between the two existing red hake stocks (Figure 1.5; NEFSC 2011), as well as between sexes with females growing to larger sizes. Since the last assessment, an additional 10,000 red hake were aged from 2008 to 2019; these had not been previously analysed. A full exploration and description of the growth data is available in Appendix 3.

We also performed an exploratory analysis of the length-at-age data, with fish broken out by existing stock definition (north/south), sex, season of collection (fall/spring), and time period (1970-1985 vs 2009-2019). For each combination we plotted the median length-at-age as well as the distribution of values (Figure 2.23). This exploratory analysis confirmed and revealed three specific findings: 1) females grow to larger sizes than males, 2) at ages greater than about 3 years red hake in the northern stock area reach a longer length-at-age than southern stock area fish, 3)

growth has shifted over the decades in both stock areas leading to reduced length-at-age. While the shift in growth over time is notable, it occurred in both stocks, leading to a continuation of the difference in length-at-age. Additionally, these initial plots suggest that there may be a pattern of initial faster growth in the southern area but lower asymptotic size, a pattern that is expected for a stock that experiences warmer water temperatures.

Further and more detailed analysis of regional size differences focussed on age-2 and age-4 red hake due to the high abundance of these age classes in the trawl surveys (see Appendix 3). These results were generally consistent with the existence of two phenotypic stocks. To summarize this work, maps of individual fish color coded by length-at-age did not indicate obvious spatial patterns, however an ANOVA revealed significant differences in size at age-2, with smaller Age-2 fish in the northern stock unit. Cluster analysis of regions using length at age-2 was generally consistent with the current units, with the exception of an anomalous grouping of fish from the southern extreme of the range, which often grouped with Gulf of Maine fish. The detailed analysis of age-4 fish (Appendix 3), revealed the opposite pattern of age-2 fish with those in the southern stock area being shorter than those in the northern stock area. This difference in age-4 lengths were significant for the early period but for the 2010 period there was a more extensive overlap in sizes. Cluster analysis tended to group the two existing stocks for the early period data, but for the recent data the patterns were less consistent.

Finally, as a further exploration of the oldest age classes we sought to evaluate patterns in length-at-age at a sub-regional scale using k-mediod clustering. As with all analyses of the age data, parsing data by age, region, sex, time period, and season results in sub-units with very low sample sizes. This is particularly prominent in recent years in the southern New England sub-regions. For this reason, we chose to analyze the three southern New England sub-regions as one unit, reducing the total number of spatial units to 7. For this analysis we calculated the median length-at-age for each sub-region for ages 4-7, by season, by time-period and by sex. The resulting matrix had 7 regions across 32 age/sex/season/time periods (i.e. 4x2x2x2). Of these 32 combinations, 4 were eliminated due to sample sizes of 0 in at least 1 sub-region (Table 2.1). As an initial evaluation we color coded regional values in this table based on whether they were above or below the average lengths for that category. This initial evaluation revealed that the 4 sub-regions currently assigned to the northern stock consistently had longer length at age than the more southerly areas. A k-mediods clustering was also run on the resulting matrix to

evaluate how regions clustered in terms of length at older age classes. The resulting clustering (Figure 2.24) provided strong support for two stocks within the existing stock boundaries (mean silhouette value=0.885). For k=3, GOM-D formed a unitary third cluster and the mean silhouette value dropped substantially (mean s=0.410).

Overall, the survey age-length data was consistent with the existence of two stocks separated at the existing stock boundaries. Since the last full assessment in 2011, a substantial effort has gone into aging red hake. This effort has revealed that a notable decline in growth has occurred, a pattern which is common for many species on the northeast U.S. continental shelf, but that regional differences in growth have been maintained. These regional differences are generally consistent with the biomass weighted average temperatures of red hake for different regions. That is, those fish that occur in warmer waters tend to initially grow faster but reach a shorter length at older ages than fish in colder waters

Otolith Microchemistry

An otolith microchemistry study was undertaken on fish collected during the 2011 Fall trawl survey. The expectation was that fish exposed to the same environment during their early life, will incorporate similar chemistry in the otolith nucleus during their early growth, and can be differentiated from fish from a different source. Fish >25 cm were collected from the Gulf of Maine (GOM-A; strata 34,36-38) and the southern New England and western Georges Bank (SNE-B; SNE-A; GB-B). Among the fish analyzed, four groupings were determined a-priori, the western Gulf of Maine, northern Gulf Of Maine, Middle Atlantic Bight shelf (i.e. mid-depths) and Middle Atlantic Bight shelf break. For the otolith chemistry, the sagittae were prepared following laboratory protocol developed at the Center for Quantitative Fisheries Ecology (CQFE) at Old Dominion University. Full details of the laboratory methodology are found in in Ashford et al. (2011, 2012b). This methodology was utilized to measure the trace and minor element concentrations in the nuclei of the otoliths representing the early life environment, and along the otolith edges.

Examining the chemistry in the otolith nuclei for population heterogeneity between sampling areas (Figs 2.24, 2.25), we found no significant spatial differences overall (MANOVA

Pillai's Trace; $F = 0.73$; df = 12; $p = 0.72$). The contrasts showed no differences between the Gulf of Maine and Mid Atlantic Bight (MANOVA Pillai's Trace; $F = 0.81$; df = 4; $p = 0.52$), as well as between areas within the Gulf of Maine (Pillai's Trace; $F = 0.57$; df = 4; $p = 0.68$) and the Mid Atlantic Bight (Pillai's Trace; $F = 0.77$; df = 4; $p = 0.55$). The univariate data corroborated these results: none of the three ratios showed significant differences for the nucleus chemistry (Table 2.2), and there was no evidence of population heterogeneity between the Gulf of Maine and Mid Atlantic Bight, or within each area, indicating that all adult red hake in the Gulf of Maine and Mid Atlantic Bight experienced a similar environment during their early life history.

Examining the chemistry along the otolith edges (Figs. 2.25, 2.26), we found no significant spatial differences (MANOVA Pillai's Trace; $F = 0.50$; df = 9; $p = 0.88$), between the Gulf of Maine and Mid Atlantic Bight (MANOVA Pillai's Trace; $F = 0.11$; df = 3; $p = 0.95$) or between areas within the Gulf of Maine (Pillai's Trace; $F = 0.51$; df = 3; $p = 0.67$) and within the MAB (Pillai's Trace; $F = 0.86$; df = 3; $p = 0.46$). The univariate data also showed no spatial differentiation (Table 2.2) indicating exposure to similar environmental conditions on the northeast United States continental shelf during summer 2011.

The approach failed to find spatial heterogeneity in the nucleus chemistry. Because it combines environmental information with the chronology delineated in the growth increments, otolith chemistry is particularly powerful for testing life history predictions that involve a physical component (Ashford et al. 2010). Nevertheless, the technique relies on several assumptions. Most importantly, sensitivity must be sufficient to differentiate spatially segregated origins. $Sr{\cdot}Ca^{-1}$ has been associated with temperature-related growth whereas $Ba{\cdot}Ca^{-1}$ reflects dissolved Ba (Campana 1999) notably in nutrient-type profiles associated with shelf and oceanic systems (Ashford et al. 2005). $Mg{\cdot}Ca^{-1}$ varies physiologically with changes in activity.

These markers have successfully tested life history hypotheses in shelf environments (e.g. Ashford et al. 2012*a*, 2012*b*), including systems characterized by mixtures of the same water masses (Ashford et al. 2010). By comparison, the northeast Atlantic margin is characterized by strong latitudinal gradients in temperature and nutrient properties as well as exchange with oceanic water offshore. These features generate strong heterogeneity along $Sr{\cdot}Ca^{-1}$ and $Ba{\cdot}Ca^{-1}$, and address the conditions necessary for large contrasts in the otolith chemistry (Ashford et al.

2007).

Another assumption is that movement and mixing do not obscure differences between groups that were originally separated. However, under a working hypothesis of discrete populations, the extensive mixing necessary would itself be a serious departure from expectation. An alternative explanation for our results is that the Gulf of Maine and Mid Atlantic Bight share a common source of recruitment and represent a single population. The working group considered these results important to consider, but also noted the pilot-project type nature of the results with low sample sizes from a single survey of fish.

Spawning, Early Life History and Larval Connectivity

Larval red hake data

The Northeast Fisheries Science Center has sampled the early-life stages of fish on the northeast United States continental shelf since the 1970s, with the two most consistent programs being the Marine Resources Monitoring, Assessment, and Prediction (MARMAP; 1977-1988) program and the Ecosystem Monitoring (EcoMon; 1999-present) program (Richardson 2010, Walsh 2015). Both programs sampled about 6 times per year from Cape Hatteras, North Carolina, to Cape Sable, Nova Scotia using either a combined fixed station -random stratified sampling design (MARMAP) or a primarily random stratified sampling design (EcoMon). EcoMon strata closely match those of the bottom trawl survey, (Azarovitz, 1981, Politis et al., 2014). Sampling protocols were similar between MARMAP and EcoMon. Both programs used a minimum of 5-minute oblique tows of 61-cm bongo nets to within 5 m of the sea floor or to a maximum depth of 200 m. Volume filtered was measured with mechanical flow meters in the mouth of the nets. Mesh size differed between the two programs (MARMAP 505-mm mesh;

EcoMon 333-mm mesh). All standard samples were preserved in 5% buffered formalin and sorted, measured, and initially identified at the Plankton Sorting and Identification Center (ZSIOP) in Szczecin, Poland.

Recent evaluation determined that previous species-level identifications of *Urophycis* larvae were not reliable. Re-examination of thousands of larvae, including genetic barcoding, led to an updated description of morphological traits to separate species of the *Urophycis* genus (Marancik et al., in press). It was possible to re-identify larvae using the new protocol, but not practical to re-identify all larvae from all years. In the end, a total of 27,591 *Urophycis* larvae were re-examined, resulting in 19,526 *U.chuss* observations available for analysis. The cruises selected for examination and analysis met three criteria: (a) spatial coverage of the entire red hake distribution from Chesapeake Bay to Portland, Maine, (b) temporal coverage during both July/August and September/October (peak spawning), and (c) physical availability for examination (samples collected prior to 1985 were destroyed in a fire at the NEFSC Sandy Hook, NJ laboratory). Based on these criteria, species level data is available for 1985, 1987, 2002, 2006, 2012, and 2013.

Larval aging

A total of 92 red hake larvae were available for otolith analysis from 2006 to 2009 and 2013. Larval lengths were measured using a dissecting microscope and image analysis software (Nikon NIS-Elements) to the nearest 0.1 mm total length. Otoliths were extracted and mounted to glass slides with Eukitt mounting medium. Increments were read by two readers using a compound microscope. Otoliths were re-read by both readers if the initial reading differed by more than two increments. If a consensus increment count that differed by two or less was found after the second reading, a mean of the consensus counts was taken. If after the second count none of the counts were within two, the otolith was discarded from analysis. The final mean increment count was rounded up to the nearest whole number to estimate larval age.

Eighty of the 92 larval Red Hake otoliths were readable. The estimated intercept of the regression of 1.56 mm (Figure 2.27) was slightly below the reported hatching size (1.8–2.0 mm, Fahay 2007) but not unreasonable due to potential shrinkage related to capture and preservation

of the larvae. Growth of the recently hatched to 8 mm larvae was estimated to be 0.31 mm per day, which resulted in an estimated age range of 1 to 25 days.

Larval distributions

U. chuss larvae were collected throughout the Northeast U.S. continental shelf, with highest abundances off the southern New England coast and on Georges Bank (Figure 2.28). A second area of high larval abundance occurs in the western Gulf of Maine. This area contains an average of 3.9% (0-20.9%) of the annual abundance on the shelf, but does frequently contain small larvae (Table 2.3). Larval distribution throughout southern New England and Georges Bank has remained relatively stable. An increase in larval abundances in the western Gulf of Maine was observed, but this is still a fraction of the number of larvae occurring in southern areas.

Unique areas of spawning were identified using hot spot analysis (Gi* statistic; Getis and Ord, 1992) of *U. chuss* larvae under 5 mm BL. This hot spot analysis identifies strata of significantly high abundance located adjacent to strata with significantly high abundance. The presence of hot spots in time and space was used to identify unique clusters of strata that support high larval abundances. This analysis identified the southern New England and Georges Bank regions as having significantly high abundances (Figure 2.29). In 2012, the number of larvae in the western Gulf of Maine was the highest observed which drives the identification of this area as a hot spot.

Larval transport evaluation methods

A number of factors influence the scale of larval dispersal including: patterns in ocean currents, spawning location and timing, larval duration, larval vertical movements, and directed horizontal swimming capabilities. We used two approaches to evaluate larval transport, a larval transport model and a drifter trajectory analysis. Larval transport models couple ocean circulation models with models of larval behavior that can range from simple to complex, allowing for the simulation of process that are difficult to evaluate in the field over relevant temporal and spatial scales. On the other hand, the accuracy of the results of these models is dependent on how well the behavioral and oceanographic model match conditions in the ocean,

both of which can be difficult to evaluate. A second approach to evaluating larval transport is to examine actual movement in the ocean as monitored by drifters, which have a buoy floating at the surface and an underwater sail, called a drogue, set at a predetermined depth (usually averaging 15 m).

A general description of the particle-tracking model can be found in Churchill et al. (2011). The larval tracking model we applied to red hake used current velocities from FVCOM (Chen et al., 2003, 2006) and the GOM-3 model dataset. Constraints on runtime limited the number of particle tracks and scenarios that could be run. We thus chose to evaluate 6 years of data, with particle release locations (5099) restricted to 5-150 m depth across a 10 minute grid from Delaware to the Scotian Shelf. Particles with a 60 day duration were released every 4 days during the months of July-September (Table 2.4). Two separate vertical behaviors were modeled: 1) an initial depth of 10 meters that switched to 20 m depth after 15 days, 2) an initial depth of 20 m that switched to 40 m after 15 days. In all cases, particles were moved to shallower depths if their target depth exceeded the bottom depth. These vertical behaviors were chosen based on results for a congener (*U. regia*) based on vertically stratified plankton sampling (Hernandez et al. 2009).

The drifter trajectory model was developed using the methodology described by Hare and Walsh (2007). The Global Drifter Program (GDP) database contains 713 drifters that have entered the Northeast US Shelf EcoMon strata (https://doi.org/10.25921/7ntx-z961). These drifters were released during all months of the year and span late 1989 to 2019. GDP drifters are all of the World Ocean Circulation Experiment (WOCE) Surface Velocity Program (SVP) design (SVPB, SVPBW, SVPC, SVPBS, SVPW) with a surface float and drogue centered at 15 m (Sybrandy and Niiler 1990).

The drifter trajectory model is a box model based on the EcoMon strata and the red hake subregions. A probability function was based on observed residence times calculated for each zone (stratum or subregion). The probability of movement from each zone to all surrounding zones was calculated from drifter tracks. Movement was interpolated to 24-hr bins to reduce the influence of tides on drifter movement. Zone-specific functions of duration and movement were used to create a probability model of transport on the shelf. Modeled drifters (n=115,000) were

released in each zone. The number of particles from a given release zone found in surrounding zones after a specified time were used to calculate estimates of retention and transport rates. Drifter locations were examined at 10, 15, 30, 45, and 60 days after release.

Spawning locations

We used the particle tracking results to evaluate the likely source location of particles of a certain duration. This approach was meant to address what the spawning location could have been for a larval fish of a particular age collected at a specific sampling site. The first step in the methodology was to generate a 3-D matrix with the matrix dimensions being: 1) the 5099 release locations used in the larval transport model, 2) Time with a resolution of 3-day and a duration of 30 days, and 3) end locations for larval transport indexed to a grid of 10 minute resolution (1/6°) across latitudes 38-46 °N and longitudes 75-61.5 °W. We populated this matrix with the number of particles that started at a simulated spawning location (Dimension-1) that were transported to a simulated collection location (Dimension-2) in a set time period (Dimension-3). The goal of this approach was to develop a representative depiction of the potential source locations for any age larva for any collection site across the EcoMon sampling domain. Similarly, we used the drifter model to evaluate the source sub-region for drifters with endpoints within the various sub-regions after specified periods of time

Comparing the drifter tracks and particle-model tracks to larval distributions, suggests that spawning most likely occurs in the subregions of and adjacent to the highest concentrations of larvae (Figures 2.30-2.33). In our larval collections, 50% of larval red hake are <3 mm (~ 10 days post-spawning) and 90% of larvae are <5 mm (~16 days post-spawning) and thus transport times are short. Larvae collected in the GOM-B are likely the result of spawning in the GOM-B.

Spawning seasonality

Length and hatch date distributions were analyzed for red hake larvae collected during cruises recently re-identified for Marancik et al. (in press). Lengths were binned in 1-mm length bins from 1 to 22. Hatch date distributions were developed by subtracting the estimated age (increment count) from the collection date for samples. Hatch date distributions were weighted

by stratified abundance (Walsh et al. 2015) of larvae collected in each EcoMon strata and summed for each week of the year.

Identifiable larval red hake lengths ranged from 1 to 22 mm and 99% of larvae were ≦6 mm (Figure 2.34). The smallest larvae (1–6 mm) were collected during all seasons from May-June to November-December. However, July-August (54 %) and September-October (45%) had the highest proportion of larvae, with a peak of 2-mm larvae in July-August and 3-mm larvae in September-October (Figure 2.36A). Small larvae were collected in the three regions (Figure 2.34B), with the highest percentages in Georges Bank (66 %), intermediate in Southern New England (26 %), and lowest in Gulf of Maine (8 %). The largest larvae (> 6 mm) accounted for less than 0.5 % of all larvae collected (Figure 2.34C), and were collected in July-August (0.25 %) to September-October (0.20 %), and November-December (0.04 %). The regional abundance of large larvae was similar to small larvae (Figure 2.34D), most abundant in Georges Bank (0.35 %) and less in southern New England (0.06 %) and Gulf of Maine (0.05 %).

Red hake larvae had estimated hatch dates ranging from week 22 to 46, the last week of May to the second week of November (Figure 2.35). The earliest hatch dates were estimated for larvae collected in the Gulf of Maine (Figure 2.35A) and peak hatch dates were during week 33. Peak hatch dates occurred for week 33 for Georges Bank larvae (Figure 2.35B). The latest peak hatch dates, week 37 to 38, were estimated for larvae collected in southern New England (Figure 2.35C). Standardized percentage of hatch date abundances larvae collected in all three regions began hatching during similar times and larvae collected in the Gulf of Maine peaked first, followed by Georges Banks and southern New England (Figure 2.35D).

Hatch date distributions estimated from larval ages indicated red hake spawn primarily during the summer (July to September). There is some evidence that spawning begins earlier in the Gulf of Maine and goes later in southern New England. Importantly, these results differ from some of those presented in the review of red hake spawning phenology, possibly due to the availability of accurate species level larval identifications for this analysis.

Adult reproductive data and spawning seasonality

Spawning phenology of red hake was evaluated using macroscopic maturity data collected during routine NEFSC spring and fall bottom trawl surveys. The macroscopic scheme includes six stages – immature, developing, ripe, running ripe, spent, and resting and criteria are described in Burnett et al (1989). Data was analyzed for each of the three stock regions (Figure 2.1). Specifically, the proportions developing, ripe, spent, and resting were calculated for each stock region and survey. The proportions in each maturity stage were also summarized by temperature bin and week of year to evaluate influence of each. These relations (binned bottom temperature and week of year) were also summarized by decade to explore temporal changes over the past few decades (1990s to 2010s).

Red hake spawn during the summer months, with most spawning occurring between the end of the spring survey and the start of the fall survey. Spawning appears to start around week 22 (early-June), but only the Gulf of Maine region was sampled this late into the year. Spawning extends to week 42 (mid-October) in the Gulf of Maine and Georges Bank. Spawning may extend later in southern New England, which was only sampled into week 41, with most fish still developing at that time. Red hake spawning appears to be more influenced by time of year than temperature. There is limited evidence of spawning extending slightly later into the fall in the recent decade in Georges Bank and southern New England.

Larval Connectivity

Connectivity matrices were developed based on the results of the particle tracking model and using the 12 defined subregions inclusive of the Scotian Shelf (Figure 2.1). A connectivity matrix defines the proportion of particles released in a source location that are transported to an end location after a predetermined period of time. These matrices thus provide an indication of how interconnected spawning and juvenile settlement areas are through larval transport, and the directionality of those connections. We used the full set of particle tracks to develop connectivity matrices for particle durations of 15 and 30 days. We then ran sensitivity analyses of the results of the 30 day runs, comparing: 1) track duration, 2) period of release (1970s/80s vs 2000s), 3) month of release, 4) particle depth behavior, and 5) bottom depth of release location. Similarly, the drifter probability model was used to develop connectivity matrices at 15

and 30 day durations.

The results of both the drifter model and particle-tracking model, in terms of connectivity, are fairly consistent and are shown in Tables 2.5-2.8 and Figures 2.31-2.32. The general patterns assume passive transport and match the average current patterns in the region and are as follows:

1. Juveniles that recruit in the three southern New England sub-regions (SNE-A—C) may be produced in the same region or sourced from areas upstream on Georges Bank. Transport to southern New England from the Gulf of Maine sub-regions is very limited even at a 30-day duration, though there is some limited transport from GOM-D, which includes northern Georges Bank.

2. Juveniles that recruit on Georges Bank are not sourced from southern New England. Supply to this region likely comes from spawning within this region, GOM-D (i.e., northern Georges Bank), and to a limited extent, GOM-C.

3. Gulf of Maine-D (northern Georges Bank – current northern stock) and Georges Bank-A (southern Georges Bank – current southern stock) are highly connected in both directions due to the clockwise circulation around Georges Bank.

4. Juveniles that recruit in the GOM-A, GOM-B and GOM-C were likely spawned in the Gulf of Maine, although there is some connectivity from Scotian Shelf-C (Bay of Fundy/Western Scotian Shelf) to Gulf of Maine-A.

The connectivity matrices from the particle-tracking model revealed notable exchange among sub-regions and among regions (Tables 2.5 and 2.6). As an example, particles released in Georges Bank-A were transported to both Gulf of Maine and Southern New England subregions. In general, the month of release (July, August, September), period of release, and depth behavior had minor influences on connectivity. However, the bottom depth at which the particles were released had a major influence (Figure 2.36). Particles released in the shallow areas of Georges Bank (<50 m) had higher levels of retention whereas particles released in the deeper areas (100-150 m) were spread more widely, likely due to entrainment in the shelf break jet (Fratantoni and Pickart 2003). In general, early stage red hake larvae occur in locations of intermediate depth and thus likely are best represented by the intermediate transport scenario.

As expected, for both the drifter model and particle-tracking model, the duration of transport had a very prominent influence on the level of exchange among regions. This raises the question of what duration most closely matches the period of passive transport for red hake early life stages. Red hake have an egg duration of 3-7 days. Around 12-days post hatch, the larvae are 5 mm, and flexion occurs. After flexion, temperate larval fishes are capable of some swimming behavior. The ~15-day egg plus pre-flexion period likely represents the minimum time of passive transport. Therefore, directly comparing the results from the 10 and 15-day model periods to observed distributions of recently hatched and nearly flexion-stage larvae (during this passive-transport phase; Fig. 2.32) identifies likely spawning locations. Post-flexion larvae transition to a pelagic juvenile stage, and then settle at around 20-50 mm. Red hake early life stages will thus remain in the water column for ~60 days, representing a maximum bound for transport periods. Importantly, during the period from post-flexion through the pelagic juvenile period, it is possible that the combination of vertical movements, in areas with vertically stratified currents, and active horizontal swimming allows an individual to either stay in or move to an area of suitable settlement habitat. The results of the 30 and 60-day model runs help understand underlying currents aiding transport to juvenile settlement locations and levels of retention, but alone cannot explain juvenile distributions. The results of any transport model should thus be interpreted with caution, and attempts should be made to validate the patterns.

Young of the Year and Recruitment

NEFSC bottom trawl survey data provides the best source of information on the distribution of young-of-the-year red hake and can be used to develop a time series of recruitment. However there are a number of notable issues with these data that should be considered including:

1. Red hake have not consistently been aged on the NEFSC trawl survey and thus a fisheries-independent recruitment time series applying annual age data is not possible. Length cutoffs must be used.

2. Red hake length-frequency distributions in the fall are bimodal, with the first maximum at ∼5 cm and the first minimum at ∼14 cm. These <14 cm fish are young-of-the year from spawning a few months earlier in the summer.

3. During the fall trawl survey, larval red hake are still being collected in the concurrent plankton survey, particularly in southern New England which is always surveyed first (i.e. in September vs October further north) and may have a later timing of spawning. This survey timing issue may cause biases in evaluating the distribution of recruitment using the fall survey.

4. It is unknown how the association of red hake with scallops affects their catchability. Scallop fishermen report seeing red hake juveniles in their catch that would otherwise pass through their gear. A similar process could happen with survey gear leading to the possibility of spatial variability in catchability.

5. In the spring, based on available aging data, there is some overlap in the length structure of age-1 and age-2 fish (75/25 at 18 cm; 52/48 at 19 cm; 22/78 at 20 cm); a perfectly clean signal of recruitment is thus not available with spring data, though a 19 cm cutoff should work well.

6. The *Albatross* (1963-2008) to *Bigelow* (2009-present) transition involved a switch from a 0.5 inch (1.27 cm) hexagon to a 1.0 inch (2.54 cm) diamond codend liner, resulting in the loss of many very small fish. Length specific calibrations were calculated for red hake, but these calibrations typically are very uncertain at the smallest sizes. Caution is thus needed in evaluating time-series of very small fish across this transition.

7. Small fish may occur inshore of the survey area thus biasing perceptions of fish distribution and time series of abundance.

While these limitations should be recognized, the trawl survey data on young of the year abundance and distribution can also provide important information..

Fall young-of-the-year

Over the 1968-2013 portion of the NEFSC trawl survey time series, the highest abundances of young-of-the-year red hake were consistently found on the top of Georges Bank, both in the subregion GB-A which is within the southern stock area boundaries and GOM-D which is within the northern stock area boundaries (Figure 2.14, 2.15). Periodically, young of the year were also sampled in both southern New England and in the northern Gulf of Maine.

From 2013-2019 there was an increase in young of the year abundance in the northern Gulf of Maine (GOM-A) (Figure 2.37). This signal in the fall trawl survey time series of increased recruitment in the northern Gulf of Maine also occurs in the the summer DFO trawl time series in the Bay of Fundy strata (adjacent to GOM-A) in Canadian waters (Figure 2.38). Since 2013 the abundance of <20 cm has increased approximately 20-fold in the Bay of Fundy strata versus 1980-2008.

Link between spawning, larval, YOY and age-1 distributions

The larval sampling indicates that a majority of larvae and spawning occur in the southern stock area and in particular on Georges Bank. In the fall the sampled young-of-the-year are also typically on Georges Bank, in a continuous distribution across strata currently assigned to both the northern and southern stock areas. Larval transport models and drifter trajectories indicate that Georges Bank is a retentive area, consistent with the clockwise recirculating gyre on Georges Bank; no barriers to larval transport occur across Georges Bank (i.e. the stock boundary). The pattern of high levels of spawning on Georges Bank and lower levels in the Gulf of Maine is consistent with the high levels of young of the year abundance on Georges Bank and the lower levels in the Gulf of Maine. However, the recent pattern of higher levels of adult biomass in the northern versus southern stock area in the fall and spring trawl survey contrasts with the higher levels of larval production in the southern stock area.

One possible explanation for the contrast between trawl survey and plankton survey distribution data is a summer migration by red hake from the Gulf of Maine to the shallow areas of Georges Bank to spawn (Figure 2.39). Such a migration could involve a seasonal crossing of the existing stock boundary along the shallow areas of Georges Bank. For a large portion of the

deep areas of the Gulf of Maine, a migration to Georges Bank to spawn would also be a shorter distance than a migration to the western Gulf of Maine. Under this scenario the product of Georges Bank spawning would recruit to Georges Bank in the fall, before moving to deeper waters in the Gulf of Maine in the winter. Different scenarios could be proposed for how northern and southern stock fish would mix during spawning and recruitment. This life history pattern would be consistent with the otolith microchemistry results from 2011. Unfortunately, no other data beyond that and survey distributions, is currently available to test this proposed life history.

The recent increase of young-of-the-year red hake in the northern Gulf of Maine in 2013, and the associated increase in age-1 fish in the summer in the Bay of Fundy points to potential;y increased spawning activity in that region. The potential source locations for those young of the year, based on the larval tracking model, was also the northern Gulf of Maine or the Bay of Fundy. Unfortunately, due to shiptime constraints, plankton sampling has not occurred during the month of August in the northern Gulf of Maine. This change in the pattern of recruitment in the northern Gulf of Maine since 2013 is one to monitor with respect to stock structure, as it also occurs near a stock boundary and is the most notable change in young of the year distribution since the start of sampling in 1968.

Use of the AIM Model

Prior to the working group meeting a proposal was put forward to use the AIM model as a means of stock identification (See TOR1 for a description of the AIM model). Specifically, the AIM model tests the hypothesis that changes in relative fishing mortality, as measured by catch divided by an index value, drive changes in population size. Changes in population size are presented as a replacement ratio, or an index value divided by the average of the index the five years prior. The proposal was that, if the appropriate stock structure is chosen, and if exploitation rates are driving population trends, then the AIM models for each stock should be significant. That is, the expectation was that this analysis would provide information on “harvest stocks” which are groups of fish that respond coherently to fishing pressure.

With three defined regions in U.S. waters, and the possibility of 1-3 defined stocks, there were 4 possible iterations of stock structure that could be tested: 1) A single unit stock, 2)

SNE+GB as a southern stock; GOM as a northern stock, 3) SNE as a southern stock, GOM+GB as a northern stock, 4) SNE, GB and GOM as three individual stocks. Southern New England and the Gulf of Maine as a stock independent of Georges Bank was not considered due to the discontinuity in the area encompassed. With these four potential stock structure scenarios for the entire shelf based on regions, there were 8 AIM models that needed to be run (3-one region, 4 two region, 1-three region). Finally, one additional iteration was also run that grouped GB-A with the Gulf of Maine and GB-B with southern New England, leading to 10 total AIM runs.

None of the 10 AIM models tested were significant (Table 2.7), with the lowest p-value among the iterations being for the GOM only region. More detailed results are shown for the AIM model runs of the northern and southern stocks under the existing stock structure as well as a single stock in U.S. waters (Figures 2.40-2.42). The working group considered these results as not providing any special insight into the appropriate stock structure to use in the assessment as none of the results were significant.

TOR3: Recommend the most likely biological stock structure among a set of alternatives from TOR2. Consider the current management unit as the null hypothesis.

The working group considered the information available insufficient to reject the null hypothesis of two stocks, and thus recommended the status quo stock structure. Specifically, we recommend two stocks, a northern stock that encompasses northern Georges Bank and the Gulf of Maine and a southern stock that encompasses southern New England and southern Georges Bank.

The working group followed the interdisciplinary approach to stock identification. In comparison to many other species, red hake is data poor with respect to information useful to determining stock structure. No genetics data or tagging data exists, and only an extremely limited effort has been put into evaluating the use of otolith microchemistry as a natural tag. For these reasons, increased weight was placed on characteristics useful for identifying phenotypic stocks, or regional groupings of fish with unique characteristics. Additionally, there was a consideration of harvest stocks, regional groups of fish that respond coherently to fishing pressure and environmental change. Both of these types of information pointed to separate northern and southern stocks of red hake. The distribution of red hake early life stages raises the likelihood of seasonal and ontogenetic movement across stock boundaries, and the potential for a shared spawning source for new recruits to each stock, but this evidence was indirect and was not considered sufficient to reject the two-stock hypothesis.

The existing (recommended) stock boundaries divide the red hake distribution on the northeast U.S. continental shelf into two regions that have distinctive life history characteristics and phenotypes. Red hake within the northern stock boundary consistently grow to larger sizes than those in the southern stock boundaries. The persistence of this difference in growth from the 1960s to the present, despite temporal trends in growth in all areas, indicates that there consistently has been little exchange of adults between the two stock areas, at least during the fall and spring when sampling has most frequently occurred. Historic data on meristic, as well as the historic and current differences in otolith morphology, are consistent with two stocks and minimal exchange among these stocks after recruitment. That is, the available evidence indicates that once a juvenile recruits to a stock they will stay within the stock boundaries at least

for the fall through spring time period when most survey effort has occurred. The red hake in U.S. waters thus group into two phenotypic stocks consistent with the stock boundaries.

The use of the management unit estimator on the 1968-present time series of red hake biomass indicated that coherent population trends occur across sub-regions within the areas defining each of the two stocks. There was moderate to meaningful support for this two-stock grouping using the management unit estimator. The management unit estimator evaluates spatial coherence in population responses relative to harvest or environmental drivers. We also sought to use the 1980-present AIM models as an additional means of evaluating the response of the survey biomass directly to fishing pressure under different stock scenarios. However, the various iterations of this approach were not significant, which may be explained by the low level of removals relative to population biomass since 1980 (see TOR4 and Appendix 1). One important note in the use of the management unit estimator, versus AIM, is the time-series used in the management unit estimator contained a period of high landings by the foreign fleets that also corresponded with the peak in relative fishing mortality. The management unit estimator thus was more likely to resolve coherent spatial population trends driven by fishing pressure, a defining characteristic of harvest stocks. Notably, previous attempts to incorporate this extended time-series into AIM were not successful, which was attributed to non-stationarity in the relationship between relative fishing mortality and population trends (NEFSC 2011). The management unit estimator does not seek to test the relationship between fishing and population trends, only the spatial coherence of trends. Overall, the fact that the management unit estimator consistently resolved the current stock boundaries when two stocks were chosen, provided additional support to the two stocks that were resolved based on phenotypic traits.

Finally, the characteristics of the fisheries within the two stock boundaries were also unique. In particular, few boats were found to harvest red hake in both stock regions and trends in fisheries-dependent metrics were coherent. Fishermen also identified differences in the fisheries in each region, and some of the target fisheries that catch red hake are unique to a specific stock (i.e. the squid fishery). While some patterns in the fishery are likely driven by regulations that have their basis in the existing stock structure, others do not. The distribution of red hake catch in the fishery indicates that the stock boundary occurs in an area with extremely

low catch. The placement of this is boundary in an area with low catch ensures that catch can be readily assigned to a stock.

Information provided by the early life stages of red hake did suggest that the stock boundary is not absolute, but rather that there may be larval, ontogenetic and seasonal spawning movements across the stock boundary on northern Georges Bank. Larval connectivity matrices indicated extensive exchange between Georges Bank and southern New England and the northern and southern portions of Georges Bank. However exchange between the western Gulf of Maine and the southern stock areas was more restricted. In the fall, young-of-the-year red hake are continuously distributed across the stock boundary on Georges Bank. Additionally, there is a mismatch between the long term trend of an increasing proportion of adult biomass in the northern stock area versus the lack of clear trend in the North-South ratio for young-of-the-year abundance. The stock boundary thus likely provides little separation for young-of-the-year fish, but this life stage is generally unexploited and contributes little to survey biomass.

No direct evidence of juvenile movement patterns exists for red hake in the form of natural or artificial tags. However, red hake occur in the shallow areas of Georges Bank as young-of-the-year in the fall but not as age-1s in the spring, whereas young-of-the-year are in low abundance in the deep basins of the Gulf of Maine in the fall but age-1s are in high abundances in the spring. These patterns suggest an overwintering movement of juvenile fish from the shallow areas of Georges Bank (both northern and southern stock areas) to the deep portions of the Gulf of Maine (northern stock area).

Larval data indicated that there were spawning areas within both the southern and northern stock areas, but the relative adult biomass during the non-spawning seasons (fall/spring) versus larval production in the two were not consistent. One possible explanation for this pattern is that a notable proportion of red hake in the northern stock may undertake a summer spawning migration from the Gulf of Maine, across the stock boundary, to Georges Bank (Figure 2.39). A similar but more extreme migration has been proposed for a congener, white hake (*Urophycis tenuis*), which is thought to migrate from the Gulf of Maine to the deep waters south of Georges Bank for spawning (Fahay and Able 1989). For fish in much of the Gulf of Maine, a spawning

migration to Georges Bank would be shorter than the migration to the shallow areas of the western Gulf of Maine.

Currently, no direct evidence exists for the migration of red hake from the Gulf of Maine to the southern flank of Georges Bank for spawning. If this migration does occur, it is possible that there is mixing of northern and southern stock fish on the summer spawning ground, and a shared source of recruits to each stock. The working group considered the lack of a second line of evidence for this hypothesis, in addition to early life stage distributions, an important data gap. In the absence of a direct tagging study, ideally it would be possible to evaluate phenotypic characteristics (length at age, meristics) of red hake on the Georges Bank spawning ground to determine if they match the northern or southern stocks or are intermediate between the two. The uncertainty concerning spawning migrations in red hake was a concern for the working group, but was not sufficient to reject the null hypothesis of two stocks.

TOR3: Recommend the most likely biological stock structure among a set of alternatives from TOR2. Consider the current management unit as the null hypothesis.

The working group considered the information available insufficient to reject the null hypothesis of two stocks, and thus recommended the status quo stock structure. Specifically, we recommend two stocks, a northern stock that encompasses northern Georges Bank and the Gulf of Maine and a southern stock that encompasses southern New England and southern Georges Bank.

The working group followed the interdisciplinary approach to stock identification. In comparison to many other species, red hake is data poor with respect to information useful to determining stock structure. No genetics data or tagging data exists, and only an extremely limited effort has been put into evaluating the use of otolith microchemistry as a natural tag. For these reasons, increased weight was placed on characteristics useful for identifying phenotypic stocks, or regional groupings of fish with unique characteristics. Additionally, there was a consideration of harvest stocks, regional groups of fish that respond coherently to fishing pressure and environmental change. Both of these types of information pointed to separate northern and southern stocks of red hake. The distribution of red hake early life stages raises the likelihood of seasonal and ontogenetic movement across stock boundaries, and the potential for a shared spawning source for new recruits to each stock, but this evidence was indirect and was not considered sufficient to reject the two-stock hypothesis.

The existing (recommended) stock boundaries divide the red hake distribution on the northeast U.S. continental shelf into two regions that have distinctive life history characteristics and phenotypes. Red hake within the northern stock boundary consistently grow to larger sizes than those in the southern stock boundaries. The persistence of this difference in growth from the 1960s to the present, despite temporal trends in growth in all areas, indicates that there consistently has been little exchange of adults between the two stock areas, at least during the fall and spring when sampling has most frequently occurred. Historic data on meristic, as well as the historic and current differences in otolith morphology, are consistent with two stocks and minimal exchange among these stocks after recruitment. That is, the available evidence indicates that once a juvenile recruits to a stock they will stay within the stock boundaries at least

for the fall through spring time period when most survey effort has occurred. The red hake in U.S. waters thus group into two phenotypic stocks consistent with the stock boundaries.

The use of the management unit estimator on the 1968-present time series of red hake biomass indicated that coherent population trends occur across sub-regions within the areas defining each of the two stocks. There was moderate to meaningful support for this two-stock grouping using the management unit estimator. The management unit estimator evaluates spatial coherence in population responses relative to harvest or environmental drivers. We also sought to use the 1980-present AIM models as an additional means of evaluating the response of the survey biomass directly to fishing pressure under different stock scenarios. However, the various iterations of this approach were not significant, which may be explained by the low level of removals relative to population biomass since 1980 (see TOR4 and Appendix 1). One important note in the use of the management unit estimator, versus AIM, is the time-series used in the management unit estimator contained a period of high landings by the foreign fleets that also corresponded with the peak in relative fishing mortality. The management unit estimator thus was more likely to resolve coherent spatial population trends driven by fishing pressure, a defining characteristic of harvest stocks. Notably, previous attempts to incorporate this extended time-series into AIM were not successful, which was attributed to non-stationarity in the relationship between relative fishing mortality and population trends (NEFSC 2011). The management unit estimator does not seek to test the relationship between fishing and population trends, only the spatial coherence of trends. Overall, the fact that the management unit estimator consistently resolved the current stock boundaries when two stocks were chosen, provided additional support to the two stocks that were resolved based on phenotypic traits.

Finally, the characteristics of the fisheries within the two stock boundaries were also unique. In particular, few boats were found to harvest red hake in both stock regions and trends in fisheries-dependent metrics were coherent. Fishermen also identified differences in the fisheries in each region, and some of the target fisheries that catch red hake are unique to a specific stock (i.e. the squid fishery). While some patterns in the fishery are likely driven by regulations that have their basis in the existing stock structure, others do not. The distribution of red hake catch in the fishery indicates that the stock boundary occurs in an area with extremely

low catch. The placement of this is boundary in an area with low catch ensures that catch can be readily assigned to a stock.

Information provided by the early life stages of red hake did suggest that the stock boundary is not absolute, but rather that there may be larval, ontogenetic and seasonal spawning movements across the stock boundary on northern Georges Bank. Larval connectivity matrices indicated extensive exchange between Georges Bank and southern New England and the northern and southern portions of Georges Bank. However exchange between the western Gulf of Maine and the southern stock areas was more restricted. In the fall, young-of-the-year red hake are continuously distributed across the stock boundary on Georges Bank. Additionally, there is a mismatch between the long term trend of an increasing proportion of adult biomass in the northern stock area versus the lack of clear trend in the North-South ratio for young-of-the-year abundance. The stock boundary thus likely provides little separation for young-of-the-year fish, but this life stage is generally unexploited and contributes little to survey biomass.

No direct evidence of juvenile movement patterns exists for red hake in the form of natural or artificial tags. However, red hake occur in the shallow areas of Georges Bank as young-of-the-year in the fall but not as age-1s in the spring, whereas young-of-the-year are in low abundance in the deep basins of the Gulf of Maine in the fall but age-1s are in high abundances in the spring. These patterns suggest an overwintering movement of juvenile fish from the shallow areas of Georges Bank (both northern and southern stock areas) to the deep portions of the Gulf of Maine (northern stock area).

Larval data indicated that there were spawning areas within both the southern and northern stock areas, but the relative adult biomass during the non-spawning seasons (fall/spring) versus larval production in the two were not consistent. One possible explanation for this pattern is that a notable proportion of red hake in the northern stock may undertake a summer spawning migration from the Gulf of Maine, across the stock boundary, to Georges Bank (Figure 2.39). A similar but more extreme migration has been proposed for a congener, white hake (*Urophycis tenuis*), which is thought to migrate from the Gulf of Maine to the deep waters south of Georges Bank for spawning (Fahay and Able 1989). For fish in much of the Gulf of Maine, a spawning migration to Georges Bank would be shorter than the migration to the shallow areas of the western Gulf of Maine.

Currently, no direct evidence exists for the migration of red hake from the Gulf of Maine to the southern flank of Georges Bank for spawning. If this migration does occur, it is possible that there is mixing of northern and southern stock fish on the summer spawning ground, and a shared source of recruits to each stock. The working group considered the lack of a second line of evidence for this hypothesis, in addition to early life stage distributions, an important data gap. In the absence of a direct tagging study, ideally it would be possible to evaluate phenotypic characteristics (length-at-age, meristics) of red hake on the Georges Bank spawning ground to determine if they match the northern or southern stocks or are intermediate between the two. The uncertainty concerning spawning migrations in red hake was a concern for the working group, but was not sufficient to reject the null hypothesis of two stocks.

TOR4: Evaluate existing experimental data on survey catchability of red hake. Examine the sufficiency of catchability data and, if appropriate, incorporate the catchability estimates into the assessment.

Indices of abundance or biomass (I) derived from fisheries-independent bottom trawl surveys are scaled to population number or biomass (N) using the survey catchability (q) parameter:

$$N = I\frac{A}{aq}$$

where A is the total area surveyed and a=the area of a tow. While catchability is often estimated internally in a stock assessment model, direct empirical estimates of catchability can also prove valuable in an assessment or for management purposes. Specifically, estimates of catchability can be used as a direct input into the assessment model, can serve as a diagnostic measure of model accuracy, or can contribute to an alternate means of providing catch advice when an assessment model is not considered acceptable.

The Northeast Fisheries Science Center (NEFSC) spring and fall bottom trawl survey has been utilizing a 4-seam 3-bridle trawl equipped with a rockhopper sweep since 2009, when a transition was made to a new survey net, tow protocol and survey vessel (*NOAA Ship Albatross IV* to *NOAA Ship Henry B. Bigelow*). Importantly, in the design of the new net and protocol, the goal was not to optimize the capture of any one species, but instead to provide consistent and representative samples that could allow for unbiased indices of abundance, size and age to be developed for a suite of many dozens of species. The choice of a rockhopper sweep, in particular, was designed to ensure consistency in the survey. This sweep allows the net to be towed over complex bottoms that could not be surveyed with a sweep that more closely tends the bottom, increasing the validity of survey indices for species that occupy regions with complex habitat. However, the tradeoff in using a rockhopper sweep, versus some alternatives, is that a higher proportion of fish are capable of passing underneath the net, potentially resulting in catchability values or gear efficiency values much less than 1.0. In order to develop accurate

empirical estimates of stock biomass it is thus necessary to determine species-specific catchability estimates of this specific survey gear.

Since 2009 the NEFSC has used a consistent towing protocol and bottom trawl across the whole sampling domain (see Politis et al. 2014 for full tow protocols). Specifically, the trawl is towed for 20 minute at 3.0 kts with an average wingspread of 13 m, resulting in approximately 0.24 km^2 swept per tow. However, direct measurements of net spread on the trawl survey indicate that the trawl tends to underspread in shallow waters and overspread in deep waters (Figure 4.1). This pattern is driven by differences in the amount of wire that must be put out across the wide depth range (20-400 m) of the survey, combined with the use of consistent gear, and in particular doors across the entire depth range. The variability in wingspread results in differences among tows in area swept. Additionally, fishermen who have worked with similar gear have raised concerns that changes in wingspread will affect catchability due to changes in gear geometry and potentially bottom contact.

One final issue in evaluating catchability and calculating biomass using trawl survey data is that there are two different measures of area swept per tow (Figure 4.2). Wingspread is the standard measure, as it encompasses the area swept by the portion of the net capable of catching fish. An alternative measure is doorspread, which is about 2.5 fold the width of wingspread on the *Bigelow* survey, and includes the area swept by the bridles. The rationale for using doorspread in some studies, is that fish may swim perpendicular to the bridles once disturbed, and enter into the area in front of the mouth of the net where they are eventually caught. This process is termed herding and has been documented for some species with some gear configurations and typically under daylight conditions (Somerton 2001; Somerton et al. 2007; Ryer 2008; Ryer et al 2010).

For red hake there are four sources of information that can inform estimates of catchability and the calculation of population abundance or biomass using NEFSC trawl survey data.

1) **Industry conversations and insights:** These can inform red hake catchability with different types of commercial gear and thus provide insights into the behavior of red hake in response to gear.

2) **HabCam estimates of population density and behavior**: HabCam is a camera system that forms the basis of a survey for sea scallops (Figure 4.3). Comparison of red hake population estimates between HabCam and the trawl survey can inform catchability, under the assumption that HabCam is 100% efficient (i.e. fish do not evade HabCam).

3) **Twin trawl sweep efficiency study:** A 2017 study comparing the catch rate of red hake using a chain sweep that strongly tends the bottom versus a standard rockhopper sweep used on the trawl survey.

4) **Twin trawl net spread study:** A 2019 study that compared catch rates between a standard survey net at an optimal spread (13 m) versus overspread and underspread conditions.

We evaluated each of these sources of information separately and then provide an integrated evaluation of red hake catchability on the NEFSC trawl survey.

Industry Conversations

Fishermen were contacted to discuss red hake based on their membership on the small mesh advisory panel, statements of interest about red hake at NEFSC Cooperative Research Branch meetings with industry, or due to their participation in the catchability studies. In total conversations were held with six fishermen, all of which have actively targeted whiting (silver hake) during a portion of their career and have thus also caught red hake. The insights provided by these fishermen were consistent with respect to the differences between silver hake and red

hake in terms of behavior relative to bottom trawl gear. Specifically, relative to silver hake, fishermen indicated that red hake had a tendency to pass under commercial gear in much higher numbers. A number of observations supported this conclusion. Red hake were found to gill in the bottom panel of a trawl gear in both directions, indicating that some went into the net and some went under the net and subsequently gilled in the mesh. Additionally, the use of a raised footrope trawl, versus other sweeps, reduces the catch of red hake but can maintain the catch of silver hake. Similarly, on Georges Bank, it was stated that there was a switch to using wide mesh nets (5 ft panels, reducing to 32 inch mesh, to 8cm mesh to 6 cm mesh) over the past decade. These sorts of nets will tend to capture silver hake and squid while shedding bottom tending species such as red hake and flatfish. The latter tend to dive to the bottom and out of the net while the former drop back into the cod end. This switch in net allowed for cleaner catches and thus less time sorting the catch, as well as reduced fuel use versus fishable area for the target species.

Questions were also asked about the tendency of red hake to herd. Some fishermen did not express an opinion on this issue due to the lack of targeting of red hake. Others indicated that herding occurs in silver hake, but does not happen with red hake. The relative catch rates of the two species when different gears were used (e.g. the big mesh nets) was provided as support for this observation.

Overall, the consensus was that red hake tend to group with flatfish in terms of their responses to gear and differ substantially from silver hake. Specifically, red hake have a tendency to pass under the gear, which can be used to reduce their catch while maintaining silver hake catch.

Habcam Studies

HabCam system and scallop survey

HabCam (Habitat mapping camera system) is a towed camera system that has been used on the annual NEFSC scallop survey since 2012 (Figure 4.3). Full details of the camera system and associated environmental monitoring systems are provided in NEFSC (2018). Briefly, the

camera takes high frequency (around 6/s) images of the sea floor from approximately 2 m above the ocean bottom while being towed at a speed of 5-7 m/s. Images are sent to the surface and stored on a hard drive.

The HabCam scallop survey occurs in May-July and covers the areas of the northeast U.S continental shelf from the Mid Atlantic Bight to Georges Bank that typically have had notable abundances of scallops (Figures 4.4 and 4.5). The focal depths of the survey are between 40-110 m and thus some areas that may contain red hake are excluded from sampling.

Due to the large number of images collected per survey only a subset (2% or 100,000) can be analyzed, in general, and of these, only a subset have been analyzed with the expertise necessary to identify red hake (vs round fish). The HabCam red hake work thus focused on a survey from a single year, 2015, with good coverage of the survey area in terms of analyzed images. This survey contained 110,931 manually annotated images, 3,540 which contained roundfish that were subsequently reannotated to species by an expert annotator. Notably, red hake can generally be readily differentiated from spotted hake based on the spots on spotted hake. However in some images the orientation of the fish obscures the spots, leading to some ambiguous identifications of *Urophycis* species.

Catchability estimates from HabCam

Unlike for some other species (e.g. yellowtail flounder; Shank and Duquette 2014) there was no evidence of evasion or reactions by red hake to HabCam. The assumption of the analysis is thus that the images of red hake provide an accurate measure of fish abundance (i.e. catchability equals 1). Estimates of red hake abundance in the HabCam images were expanded to an estimated population number across the survey. These HabCam estimates were then compared to the minimum swept area abundances estimates for that area from the 2015 trawl and dredge surveys in order to obtain estimates of catchability.

HabCam tow lines, dredge stations, trawl stations and red hake abundances on each are shown for the Mid Atlantic (Figure 4.4) and Georges Bank (Figure 4.5). HabCam based estimates of the number of red hake were 262 million for the Georges Bank survey area and 196 million for the Mid Atlantic survey area. Table 4.1 shows the matching estimates for the fall and spring trawl survey under the assumption that wing spread and door spread measure the area

fished by a trawl. The swept area numbers of the scallop dredge are also shown. The trawl survey was estimated to have an efficiency of 0.15 for the fall on Georges Bank, with lower values for the spring. The lower spring efficiency values are likely an underestimate, as fish may migrate into the HabCam survey area between the spring trawl survey and summer HabCam survey. The Mid-Atlantic efficiency values were also lower for the fall and spring than the fall Georges Bank values. One concern is that spotted hake are being misidentified as red hake in the HabCam images, as the spots of spotted hake may be obscured. This would inflate the Mid Atlantic population estimate of red hake and reduce the catchability estimate of the trawl gear. When the red hake-spotted hake complex imaged on HabCam was reapportioned to match the ratio on the trawl survey (45% spotted to 55% red hake), the HabCam red hake population estimate was reduced from 196 million fish to 128 million fish, and the trawl survey efficiency value was increased to 0.14, a value similar to that estimated on Georges Bank.

Overall, the analysis of HabCam data demonstrated that it can be used to provide an estimate of finfish abundance, with much different processes affecting the detectability of fish relative to towed gear. The comparison of HabCam to the trawl survey in 2015 suggested a red hake catchability value of around 0.14-0.15 for the number of fish. A catchability value to apply to biomass or by length was not estimated. Future work focused on annotating more years of images, and developing automated annotation routines should allow for the estimate of catchability to be continually refined. The conclusion of the working group was that the HabCam work provided an important context for evaluating trawl survey catchability and red hake behavior and should continue to be pursued.

Twin Trawl Sweep Efficiency Study

Paired-gear studies have long been used to estimate the efficiency of one fishing gear relative to another (e.g., Gulland 1964; Bourne 1965). These types of studies are critical for informing abundance time series from fishery-independent surveys when there are changes in the vessel and (or) gears over time due to gear failures or improved technology.

In conducting paired-gear studies, it is ideal to have the two gears deployed as close together spatially and temporally as possible to reduce variation between the gears in densities of the species being captured. One fishing method that approaches this ideal is the twin-trawl

rigging where two trawls can be fished simultaneously from a single vessel (ICES 1996). The basic methods we used here are the same as those used by Miller (2013) to estimate size effects on relative catch efficiency of the *Bigelow* to the *Albatross IV* and to make similar estimates for groundfish, TRAC stocks and summer flounder (Miller et al. 2017a,b).

Sweep efficiency study design

Data were collected during three field experiments carried out in 2015, 2016, and 2017, respectively, aboard the *F/V Karen Elizabeth*, a 78 ft stern trawler capable of towing two trawls simultaneously side-by-side. However, red hake were only counted and measured during the 2017 field experiments. One side of the twin-trawl rig towed a NEFSC standard 400 x 12 cm survey bottom trawl rigged with the NEFSC standard rockhopper sweep (Politis et al. 2014) (Figure 4.6). The other side of the twin-trawl rig towed a version of the NEFSC 400 x 12 cm survey bottom trawl modified to maximize the capture of flatfish. The trawl was modified by reducing the headline floatation from 66 to 32, 20 cm, spherical floats, reducing the port and starboard top wing-end extensions by 50 cm each and utilizing a chain sweep. The chainsweep was constructed of 1.6 cm (5/8in) trawl chain covered by 12.7cm diameter x 1 cm thick rubber discs on every other chain link (Figure 4.7, Figure 4.8). Two rows of 1.3 cm (½ inch) tickler chains were attached to the 1.6 cm trawl chain by 1.3 cm shackles (Figure 4.7). To ensure equivalent net geometry of each gear, 32 m restrictor ropes, made of 1.4cm (9/16 inch) buoyant, Polytron rope, were attached between each of the trawl doors and the center clump. 3.4 m^2 Thyboron Type 4 trawl doors were used to provide enough spreading force to ensure the restrictor ropes remained taut throughout each tow. Each trawl used the NEFSC standard 36.6 m bridles. All tows followed the NEFSC standard survey towing protocols of 20 minutes at 3.0 knots. A total of 103 (61 day, 42 night) paired tows were conducted in waters off of southern New England and in the Gulf of Maine (Figure 4.9). Paired tows were denoted as “day" and “night" by whether the sun was above or below the horizon at the time of the tow.

Red hake were caught in 73 paired tows (40 day, 33 night). Overall 12,585 red hake were measured for length. The subsampling fractions implied an estimated 47,275 red hake were captured across all paired tows. A total of 8,587 and 3,998 length measurements were made for the chainsweep and rockhopper gears, respectively. During the day, 4,908 and 1,706 red hake were measured in catches by the respective gears whereas during the night 3,679 and 2,292 were measured in catches by the respective gears.

Paired Tow Analysis

We use the hierarchical modeling approach from Miller (2013) to estimate the relative efficiency of chain sweep to the rockhopper sweep used by the NEFSC bottom trawl survey. As in Miller (2013), we compared a set of models with different assumptions about variation of relative efficiency between paired gear tows, size effects on the relative efficiency, and extra-binomial variation of observations within paired gear tows. We began with the same 13 models considered by Miller (2013), and then included diel effects on relative catch efficiency and interactions with size effects with the best performing model of the original 13 models. Table 4.2 provides a description of the fitted models and pseudo-formulas comparable to those used for fitting models in R and the mgcv package (R Core Team 2019; Wood 2006). The analyses are analogous to those by Miller et al. (2017a,b, 2018), but here we have generalized the model fitting software to fit multiple smooth effects on relative catch efficiency so that models do not have to be fit separately to observations occurring during the day and night. Therefore when diel effects are considered, many parameters can be allowed to be common to the day and night observations.

Length-weight analysis

We fit length-weight relationships to the length and weight observations for each survey each year. We assumed weight observation *j* from survey *i*, was log-normal distributed,

$$\log W_{ij} \sim N\left(\log \alpha_i + \beta_i \log L_{ij} - \frac{\sigma_i^2}{2}, \sigma_i^2\right) \quad (1)$$

We used a bias correction to ensure the expected weight $E(W_{ij}) = \alpha_i L_{ij}^{\beta_i}$.

We estimated parameters by maximizing the model likelihood programmed in TMB (Kristensen et al. 2016) and R (R Core Team 2019). Like the relative catch efficiency, bootstrap predictions of weight-at- length were made by sampling with replacement the length-weight observations within each annual survey and refitting the length-weight relationship to each of the bootstrap datasets.

Biomass estimates

We estimated biomass for each annual survey in terms of chainsweep efficiency by scaling the survey tow observations by the relative efficiency of the chainsweep and rockhopper sweep gears. First, the tow-specific catches

First, the tow-specific catches at length were rescaled,

$$\tilde{N}_{hi}(L) = N_{hi}(L)\hat{\rho}_i(L) \quad (2)$$

where N_{hi} is the number at length L in tow i from stratum n tow i from stratum h and $\hat{\rho}_i(L)$ is the relative efficiency of the chain sweep to rockhopper sweep at length L estimated from the twin trawl observations, that may depend on the diel characteristic of tow i if that factor is in the best model fitted to the twin-trawl observations. Note that we have omitted any subscripts denoting the year or survey.

The stratified abundance estimate is then calculated using the design-based estimator,

$$\hat{N}(L) = \sum_{h=1}^{H} \frac{A_h}{An_h} \sum_{i=1}^{n_h} \tilde{N}_{hi}(L) \quad (3)$$

where A_h is the area of stratum h, and n_h is the number of tows that were made in stratum h. The corresponding biomass estimate is then:

$$\hat{B} = \sum_{l=1}^{n_L} \hat{N}(L = l)\hat{w}(L = l) \quad (4)$$

where $\hat{w}$ is the estimated weight at length from fitting length-weight observations described above. Length is typically measured to the nearest cm so n_L indicates the number of 1 cm length categories that were observed during the survey.

To estimate uncertainty in biomass, we used bootstrap results for the relative catch efficiency and weight-at-length estimates along with bootstrap samples of the survey data. Bootstrap data sets for each of the annual surveys respected the stratified random designs by resampling with replacement within each stratum (Smith 1997). For each of the 1000 combined bootstraps, survey observations for bootstrap b were scaled with the corresponding bootstrap

estimates of relative cookie sweep to rockhopper sweep efficiency and predicted weight-at-length, using Eqs. 3 and 4.

Sweep efficiency results and discussion

As measured by AIC, the best performing model before considering day/night effects was the conditional beta-binomial model BB_6 (Table 4.2). The best beta-binomial model had an AIC more than 13 units lower than the best binomial model. Allowing variation in smooth size-effects on relative catch efficiency among paired-tows and extra-binomial variation within paired-tows (overdispersion via the beta-binomial assumption) provided primary improvements in model performance. Including diel effects on relative efficiency for the twin-trawl observations improved performance of the beta-binomial model. Initially separate smooth size effects for day and night tows were considered for the beta-binomial model (BB_8), but the correlation of non-smoother related random effects across stations was not estimable. Those random effects were therefore assumed uncorrelated (BB_9). Allowing different smooth size effects of relative efficiency for day and night observations was considered (BB_{10}), but it did not improve model performance. The relative efficiency of the chain sweep gear to the rockhopper sweep gear generally declines with increased size whether the tow occurred during day or night, but the increase in efficiency of the chainsweep was generally greater for tows occurring during the day (Figure 4.9).

Stock-specific trends in annual biomass estimates from 2009 to 2019 for the NEFSC spring and fall survey were generally the same. For northern red hake both the spring and fall biomass estimates increased in 2014 and have remained higher than previous years (Figure 4.11 and Table 4.3). The scale of the biomass estimates is also similar for the spring and fall surveys. For southern red hake, the spring biomass generally declined until 2017 and then has increased for the last two years whereas the fall biomass has remained relatively stable (Figure 4.10 and Table 4.3).

The efficiency of the rockhopper gear relative to the chainsweep in terms of biomass changes from year to year due primarily to corresponding changes in the estimated numbers at length (Table 4.4). Annual biomass relative efficiency for northern red hake varied between 0.19 and 0.25 in the spring and 0.21 and 0.33 in the fall. Values range between 0.15 and 0.26 for the spring and 0.19 and 0.39 in the fall for southern red hake.

Because the length-weight relationship, which is used with the numbers at length to

estimate biomass, is estimated by survey and year there is a possibility that poor sampling in a given year could adversely affect the biomass estimates. We therefore calculated the ratios of the annual uncalibrated biomass estimates using just the aggregate catch data to the biomass estimates made using the numbers at length and estimated weight at length (i.e., Eqs. 3 and 4 without the relative efficiency-at -size). These ratios should be approximately 1. The ratios for all years and seasons for both northern and southern red hake varied from 0.96 to 1.04 (Table 4.5).

Twin Trawl Wingspred Study

The net fished by the NOAA Ship *Henry B. Bigelow* during the Northeast Fisheries Science Center (NEFSC) bottom trawl survey tends to exhibit increased wingspread width, and thus area swept, as the depth the net is fished at increases (Figure 4.1). Observations by fishermen of their own gear has led to questions and speculation about how departures from optimal wing spread alter the physical dynamics at play in the survey net as it is fished, potentially leading to decreases in net efficiency at different depths. To address this issue, an experiment was planned and implemented under the guidance of the Northeast Trawl Advisory Panel (NTAP). Here we describe the results of this experiment for a single species: red hake (*Urophycis chuss*). Several Northeast Trawl Advisory Panel members expected a roughly unimodal relationship of catch efficiency with wingspread (Figure 4.12), and we treat that as our working hypothesis when analyzing the experimental results.

Experimental Design

The F/V *Karen Elizabeth*, captained by Chris Roebuck, was chartered for 14 sea days. The vessel towed two nets in a twin-trawl rig: the control net maintained a constant target opening similar to the *Bigelow* target net spread of 13 m, while the other tested a range of openings seen in *Bigelow* operations (9-16 m). The targeted wingspread of each net was achieved using restrictor cables, and monitored throughout each experimental tow with mensuration systems attached the wings of each net.

The first cruise leg covered shallow depths off of southern New England, targeting windowpane and winter flounder, as well as deep stations in the Gulf of Maine, targeting witch flounder and American plaice. Based on data from that leg, the second leg targeted shallow water to better capture more windowpane flounder and winter flounder. The fishing gear used

for this experiment mimicked the net on the *Bigelow* (both trawl net and sweep), with some subtle changes to accommodate the twin trawl configuration. Specifically, trawl doors were larger than the NEFSC standard survey doors, a clump weight was used between nets, and warp to depth ratios were more consistent with industry standards. These changes helped to consistently achieve the target net spreads.

The field experiment completed paired tows at 170 stations (Figure 4.15) using standard tow protocols and with catch processing and subsampling followed NEFSC survey protocols. During the data quality control process, special attention was paid to the net mensuration data for each set of paired tows. Tows that were marked as non-representative by field scientists were excluded from further analyses (e.g., a station where the nets crossed one another). Net mensuration data was trimmed slightly and a mean width for each net was calculated (Figure 4.16). Stations where the control net width varied too greatly (+- 0.5) from the 13 m target were also excluded from further analyses. The mean achieved spreads of the treatment net were used for further analysis.

Analysis

Two distinct analyses were conducted. First, an exploratory weight-based analysis of the catch rates for all species were compared. Second, a more thorough length-based analysis was conducted for red hake.

The exploratory analysis calculated the summed weight (kg) of red hake and other species caught at each station for each net (control and treatment). A percent difference was then computed between the summed weights to estimate the discrepancies in catch. Next, catch per swept area (kg/m^2) was calculated for each net. The influence of net wingspread on the red hake catch and catch efficiency was evaluated by plotting the percent difference as a function of net width. A basic generalized additive model was applied to help visualize the pattern in the relationship between wingspread and total catch (kg/tow) and catch efficiency (kg/m^2).

For the length-based analysis, a set of statistical models were fit to the numbers of red hake caught and measured for length in each net at each station data. These hierarchical-generalized additive models were similar to those fit in Miller (2013) for estimating relative efficiency of the *Albatross IV* and *Bigelow* and for estimating the efficiency of the rockhopper gear used by the *Bigelow* (see above). The fitted models assumed random variation in and size

effects on relative efficiency between the control and treatment. Model fits were then compared using AIC values (Akaike 1974). Effects of wingspread and day/night on the average relative efficiency across pairs were then added to the best models. All models accounted for subsampling for length measurements and differences in swept area between each paired tow. We assumed that the control wingspread was 13 m and used the wingspread of the treatment measured using gear mensuration data rather than targeted treatment wingspread.

Wingspread study results and conclusions

Approximately 4,800 kg of red hake in total were caught in both nets for the stations that were included in the analyses (Table 4.6). On average 7.75 stations were successfully sampled with each treatment net width (Table 4.7). The exploratory analyses suggest that the effect of wingspread on catch is subtle and that swept area may have a larger effect on catch rates of red hake (Figure 4.16). Specifically, there appears to be a slight positive relationship between wingspread and red hake catch prior to correcting weight totals to account for differences in swept area. Once swept area conversions had been applied there was limited evidence for a relationship between wingspread and the red hake catch measured in weight-per-tow.

Results from model comparisons in the length-based analysis suggest that models that included wingspread (models number four and ten) did not provide the best fit to the data (Table 4.8). Instead, models that included only smooth size effects, and potentially day/night effects (models 9 and 11), were the best performing. Based on these comparisons our findings are that there was a non-significant effect of the net wingspread on catches in the control and treatment nets (Figure 4.17). Finally, plotting out the mean number of individuals at each length for experimental net wingspread we also see limited evidence of a difference in the catch efficiency at different net widths (Figure 4.18).

This study and analysis indicates no evidence for reduced catch efficiency for red hake when wingspread departs from optimal conditions. Future work to standardize the *Bigelow* survey data by incorporating the measured area swept at each station may be warranted. Preliminary work suggests that this will have a minimal effect on trends for red hake and a limited effect (<10%) on scale.

Catchability Summary

The working group reached five consensus conclusions regarding the catchability of red

hake. First, the design of the sweep efficiency study was determined to be appropriate for providing an estimate of the maximum catchability of red hake. This study design had previously only been evaluated in flatfish assessments (NEFSC 2017), but based on the available information on red hake behavior from commercial fishermen, the study samples sizes and data, and HabCam images documenting red hake behavior, it was determined that the sampling results could be applied to red hake. Second, the analysis of relative catch efficiency was determined to be appropriate for estimating a maximum catchability of red hake and a minimum biomass; variations of this methodology has been through numerous peer reviews (Miller 2013, Miller et al. 2017a, 2017b, 2018). Third, the use of area swept by the wings should be used in calculating the swept area biomass. This conclusion recognized the low likelihood of herding by by red hake with this gear, similar to the conclusions drawn for flatfish in previous applications of these studies. Fourth, the group agreed that the HabCam survey provided an important additional piece of information in assessing catchability of the trawl survey, but that the data currently available does not allow for this study to be used as the primary source of catchability information. The work group was reassured that the HabCam estimate of catchability (0.14-0.15 for number per tow) was similar to the chain sweep estimate of catchability (≈0.23 for biomass per tow). It was noted that due to the increasing catchability with size of the rockhopper gear the higher catchability value for biomass per tow makes sense. Fifth, the working group also agreed that the data to date did not provide any evidence that the efficiency of the gear for red hake declined at wider or narrower net width. However, the group did recommend that future calculations of swept area biomass should explore directly accounting for measured wingspread rather than applying the average wingspread to all tows.

TOR5: Apply the existing assessment model framework to the stock structure based on TOR 3 and 4 to ensure its utility in subsequent management track assessments. Evaluate existing reference points.

The working group failed to reject the null hypothesis that red hake on the northeast U.S. continental shelf are comprised of two stocks, and thus maintained the status quo stock structure for future assessments. The AIM models that had previously been applied to each stock of red hake were thus updated to evaluate significance levels and reference points (Tables 2.7, 2.8 Figures 2.41, 2.42).

Full details of the AIM approach are available in Anon. (2002). The application of AIM to red hake, and the decision to use the spring index and the shortened time series since 1980 is detailed in NEFSC (2011). Briefly, AIM (An Index Method) fits a linear regression to the relationship between the natural-log of relative fishing mortality (RelF) as measured by Catch/Index and the natural log of the replacement ratio (change in index). The method tests whether fishing mortalities drive trends in the stock and calculates a relative fishing mortality that allows the stock to replace itself (i.e. RelF at replacement ratio=1). Importantly, this approach cannot use a standard test of significance. As stated in the report: "*The relation between Q_t and $relF_t$ is of the general form of Y/X vs X where X and Y are random variables. The expected correlation between Y/X and X is less than zero and is the basis for the oft stated criticism of spurious correlation."* (Anon 2002) Because of this concern about spurious correlations, a randomization test was developed to evaluate the significance of the model. This test involved generating new time series of catch and index values by sampling the available values with replacement. For each randomization the correlation statistic is then calculated and compared to the model correlation statistic from the true time series. The frequency with which the true correlation statistic exceeds the resampled correlation statistics is provided as a measure of significance.

The AIM model run for the southern stock of red hake was not significant (p=0.457) and the relative F for a replacement ratio of 1, which is used to guide catch levels, was estimated at 177 mt/ kg tow^{-1} in *Bigelow* survey index units (previous assessments used the *Albatross IV* index units). The conversion of kg tow^{-1} to metric tons followed the standard approach and the average catchability value across years (TOR4) for the spring survey:

$$B = I\frac{A}{qa} = 1\frac{128{,}230}{0.21 * 0.024} = 25{,}442\ mt$$

The updates AIM model thus indicates that an exploitation rate of 177/25,422 mt, or 0.7% results in a replacement ratio of 1 (population stability). The combination of the lack of significance of the model and the very low exploitation rate were considered and the working group determined this approach should not be used in subsequent management track assessments of the southern stock.

The AIM model run for the northern stock of red hake was also not significant (p=0.127) and the relative F for a replacement ratio of 1, which is used to guide catch levels, was estimated at 49 mt/ kg tow^{-1} in the *Bigelow* survey index units (previous assessments used the *Albatross* index unit). The conversion of kg tow^{-1} to metric tons followed the standard approach and the average catchability value across years for the spring survey:

$$B = I\frac{A}{qa} = 1\frac{81{,}397}{0.20 * 0.024} = 16{,}957\ mt$$

The updates AIM model thus indicates that an exploitation rate of 49/16,957 mt, or 0.2%, results in a replacement ratio of 1. The combination of the lack of significance of the model and the very low exploitation rate were considered. As with the southern stock, the working group determined this approach should not be used in subsequent management track assessments.

The recommendation to not use the AIM model in future assessments created the need to develop an alternate means of providing catch advice and reference points. Unlike in previous assessments of red hake, the working group was able to make use of a well-designed experiment that generated estimates of length-specific catchability on the NEFSC survey. The working group reached a consensus that the results of this catchability study should be directly incorporated into the assessment.

An assessment for both the northern and southern stocks of red hake is presented in Appendix 4 (Miller TJ, "*An empirical approach to assessing northern and southern red hake*"). The working group reached a consensus that this paper and the analyses were technically sound, and that they provided the best approach available for assessing both stocks of red hake. The working group also noted that there was a precedence for utilizing this technique in past analyses of butterfish (Miller and Rago 2012; Miller et al. 2013) and scallops (Applegate et al. 1998). The full details of the approach are available in the Appendix; a brief summary is presented below.

The empirical approach to assessing red hake used bottom trawl survey data, weight-at-length data and estimates of catchability-at-length, to develop estimates of recruitment, exploitable biomass and spawning stock biomass for the 2009-2019 period (i.e. the *Bigelow* time series). Calculations of numbers of recruits used a length cut off of 19 cm and utilized the spring survey data. Age-length keys for the spring were used to determine this length cutoff. Exploitable biomass also used the 19 cm recruitment cutoff. Fish <19cm were considered to have a selectivity of 0 in the fishery consistent with length frequency distributions of fish sampled from the fishery. Spawning stock biomass was calculated using both the fall and spring survey data, with length cutoffs of 23 cm for the southern stock and 24 cm for the northern stock. Maturity data collected during the trawl survey informed these length cutoffs.

Annual fishing mortality rates were calculated using the catch data for a given year and an assumed natural mortality (M) rate of 0.4 (CV=0.3). The candidate reference points were F_{40} and SSB_{40}, or the equilibrium fishing mortality rates associated with a 40% spawning potential ratio. The candidate reference points are consistent with many other assessments in the northeast United States (NEFSC 2019). Two possibilities were considered in calculating F_{40} and SSB_{40}. The first was to use the entire time series of growth and maturity data and the second was to use only the values from the recent decade, during which red hake growth have reached shorter asymptotic lengths-at-age. While reference points using both approaches were calculated, the working group recommends the use of the recent period of growth.

For the northern stock of red hake fishing mortality since 2009 has been very low (0.001-0.004) relative to the F_{40} value of 0.247. Spawning stock biomass has ranged from about 75,000 mt to 273,000 mt which is above SSB_{40} of 46,581 mt. The northern stock is thus

estimated to not be overfished with overfishing not occuring.

For the southern stock of red hake fishing mortality since 2009 has been higher than the northern stock (0.02-0.05) but still low relative to the F_{40} value of 0.333. Spawning stock biomass has ranged from about 35,000 mt to 93,000 mt which is above the SSB_{40} of 12,020 mt. The southern stock is also estimated to not be overfished with overfishing not occuring.

One focal point of discussion of these results concerns the use of only the 2009-2018 recruitment values from the survey in developing the SSB_{40} reference points. The 2009-2018 time series is based on the duration of the survey on the *Bigelow*. Use of this time series eliminates the need to incorporate the results of the *Albatross* to *Bigelow* calibration at short lengths, which would introduce substantial levels of uncertainty. For the northern stock of red hake there is consistent evidence that the stock has been near time series highs of biomass and has experienced negligible rates of exploitation over the past decades. The status of not overfished for this stock matched all data available for this stock. On the other hand southern red hake are at lower biomass levels than historically, though recent fishing mortality has also been well below F_{40}. If it was possible to use a longer time series of recruitment, SSB_{40} would possibly be higher, which in turn might change the not overfished status. Notably, the use of truncated time series of recruitment in determining reference points and running projections has been a topic of discussion in general in other assessments. Specifically, the assessment of the southern New England stock of yellowtail flounder uses a truncated time series to address the decline in recruitment that coincided with warming water temperatures (NEFSC 2019). Overall the working group considered expanding the time series of recruitment to be worth evaluating in the future, but also strongly endorsed the approach detailed in Appendix 4.

TOR6: Identify gaps in the existing research with respect to red hake stock structure. Develop a prioritized list of research recommendations to address these gaps. Comment on the feasibility and time horizon of the proposed research recommendations.

Research recommendations developed by the working group were both specific to the topic of red hake stock structure and more general on the topics of stock structure for northeast fish and the utilization of catchability data. We will focus on these separately

Red hake specific research recommendations:

1) Implement a population genetics study on red hake. (**Priority:** High; **Cost estimate-** $120,000**) —**A population genetics study was considered a high priority with the cost estimate based on running 500 fish (5 regions X 100 individual/region). Temporal stability in genetic signatures was considered important. Larval red hake were also noted as being available across many areas and potentially useful for such a study, due to their link to specific spawning grounds. Due to the importance of this research recommendation a more thorough description was developed and is presented below.

2) Analysis of natural tags to evaluate the hypothesis that red hake move from the Gulf of Maine (northern stock area) to Georges Bank (southern stock area) to spawn. **(Priority-**High**; Cost-**$5,000-$20,000**)—** If this movement pattern is in fact occurring, the characteristics of red hake caught during the spawning season on Georges Bank should match those of Gulf of Maine fish during the non-spawning season or be a mixture of non-spawning season Gulf of Maine and Georges Bank characteristics. An updated meristics study or length at age analysis were discussed as a potential cost-effective option for implementing this sort of study.

3) Otolith microchemistry study **(Priority:** medium**) —**Otolith microchemistry work can provide important information on lifetime movements not available through other means. While specific numbers of samples and costs were not estimated, it was noted that this is an expensive and time-intensive option to apply.

4) Tagging study (Considered not practical)—A tagging study on red hake was determined to not be practical. A number of factors led to this decision, including that fishing mortality in the

red hake fishery is estimated to be low and a notable proportion of fish are discarded. These factors suggest low recapture and return rates.

***5) Continue aging of red hake samples*—(Priority:** high**) —**Aging of red hake since the 2010 assessment provided important insights including the decline in growth in all regions. Continuing this work and adding archived samples is important and would contribute to the ability to pursue an age-structured assessment.

***6) Explore an age structured assessment for red hake*—(Priority:** medium**) —**This recommendation is carried over from the last assessment. The work is feasible, but does require a notable investment of time by the stock assessment scientist.

7) Further document Fishermen's Ecological Knowledge for red hake **(Priority:** medium As a non-target species FEK on red hake is not as well-developed as it is with other higher value species. However, the limited effort to document this information for this assessment still proved valuable.

<u>General recommendations (All considered High Priority)</u>

1) ***Index based stock assessment methods that incorporate catchability estimates should continue to be developed and tested*** **(**Priority: High**)—**As noted in TOR5, work directly utilizing the catchability estimates in developing reference points was considered a notable step forward from the previous AIM model. Further work exploring and refining these approaches should be pursued for red hake and other species. It was noted that this sort of work will be considered at the Index Based Working Group scheduled for the fall of 2020.

2) ***The Northeast Fisheries Science Center should develop prioritized lists of species that A) are due for an updated review and evaluation of stock structure, and B) should be the focus of new research using approaches pertinent to evaluating stock structure.*** There are a number of species with information developed in recent years that is pertinent to the evaluation of stock structure. For these species a comprehensive review of stock structure may be warranted. Additionally, there are species that have notable uncertainty in stock structure that should be the target of additional studies using new techniques. Currently, there is not a prioritized list of species for these two topics that can form the basis of determining which species are scheduled

for future reviews and which should be the focus of future research. Prioritized lists may lead to the more efficient use of limited resources.

3) ***Maintain ichthyoplankton monitoring*** **(**Priority: High**) —**Failures to obtain full spatial coverage during the recent EcoMon plankton surveys in August contributed to the uncertainty in discussions of potential recent shifts in spawning activity. Returning the EcoMon sampling to a full set of sea day would address this issue for red hake and other species.

Further description of the research recommendation on population genetics

One major deficiency in the investigations to date of the stock structure of red hake is the absence of any studies examining its genetic population structure. Unlike the other analyses included in this report, population genetics studies can definitively determine if separate reproductively isolated units exist within a species' distribution, the number of such units, and potentially their geographic boundaries. For these genetic units to form and persist requires a high degree of integrity within units and an almost total absence of migration between them.

Populations of marine fishes, such as red hake, had long been viewed as being highly connected demographically because of vagile pelagic egg and larval stages, extended duration of these early life-stages, and high adult migratory potential; however, recent empirical genetic evidence suggests that may not always be the case. With increasingly sensitive genetic techniques and the ability to process larger numbers of specimens, the opportunity to detect significant genetic population structure in marine fishes has increased in recent times. Rather than being demographically open, marine fishes often exhibit significant stock structure on fine geographic and temporal scales due to processes that limit dispersal and promote self-replenishment of local populations and that promote spawning site fidelity, egg and larval retention at those sites, and local adaptation. Not only have molecular techniques revealed greater levels of heterogeneity of genetic structure in marine fishes than previously thought, concomitant variation in ecologically important traits sometimes indicate the presence of extensive adaptive differentiation. This may be especially true for marine groundfish species such as red hake. For example, it has been known for a while that Atlantic cod in U.S. waters

exhibit significant genetic population structure, but it was very recently demonstrated that genetic structure in cod was in large part due to variation at loci under significant natural selection

Molecular techniques at the DNA level that can be used to investigate for genetic population structure in fishes have evolved over time from restriction fragment length polymorphism (RLFP) or sequencing of mitochondrial DNA (mtDNA), through analysis of variable copy numbers of short tandem-repeated nucleotide motifs (microsatellites), to single nucleotide polymorphism analysis (SNPs). Analysis has shifted from the use of "genetic" approaches that examine only a limited number of genetic markers (10s-100s) to "genomic" approaches that screen much of the genome and analyze >1000s of marker loci. The shift from "genetic" to "genomic" approaches also witnessed the evolution of analysis from selectively neutral loci to use of "genomic" approaches that screen much of the genome for informative markers whose allelic frequencies are controlled by temperature driven adaptive divergence.

Thus, a high priority recommendation of this committee is the application of a modern DNA-based genetics investigation of red hake population structure focusing on a total of 5 collection sites within the two putative stocks supported by this report and including 2-3 locales within each the geographic bounds of each of the two stocks.

REFERENCES

Akaike H, 1974. A new look at the statistical model identification. In Selected Papers of Hirotugu Akaike (pp. 215-222). Springer, New York, NY.

Almeida FP, Anderson ED. 1981. Status of the red hake resource off the northeast coast of the United States – 1981. Northeast Fisheries Center, Woods Hole Lab. Ref. Doc. 81-37.

Anderson ED. 1974a. Assessment of red hake in ICNAF Subarea 5 and Statistical Area 6. ICNAF Res. Doc. 74/19.

Anderson ED. 1974b. Comments on the delineation of red and silver hake stocks in ICNAF Subarea 5 and Statistical Area 6. ICNAF Res. Doc. 74/100.

Anderson ED, Ed. 1984. Status of the fishery resources off the northeastern United States for 1983. NOAA Tech. Mem. NMFS-F/NEC-29.

Anderson ED. 1998. The history of fisheries management and scientific advice – the ICNAF/NAFO history from the end of World War II to the present. J. Northw. Atl. Fish. Sci., 23: 75–94.

Anon (Working group on re-evaluation of biological reference points for New England groundfish). 2002. Re-evaluation of biological reference points for New England groundfish. Northeast Fish. Sci. Cent. Ref. Doc. 02-04; 395 p.

Applegate A, Cadrin S, Hoenig J, Moore C, Murawski S, Pikitch E. 1998. Evaluation of existing overfishing definitions and recommendations for new overfishing definitions to comply with the Sustainable Fisheries Act. Final Report of the Overfishing Definition Review Panelto the New England Fishery Management Council,Newburyport, Massachusetts.

Ashford JR, Jones CM, Hofmann EE, Everson I, Duhamel G, Moreno C, Williams R. 2005. Can otolith elemental signatures record the capture site of a fully marine fish, *Dissostichus eleginoides*, in the Southern Ocean? Can. J. Fish. Aquat. Sci. **62**(12): 2832-2840.

Ashford JR, Arkhipkin AI, Jones CM. 2007. Otolith chemistry reflects frontal systems in the Antarctic Circumpolar Current. Mar. Ecol. Prog. Ser. **351**: 249-260.

Ashford JR, La Mesa M, Fach BA, Jones C, Everson I. 2010. Testing early life connectivity using otolith chemistry and particle-tracking simulations. Can. J. Fish. Aquat. Sci. **67**: 1303-1315.

Ashford JR, Serra R, Saavedra JC, Letelier J. 2011. Otolith chemistry indicates large-scale connectivity in Chilean jack mackerel (*Trachurus murphyi*), a highly mobile species in the southern Pacific Ocean. Fish. Res. **107**: 291-299.

Ashford JR, Dinniman M, Brooks C, Andrews AH, Hofmann E, Cailliet G, Jones CD, Ramanna, N. 2012*a*. Does large-scale ocean circulation structure life history connectivity in Antarctic toothfish (*Dissostichus mawsoni*)? Can. J. Fish. Aquat. Sci. **69**: 1903-1919.

Ashford JR, Fach BA, Arkhipkin AI, Jones CM. 2012*b*. Testing early life connectivity supplying a marine fishery around the Falkland Islands. Fish. Res. **121-122**: 144-152.

Azarovitz TR. 1981. A brief historical review of the Woods Hole Laboratory trawl survey time series. Can. Special Pub. Fish. Aquat. Sci. 58: 62-67.

Berrien PL, Sibunka JD. 2006. A laboratory guide to the identification of marine fish eggs collected on the northeast coast of the United States, 1977-1994. U.S. Dept. Comm., Northeast Fish. Sci. Cent. Ref. Doc. 06-21, Woods Hole, MA.

Bigelow HB, Schroeder WC. 1953. Fishes of the Gulf of Maine. Fish. Bul. 53.

Booke HE. 1981. The conundrum of the stock concept—Are nature and nurture definable in fishery science? Can. J. Fish. Aquat. Sci. 38: 1479–1480.

Bourne N. 1965. A comparison of catches by 3- and 4-inch rings on offshore scallop drags. J. Fish. Res. Board Can. 22(2): 313-333.

Brown BE. 1974. Species mixture in the boundary areas between 5ZE and 5ZW. ICNAF Res. Doc. 74/101.

Brown SK, Mahon R, O'Boyle R, Zwanenburg K, Buja K, Claflin L, Atkinson B, Howell G, Sinclair M, Monaco M. 1996. East coast of North America groundfish: initial explorations of biogeography and species assemblages. Silver Spring, MD: Strategic Environmental

Assessments Division, National Oceanic and Atmospheric Administration, and Dartmouth, NS: Marine Fish Division, Department of Fisheries and Oceans. 102 pp.

Burnett J, O'Brien L, Mayo RK, Darde JA, Bohan M. 1989. Finfish maturity sampling and classification schemes used during Northeast Fisheries Center bottom trawl surveys, 1963-1989. NOAA Technical Memorandum. NMFS-F/NEC 76

Cadrin SX, Kerr LA, Mariani S. (eds) 2014. Stock identification methods: Applications in Fishery Science-Second Edition. Elsevier, Amsterdam 589 pages

Campana SE. 1999. Chemistry and composition of fish otoliths: pathways, mechanisms, and applications. Mar. Ecol. Prog. Ser. **188**: 263-297.

Chen C, Liu H, Beardsley RC. 2003. An unstructured,finite-volume, three-dimensional, primitive equation ocean model: application to coastal ocean and estuaries. J. Atmos. Oceanic Technol. 20: 159–186.

Chen C, Beardsley RC, Cowles G. 2006. An unstructured grid, finite-volume coastal ocean model (FVCOM) system. Oceanogr. 19: 78–89.

Churchill, JH, Runge J, Chen C. 2011, Processes controlling retention of spring-spawned Atlantic cod (*Gadus morhua*) in the western Gulf of Maine and their relationship to an index of recruitment success. Fish. Oceanogr. 20:32-46

Cohen DM, Inada T, Iwamoto T, Scialabba N. 1990. FAO species catalogue. Vol. 10. Gadiform fishes of the world (Order Gadiformes). An annotated and illustrated catalogue of cods, hakes, grenadiers and other gadiform fishes known to date. FAO Fish. Synop. 125(10). Rome: FAO. 442 p.

Cope JM, Punt AE. 2009. Drawing the lines: resolving fishery management units with simple fisheries data. Can. J. Fish. Aquat. Sci. 66:1256-1273.

Derry DM. 1988. Red Hake. pp: 49-57 In: Penttila J, Dery LM (Eds) Age determination methods for Northwest Atlantic Species. NOAA Technical Report NMFS 72J.

Edwards RL, Lux FE. 1958. New England's industrial fishery. Commercial Fisheries Review. 20: 1-6.

Fahay MP, Able KW. 1989. White hake, *Urophycis tenuis*, in the Gulf of Maine: spawning seasonality, habitat use, and growth in young of the year and relationships to the Scotian Shelf population. Can. J. Zool. 67: 1715-1724.

Fahay MP. 2007. Early stages of fishes in the western North Atlantic Ocean (Davis Strait, Southern Greenland and Flemish Cap to Cape Hatteras). Dartmouth: Northwest Atlantic Fisheries Organization.

Fey MS, Regenstein JM. 1982. Extending shelf-life of fresh wet red hake and salmon using CO_2-O_2 Modified atmosphere and potassium sorbate ice at 1° C. J. Food Sci.. 47: 1048-1054.

Fratantoni PS, Pickart RS. 2003. Variability of the shelf break jet in the Middle Atlantic Bight: Internally or externally forced? J. Geophy. Res. Oceans. 108: 1-16.

Friedland KD, Langdon JA, Large SI, Selden RL, Link JS, Watson RA, Collie JS. 2020. Changes in higher trophic level productivity, diversity and niche space in a rapidly warming continental shelf ecosystem. Sci.Tot. Env.. 704:135270

Getis, A, Ord JK. 1992. The analysis of spatial association by use of distance statistics. Geograph. Anal. 24: 189-206.

Gill TA, Keith RA, Smith Lall B. 1979. Textural deterioration of red hake and haddock muscle in frozen storage as related to chemical parameters and changes in myofibrillar proteins. J. Food Sci. 44: 661-667.

Grabowski JH, Clesceri EJ, Bakus AJ, Gaudette J, Weber M, Yund PO. 2010. Use of herring bait to farm lobsters in the Gulf of Maine. PLOS One. 5: e10188.

Gulland JA. 1964. Variations in selection factors, and mesh differentials. J. Cons. Int. Explor. Mer. 29(2): 158-165.

Hare JA, Walsh HJ. 2007. Planktonic linkages among marine protected areas on the south Florida and southeast United States continental shelves. Can. J. Fish. Aquat. Sci. 64: 1234-1247.

Hernandez FJ, Hare JA, Fey DF. 2009.Evaluating diel, ontogenetic and environmental effects on larval fish vertical distribution using generalized additive models for location, scale and shape. Fish. Oceanogr. 18: 224-236

Hogan F, Didden J, Gustafson K, Keane E, Legault C, Linden D, Murray K, Palmer D, Potts D, Tholke C, Weeks S, Wigley S. 2019. Standardized bycatch reporting methodology 3-year review report-2018. NOAA Technical memorandum NMFS-NE-257. 196 pgs.

ICES. 1996. Manual of methods of measuring the selectivity of towed fishing gears. (Eds.) Wileman DA, Ferro RST, Fonteyne R, Millar RB. ICES Coop. Res. Rep. No. 215.

ICES, 2009. Report of the workshop on redfish stock structure. ICES CM 2009/ACOM:37.

Kleisner KM, Fogarty MJ, McGee S, Barnett A, Fratantoni P, Greene J, Hare JA, Lucey SM, McGuire C, Odell J, Saba VS, Smith L, Weaver KJ, Pinsky ML. 2016. The effects of sub-regional climate velocity on the distribution and spatial extent of marine species assemblages. PLOS ONE DOI:10.1371/journal.pone.0149220.

Kristensen K, Nielsen A, Berg CW, Skaug H, Bell BM. 2016. TMB: Automatic differentiation and Laplace approximation. J. Stat. Soft. 70(5): 1-21.

Lewis LA, Richardson DE, Zakharov EV, Hanner R. 2016. Integrating DNA barcoding of fish eggs into ichthyoplankton monitoring programs. Fish. Bul. 114: 153-168.

Licciardello JJ, Ravesi EM, Lundstrom RC, Wilhelm KA, Correia FF and Allsup MG. 1982. Time-temperature tolerance and physical-chemical quality tests for frozen red hake. J. Food Qual. 5: 215-234.

Lindsey CC. 1988. Factors controlling meristic variation, in (eds) Hoar WS, Randall DJ. Fish physiology, viviparity and posthatching juveniles, Academic Press, New York NY, pp. 197–274.

Maechler M, Rousseeuw P, Struyf A, Hubert M, Hornik K. 2019. cluster: Cluster analysis basics and extensions. R package version 2.0.8.

Marancik KE, Richardson DE, Konieczna M. in press. Updated morphological descriptions of the larval stage of *Urophycis* species (family: Phycidae) from the northeast United States continental shelf. Copeia

McBride RS, Smedbol RK (eds), In Press. An Interdisciplinary Review of Atlantic Cod (*Gadus morhua*) Stock Structure in the Western North Atlantic Ocean. NOAA Technical Memorandum NMFS-NE-XXX

Miller TJ, Das C, Politis PJ, Miller AS, Lucey SM, Legault DM, Brown RW and Rago PJ. 2010. Estimation of *Albatross IV* to *Henry B. Bigelow* calibration factors. Northeast Fisheries Science Center Ref. Doc. 10-05. 230 pgs.

Miller TJ, Rago PJ. 2012. Empirical exploration of feasible bounds on butterfish stock size and fishing mortality rates, 1975-2011. Report to the Mid-Atlantic Fishery Management Council Scientific and Statistical Committee, May 2, 2012.

Miller TJ, Adams C, Rago PJ. 2013. Feasible bounds on historic butterfish stock size and fishing mortality rates from survey and catch data. Report to the Mid-Atlantic Fishery Management Council Scientific and Statistical Committee, April 12, 2013.

Miller TJ. 2013. A comparison of hierarchical models for relative catch efficiency based on paired-gear data for U.S. Northwest Atlantic fish stocks. Can. J. Fish. Aquat. Sci. 70(9): 1306-1316

Miller TJ, Martin M, Politis P, Legault CM, Blaylock J. 2017a. Some statistical approaches to combine paired observations of chain sweep and rockhopper gear and catches from NEFSC and DFO trawl surveys in estimating Georges Bank yellowtail flounder biomass. TRAC Working Paper 2017/XX. 36p,.

Miller TJ, Richardson DE, Politis P, Blaylock J. 2017b. NEFSC bottom trawl catch efficiency and biomass estimates for 2009-2017 for 8 flatfish stocks included in the 2017 Northeast Groundfish Operational Assessments. 2017 Groundfish Operational Assessment working paper. Northeast Fisheries Science Center.

Miller TJ, Politis P, Blaylock J, Richardson DE, Manderson J, Roebuck C. 2018. Relative efficiency of a chain sweep and the rockhopper sweep used for the NEFSC bottom trawl survey and chainsweep-based swept area biomass estimates for 11 flatfish stocks. SAW 66 summer flounder Data/Model/Biological Reference Point meeting. National Marine Fisheries Service, Northeast Fisheries Science Center, Woods Hole, MA. September 17-21, 2018

Northeast Fisheries Center (NEFC). 1985. Status of the fishery resources off the Northeastern United States for 1985. NOAA Tech. Mem. NMFS-F/NEC-42.

New England Fishery Management Council (NEFMC). 1990. Amendment #4 to the Fishery Management Plan for the Northeast Multispecies Fishery. https://s3.amazonaws.com/nefmc.org/amendment_4_combined.pdf

Northeast Fisheries Center (NEFC). 1986. Report of the second NEFC stock assessment workshop. NEFC Wood Hole Lab. Ref. Doc. 86-09.

Northeast Fisheries Center (NEFC). 1986. Report of the eleventh NEFC stock assessment workshop, Fall 1990. NEFC Wood Hole Lab. Ref. Doc. 90-09.

Northeast Fisheries Science Center (NEFSC). 2011. 51st Northeast regional stock assessment workshop (51st SAW) assessment report. US Dept Commer, Northeast Fish Sci Cent Ref Doc. 11-02 856 p., Woods Hole, MA.

Northeast Fisheries Science Center (NEFSC). 2017. Operational assessment of 19 Northeast groundfish stocks, updated through 2016. US Dept Commer, Northeast Fish Sci Cent Ref Doc. 17-17 259 p., Woods Hole, MA.

Northeast Fisheries Science Center (NEFSC). 2018. 65th Northeast regional stock assessment workshop (65th SAW) assessment report. US Dept Commer, Northeast Fish Sci Cent Ref Doc. 18-11 659 p., Woods Hole, MA.

Northeast Fisheries Science Center (NEFSC). 2019. Operational Assessment of 14 Northeast Groundfish Stocks, Updated Through 2018.

Nye JA, Link JS, Hare JA, Overholtz WJ. 2009. Changing spatial distribution of fish stocks in relation to climate and population size on the Northeast United States continental shelf. Mar. Ecol. Prog. Ser. 393: 111–129.

Pinsky ML Fogarty MJ. 2012. Lagged social-ecological responses to climate and range shifts in fisheries. Clim. Change. 115: 883–91.

Pol MV, Herrmann B, Rillahan C, He P. 2016. Impact of codend mesh sizes on selectivity and retention of Acadian redfish *Sebastes fasciatus* in the Gulf of Maine trawl fishery. Fish. Res. 184: 54-63.

R Core Team. 2019. R: A language and environment for statistical computing. R Foundation for statistical computing, Vienna, Austria.

Richardson DE, Hare JA, Overholtz WJ, Johnson DL. 2010. Development of long-term larval indices for Atlantic herring (*Clupea harengus*) on the northeast U.S. continental shelf. ICES J. Mar. Sci. 67: 617-627.

Richardson DE. Palmer MC, Smith BE. 2014. The influence of forage fish abundance on the aggregation of Gulf of Maine Atlantic cod (*Gadus morhua*) and their catchability in the fishery. Can. J. Fish. Aquat. Sci. 71: 1349-1362.

Richter VA. 1968. Results of research on the distribution, age, growth, and general,mortality of stocks of red hake, *Urophycis chuss* Walbaum, on Georges Bank and in adjacent waters, 1965-1966. ICNAF Res. Doc. 68/38.

Richter VA. 1970. Dynamics of some biological indices. abundance and fishing of red hake (*Urophycis chuss* W.) in the Northwest Atlantic, 1965-1968. ICNAF Res. Doc. 70/39.

Ryer CH. 2008. A review of flatfish behavior relative to trawls. Fish. Res. **90**:138-146.

Ryer CH, Rose CS, Iseri PJ. 2010. Flatfish herding behavior in response to trawl sweeps: a comparison of diel responses to conventional sweeps and elevated sweeps. Fish. Bull. (Seattle) 108:145-154.

SARC (Stock Assessment Review Committee). 2011. SARC 51 Panel Summary Report. 55 pgs. Available at: https://www.nefsc.noaa.gov/saw/saw51/SAW51PanelSummary.pdf.

SEDAR. 2018. SEDAR 58 – Cobia Stock ID process report compilation. SEDAR, North Charleston SC. 116 pp. available online at:http://sedarweb.org/sedar-58-stock-id-process

Shank B, Duquette J. 2014. Gear avoidance behavior of yellowtail flounder associated with the HabCam towed imaging vehicle. Transboundary Resources Assessment Committee: 2016/16

Showell MS. 1987. Red hake. pp. 11 In (ed) Bowen WD. A Review of stock structure in the Gulf of Maine area: A workshop report. Canadian Atlantic Fisheries Scientific Advisory Committee (CAFSAC) Res. Doc. 87/21.

Smith SJ. 1997. Bootstrap confidence limits for groundfish trawl survey estimates of mean abundance. Can. J. Fish. Aquat. Sci. 54:616-630.

Snow GW. 1950, Development of trash fishery at New Bedford, Massachusetts. Com. Fish. Rev.. 12: 8-10.

Somerton DA, Munro P. 2001. Bridle efficiency of a survey trawl for flatfish. Fish. Bull. (Seattle) **99**:641-652.

Somerton DA, Munro PT, Weinberg KL. 2007. Whole-gear efficiency of a benthic survey trawl for flatfish. Fish. Bull. (Seattle) **105**:278-291.

Sosebee K. 1998. Red hake. In (ed) Clark SH. Status of the fishery resources off the northeastern United States for 1998. p. 64-66. NOAA Tech. Mem. NMFS-NE-115.

Steimle FW, Morse WW, Berrien PL, Johnson DL. 1999. Essential fish habitat source Document: Red Hake, *Urophycis chuss*, life history and habitat characteristics. NOAA Technical Memorandum NMFS-NE-133.

Steiner WW, Luczkovich JJ, Ola BL. 1982 . Activity, shelter usage, growth and recruitment of juvenile red hake *Urophycis chuss*. Mar. Ecol. Prog. Ser. 7: 125-135.

Sybrandy AL, Niiler PP. 1990. The WOCE/TOGA SVP Lagrangian drifter construction manual. Scripps Institution of Oceanography, University of California, San Diego, SIO Reference No. 90-248.

Walsh HJ, Richardson DE, Marancik KE, Hare JA. 2015. Long-term changes in the distributions of larval and adult fish in the Northeast U.S. Shelf Ecosystem. PLOS ONE 10:e0137382.

Wood SN. 2006. Generalized additive models: An Introduction with R. Chapman & Hall, Boca Raton, Florida, 392 pp.

Tables

Table 1.1. Morphological comparisons reported by Richter (1968) including degrees of freedom (df), t-statistic (t), probability (P) and 95% significance, adjusted for multiple comparisons.

character	df	t	P	significance
Northern Georges Bank vs. Southern Georges and southern New England Slope				
vertebrae	397	3.70	0.0002	*
1st dorsal rays	397	1.90	0.0582	
2nd dorsal rays	397	1.20	0.2309	
pectoral rays	397	8.10	0.0000	*
anal fin rays	397	0.20	0.8416	
otolith wt 36cm female	21	3.71	0.0013	*
otolith wt 38cm female	38	5.04	0.0000	*
Scotian Shelf vs. Southern Georges and southern New England Slope				
vertebrae	268	0.94	0.3481	
1st dorsal rays	268	3.60	0.0004	*
2nd dorsal rays	268	3.80	0.0002	*
pectoral rays	268	3.10	0.0021	*
anal fin rays	268	11.05	0.0000	*
Southern Georges and southern New England Slope vs. Mid Atlantic slope				
otolith wt 36cm female	37	4.00	0.0003	*
otolith wt 38cm female	28	4.47	0.0001	*
otolith wt 32cm male	54	4.10	0.0001	*
otolith wt 34cm male	39	3.45	0.0014	*
otolith wt 36cm male	32	4.62	0.0001	*

Table 2.1. Median-length-at-age by time period of sampling, sex, and season. Cells are color-coded based on whether they are above (blue), below (orange) or at (white) the average regional length-at-age. Black cells lacked red hake of that age in that category.

				Sub-region						
Age	**Period**	**Sex**	**Season**	**GOM-A**	**GOM-B**	**GOM-C**	**GOM-D**	**GB-A**	**GB-B**	**SNE**
4	70s/80s	Male	Spring	38	39	38	38	34	35	35
4	2010s	Male	Spring	29	29	30	32	29	29.5	29
4	70s/80s	Female	Spring	43	44	43	44	39	39	40
4	2010s	Female	Spring	32	34	35	32	32	34	34
4	70s/80s	Male	Fall	40	40	38	40.5	35	36	35
4	2010s	Male	Fall	32	31	33	33	31	30	31
4	70s/80s	Female	Fall	46	45	45	44	40	41	41
4	2010s	Female	Fall	35	35	37	38	35.5	34	36
5	70s/80s	Male	Spring	40	40.5	40	40	35	36	36
5	2010s	Male	Spring	33	32.5	33	33	30	31	31.5
5	70s/80s	Female	Spring	46	46	46	48	40	40	41
5	2010s	Female	Spring	37.5	37	39	38	35	35	36
5	70s/80s	Male	Fall	41.5	41	39	42	35.5	36	36
5	2010s	Male	Fall	33	33	35	34	32	32	32
5	70s/80s	Female	Fall	48	48	47.5	47	42	42	43
5	2010s	Female	Fall	40	39.5	41	41	36	37	37.5
6	70s/80s	Male	Spring	42	42	42	45	36	36	36
6	2010s	Male	Spring	34.5	34	35	33	31.5	34	35.5
6	70s/80s	Female	Spring	48	48	48.5	49.5	41	41	43
6	2010s	Female	Spring	39	41	41	41	35	36	38
6	70s/80s	Male	Fall	44.5	41	38	44	36	36	36
6	2010s	Male	Fall	36	34	37	40.5	32	34	NaN
6	70s/80s	Female	Fall	50	49	48.5	49	42	43	45
6	2010s	Female	Fall	42	42	42	42	37	37	40
7	70s/80s	Male	Spring	42	45	45	45	37	36	36.5
7	2010s	Male	Spring	36	34.5	36	35.5	31	NaN	NaN
7	70s/80s	Female	Spring	51	49	51	51	44	42	44
7	2010s	Female	Spring	41	41	42	41.5	39.5	42	38
7	70s/80s	Male	Fall	45	43	39	44	36	37	37
7	2010s	Male	Fall	42	NaN	37	39	34	NaN	NaN
7	70s/80s	Female	Fall	53	51	49.5	51	43.5	42.5	45
7	2010s	Female	Fall	42	42	43.5	42.5	41	NaN	NaN

Table 2.2. Mean square estimates for chemistry from randomized block analyses of variance (ANOVA), testing for differences in concentrations of $Mg \cdot Ca^{-1}$, $Sr \cdot Ca^{-1}$, and $Ba \cdot Ca^{-1}$ a) in nuclei and b) along the edges of otoliths from adult red hake sampled from the Gulf of Maine and Mid-Atlantic Bight. * $p < 0.05$ (significant comparison-wise only).

	df	Mg/Ca	Mn/Ca	Sr/Ca	Ba/Ca
Nucleus					
Slide (block)	9	0.00114	0.0077	1.95×10^{-9}	0.0221
Sampling area	3	0.00014	0.0099	6.93×10^{-10}	0.0182
Length	1	0.00032	0.0246	7.72×10^{-9}	0.0613*
Residual	66	0.00093	0.0078	3.20×10^{-9}	0.0144
Edge					
Slide (block)	9	0.00143		4.55×10^{-6}	0.0576
Sampling area	3	0.00019		2.26×10^{-5}	0.0921
Length	1	0.00001		1.03×10^{-4}*	0.3674*
Residual	66	0.00233		1.03×10^{-5}	0.0849

Table 2.3. Seasonal relative percentage of red hake larvae caught in July-August and September-October from 9 sub-regions (see Figure 2.1)

Year	Season	SNE_C	SNE_B	SNE_A	GB_B	GB_A	GOM_D	GOM_C	GOM_B	GOM_A
1985	Jul-Aug	0.7	0.7	2.1	1.8	17.1	1.5	0.0	0.0	0.0
	Sep-Oct	2.4	8.1	21.2	22.9	18.7	0.1	0.3	2.3	0.0
1987	Jul-Aug	5.1	2.4	5.9	0.3	0.9	0.0	0.0	0.0	0.0
	Sep-Oct	25.2	5.2	27.9	9.1	4.1	1.5	0.0	12.1	0.2
2002	Jul-Aug	0.3	0.7	3.9	44.2	13.0	2.6	0.1	1.1	0.0
	Sep-Oct	0.8	4.6	9.5	14.8	2.5	1.7	0.0	0.1	0.0
2006	Jul-Aug	0.6	3.0	1.4	17.5	23.1	1.9	0.6	6.9	0.1
	Sep-Oct	3.2	17.7	13.9	3.8	3.4	2.2	0.6	0.0	0.0
2012	Jul-Aug	1.1	1.0	5.8	40.8	18.6	6.3	1.4	20.9	0.5
	Sep-Oct	0.3	1.1	1.4	0.4	0.2	0.1	0.1	0.0	0.0
2013	Jul-Aug	0.3	0.0	0.0	32.5	15.7	1.8	0.2	0.0	0.2
	Sep-Oct	2.3	7.9	15.5	17.2	2.2	0.1	0.4	3.3	0.1

Table 2.4. Details of the particle-tracking model.

Metric	Description
Year of Release	1978, 1981, 1984, 2000, 2004, 2010
Seasonality	July, August, September
Frequency	Every 4 days
Duration	60 days
Vertical behavior	a) 10 m for 0-15 d; 20 m for 15-60 d
	b) 20 m for 0-15 d; 40 m for 15-60 d
Bottom Depth	5-150 m
Region	Delaware Bay to Mid-Scotian Shelf
Spatial Resolution	0.065 degrees
Release Locations	5099
Total Releases used	1,402,225

Table 2.5: Connectivity matrix for particles after a 15-day duration across all months, years, and depth behaviors. Rows correspond to the release locations and columns indicate the end locations.

Source	SS-A	SS-B	SS-C	GOM-A	GOM-B	GOM-C	GOM-D	GB-A	GB-B	SNE-A	SNE-B	SNE-C
SS-B	0.15%	47.86%	17.80%	0.59%	0.00%	2.56%	0.04%	2.66%	0.01%	0.00%	0.00%	0.00%
SS-C	0.00%	3.62%	69.60%	15.26%	0.45%	1.72%	0.07%	1.93%	0.03%	0.00%	0.00%	0.00%
GOM-A	0.00%	0.00%	0.19%	62.91%	16.15%	11.67%	0.85%	0.06%	0.00%	0.00%	0.00%	0.00%
GOM_B	0.00%	0.00%	0.03%	3.25%	49.08%	11.43%	9.16%	0.36%	0.38%	0.00%	0.00%	0.00%
GOM-C	0.00%	0.00%	0.41%	1.02%	1.41%	59.90%	21.10%	5.90%	2.47%	0.04%	0.00%	0.00%
GOM-D	0.00%	0.00%	0.17%	0.22%	0.32%	10.38%	21.33%	51.65%	7.32%	0.69%	0.01%	0.00%
GB-A	0.00%	0.03%	0.13%	0.01%	0.00%	5.56%	19.83%	29.74%	20.99%	9.92%	2.08%	0.30%
GB-B	0.00%	0.00%	0.00%	0.00%	0.00%	0.62%	1.80%	0.09%	10.18%	47.18%	20.76%	6.18%
SNE-A	0.00%	0.00%	0.00%	0.00%	0.00%	0.00%	0.00%	0.01%	0.06%	16.71%	47.91%	23.79%
SNE-B	0.00%	0.00%	0.00%	0.00%	0.00%	0.00%	0.00%	0.00%	0.02%	0.51%	26.94%	60.37%
SNE-C	0.00%	0.00%	0.00%	0.00%	0.00%	0.00%	0.00%	0.00%	0.01%	0.00%	0.81%	63.91%

Table 2.6: Connectivity matrix for particles after a 30-day duration across all months, years, and both depth behaviors. Rows correspond to the release locations and columns indicate the end locations.

Source \ End Location	SS-A	SS-B	SS-C	GOM-A	GOM_B	GOM-C	GOM-D	GB-A	GB-B	SNE-A	SNE-B	SNE-C
SS-B	0.19%	33.13%	17.35%	5.65%	0.24%	2.24%	0.06%	4.37%	0.93%	0.16%	0.10%	0.02%
SS-C	0.00%	4.13%	54.13%	23.46%	1.88%	5.00%	0.41%	1.86%	0.64%	0.14%	0.05%	0.02%
GOM-A	0.00%	0.00%	0.79%	43.08%	17.42%	22.78%	2.83%	1.36%	0.25%	0.00%	0.00%	0.00%
GOM_B	0.00%	0.00%	0.18%	3.67%	32.39%	15.73%	9.44%	1.01%	2.26%	0.24%	0.00%	0.00%
GOM-C	0.00%	0.01%	2.00%	5.17%	1.06%	51.93%	10.56%	11.50%	5.81%	1.47%	0.05%	0.02%
GOM-D	0.00%	0.02%	0.66%	1.00%	0.32%	12.78%	18.18%	32.76%	17.06%	6.43%	0.70%	0.22%
GB-A	0.00%	0.16%	0.39%	0.29%	0.02%	10.72%	13.61%	17.18%	14.15%	15.99%	7.95%	5.67%
GB-B	0.00%	0.00%	0.01%	0.01%	0.01%	0.69%	0.94%	0.34%	3.11%	24.62%	27.45%	24.03%
SNE-A	0.00%	0.00%	0.00%	0.00%	0.00%	0.00%	0.00%	0.01%	0.10%	6.14%	30.40%	39.98%
SNE-B	0.00%	0.00%	0.00%	0.00%	0.00%	0.00%	0.00%	0.02%	0.05%	0.61%	16.88%	48.95%
SNE-C	0.00%	0.00%	0.00%	0.00%	0.00%	0.00%	0.00%	0.04%	0.01%	0.02%	0.75%	38.24%

Table 2.7: Connectivity matrix for the drifters after 15-day duration. Rows correspond to the release locations and columns indicate end locations.

source	SNE-C	SNE-B	SNE-A	GB-B	GB-A	GOM-D	GOM-C	GOM-B	GOM-A
SNE-C	32.65%	1.91%	0.53%	0.62%	1.32%	0.20%	0.25%	0.00%	0.07%
SNE-B	19.55%	18.00%	5.88%	0.86%	0.91%	0.17%	0.19%	0.00%	0.05%
SNE-A	7.33%	19.73%	24.71%	4.45%	1.29%	0.63%	0.19%	0.00%	0.03%
GB-B	1.50%	6.93%	18.94%	20.70%	11.16%	6.65%	1.71%	0.03%	0.26%
GB-A	0.44%	0.79%	3.70%	10.56%	43.58%	10.19%	2.69%	0.04%	0.21%
GOM-D	0.14%	0.27%	1.67%	7.53%	40.43%	22.28%	11.01%	0.26%	1.19%
GOM-C	0.11%	0.09%	0.58%	3.64%	23.78%	23.06%	24.51%	1.13%	5.70%
GOM-B	0.03%	0.04%	0.31%	2.35%	18.05%	24.28%	22.88%	22.34%	2.20%
GOM-A	0.08%	0.05%	0.17%	1.07%	5.84%	10.12%	21.63%	2.00%	35.26%

Table 2.8: Connectivity matrix for the drifters after 30-day duration. Rows correspond to the release locations and columns indicate end locations.

source	SNE-C	SNE-B	SNE-A	GB-B	GB-A	GOM-D	GOM-C	GOM-B	GOM-A
SNE-C	15.59%	1.44%	0.92%	0.99%	2.21%	0.62%	0.54%	0.01%	0.20%
SNE-B	12.54%	4.87%	3.05%	1.29%	2.10%	0.59%	0.47%	0.01%	0.17%
SNE-A	9.03%	8.85%	8.09%	2.67%	2.82%	1.03%	0.55%	0.01%	0.18%
GB-B	4.13%	6.63%	9.62%	6.92%	11.68%	4.73%	2.18%	0.07%	0.49%
GB-A	1.25%	2.11%	4.73%	7.77%	27.85%	7.99%	3.20%	0.09%	0.55%
GOM-D	0.75%	1.28%	3.75%	8.02%	32.00%	12.33%	7.13%	0.31%	1.74%
GOM-C	0.47%	0.71%	2.30%	6.21%	27.44%	14.98%	12.13%	0.82%	4.79%
GOM-B	0.30%	0.54%	1.82%	5.50%	27.52%	18.20%	15.20%	6.75%	3.43%
GOM-A	0.35%	0.33%	1.00%	3.30%	15.03%	13.05%	17.16%	1.56%	16.72%

Table 2.7. AIM model results from runs on the individual components of various stock configurations. "Two stocks" is the status quo stock configuration, "Alt. two stocks" moves the Georges Bank region from the southern stock to the northern stock, and "Alt. Alt. two stocks" leaves western Georges Bank (GB-B) in the southern stock and adds the eastern Georges Bank region (GB-A) to the northern stock. Three stocks makes each region a separate stock. The survey index input was from the following year (for example catch from 2018, survey index from spring 2019) for the runs where lagging is "yes". Lagging did not improve the fit. The p value is generated by a randomization test. Reported landings and total estimated catch are for reference, and the F_{msy} proxy and relative F are AIM model outputs.

Model	Lagging (catch = y, survey index = y+1)	P value	Reported landings (5 yr mean, mt)	Total 2018 catch used in model (mt)	F_{msy} proxy (Rel F for rep ratio = 1) in mt per kg/tow	AIM Rel F 2018 (3yr running avg) in mt per kg/tow
One stock	Yes	0.339	493	2057	380	345
Two stocks - North	Yes	0.127	109	281	49	20
Two stocks - South	Yes	0.457	407	1771	177	1,566
Alt. two stocks - North	Yes	0.497	108	640	93	68
Alt. two stocks - South	Yes	0.213	378	1340	475	1,851
Alt. Alt. two stocks - North	No	0.156	379	416	107	35
Alt. Alt. two stocks - South	No	0.878	107	1601	419,326,900	2910
Three stocks - GOM	No	0.075	109	281	54	18
Three stocks - GB	No	0.973	30	396	855	215
Three stocks - SNE	No	0.910	378	1340	1,350,994	4,467

Table 2.8. Table of catch and survey index input values for AIM runs for one stock, and status quo two stocks. Removals are the sum of reported red hake landings, the estimated proportion of red hake in reported mixed hake landings, estimated recreational catch, reported vessel-to-vessel bait sales, and estimated discards. Survey index is the stratified mean kilograms per tow, in *Bigelow* units, of the NEFSC spring bottom trawl survey.

Year	One stock removals (mt)	One stock survey index in kg per tow (y+1)	Two stock north removals (mt)	Two stock north survey index in kg per tow (y+1)	Two stock south removals (mt)	Two stock south survey index in kg per tow (y+1)
1981	6323.9	9.99	2615.5	7.46	3708.38	11.54
1982	7300.9	8.12	2669.6	11.05	4631.36	6.31
1983	7562.9	5.78	2242.5	8.93	5320.32	3.84
1984	7685	6.55	2385.3	10.89	5299.76	3.88
1985	6093.9	6.86	2271.9	9.75	3821.98	5.08
1986	6941.5	5.53	2690.3	10.34	4251.26	2.56
1987	6638.8	3.93	2119.1	5.87	4519.66	2.72
1988	6633.3	3.33	1883.8	5.95	4749.49	1.76
1989	8821.4	3.42	2482.2	4.87	5971.05	2.53
1990	8178.7	3.59	1503.8	5.97	6420.22	2.13
1991	5278.6	3.61	1530.1	7.33	3775.49	1.31
1992	8933.9	4.12	1663.8	8.7	8547.43	1.29
1993	14788.9	3.85	1404.7	6.03	16651.98	2.5
1994	6868.8	3.15	748.7	5.86	6522.98	1.48
1995	2567.4	2.93	202.7	5.46	2400.8	1.37
1996	2596.2	4.22	956.1	5.48	1353.63	3.44
1997	3058.7	3.23	467.8	7.43	3108	0.63
1998	9720.9	3.51	192.3	7.14	7979.15	1.27
1999	8393.8	4.37	614.9	9.48	5381.91	1.22
2000	3955.2	5.41	237.2	11.16	4191.35	1.87
2001	4081.8	6.39	332.5	14.13	2922.45	1.64
2002	1402.8	2	381.6	3.95	939.26	0.8
2003	1192.5	2.44	311.6	5.66	856.14	0.45
2004	1318.2	2.05	170.7	3.45	1142.89	1.18
2005	1458.1	1.8	141.1	2.84	1455.79	1.16
2006	1523.6	4.03	265.8	6.33	1244.69	2.62
2007	1852.5	5.1	196.3	11.05	1727.43	1.43
2008	1431.9	4.71	121.6	5.46	1255.93	4.24
2009	1851.5	5.01	200.9	8.86	1666.27	2.63
2010	1678.9	5.56	304.5	6.42	1446.87	5.03
2011	1816.7	4.06	248.9	5.6	1551.02	3.12
2012	1915.7	2.86	368	4.55	1425.45	1.82
2013	1493.9	5.65	260.6	10.28	1117.36	2.26
2014	1500.4	8.78	261.3	20.3	1207.34	1.67
2015	1728.3	6.47	347.9	15.31	1274.41	1.01
2016	1805.9	6.15	368.3	14.95	1438.89	0.72
2017	1099.5	6.9	219.5	16.83	874.67	0.76
2018	2056.6	4.84	280.5	9.58	1771.37	1.91

Table 2.9. Catch and survey index input values for AIM runs for three stocks. Removals are the sum of reported red hake landings, the estimated proportion of red hake in reported mixed hake landings, estimated recreational catch, reported vessel-to-vessel bait sales, and estimated discards. Survey index is the stratified mean kilograms per tow, in *Bigelow* units, of the NEFSC spring bottom trawl survey.

Year	Three stock GOM removals (mt)	Three stock GOM survey index in kg per tow	Three stock GB removals (mt)	Three stock GB survey index in kg per tow	Three stock SNE removals (mt)	Three stock SNE survey index in kg per tow
1981	1860.55	21.56	336.58	15.46	4126.35	18.4
1982	1947.95	7.46	415.44	3.01	4937.03	16.28
1983	1628.53	11.05	528.74	4.34	5405.08	7.41
1984	1796.42	8.93	510.47	1.77	5377.61	4.99
1985	1599.52	10.89	375.34	4.2	4118.63	3.7
1986	2147.07	9.75	434.28	12.42	4359.73	0.99
1987	1682.25	10.34	443.72	3.08	4512.4	2.26
1988	1601.39	5.87	485.49	2.59	4545.95	2.8
1989	2482.23	5.95	464.01	2.58	6809.59	1.3
1990	1503.8	4.87	763.27	2.69	4532.58	2.44
1991	1530.13	5.97	232.1	2.08	3658.1	2.16
1992	1663.84	7.33	1358.87	0.93	7399.07	1.52
1993	1404.72	8.7	389.2	1.77	14028.06	1.03
1994	748.75	6.03	8233.99	3.99	3638.3	1.68
1995	204.08	5.86	70.89	2.88	2449.23	0.69
1996	956.08	5.46	177.66	3.49	916.49	0.19
1997	467.78	5.48	1187.18	8.24	2888.36	0.79
1998	192.33	7.43	76.3	0.55	6658.22	0.68
1999	614.91	7.14	621.01	2.48	5556.11	0.6
2000	237.23	9.48	4085.78	2.84	1401.6	0.32
2001	332.5	11.16	147.23	0.81	2868.45	2.46
2002	381.59	14.13	197.35	3.88	900.61	0.38
2003	311.58	3.95	516.1	1.85	366.44	0.21
2004	170.73	5.66	459.67	0.34	794.63	0.51
2005	141.13	3.45	338.64	2.38	1130.07	0.51
2006	265.82	2.84	966.78	2.01	370.82	0.68
2007	196.26	6.33	2595.52	6.54	322.69	0.43
2008	121.95	11.05	701.46	1.74	728.78	1.27
2009	200.92	5.46	501.19	10.24	1010.6	0.88
2010	304.53	8.86	838.58	5.7	793.55	0.93
2011	248.97	6.42	1010.43	12.18	694.65	1.06
2012	367.99	5.6	588.16	4.79	1085.64	2.19
2013	260.6	4.55	853.15	4.74	609.46	0.2
2014	261.38	10.28	426.73	3.75	938.09	1.16
2015	347.96	20.3	603.84	3.57	673.71	0.62
2016	368.38	15.31	691.3	2.03	923.75	0.44
2017	219.52	14.95	198.53	1.81	626.8	0.11
2018	280.52	16.83	396.11	1.68	1340.24	0.25

Table 4.1. Estimate of red hake abundance based on different surveys and the associated gear efficiency assuming that HabCam is 100% efficient.

Survey	GB	GB Eff	MA	MA Eff**	Overall	Eff**
Habcam	262	1	196	1	458	1
Fall Trawl (wings)	39.3	0.15	18.3	0.09	57.6	0.13
Fall Trawl (doors)	15.9	0.06	7.4	0.04	23.3	0.05
Spring Trawl* (wings)	28.4	0.11	2.4	0.01	35.8	0.08
Spring Trawl* (doors)	11.5	0.04	1.0	0.005	12.4	0.03
Scallop Dredge	79.5	0.30	NA	NA	NA	NA

*Likely underestimated due to seasonal migration

** May be underestimated due to misidentification of spotted hake in the Habcam survey

Table 4.2. Description of relative catch efficiency (ρ) and dispersion (φ) parameterizations for conditional binomial and beta-binomial models and corresponding maximized marginal log-likelihoop, number of fixed effects parameters (P) and ΔAIC.

Model	log (ρ)	log(φ)	log-likelihood	P	ΔAIC	Description
BI_0	~ 1	–	-2735.83	1	1916.85	population-level mean for all observations
BI_1	~ 1+1|pair	–	-1940.50	2	328.2	population- and random station-level ρ
BI_2	~ s(length)	–	-2640.32	3	1729.83	population-level smooth size effect on ρ
BI_3	~ s(length) + 1|pair	–	-1875.95	4	203.09	population-level smooth size effect and random station level intercept for ρ
BI_4	~ s(length) + s(length)|pair	–	-1794.11	7	45.41	population-level and random station-level smooth size effects for ρ
BB_0	~ 1	~ 1	-2106.24	2	659.68	population-level ρ and φ
BB_1	~ 1+1|pair	~ 1	-1874.80	3	198.78	population-level and random station-level intercept for ρ and population-level φ
BB_2	~ s(length)	~ 1	-2086.04	4	623.26	population-level smooth size effect on ρ and population level on φ
BB_3	~ s(length)	~ s(length	-2072.37	6	599.93	population-level smooth size effect on ρ and φ
BB_4	~ s(length) + 1|pair	~ 1	-1837.48	5	128.15	population-level smooth size effect and random station-level intercept for ρ and population-level φ
BB_5	~ s(length) + 1|pair	~ s(length	-1817.24	7	91.66	population-level smooth size effect on ρ and φ and random station-level intercepts for ρ
BB_6	~ s(length) + s(length)|pair	~ 1	-1786.58	8	32.35	population-level and random station-level smooth size effects on ρ and population-level φ
BB_7	~ s(length) + s(length)|pair	~ s(length	-1784.99	10	33.18	population-level and random station-level smoth size effects on ρ and population-level smooth size effects on φ
BB_8	~ dn+ s(length) + s(length)|pair	~ 1	-1772.30	9	5.79	population-level smooth size and day/night effects and random station-level smooth size effects on ρ and population-level smooth size effects on φ
BB_9	~ dn+ s(length) + s(length)|pair	~ 1	-1770.40	8	0	BB8 with no correlation of station-specific random effects
BB_{10}	~ dn+ s(length) + s(length)|pair	~ 1	-1769.99	10	3.18	BB_9 with interaction of population level day/night and smooth size effects

Table 4.3. Estimated chain sweep swept area seasonal survey biomass (mt) for each stock between 2009 and 2019 using relative efficiency estimates from the best performing model (BB9).

Year	Northern red hake spring	Northern red hake fall	Southern red hake spring	Southern red hake fall
2009	92,125	75,194	98,202	49,021
2010	151,491	86,754	58,693	100,097
2011	104,590	138,232	167,537	58,182
2012	99,371	105,424	93,450	47,492
2013	79,322	107,243	41,582	41,727
2014	179,416	234,429	64,014	59,312
2015	372,848	235,387	40,560	39,935
2016	206,779	235,264	25,138	53,187
2017	275,022	219,999	19,267	93,945
2018	280,428	226,800	24,810	87,891
2019	163,439		72,787	

Table 4.4. Implicit annual and seasonal efficiencies of unconverted swept area biomass estimates as measured by the ratio to the chainsweep-based estimates in Table 4.3.

Year	Northern red hake spring	Northern red hake fall	Southern red hake spring	Southern red hake fall
2009	0.21	0.33	0.25	0.39
2010	0.20	0.25	0.26	0.25
2011	0.22	0.21	0.18	0.26
2012	0.20	0.24	0.19	0.29
2013	0.20	0.33	0.25	0.34
2014	0.20	0.24	0.20	0.25
2015	0.19	0.29	0.24	0.27
2016	0.25	0.23	0.22	0.29
2017	0.19	0.26	0.22	0.25
2018	0.21	0.25	0.17	0.19
2019	0.20		0.15	

Table 4.5. Ratios of annual and seasonal unconverted biomass estimates made using numbers at length and estimated weight at length to those using the aggregate catch (kg) per tow observations.

Year	Northern red hake spring	Northern red hake fall	Southern red hake spring	Southern red hake fall
2009	1.01	1.00	1.00	0.99
2010	1.01	1.02	0.98	1.02
2011	0.97	1.03	0.97	1.02
2012	1.01	1.02	0.99	1.04
2013	1.02	1.02	0.98	0.98
2014	0.99	0.99	0.98	1.03
2015	1.01	1.02	0.99	1.00
2016	1.01	1.01	1.02	1.02
2017	1.00	1.01	0.96	1.00
2018	1.01	1.01	1.03	1.02
2019	1.01		0.98	

Table 4.6: Breakdown of summed weights of red hake caught in the 2019 *F/V Karen Elizabeth* experiments. Note that the totals caught in a 13 m wide net are much higher because a control net was fished at each station.

Red hake catch weights for each net width (m). Weights are summed kilograms for both nets.

Species	9	10	11	12	13	14	15	16	Total
Red Hake	372.6	483.4	1057.5	871.3	1204.4	193.0	444.4	223.9	4850.4

Weights represent totals after 25 non-representative stations were removed from the data set.

Table 4.7: The number of stations for each net width where red hake were caught

Count of positive stations for red hake at each net width (m) where both nets caught each species

Treatment net widths (m)	9	10	11	12	13	14	15	16	Total
Red hake	3	10	9	10	15	6	6	3	62

Count represent totals after 25 non-representative stations were removed from the data set.

Table 4.8: Results of length-based model comparisons for both binomial and beta-binomial models. Model statistics (Δ AIC and the number of parameters) for the eleven models fit to the data from the experiment are shown. The models which had the lowest AIC value are shown in white (with a Δ AIC of zero). Additionally, a description of the model components is given for each model, with 'Y' indicating a specific component was included in that model.

Model specifications
to estimate relative catch efficiency

Model Component	Binomial						Beta-binomial				
	1	2	3	4	5	6	7	8	9	10	11
Model AIC difference	699.4	229.4	227.8	231.3	228.3	292.5	2	1.8	0	3.8	0
Number model parameters	2	5	7	9	8	3	6	8	10	12	11
Day/night effect on overall global mean relative efficiency	N	N	N	N	Y	N	N	N	N	N	Y
Smooth size effect on overall global mean relative efficiency	N	N	Y	Y	Y	N	N	N	Y	Y	Y
Smooth size effect on overdispersion parameter	N	N	N	N	N	N	N	Y	Y	Y	Y
Random variation in smooth size effects on relative catch efficiency from pair to pair	N	Y	Y	Y	Y	N	Y	Y	Y	Y	N
Smooth wingspread effect on overall global mean relative efficiency	N	N	N	Y	N	N	N	N	N	Y	N
Random variation in relative catch efficiency from pair to pair	Y	N	N	N	N	Y	N	N	N	N	N

Figures

Figure 1.1. Red hake images. A) Red hake photographed *in situ* with the HabCam system. B) Side-by-side images of white hake (top) and red hake (bottom) showing the difficulty in differentiating the two species.

A. Red hake in HabCam

B. White hake (top) and Red hake (bottom)

Figure 1.2. Distribution of red hake based on trawl surveys. Figure from Brown et al. 1996.

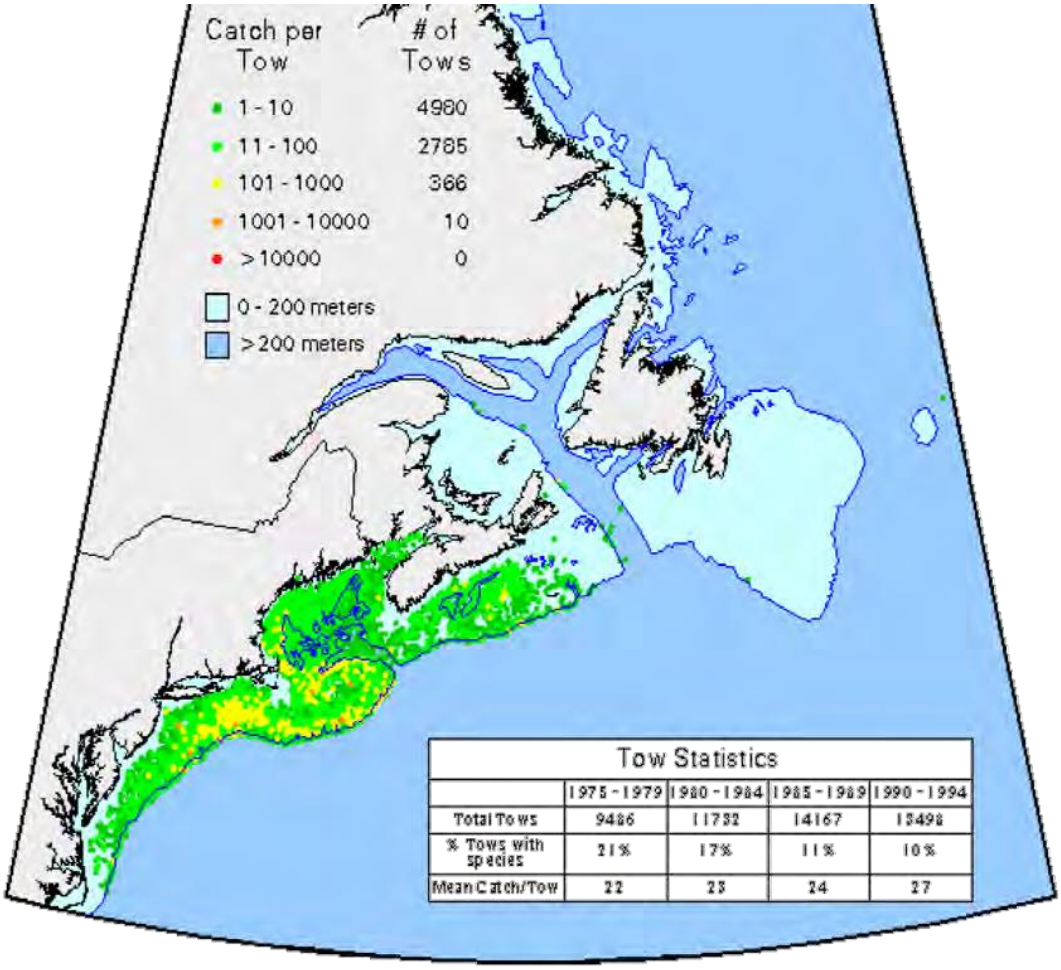

Figure 1.3: Distribution maps based on fall trawl survey data showing the overlap of the three species of *Urophycis* on the northeast U.S. continental shelf, white hake (*U. tenuis*), red hake (*U. chuss*) and spotted hake (*U. regia*) during two time periods.

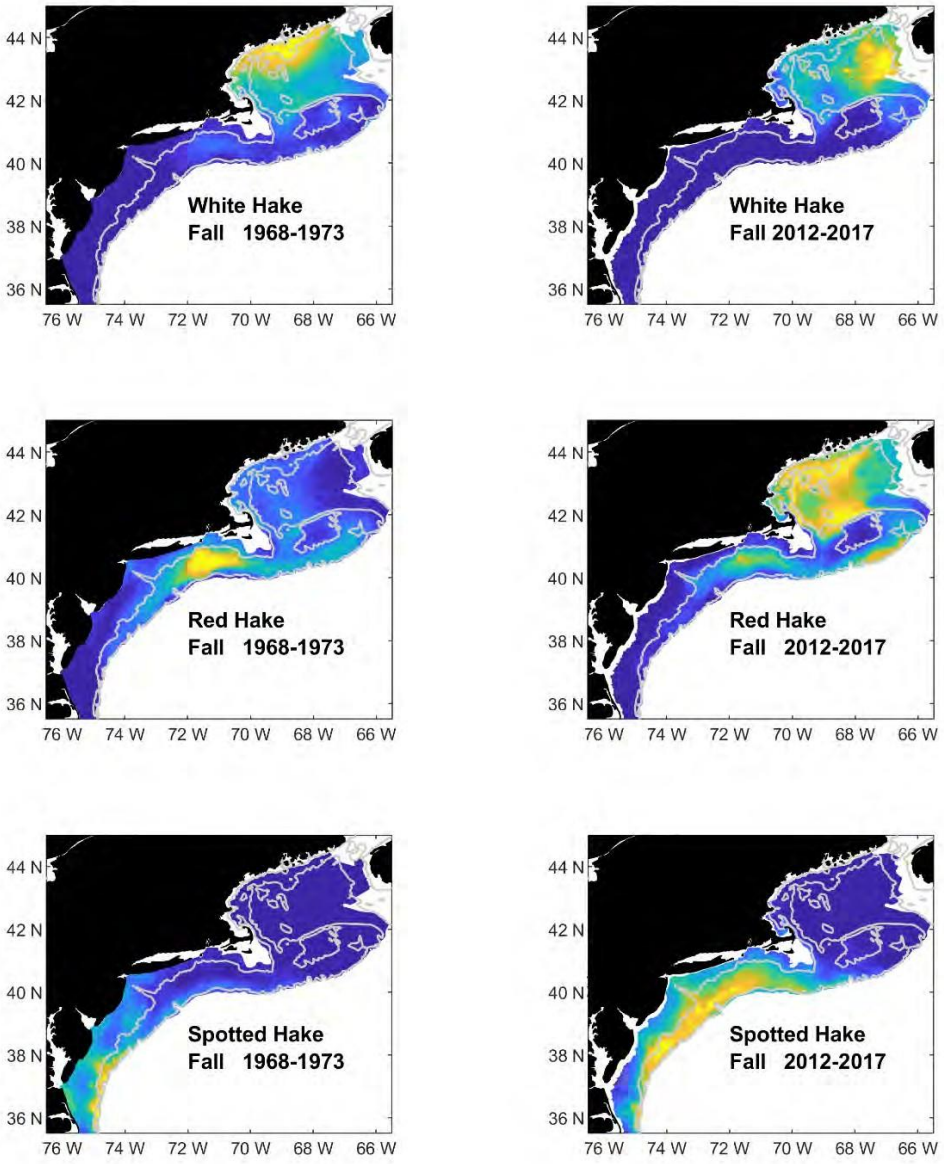

Figure 1.4: Image of a larval red hake from Marancik et al. (in press). The characters to reliably identify *Urophycis* larvae were only recently determined.

Figure 1.5. A) Location of the trash fishery in the 1950s and a B) depiction of the seasonal timing of catch per unit effort in this fishery based on interviews with fishermen. Figures from Snow 1950.

A.

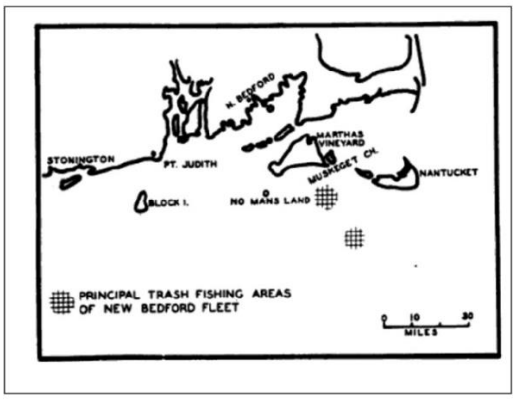

B.

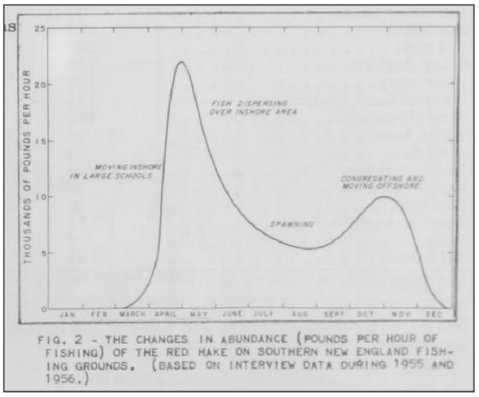

FIG. 2 - THE CHANGES IN ABUNDANCE (POUNDS PER HOUR OF FISHING) OF THE RED HAKE ON SOUTHERN NEW ENGLAND FISHING GROUNDS. (BASED ON INTERVIEW DATA DURING 1955 AND 1956.)

Figure 1.6. Map of the small mesh exempted areas in the Gulf of Maine and the seasonal timing of their opening. The small mesh exempted areas were designed to minimize bycatch in the whiting fishery.

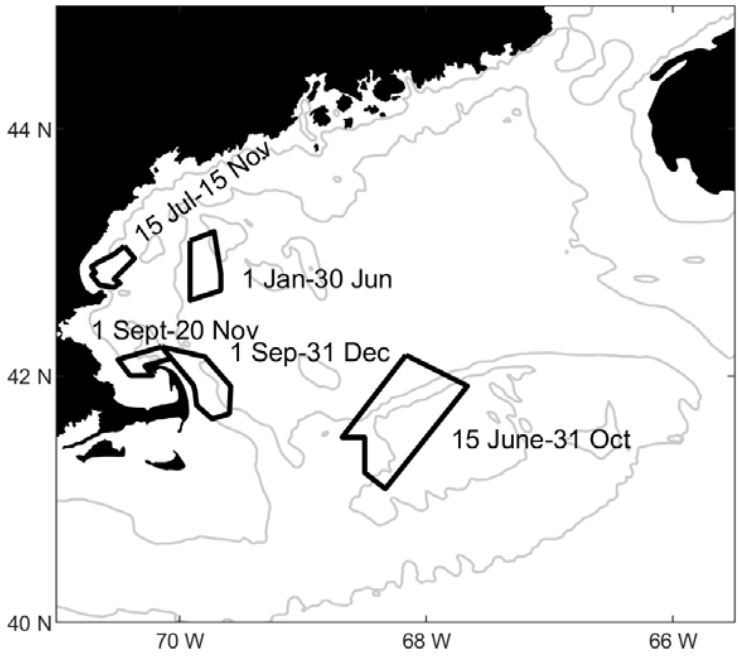

Figure 1.7. Maps of the observed catches of red hake (deciles of catch) based on the declared primary target species. The declaration of red hake as a primary target species is extremely rare.

A. Observed red hake catch (1994-2018) All target species

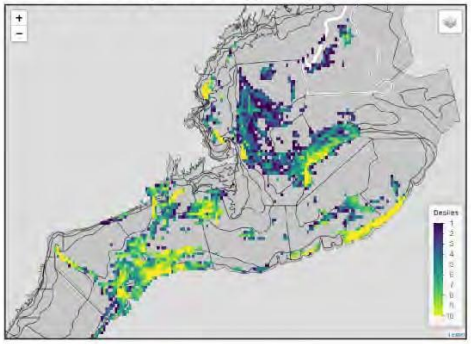

B. Observed red hake catch (1994-2018) Whiting target

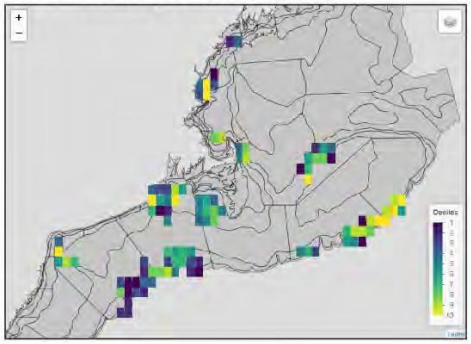

C. Observed red hake catch (1994-2018) Squid target

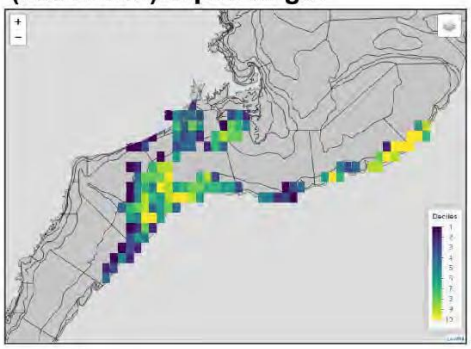

D. Observed red hake catch (1994-2018) Other target species

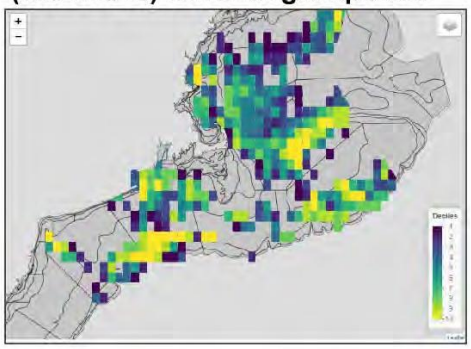

Figure 1.8 Maps of the observed catches of red hake (deciles of catch) by three-month time block in all fisheries.

A. Observed red hake catch (1994-2018) January-March

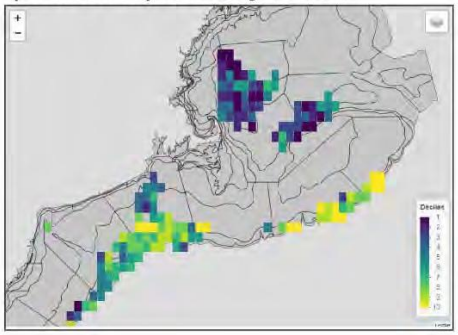

B. Observed red hake catch (1994-2018) April-June

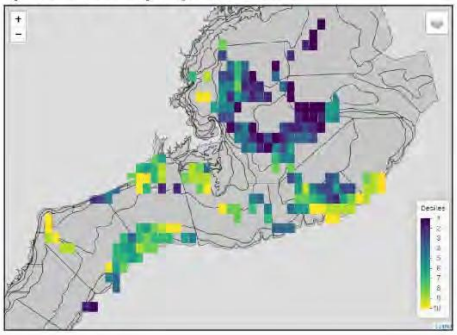

C. Observed red hake catch (1994-2018) July-September

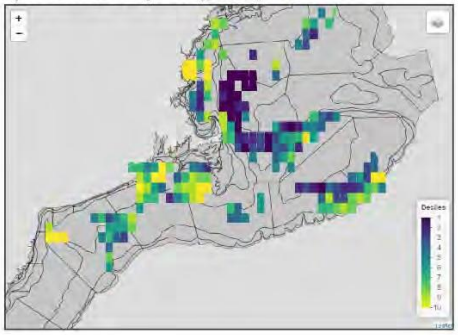

D. Observed red hake catch (1994-2018) October-December

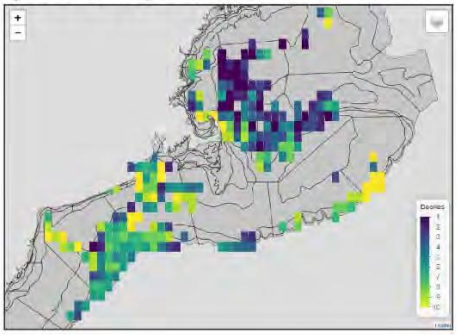

Figure 1.9. Number of tows with primary targets of squid, whiting, red hake, and butterfish. These taxa make up the majority of the small mesh targeted species with notable catches of red hake.

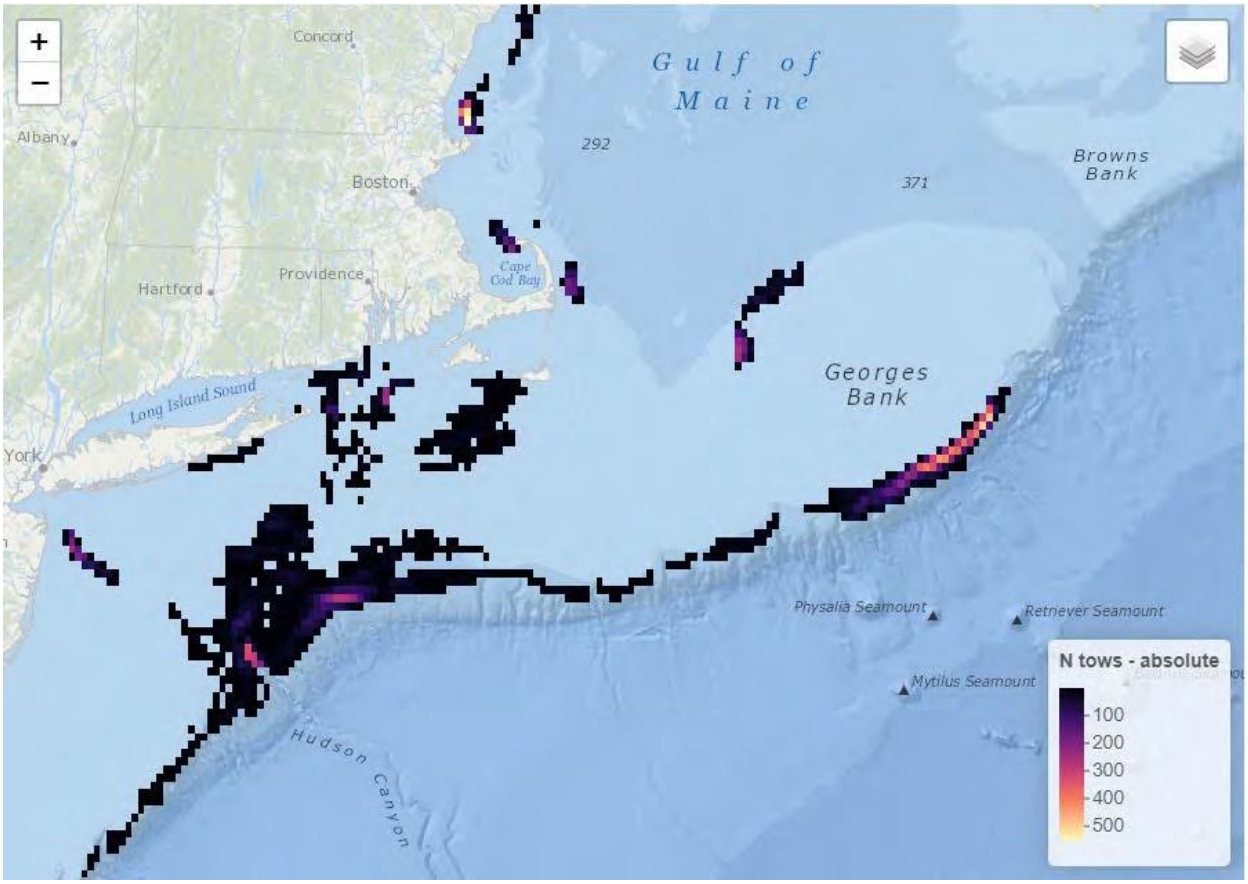

Figure 1.10. Red hake fishing grounds sampled by Richter (1968), referred to as Scotian Shelf (I), northern Georges Bank (II), southern Georges Bank-southern New England slope (III), and Mid Atlantic slope (IV).

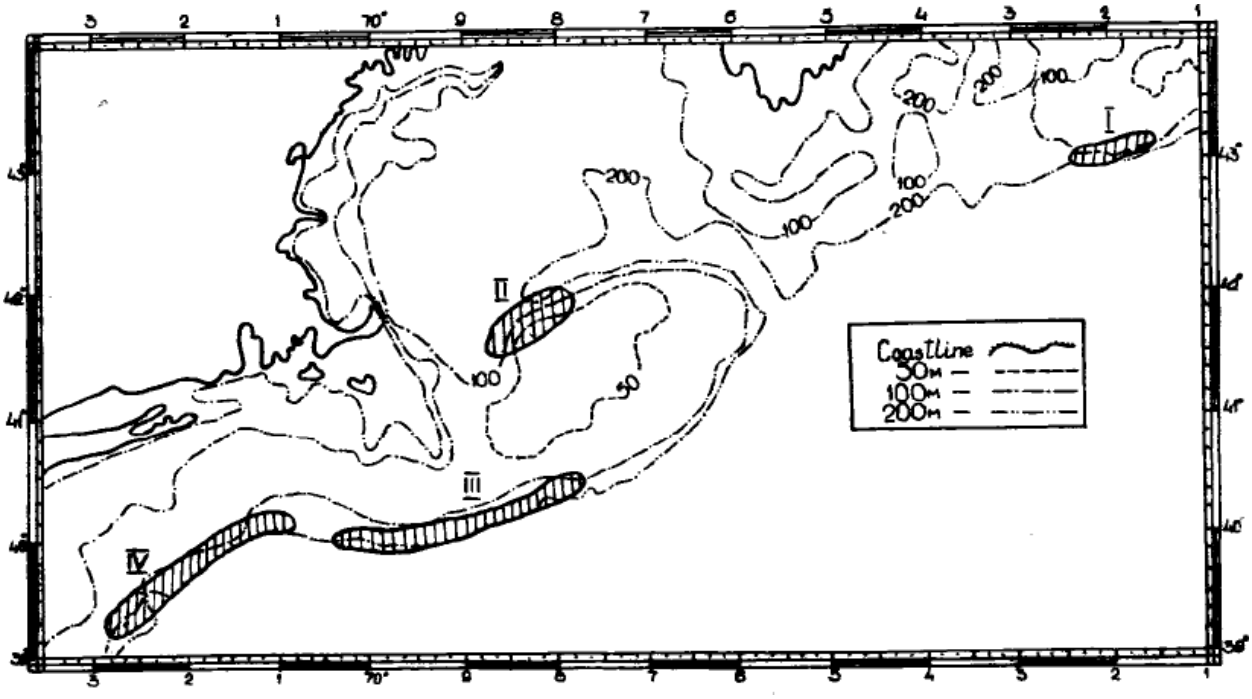

Figure 1.11. Size at age by fishing areas reported by Richter (1970) referred to as southern Georges Bank-southern New England (I), and southern New England-Mid Atlantic Bight (IV).

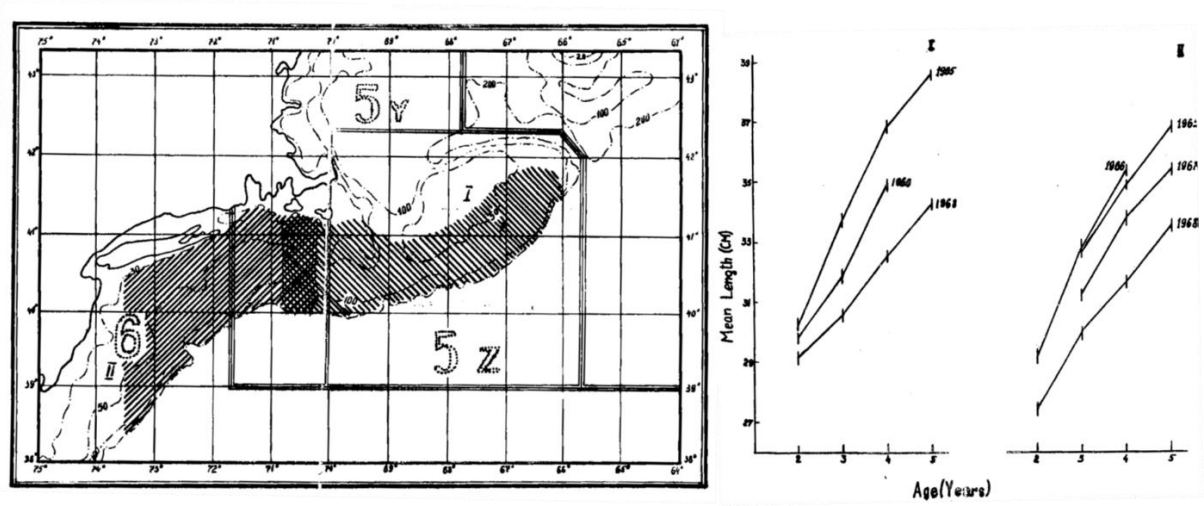

Figure 1.12. Distribution of red hake during the winter (top) and summer (bottom) groundfish surveys (from Anderson 1974b).

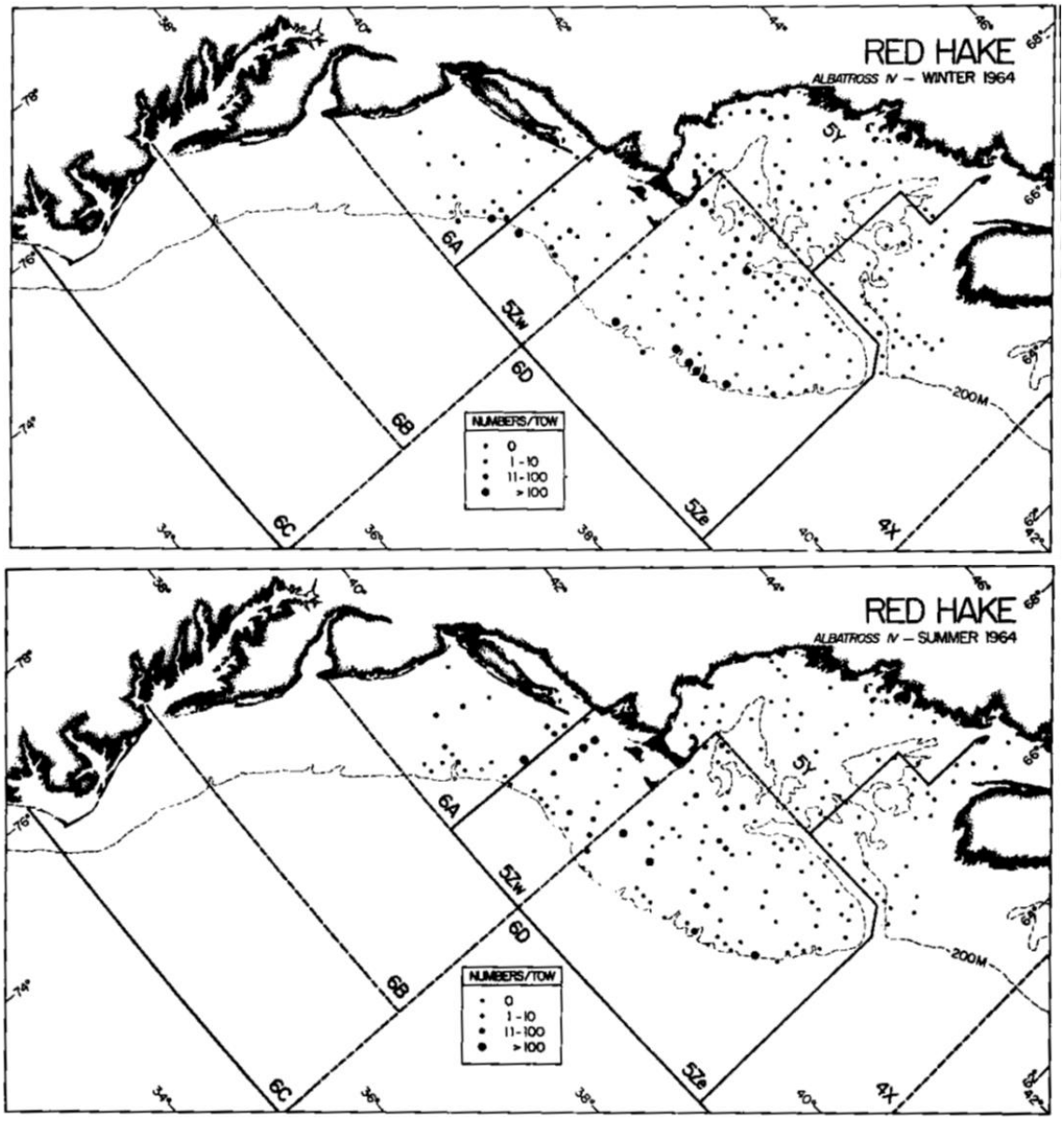

Figure 1.13. Statistical areas used to define the northern and southern red hake stocks (from NEFSC 2011).

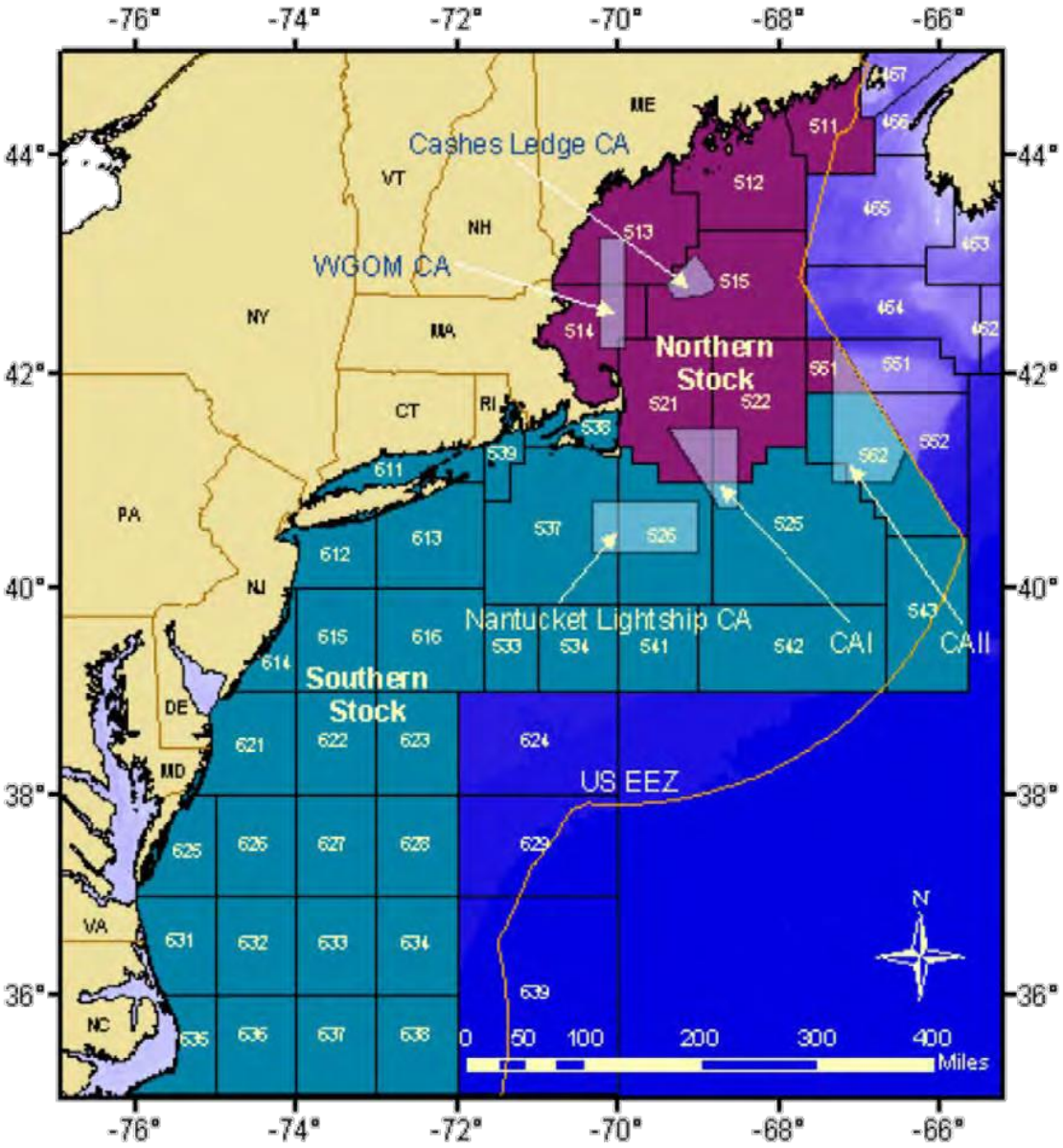

Figure 1.14. Size (cm total length) at age comparison between red hake caught in strata 1-19, 61-76 (southern stock) and strata 20-40 (northern stock) for 1957-1974 cohorts (NEFSC 2011).

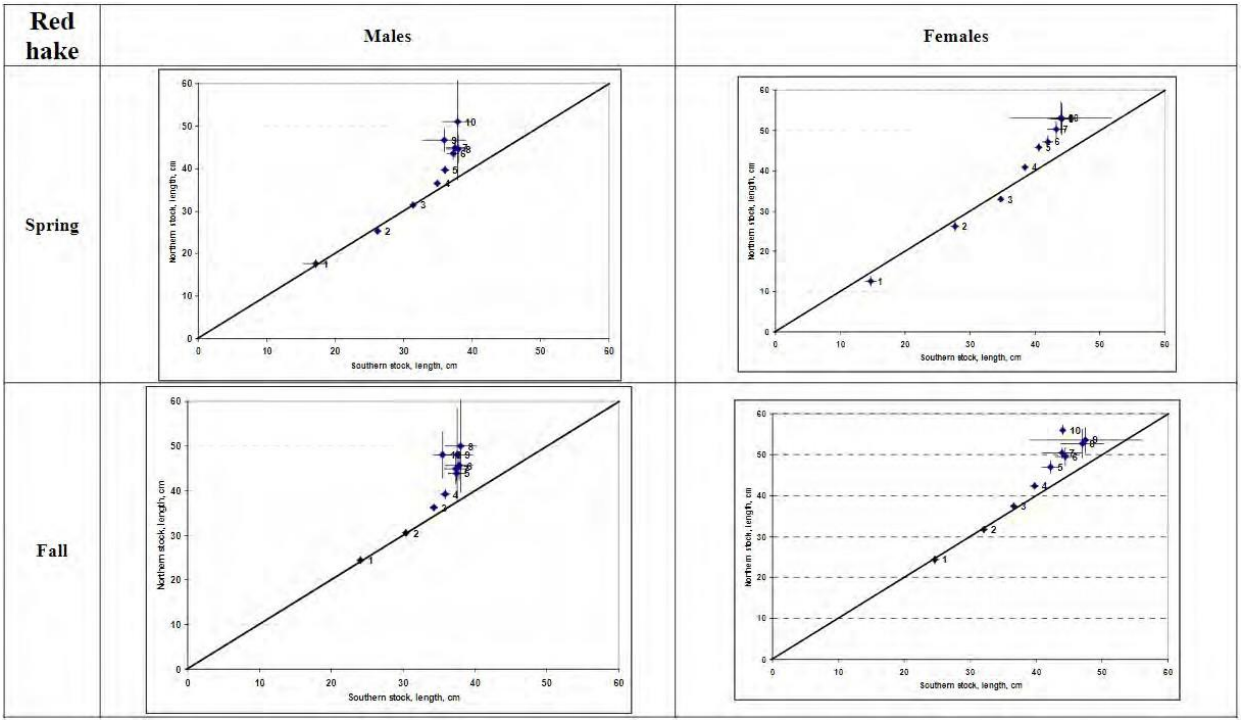

Figure 2.1. Map of the four regions (SS: Scotian Shelf, GOM: Gulf of Maine, GB: Georges Bank, SNE: southern New England) and 12 sub-regions used in analyses of the fisheries-independent survey data. Sub-regions are defined based on groupings of survey strata. The listed survey strata are from the NEFSC trawl survey and for the Scotian Shelf, the Canadian Department of Fisheries and Oceans (DFO) summer trawl survey.

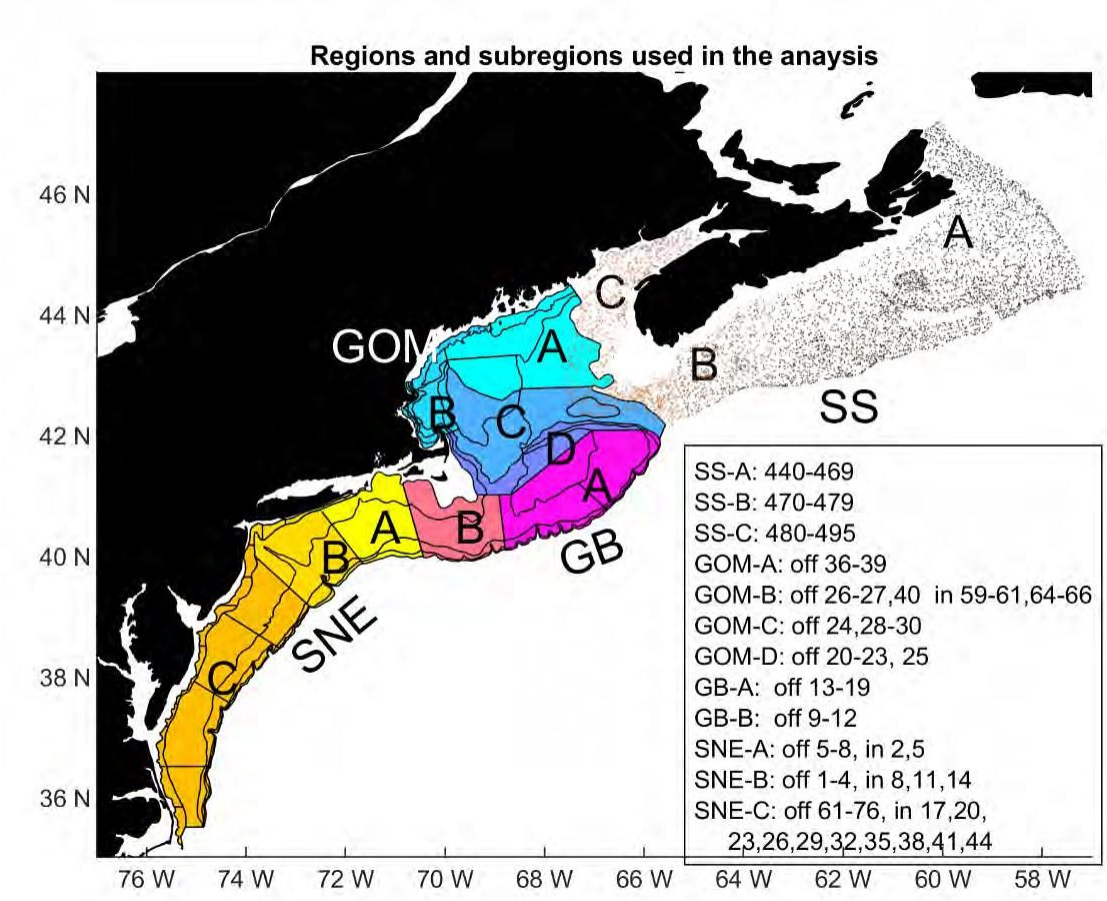

Figure 2.2. Hierarchical clustering results from the DMIS data set. Results indicate that most vessels have landed the southern stock (shown in yellow). A smaller proportion of vessels have landed both stocks, but these vessels have landed smaller numbers of red hake. The vessels participating in Study Fleet are highlighted (labels with darker text). Note, Study Fleet vessels exist in all but one cluster (blue for vessels > 50,000 lbs).

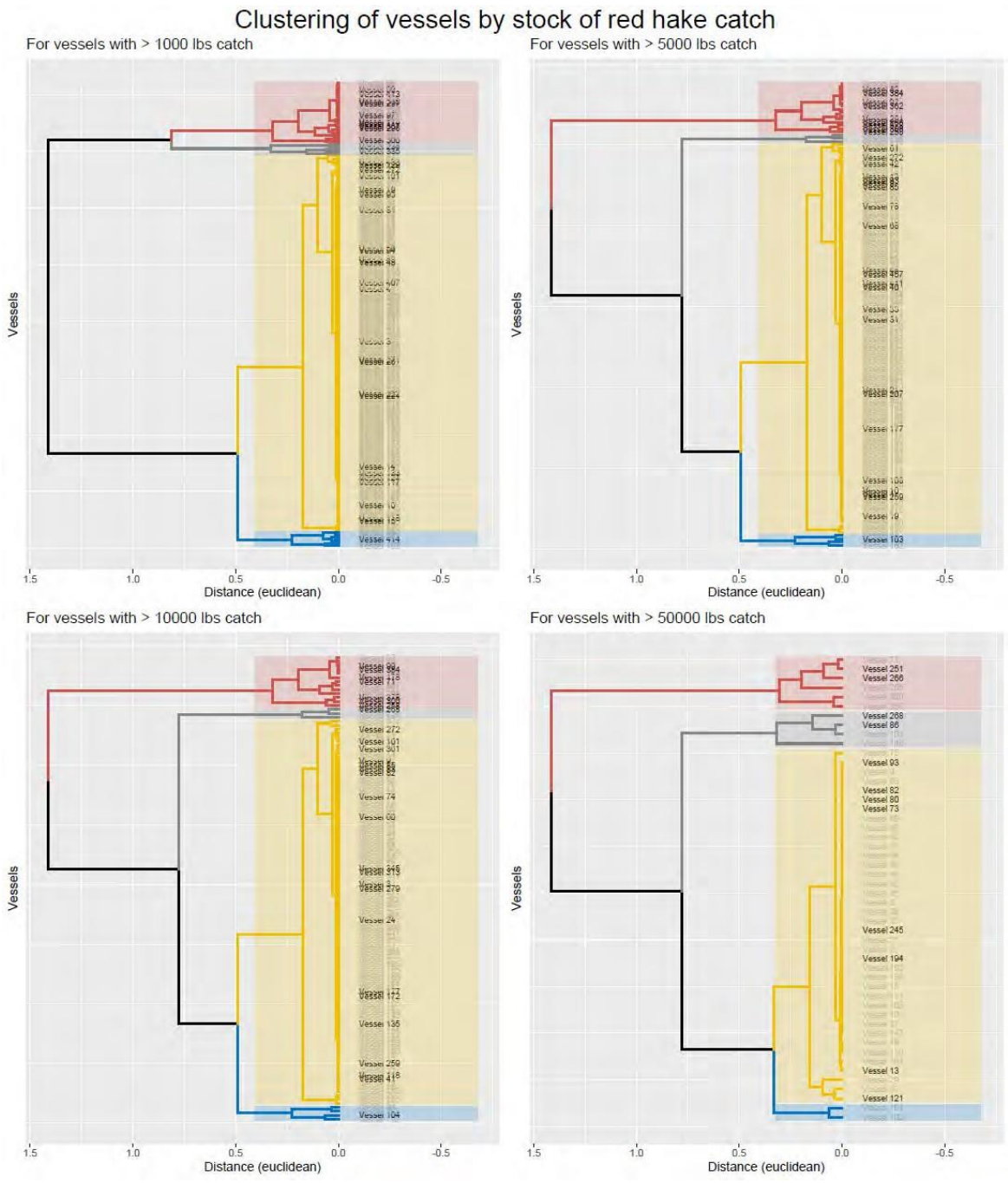

Figure 2.3. Proportions of landings from each of the current stocks from the DMIS data set for each vessel. Landings (in lbs) are summed across the entire time period (one point per vessel). Generally results did not vary much from year to year. Note: axes are not equal.

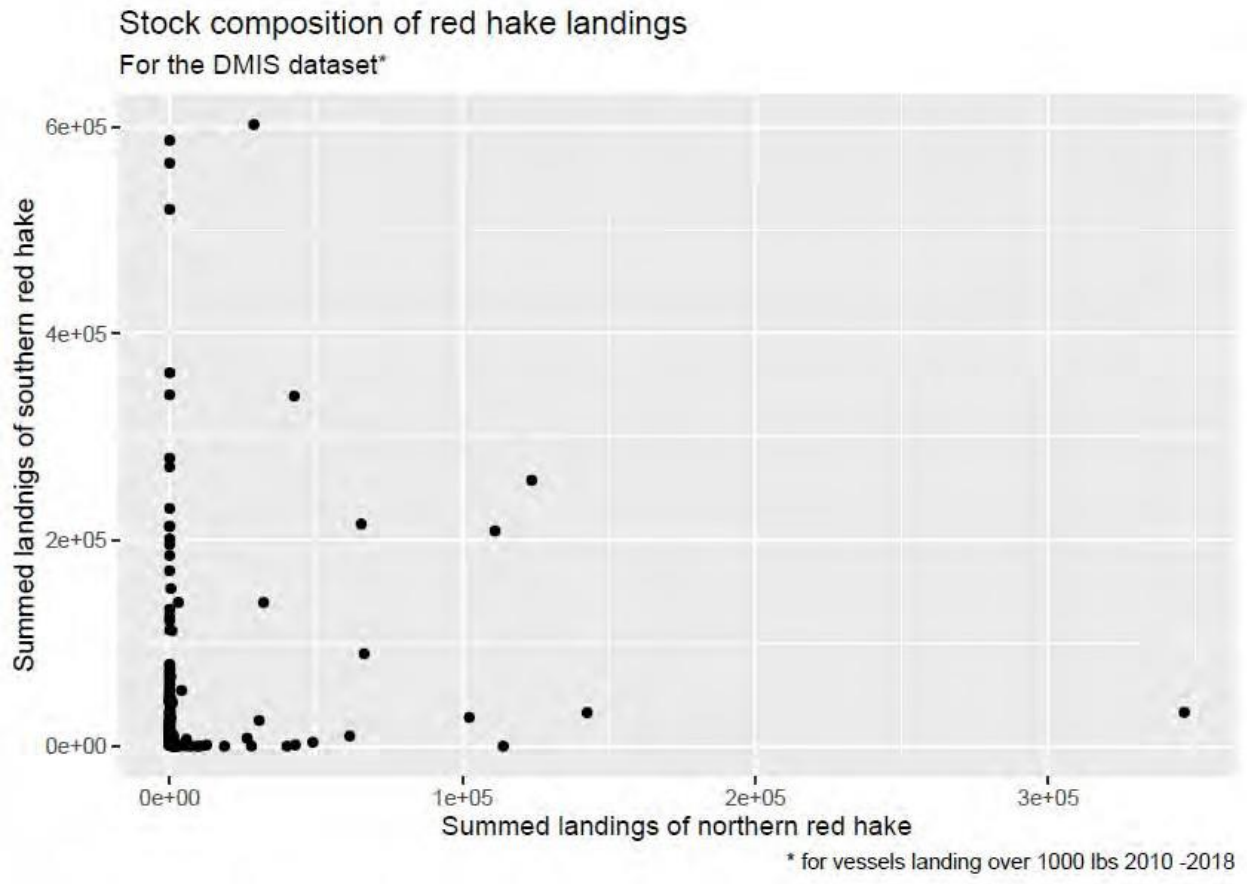

Figure 2.4. Trends in stratified mean biomass per tow for each of the 12 sub-regions. The Scotian Shelf data is from the summer Canadian DFO trawl survey and the Gulf of Maine (GOM), Georges Bank (GB) and Southern New England (SNE) data is from the fall (grey) and spring (black).

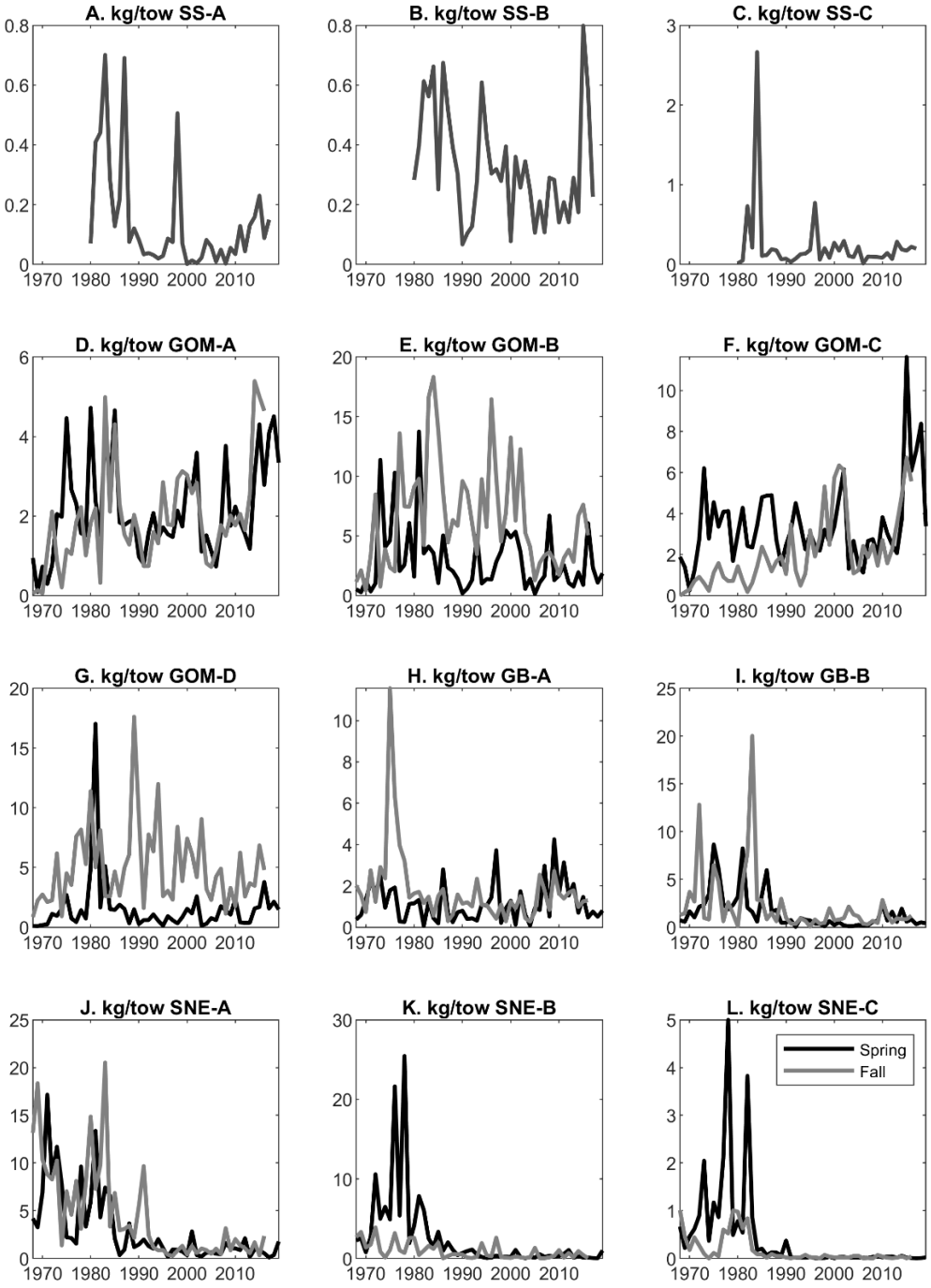

Figure 2.5. Survey indices for the entire shelf, broken out by region and subregion, for the spring and fall.

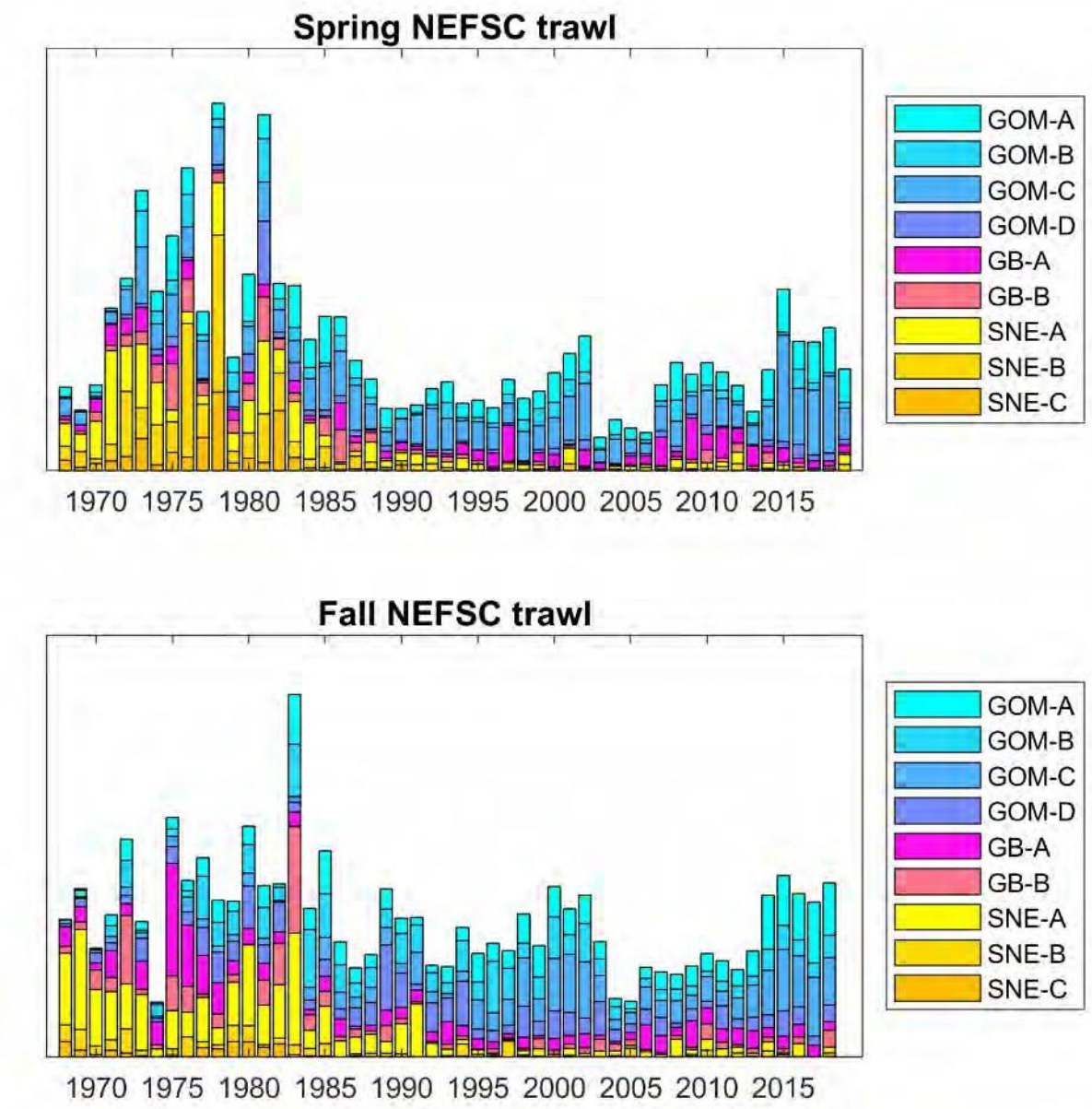

Figure 2.6. Distribution of red hake during the winter (1992-2007), spring (1968-2019), summer (1977-1983), and fall (1968-2018) on the northeast U.S. continental shelf. The strata boundaries are shown with sub-regions demarcated by the colors noted in Figure 2.1.

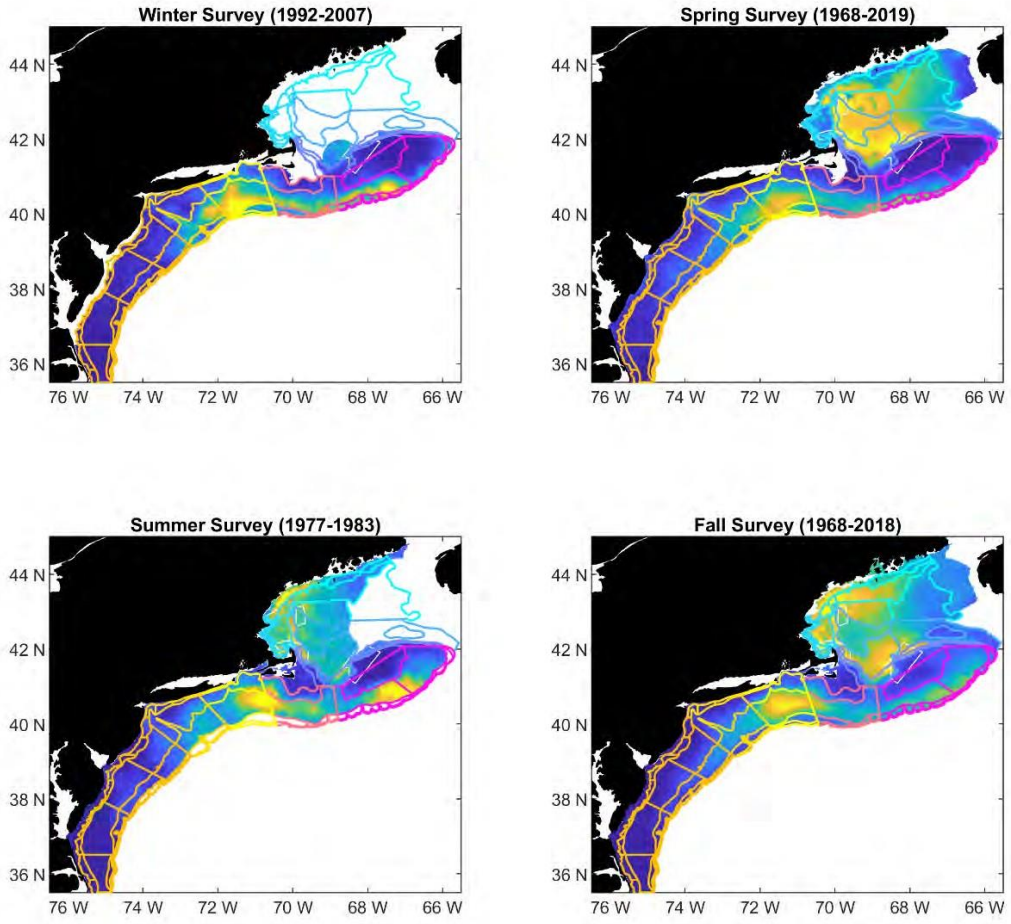

Figure 2.7. Distribution of red hake biomass on the Spring NEFSC trawl survey in blocks of 4-5 years

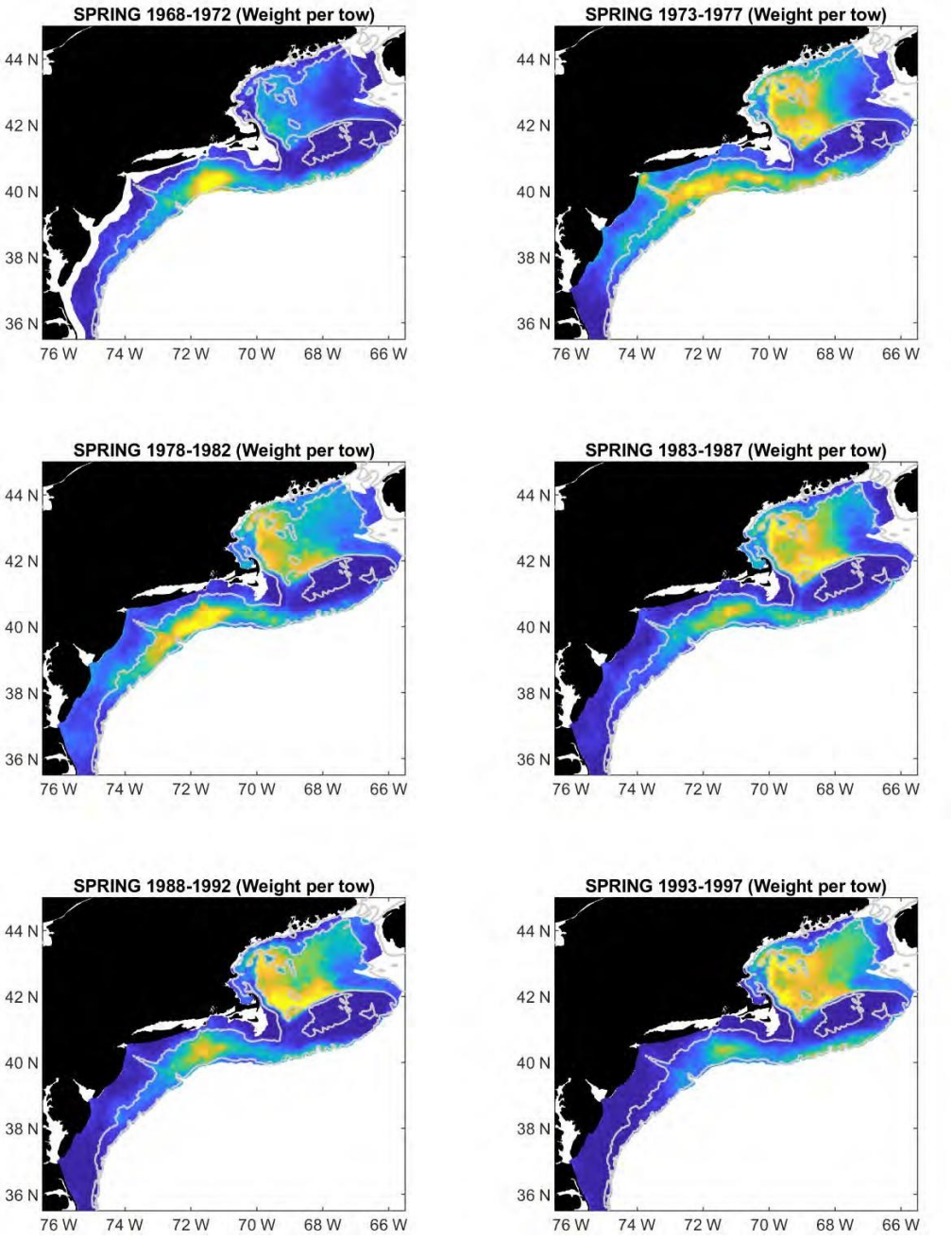

Figure 2.7. cont

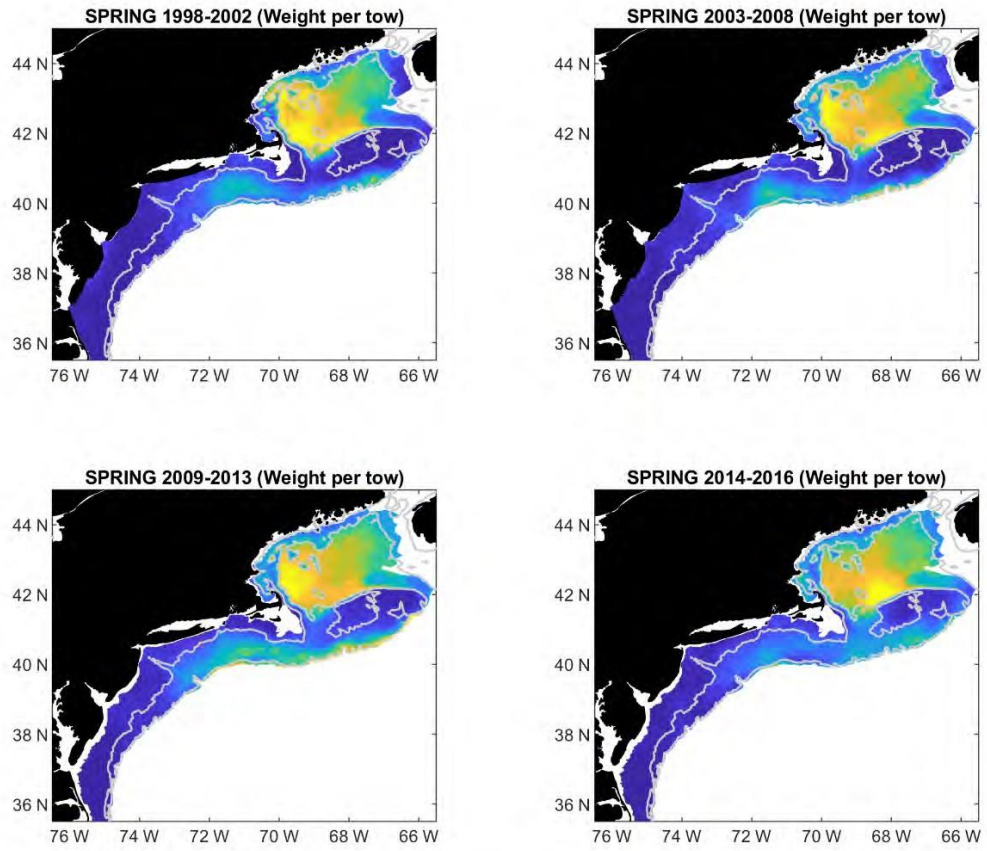

Figure 2.8. Distribution of red hake biomass on the Fall NEFSC trawl survey in blocks of years

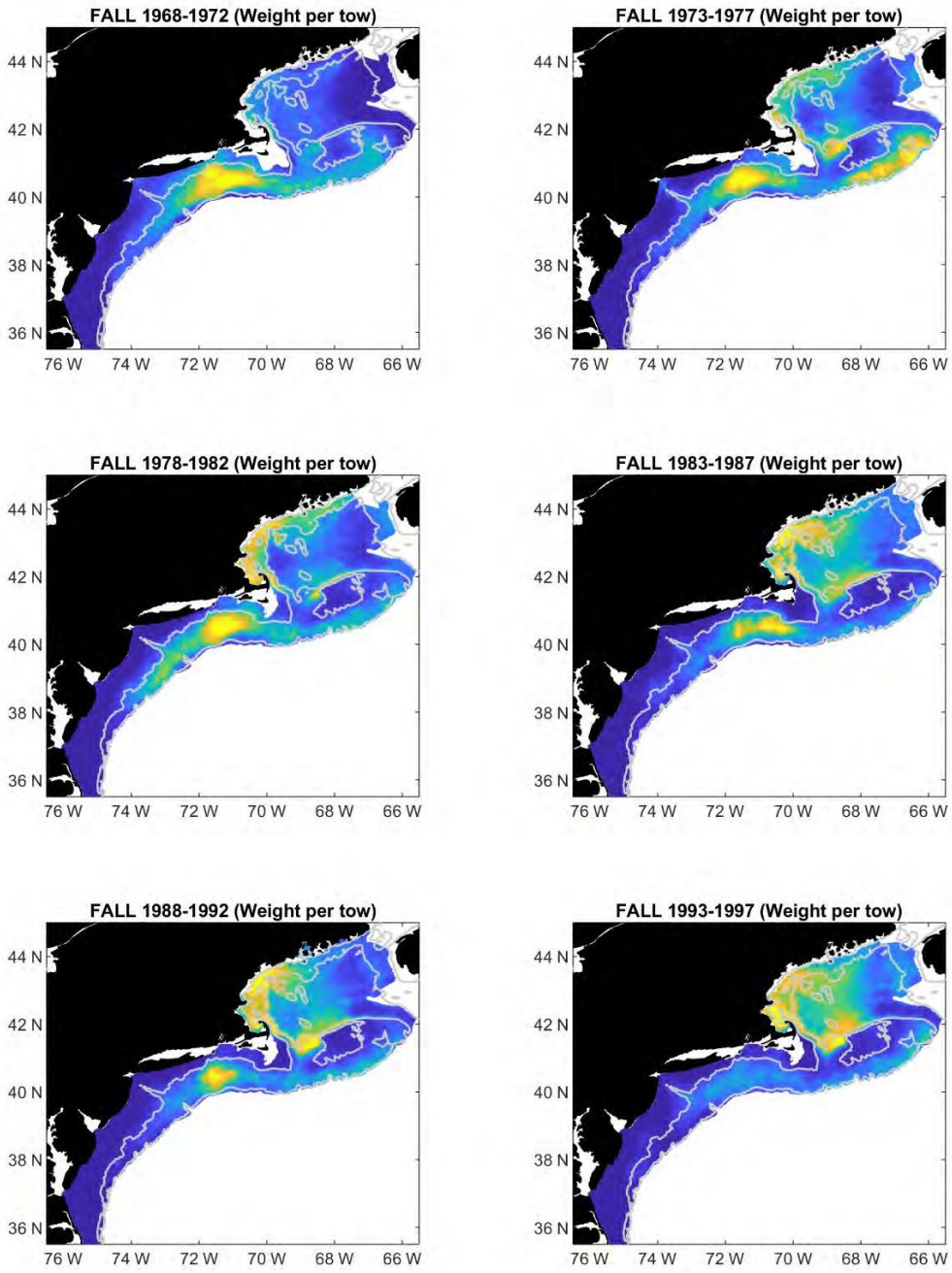

Figure 2.8. (cont)

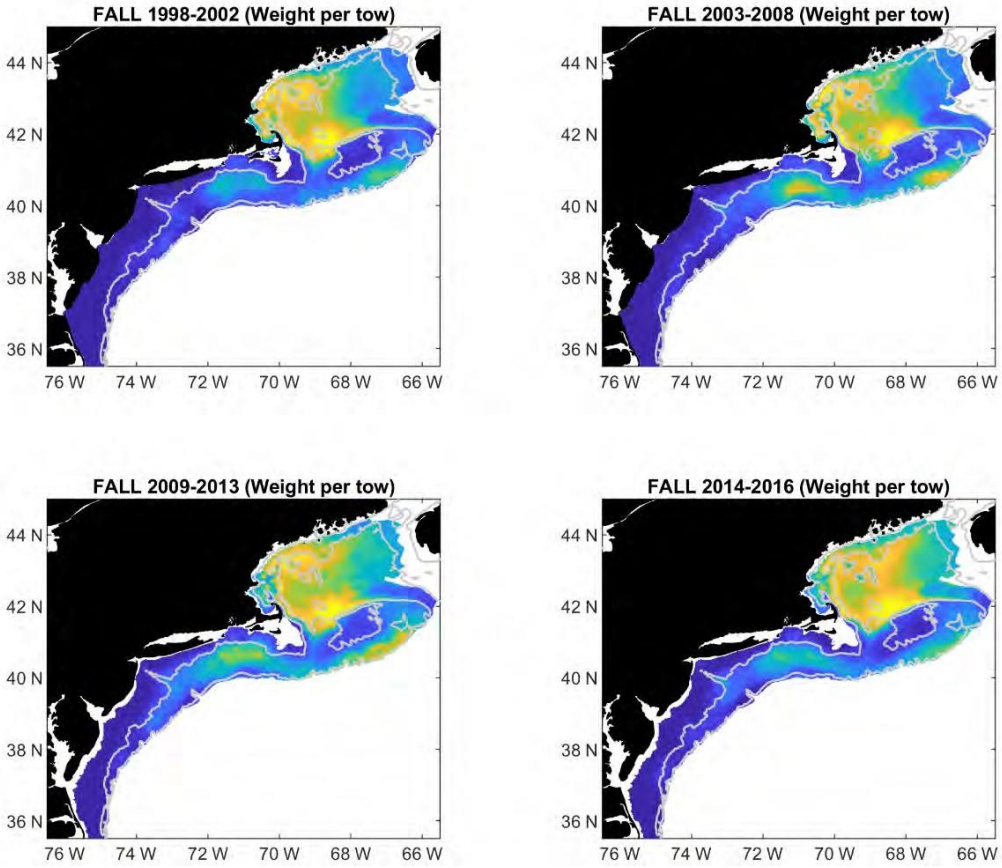

.

Figure 2.9. Weighted mean latitude, longitude and depth for red hake sampled on the Northeast Fisheries Science Center trawl survey.

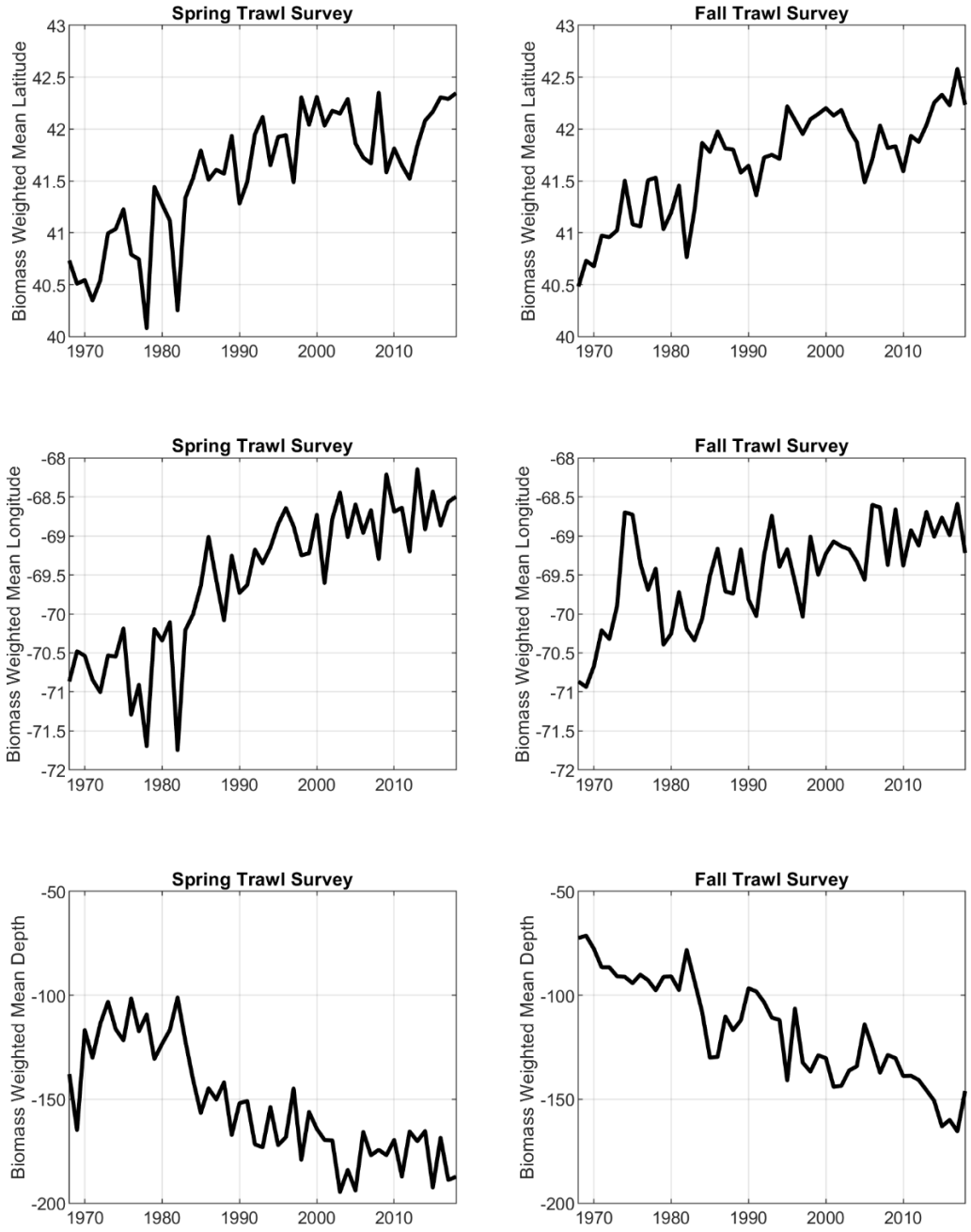

Figure 2.10. Weighted mean depth across the time series by sub-region and season. Sub-regional definitions are in Figure 2.1.

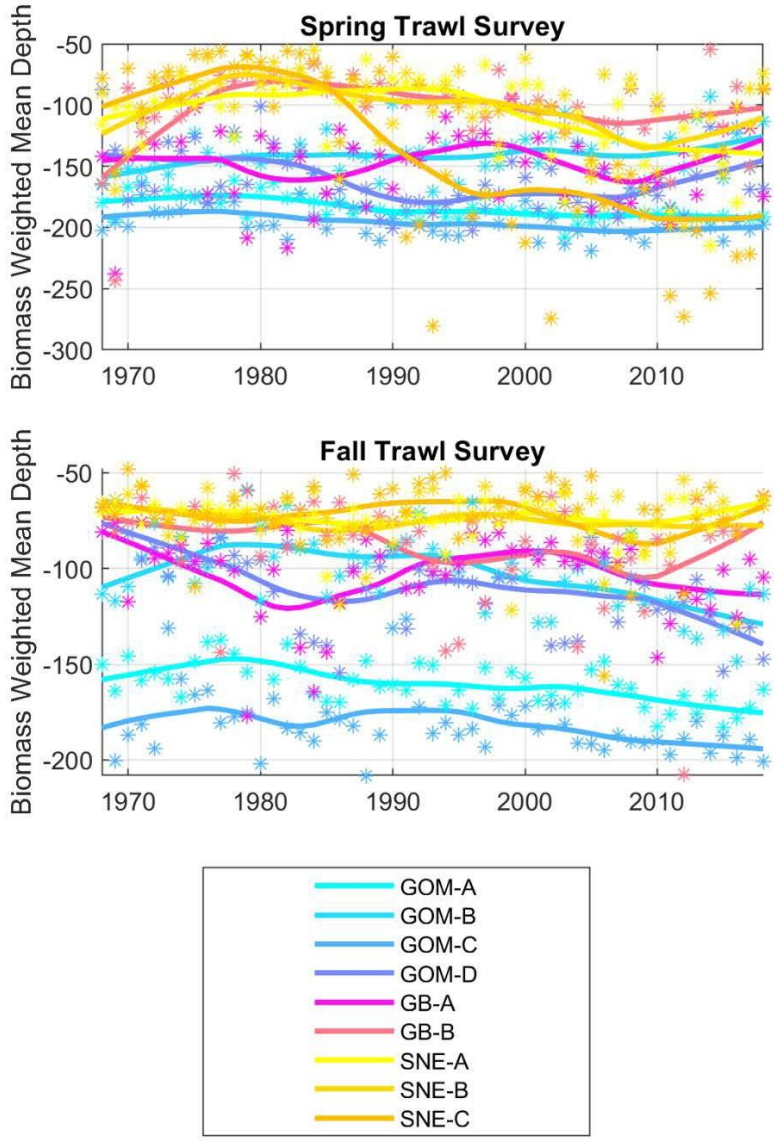

Figure 2.11. Weighted mean temperature of collection by subregion on the NEFSC trawl survey. The black line corresponds the shelfwide average temperature of collection. Sub

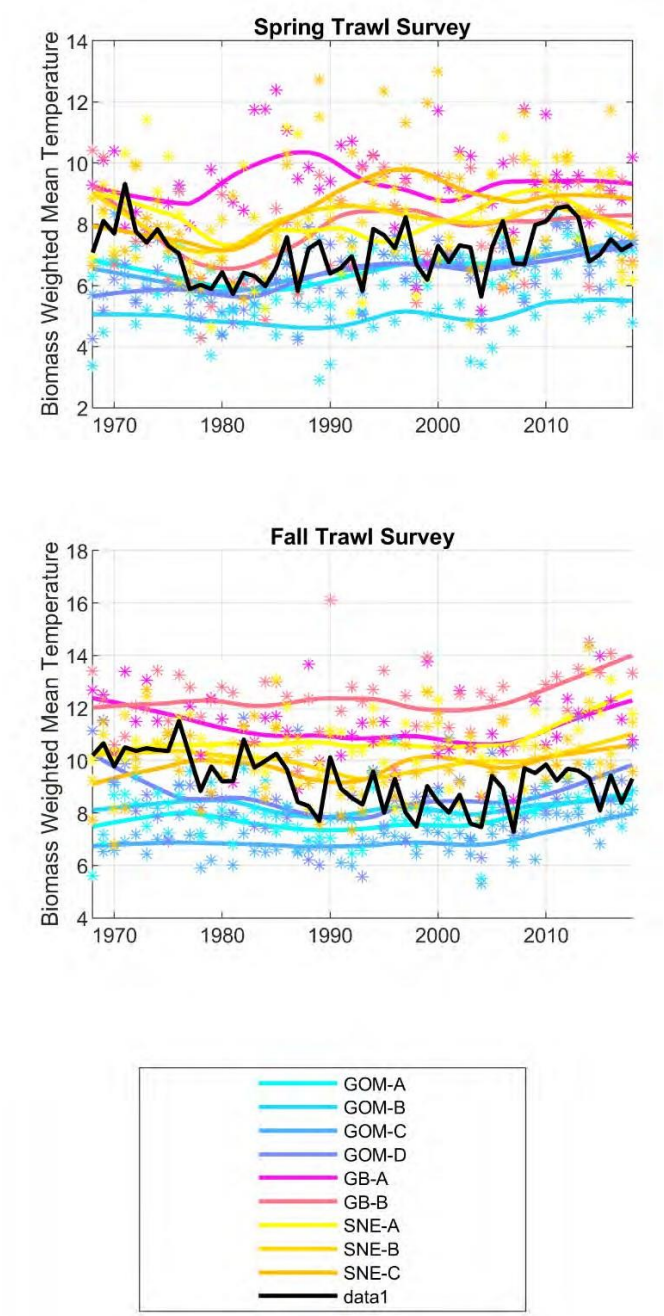

Figure 2.12. Proportion of abundance by length class in each of the 9 sub-regions over time on the spring trawl survey.

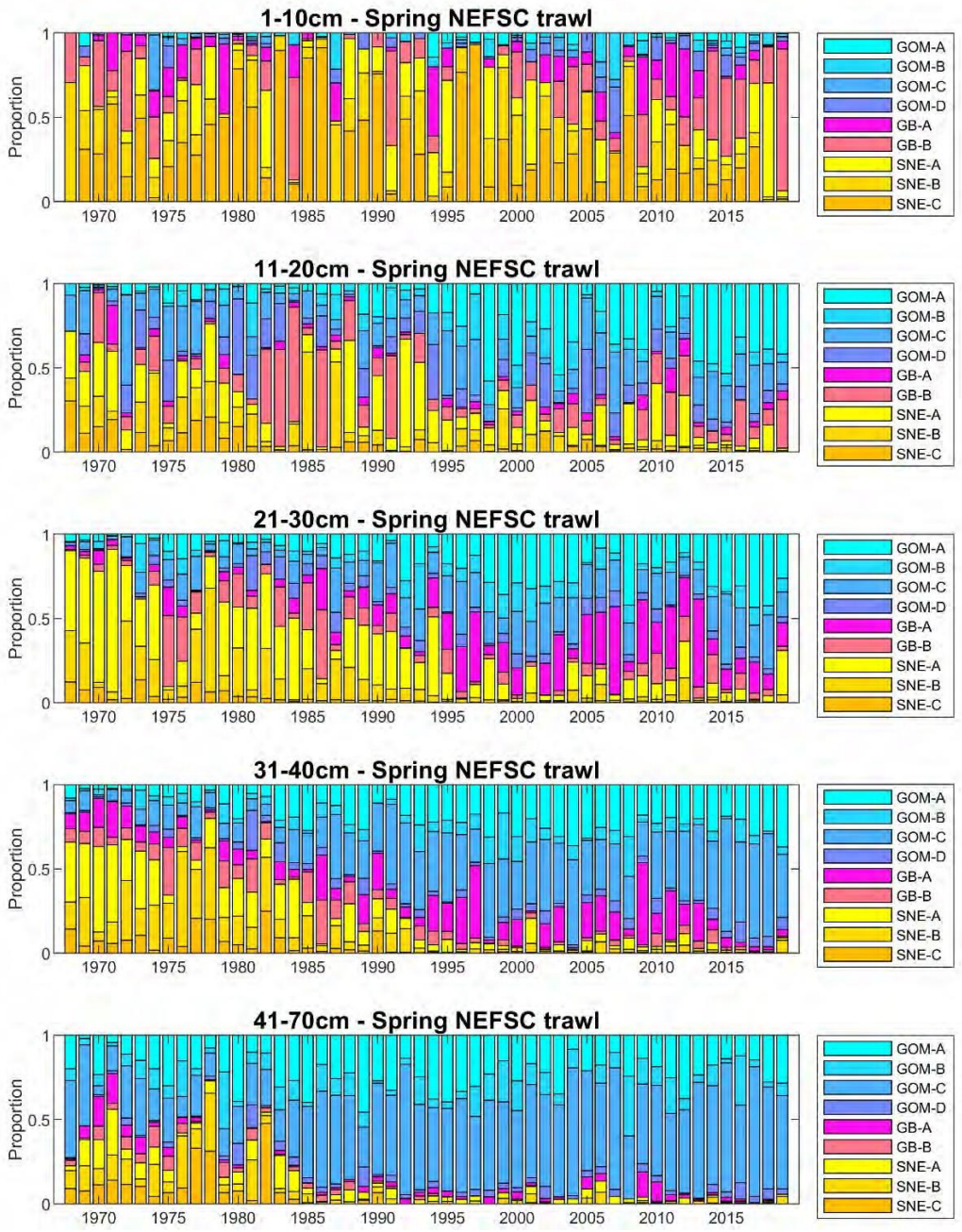

Figure 2.13. Length-frequency distribution on the spring trawl survey over time broken out by sub-region.

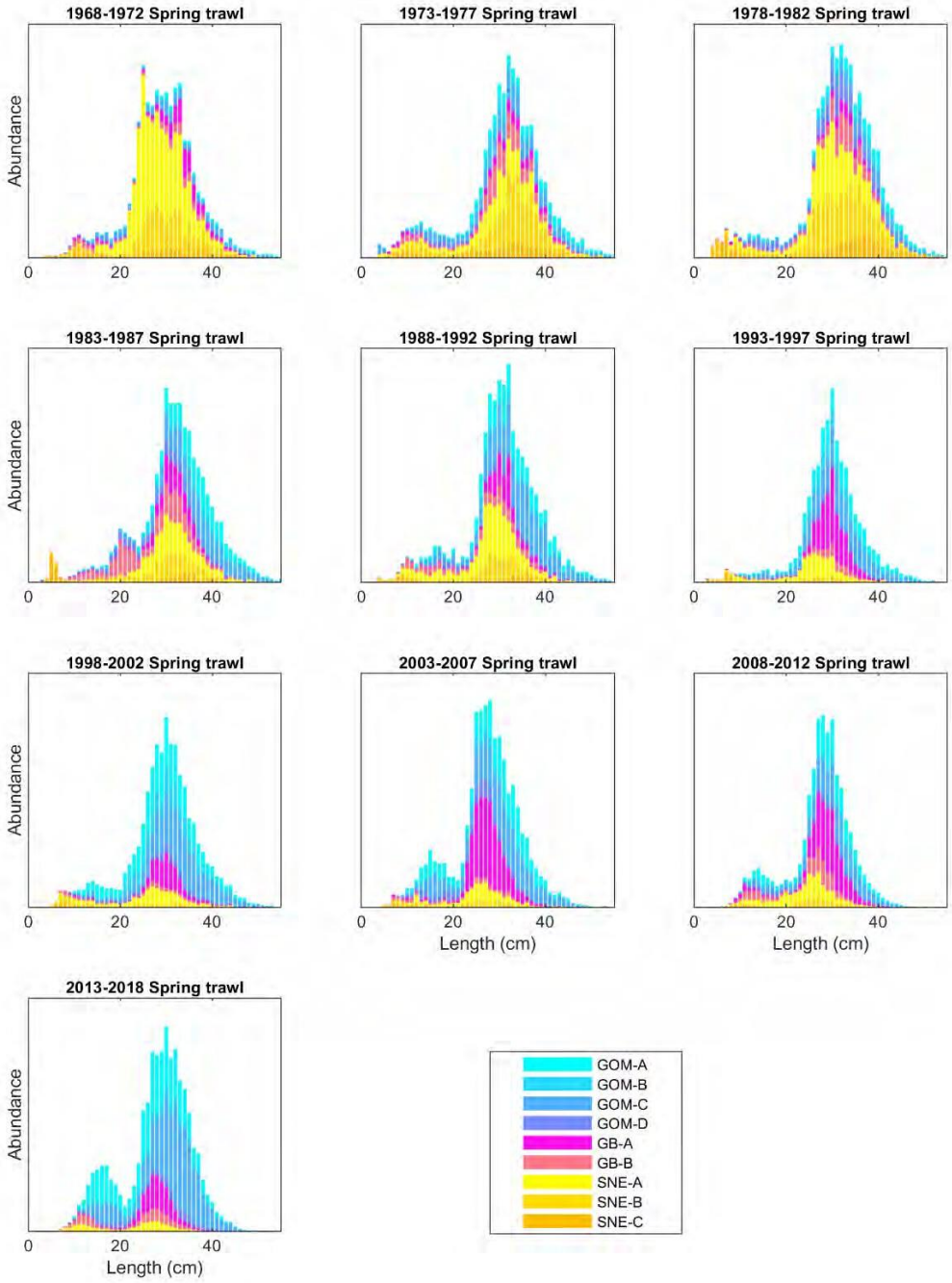

Figure 2.14. Proportion of abundance by length class in each of the 9 sub-regions on the fall trawl survey.

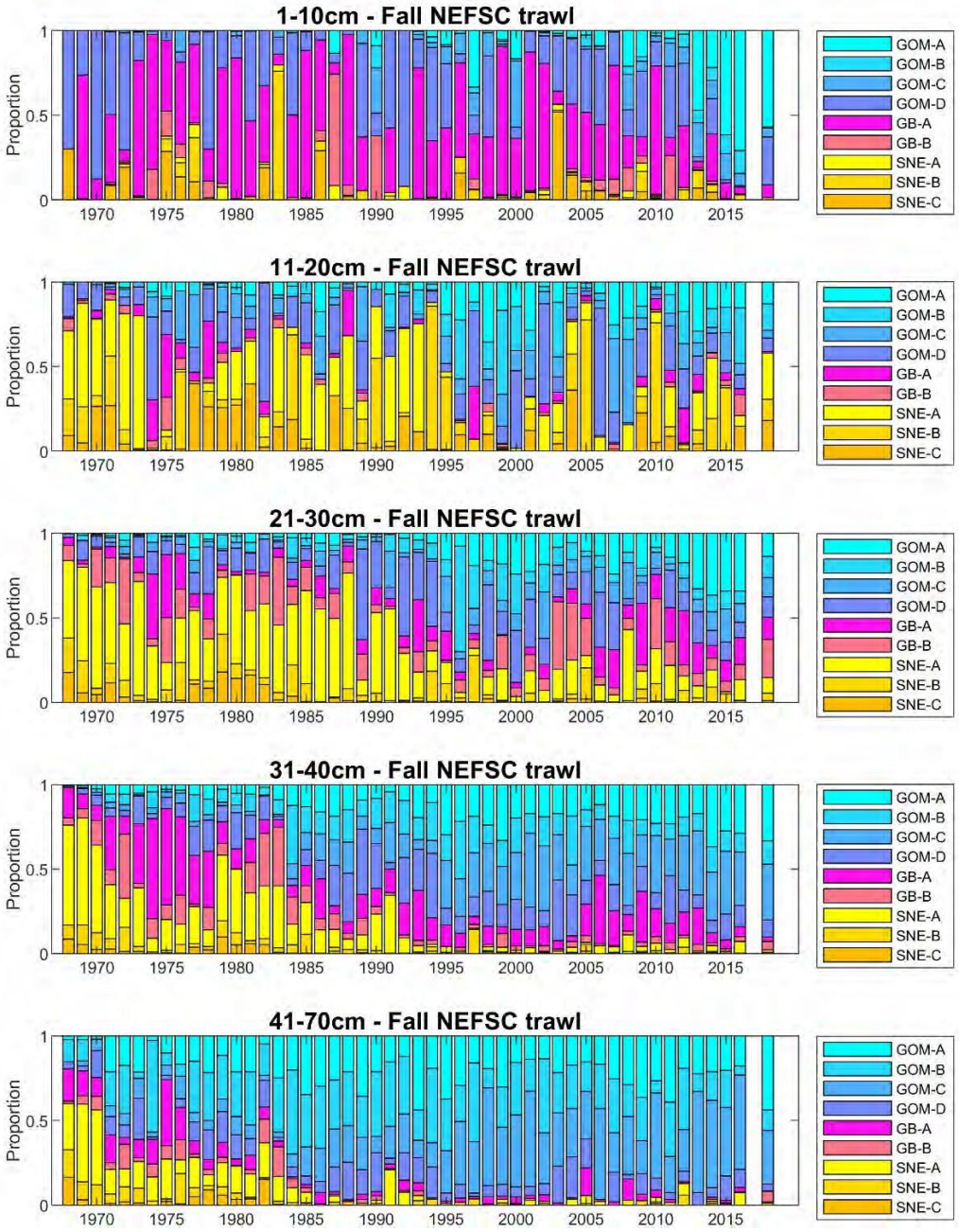

Figure 2.15. Length-Frequency distribution on the fall trawl survey over time broken out by sub-region.

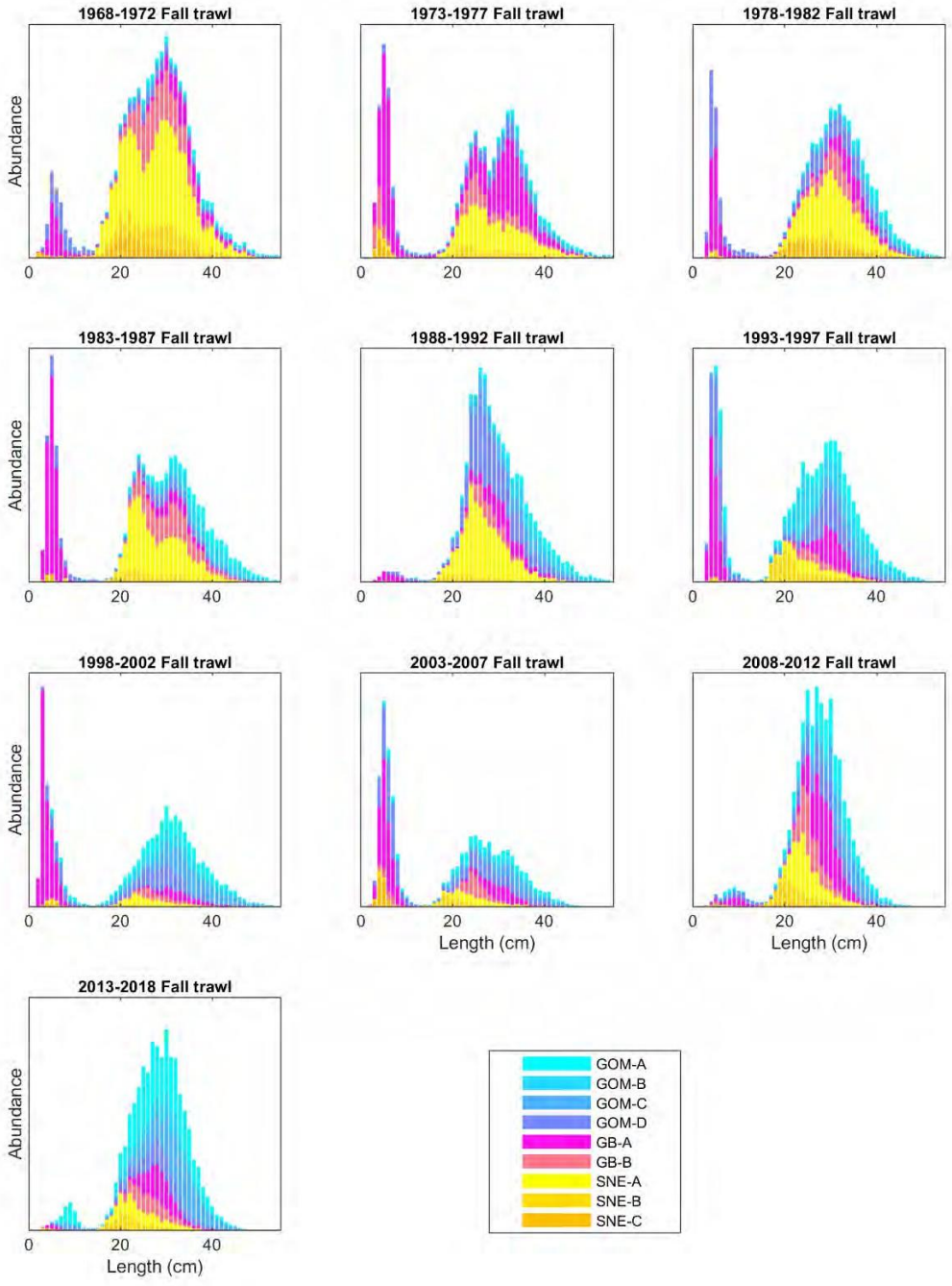

Figure 2.16. The 90th percentile of the cumulative length frequency distribution for each of the sub-regions when only >17cm fish (i.e. young-of-year excluded) are considered.

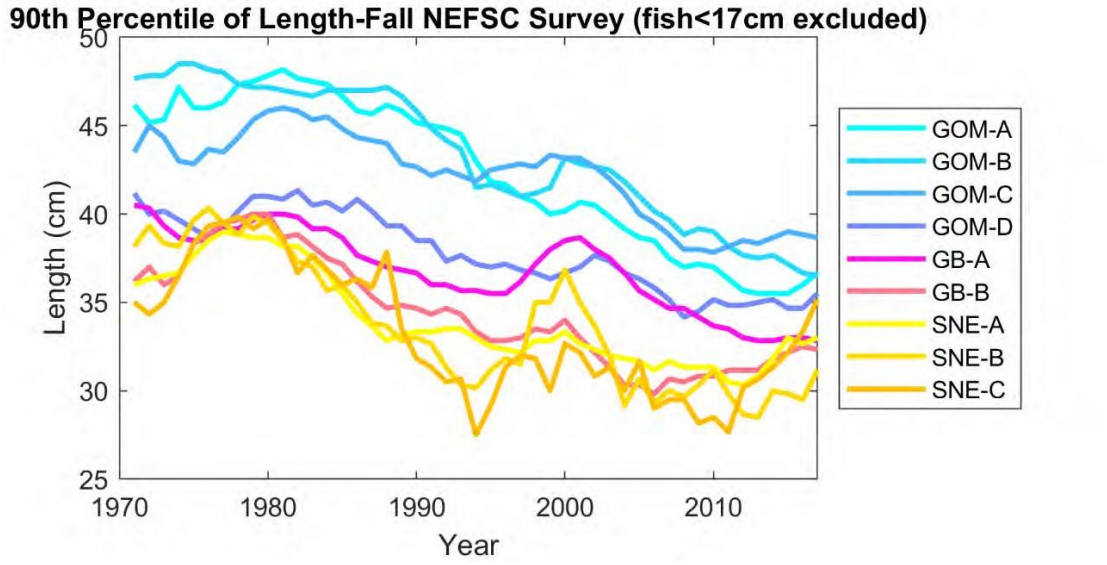

Figure 2.17. Schematic of the methodology used in the implementation of the management unit estimator from Cope and Punt (2009).

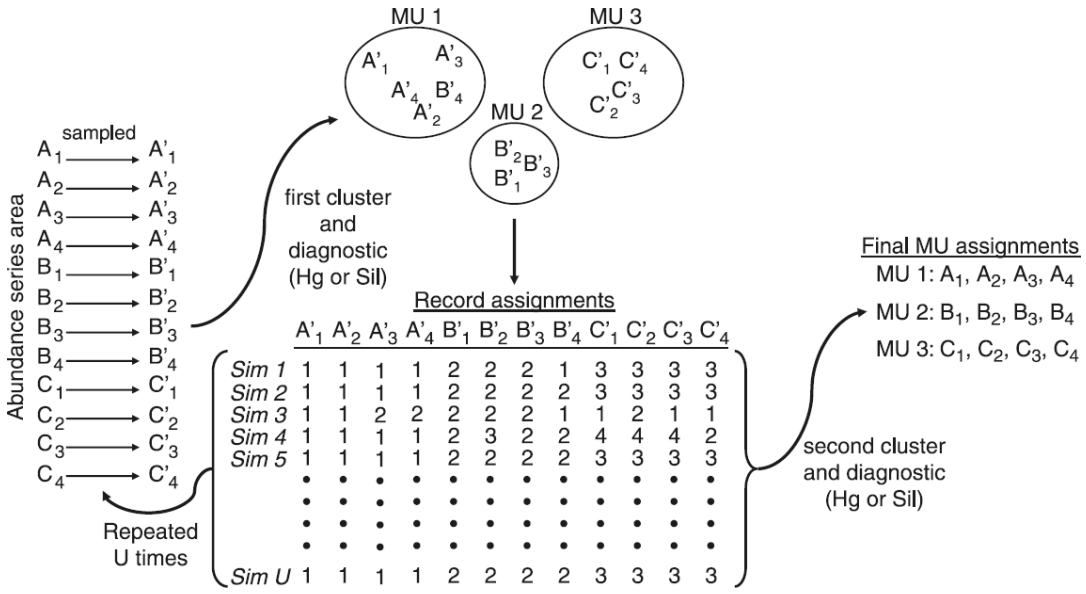

Figure 2.18. Results of the management unit estimator when both the spring and fall data are used. The left hand plots show the sub-region groupings when the number of units (k) is set to 2-4. The right hand plots show the associates silhouette values for each sub-region as well as the average values. Higher silhouette values indicate more support for the clustering. Sub-region designations are shown in Figure 2.1.

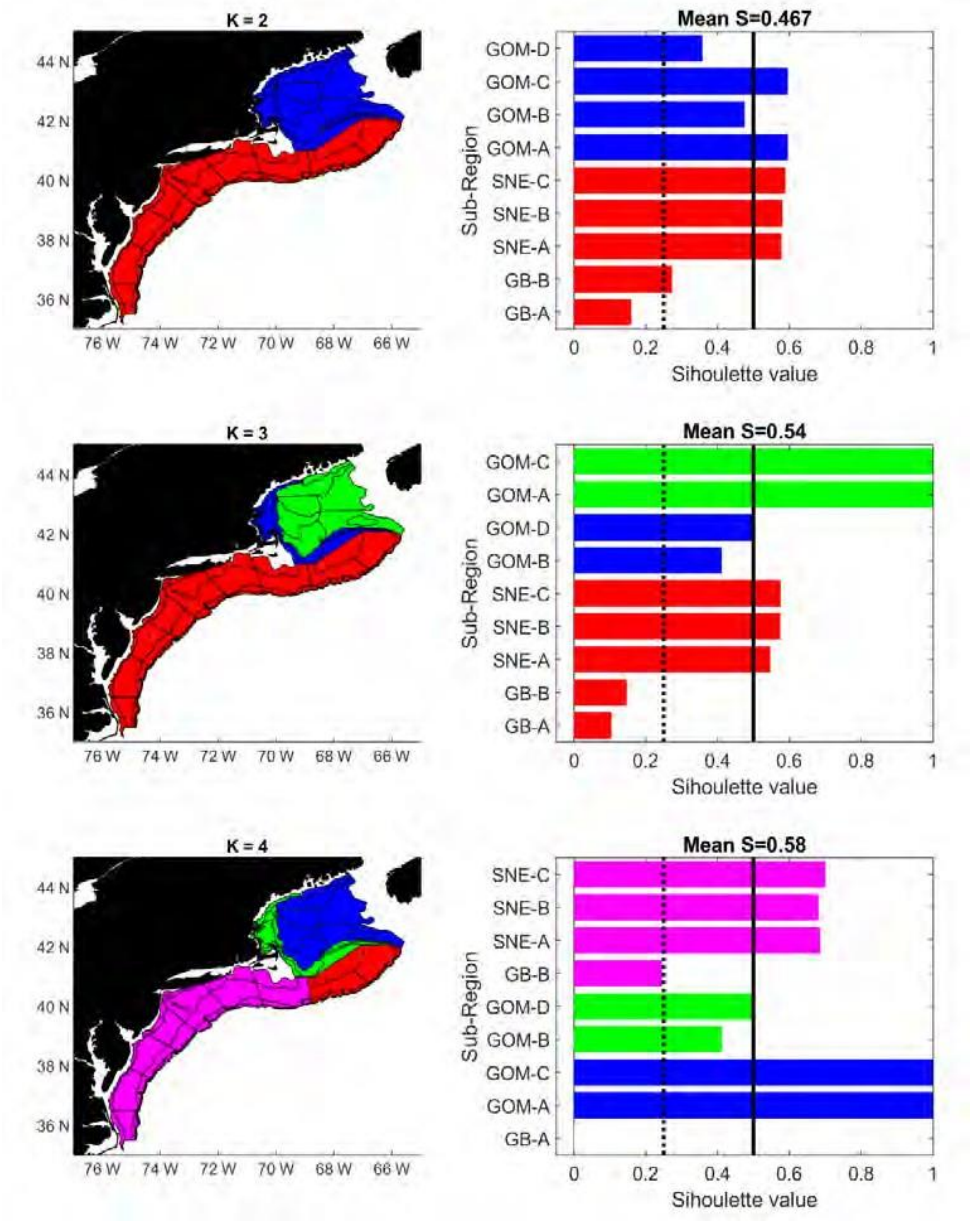

Figure 2.19. Results of the management Unit estimator when only the spring data are used. The left hand plots show the sub-region groupings when the number of units (k) is set to 2-4. The right hand plots show the associates silhouette values for each sub-region as well as the average values. Higher silhouette values indicate more support for the clustering. Sub-region designations are shown in Figure 2.1.

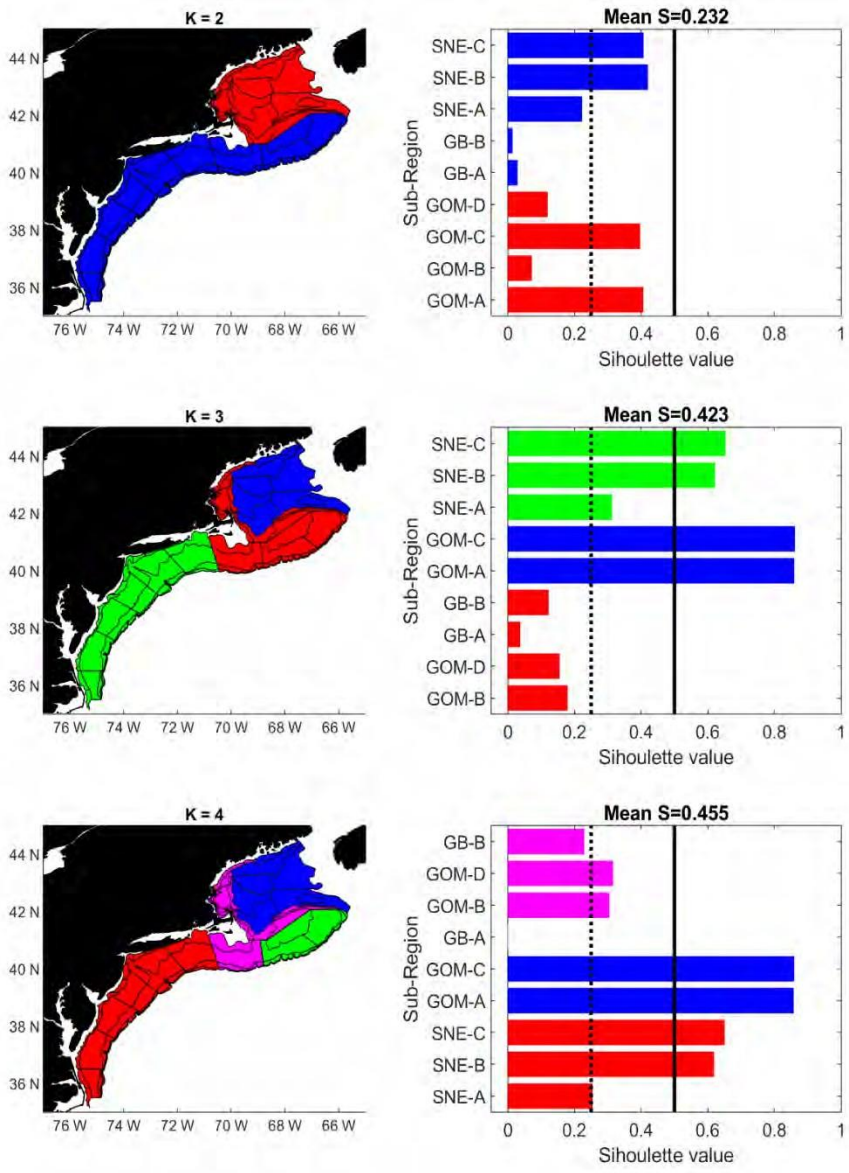

.

Figure 2.20. Results of the management unit estimator when only the fall data are used. The left hand plots show the sub-region groupings when the number of units (k) is set to 2-4. The right hand plots show the associates silhouette values for each sub-region as well as the average values. Higher silhouette values indicate more support for the clustering. Sub-region designations are shown in Figure 2.1.

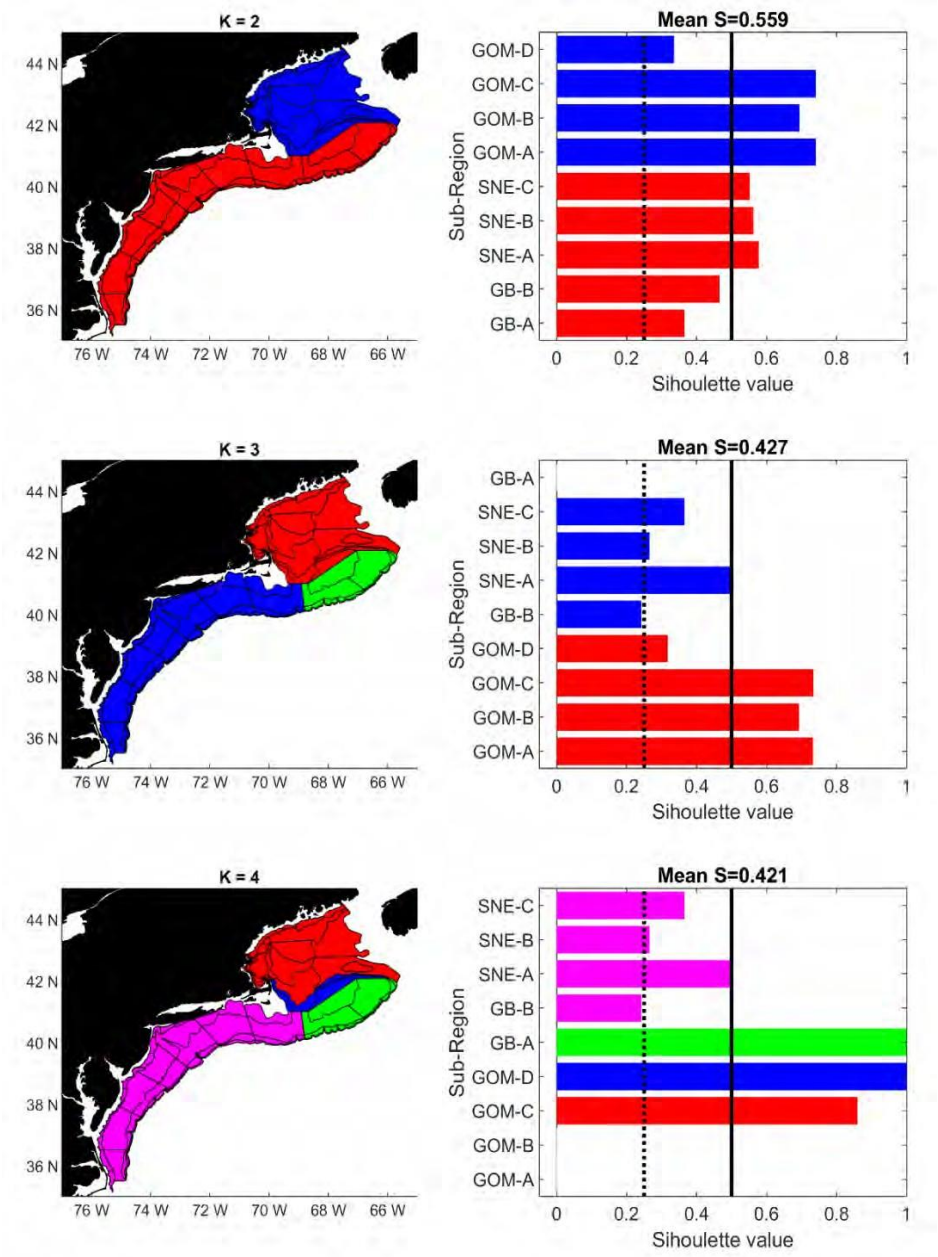

Figure 2.21. Results of the occupational probability models for red hake in the spring. A) and B) Variables included in the model, lower mean minimum depth, and higher times the root, Gini decrease and accuracy decrease all indicate increased importance in the model. C. Map of average occupational probability and D) change in occupational probability across the northeast shelf. E) Sub-regional trends in average occupational probability.

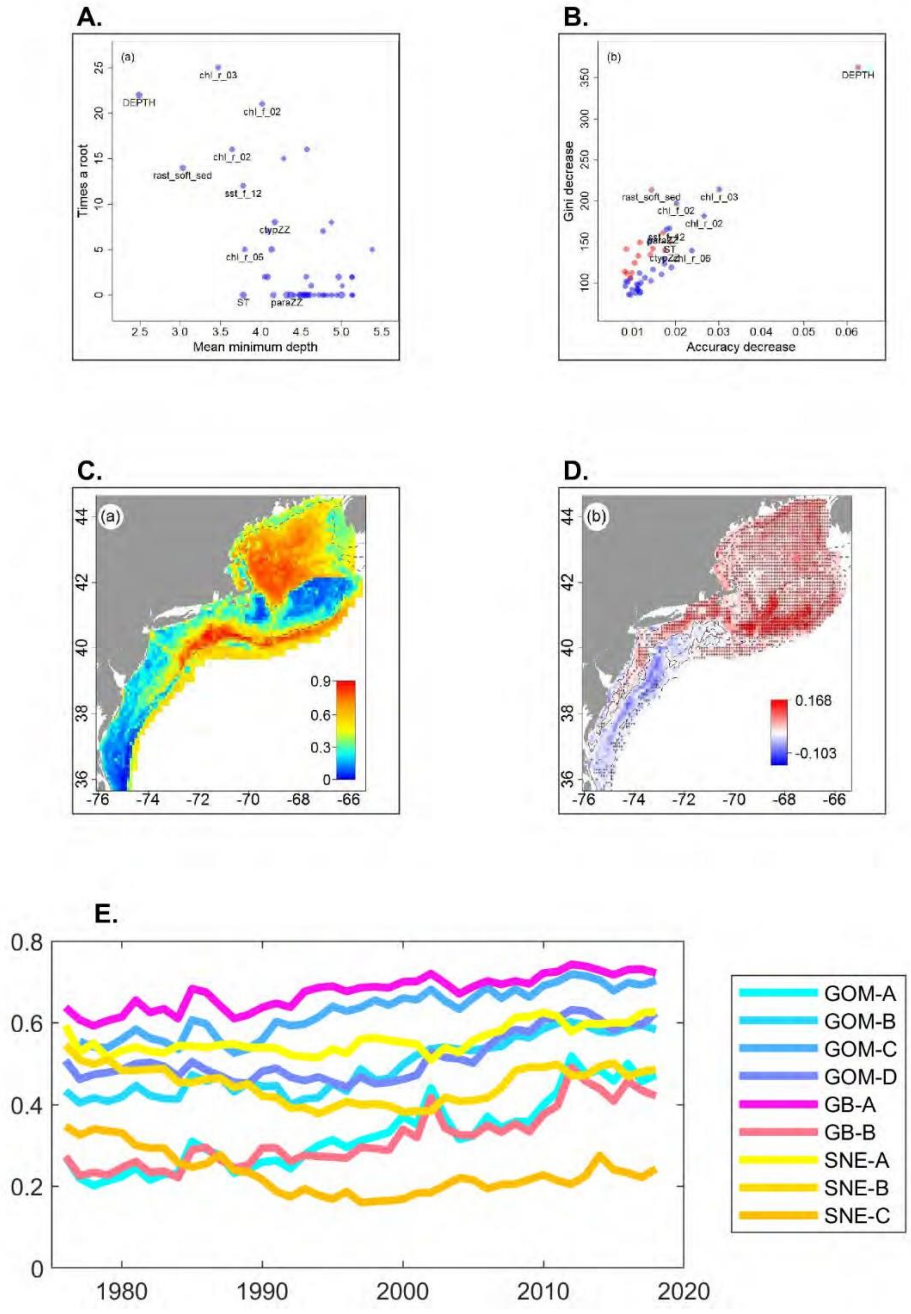

Figure 2.22 Results of the occupational probability models for red hake in the fall. A) and B) Variables included in the model, lower mean minimum depth, and higher times the root, Gini decrease and accuracy decrease all indicate the level of importance in the model. C) Map of average occupational probability and D) change in occupational probability across the northeast shelf. E) Sub-regional trends in average occupational probability.

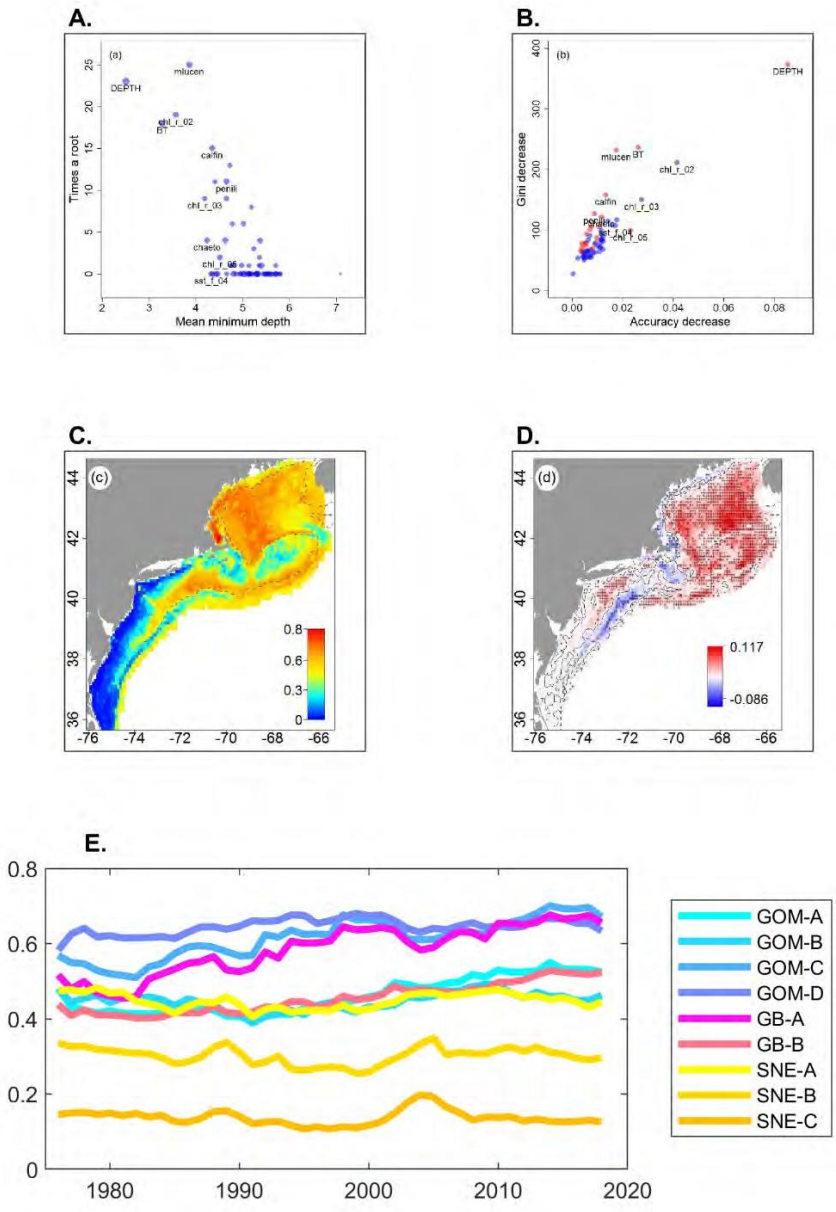

Figure 2.23. Plots of length-at-age data. The median length-at-age (large dots) and individual (small dots with offsets to allow visualization of points) are shown. For this evaluation fish are grouped based on the existing stock boundaries.

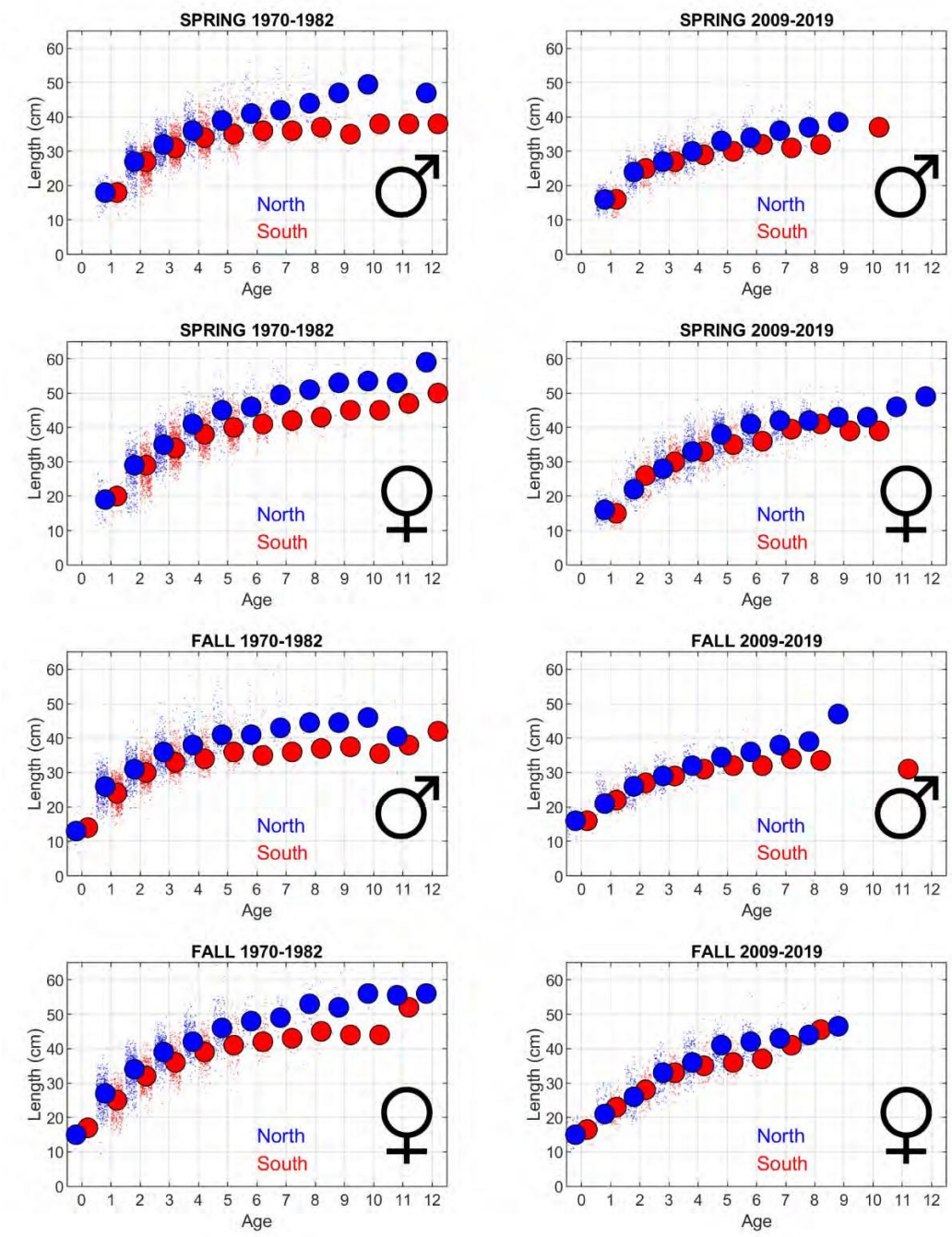

Figure 2.24. K mediods clustering of median length-at-ages 4-7 when data are grouped by sex, time period and season.

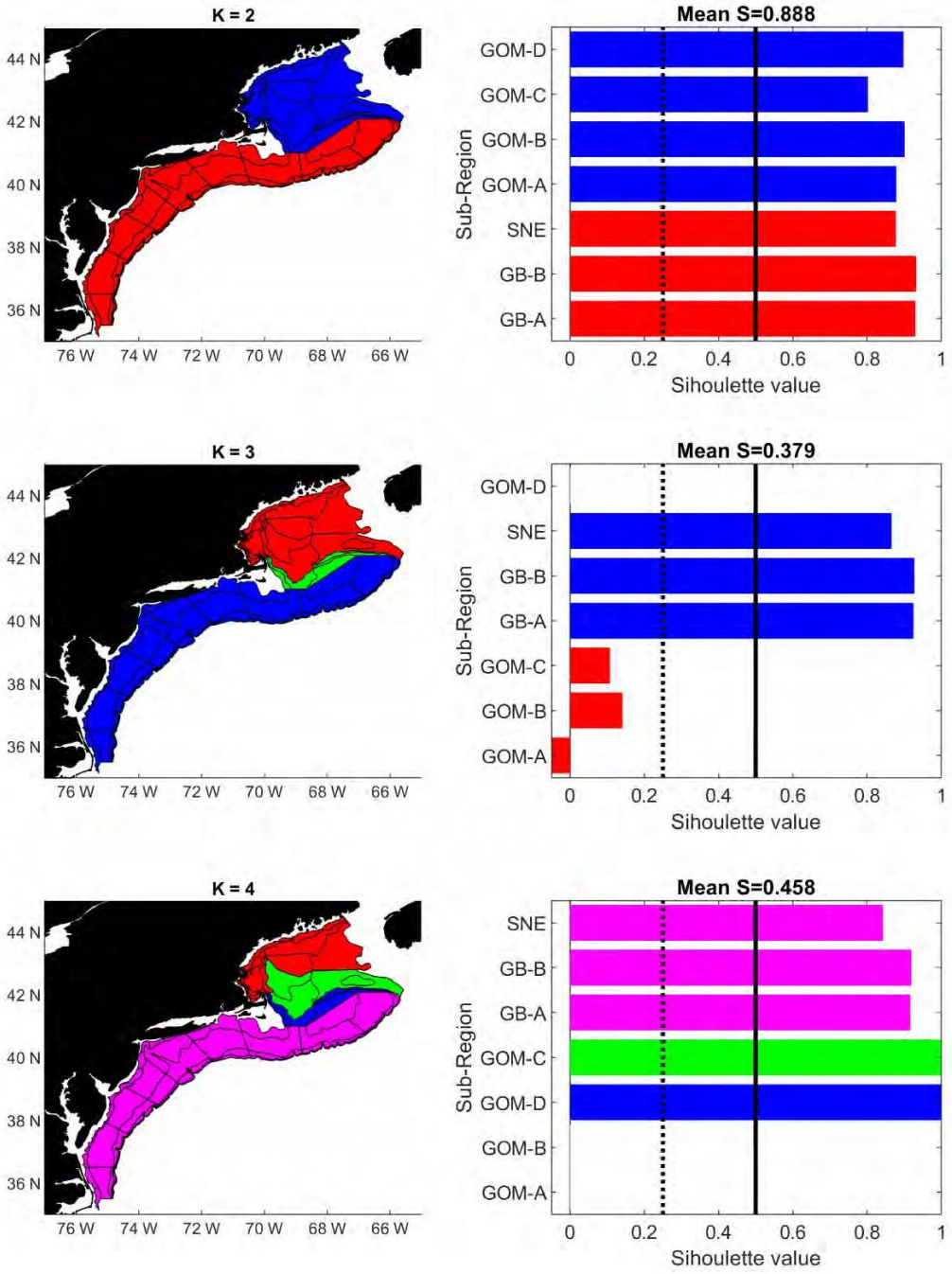

Figure 2.25. Mean (±SE) chemistry measured in (left panels) nuclei ($Mg \cdot Ca^{-1}$, $Mn \cdot Ca^{-1}$, $Sr \cdot Ca^{-1}$, $Ba \cdot Ca^{-1}$) and (right panels) edges ($Mg \cdot Ca^{-1}$, $Sr \cdot Ca^{-1}$, $Ba \cdot Ca^{-1}$) of otoliths taken from red hake caught along the northeast United States continental shelf. $Mn \cdot Ca^{-1}$ did not exceed detection limits for edge data, and are not shown.

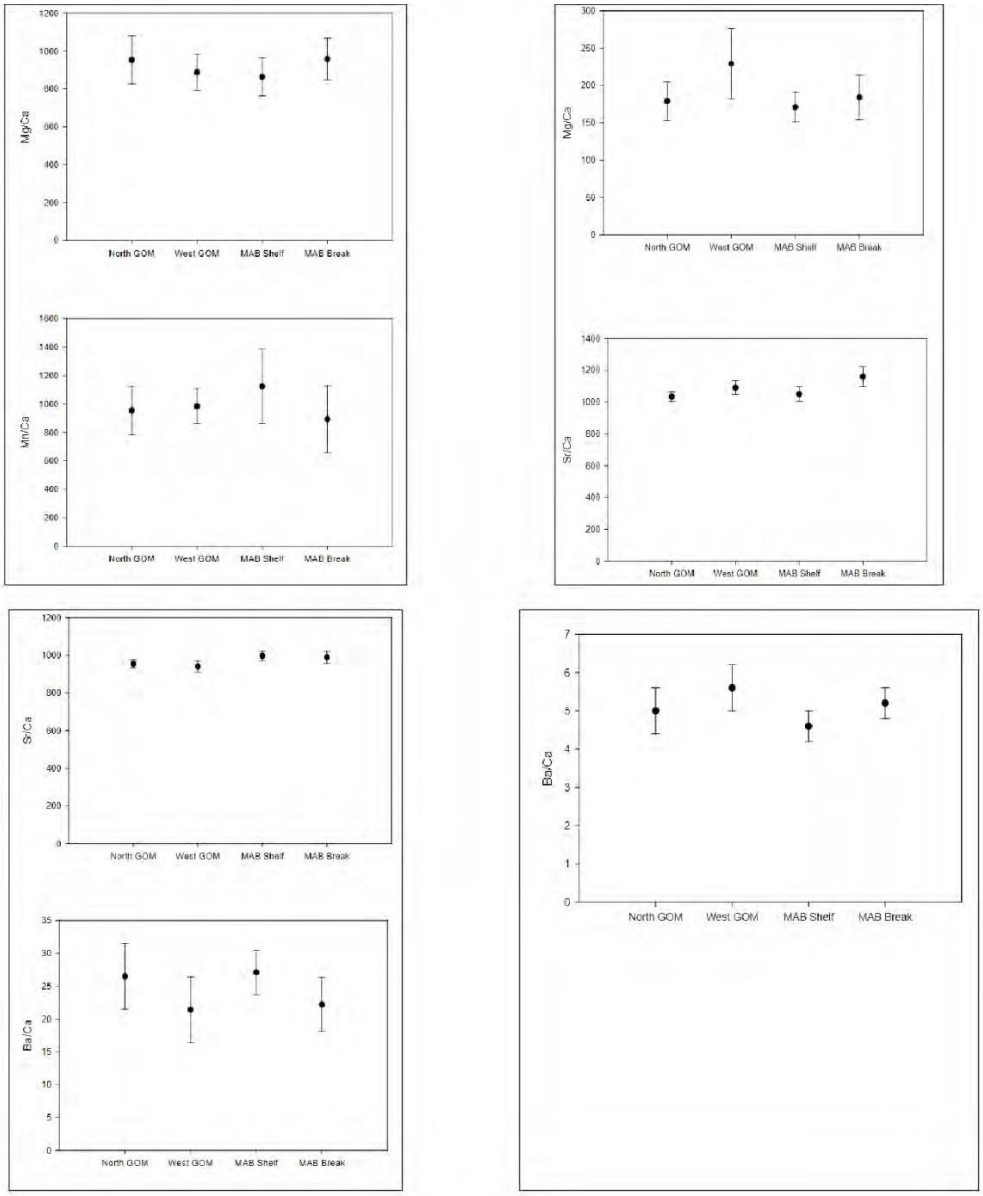

Figure 2.26. Chemistry from otolith a) nuclei and b) edges of red hake, showing relationships between fish caught along the Northeast United States continental shelf using canonical discriminant variates. North Gulf of Maine ●; West Gulf of Maine ○; Middle Atlantic Bight shelf +; Middle Atlantic Bight shelf-break ×.

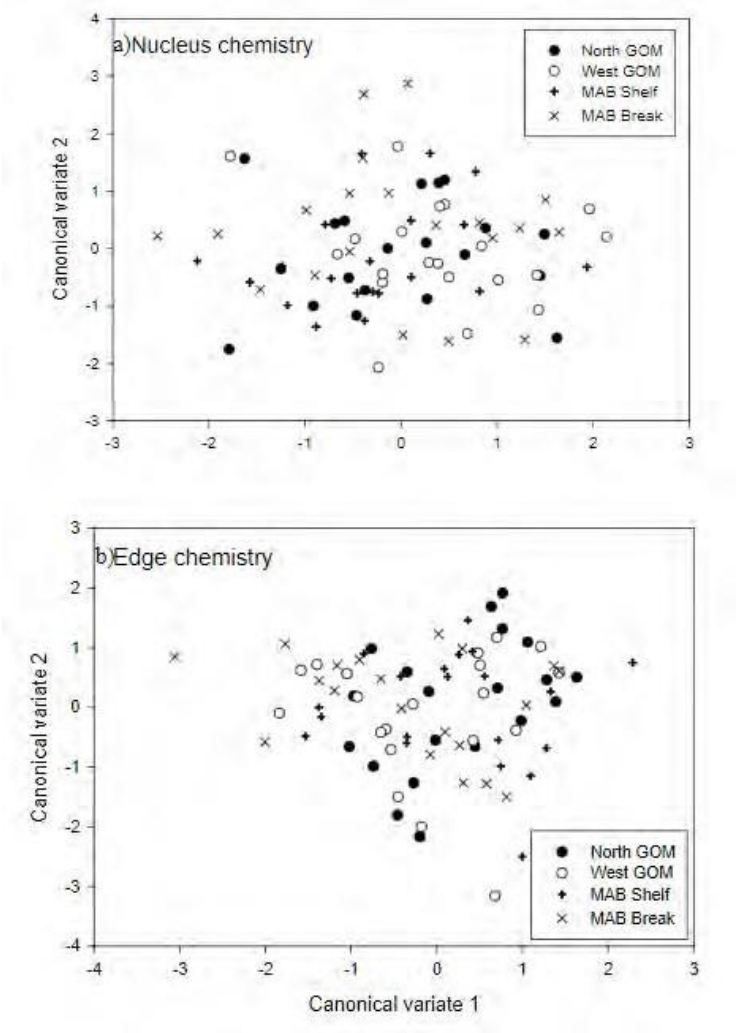

Figure 2.27. Regression of 80 larval red hake (*Urophycis chuss*) length (mm) and number of otolith increments collected during Ecosystem Monitoring surveys. The dashed line represents the mean growth rate.

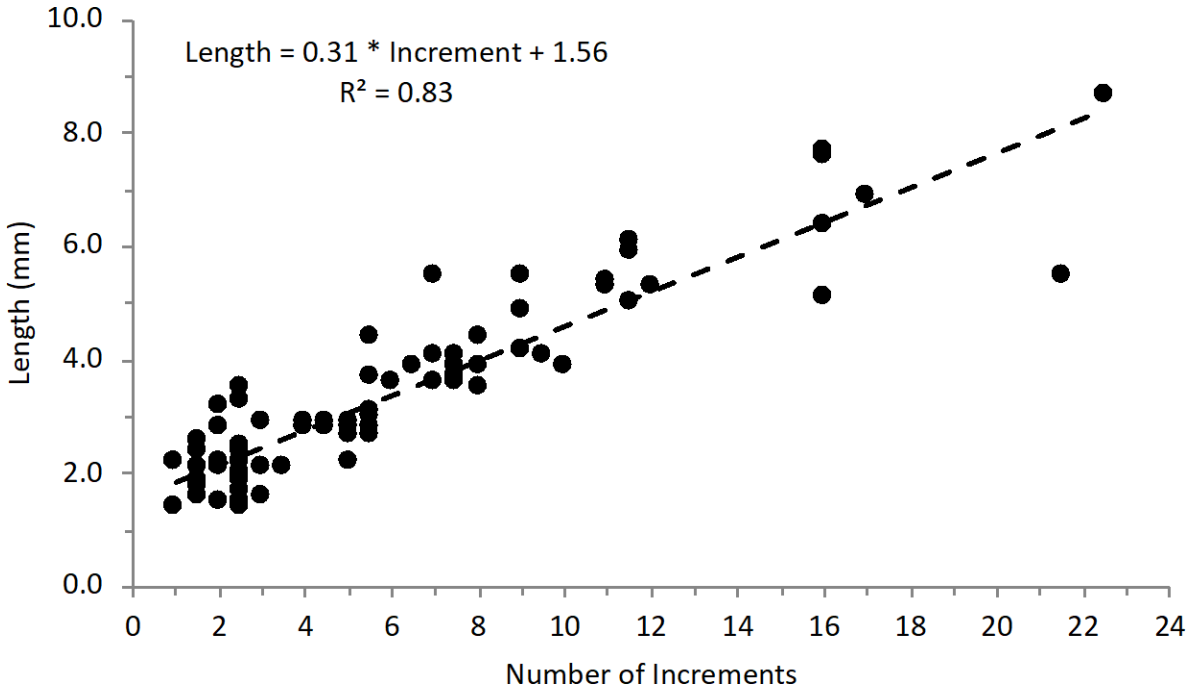

Figure 2.28. Comparison of the distributions of larval abundances (larvae 1-5mm BL) between the 1980s and the 2000s and 2010s, separated by sampling seasons.

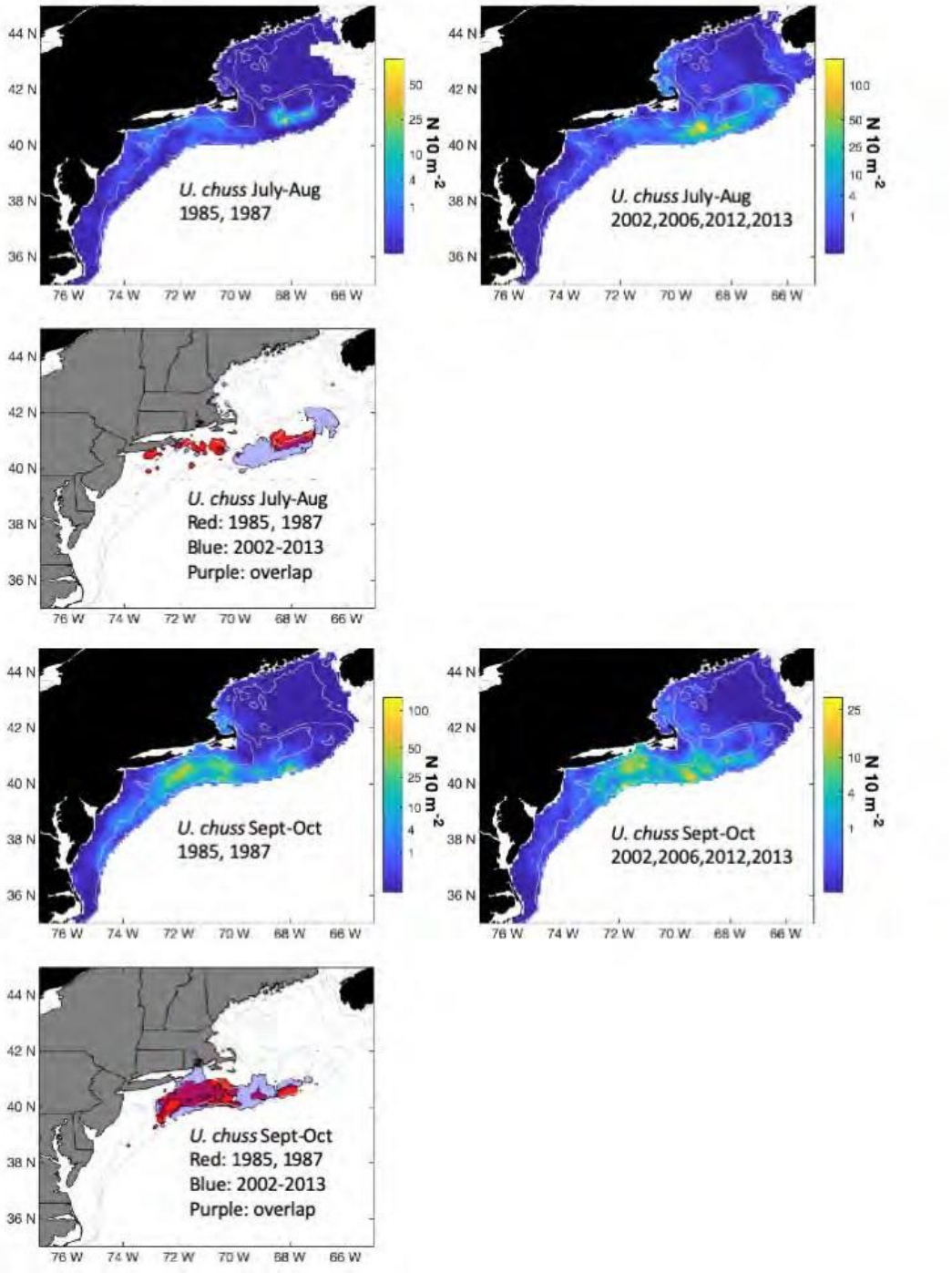

Figure 2.29. Figure 2: results of the Gi* hot spot analysis. Red-filled strata indicate significanly high abundances or hot spots. Blue-filled strata indicate areas of significanly low abundances.

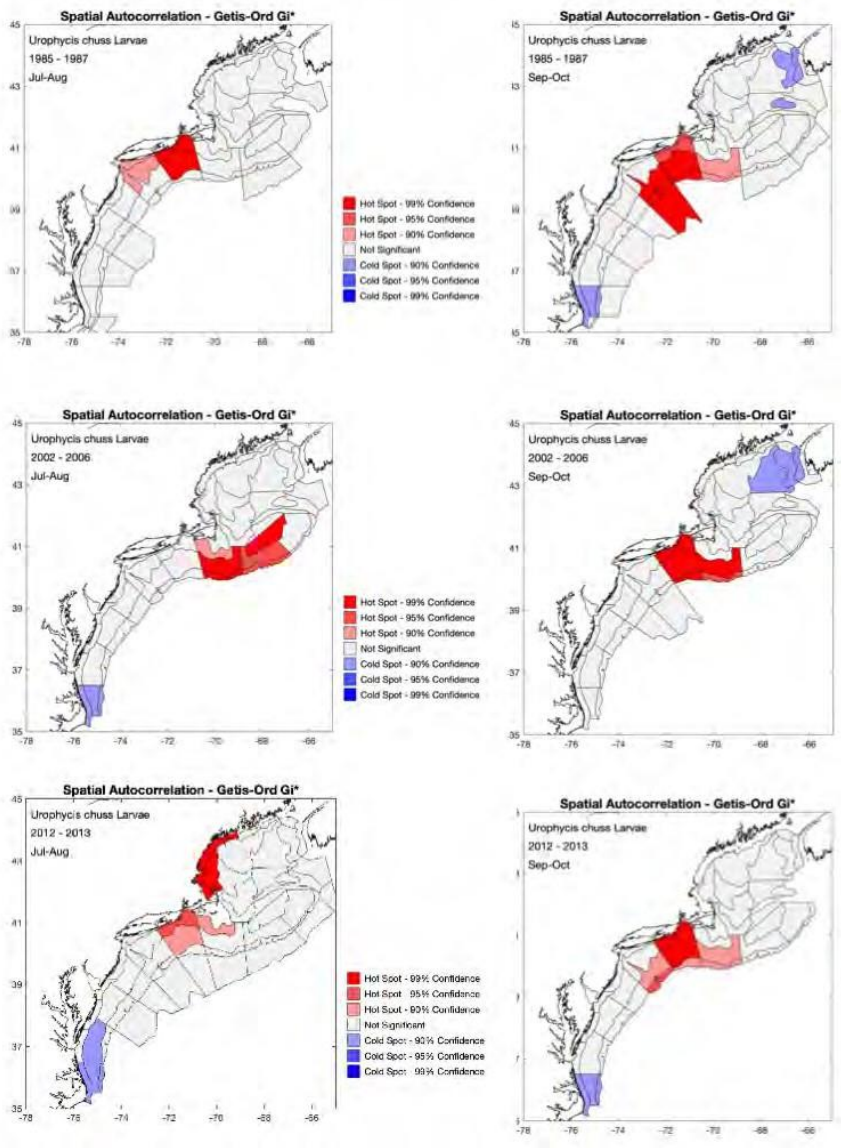

Figure 2.30: Map locations of 1-1.5mm (top) and 1.5-5mm (bottom) larval Red Hake, representing the distribution of larvae after 7-10 days post spawning, the end of the egg stage, and approximately 15 days post spawning, the beginning of flexion and the majority of larvae collected. MARMAP used 505um nets that did not effectively retain <1.5 mm larvae. However, the distributions of larvae that were collected suggest similar areas of high concentrations over time. The distribution of larvae throughout this range of sizes Identifies 4 subregions of highest concentrations (see Marancik et al., larval distribution working paper): SNE-A, GB-B, GB-A, and GOM-B.

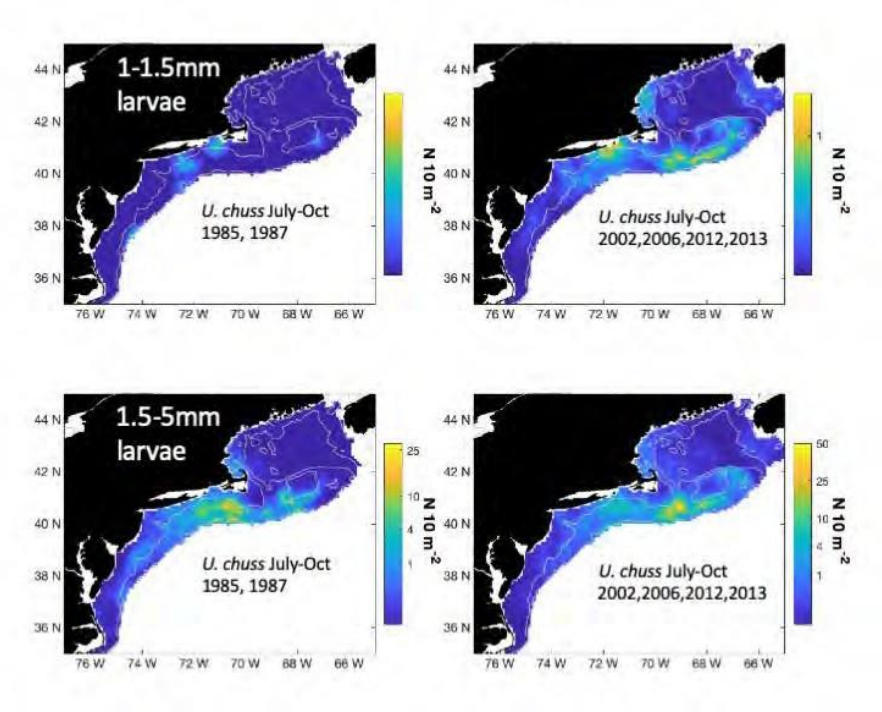

Figure 2.31. Drifter model projections of 10 days (egg duration) and 15 days (flexion) for the 4 subregions identified by larval Red Hake. 10 day and 15 day distributions of drifters are fairly similar. GOM-B released drifters remain in GOM-B (34.6%; 22.3%) or move into GOM-C (24.1%; 22.9%) and GOM-D (23.9%; 24.3%). GB-A-released drifters remain in GB-A (52.9%; 43.6%) or move to GB-B (11%; 10.6%) and GOM-D (10.4%; 10.2%). GB-B-released drifters remained in GB-B (33.9%; 20.7%) or move into SNE-A (20.8%; 18.9%). SNE-A-released drifters remain in SNE-A (38.3%; 24.7%) and move into SNE-B (22.3%; 19.7%).

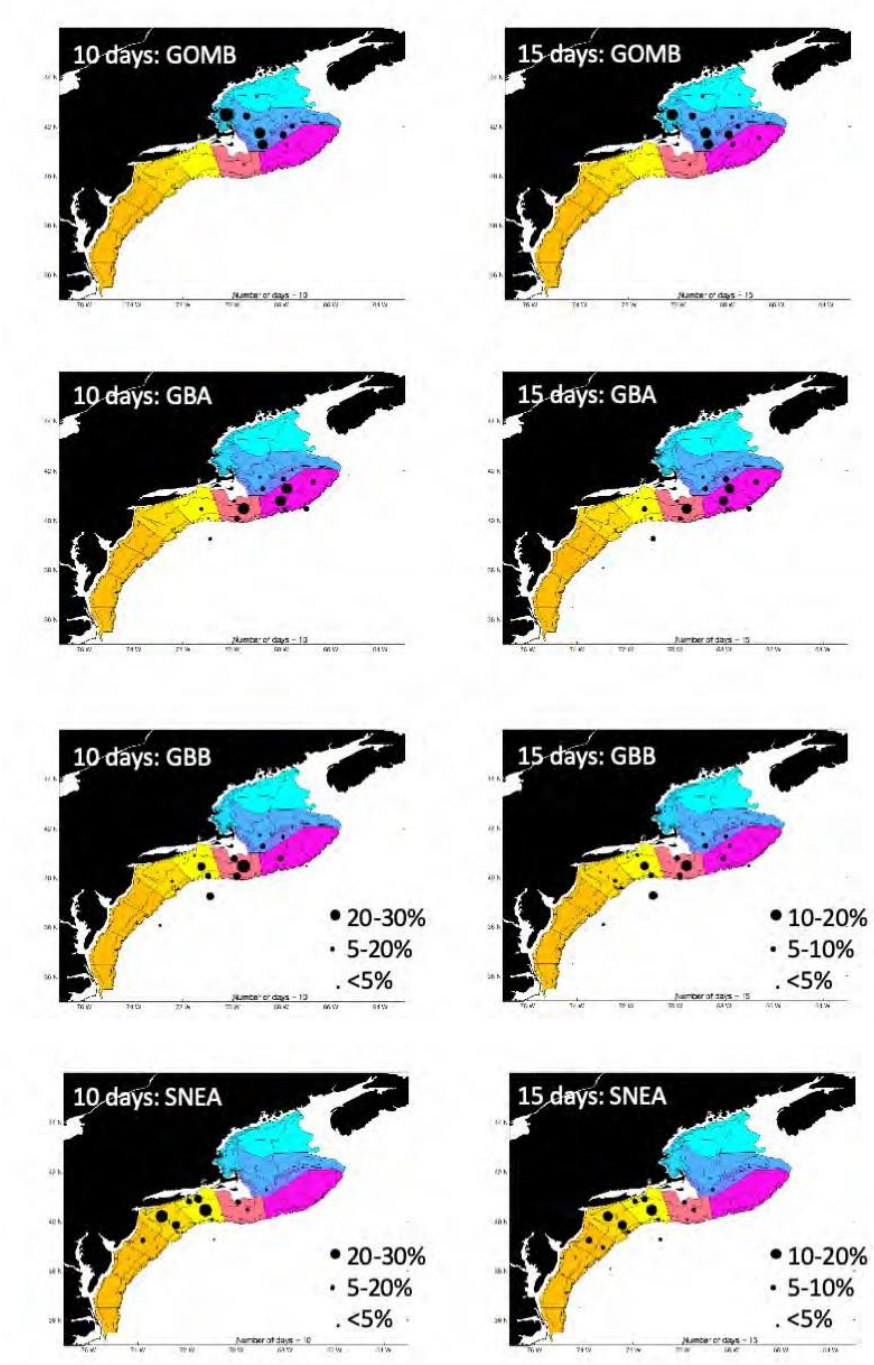

Figure 2.32. Proportion of particles from each subregion that reach each of the 4 subregions identified by larval Red Hake distributions after 10, 15, 30, 45, or 60 days. The 10 and 15 days results are similar between the two models for all subregions. The drifter model projections for 30-60 days are less matched, although still fairly similar. Drifters and particles that reach SNE-A, mostly come from SNE-A and GB-B. After 30 days, the GOM subregions have some drifters/particle reach the SNE-A. Drifters and particles that reach GB-B mostly came from GB-B and GB-A. After 30 days, GOM-D drifters/particles reach the GB-B. The particle-tracking model shows a higher percentage of particles from the GOM reaching the GB-B after 30 days than the drifters. Drifters and particles that reach the GB-A mostly came from the GB-A and GOM-D. After 30 days, the drifter model shows more drifters from the GOM reaching the GB-A than the particle-tracking model. Drifters and particles that reach the GOM-B mostly came from the GOM-B. The particle-tracking model shows more particles from the GOM-A reaching GOM-B than the drifter model.

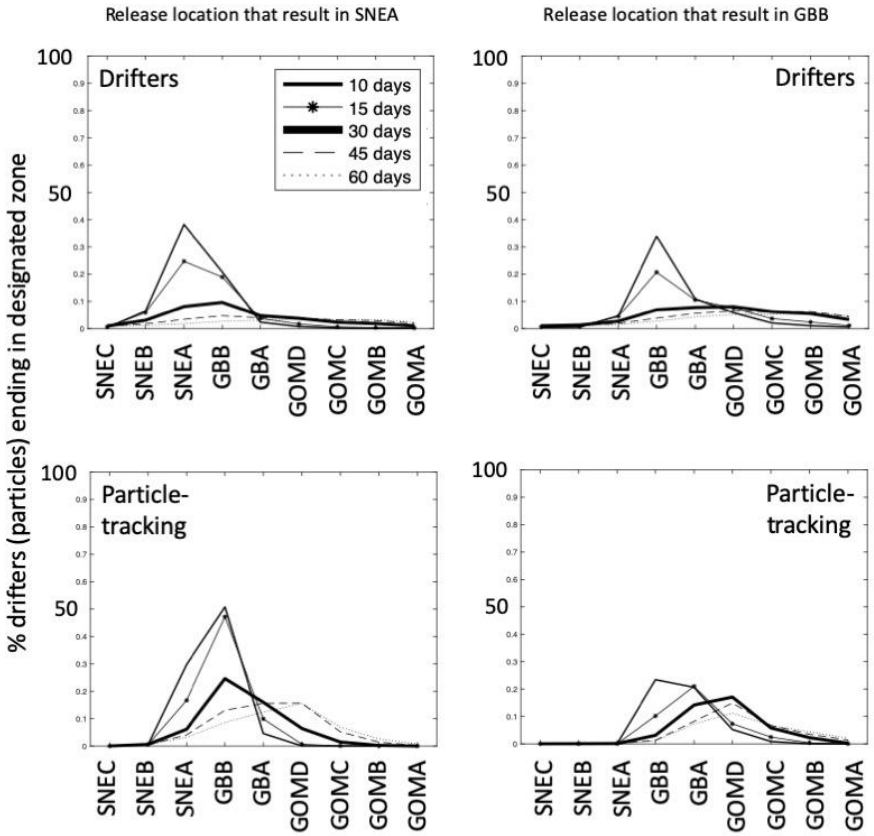

Figure 2.32 continued

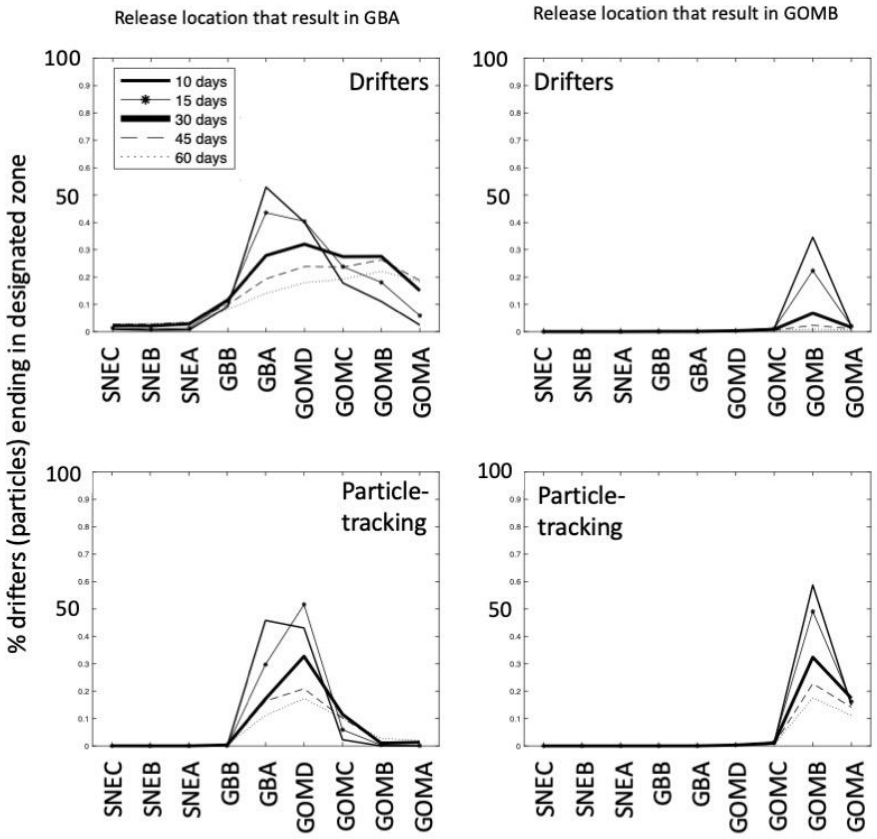

Figure 2.33. Particle-tracking model results showing the distribution of source locations for particles that occur at the red dots after durations of 7-9 days, 16-18 days, and 28-30 days. The source locations tend to be adjacent to the sink locations, and the spread of potential source locations increases with time at large.

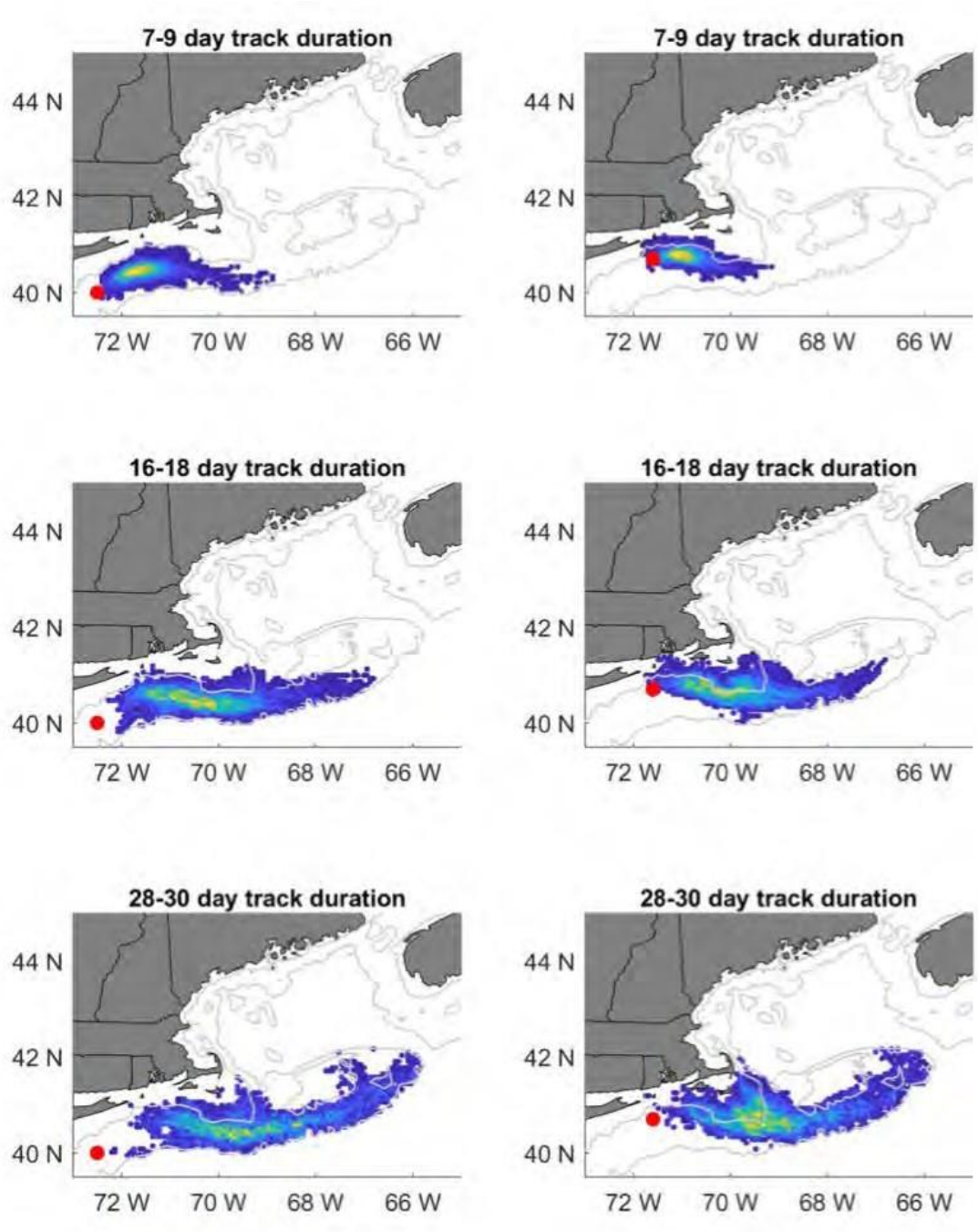

Figure 2.33 continued

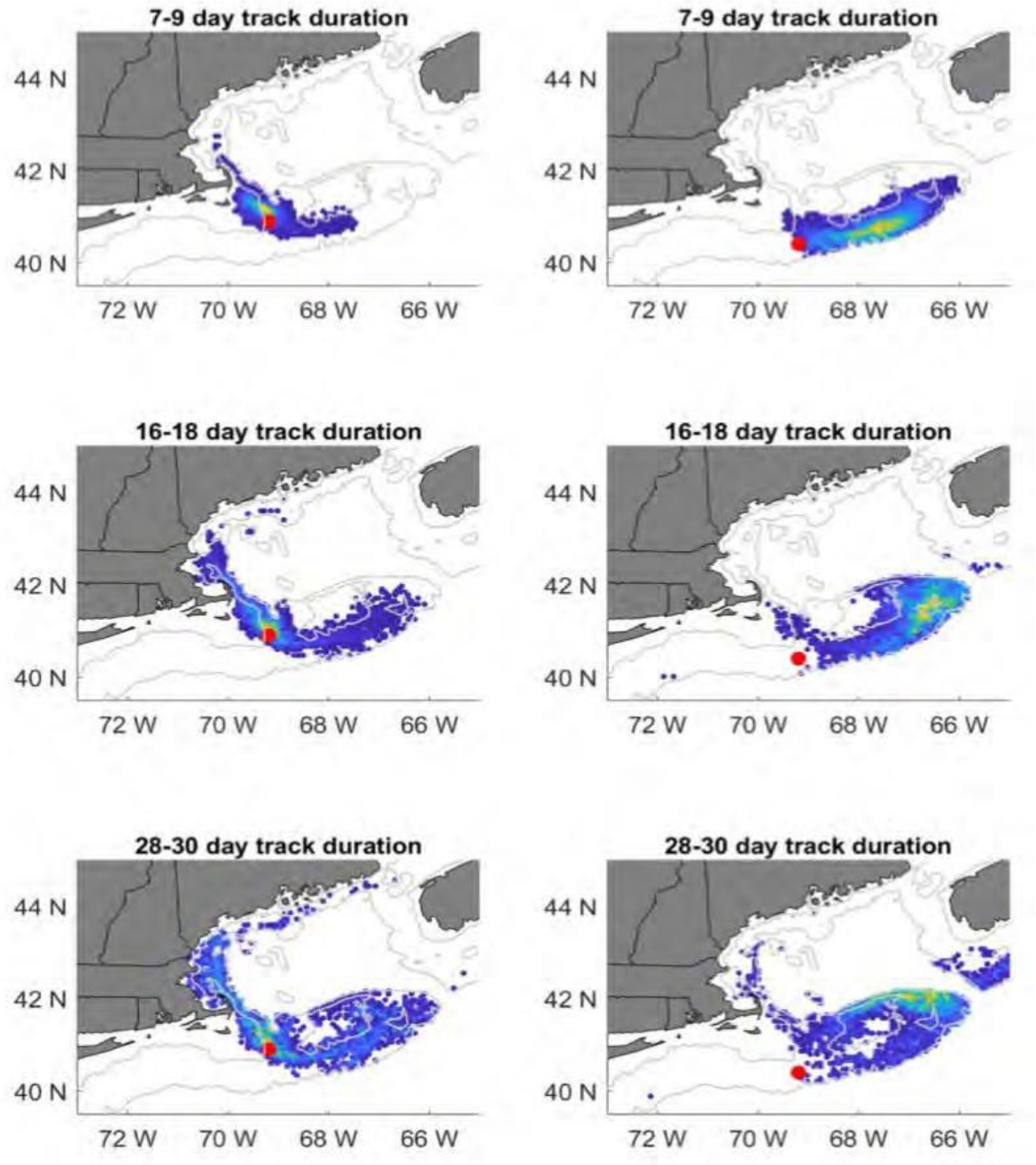

Figure 2.33 Continued.

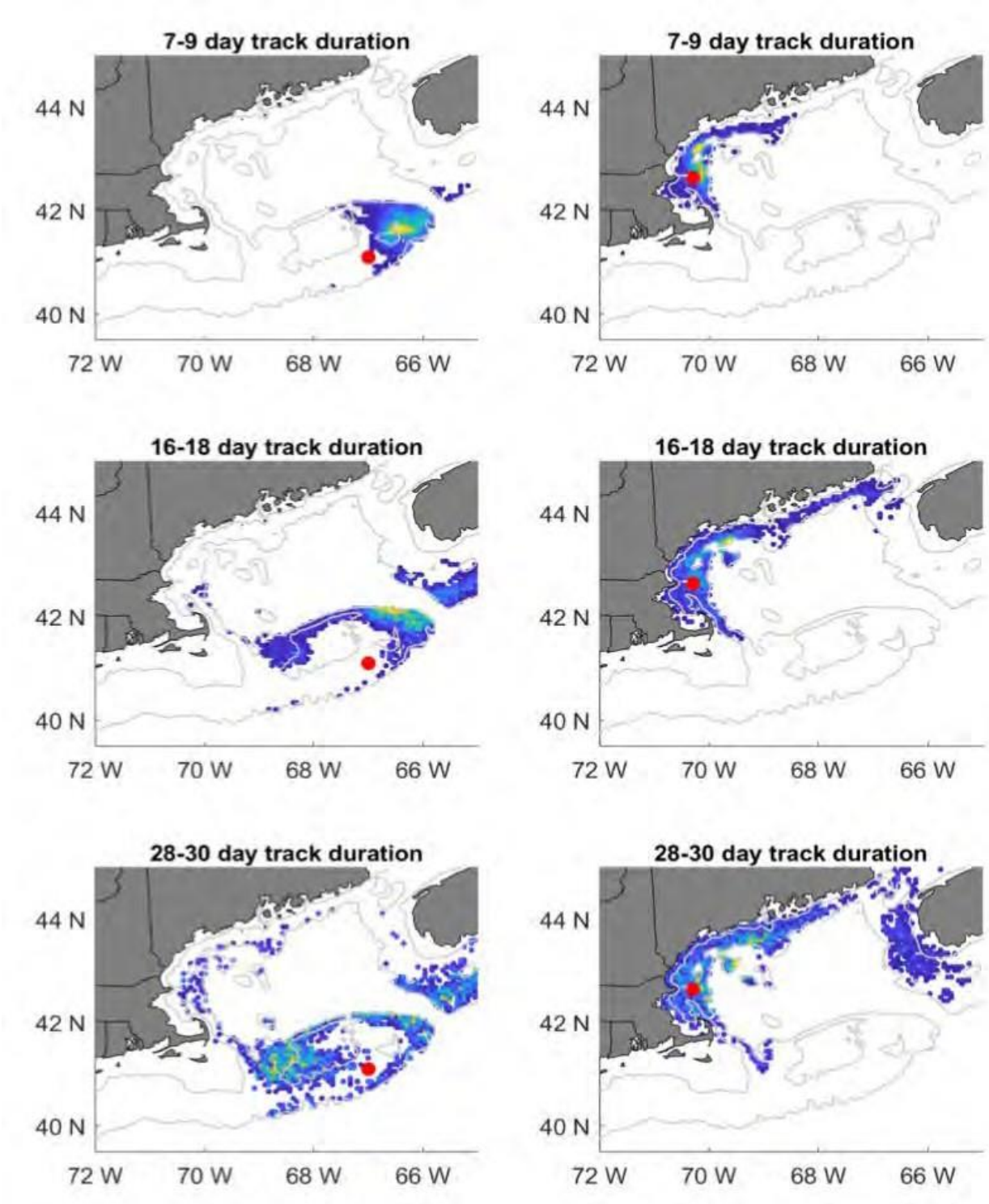

Figure 2.34. Total abundance of small (<7 mm, A-B) and large (>6 mm, C-D) Red Hake larvae collected during Ecosystem Monitoring surveys (see Table 2). Seasonal (A, C) and regional (B, D) percentages of the each size class were based on the total abundance of all larvae identified.

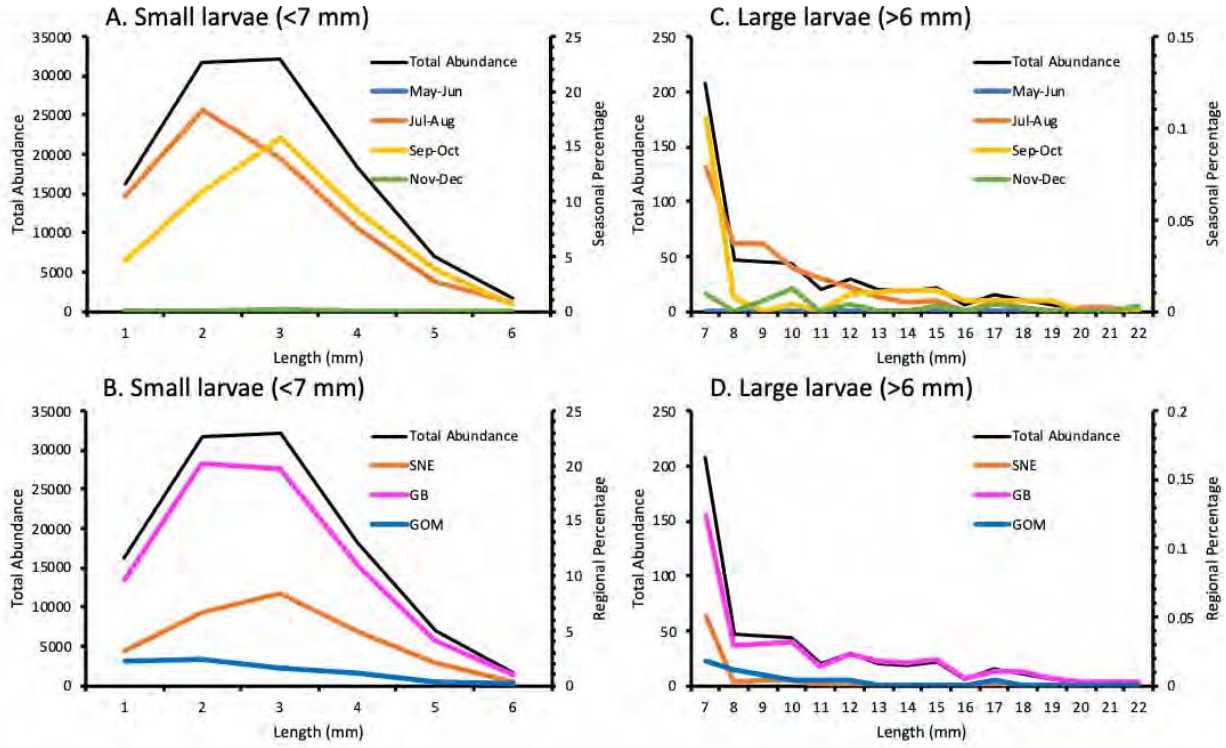

Figure 2.35. Hatch date distributions of Red Hake larvae collected during Ecosystem Monitoring surveys (see Table 2) for three regions (A-C) based on abundance. Regional percentages were based on all larvae collected from 1 to 8 mm in length.

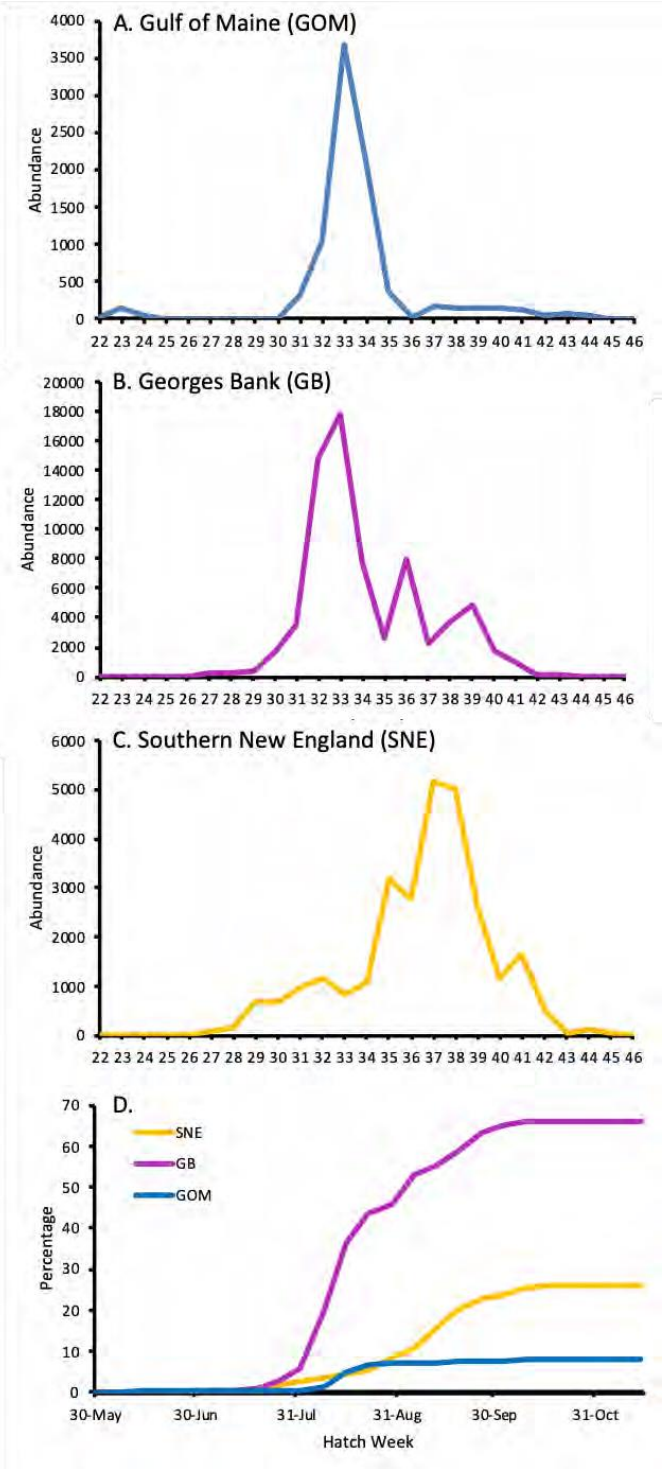

Figure 2.36. Sensitivity analysis of the particle-tracking model. Only the end locations for particles released in GB-A are shown. Except for panel A, all analyses were done for a 30-day duration.

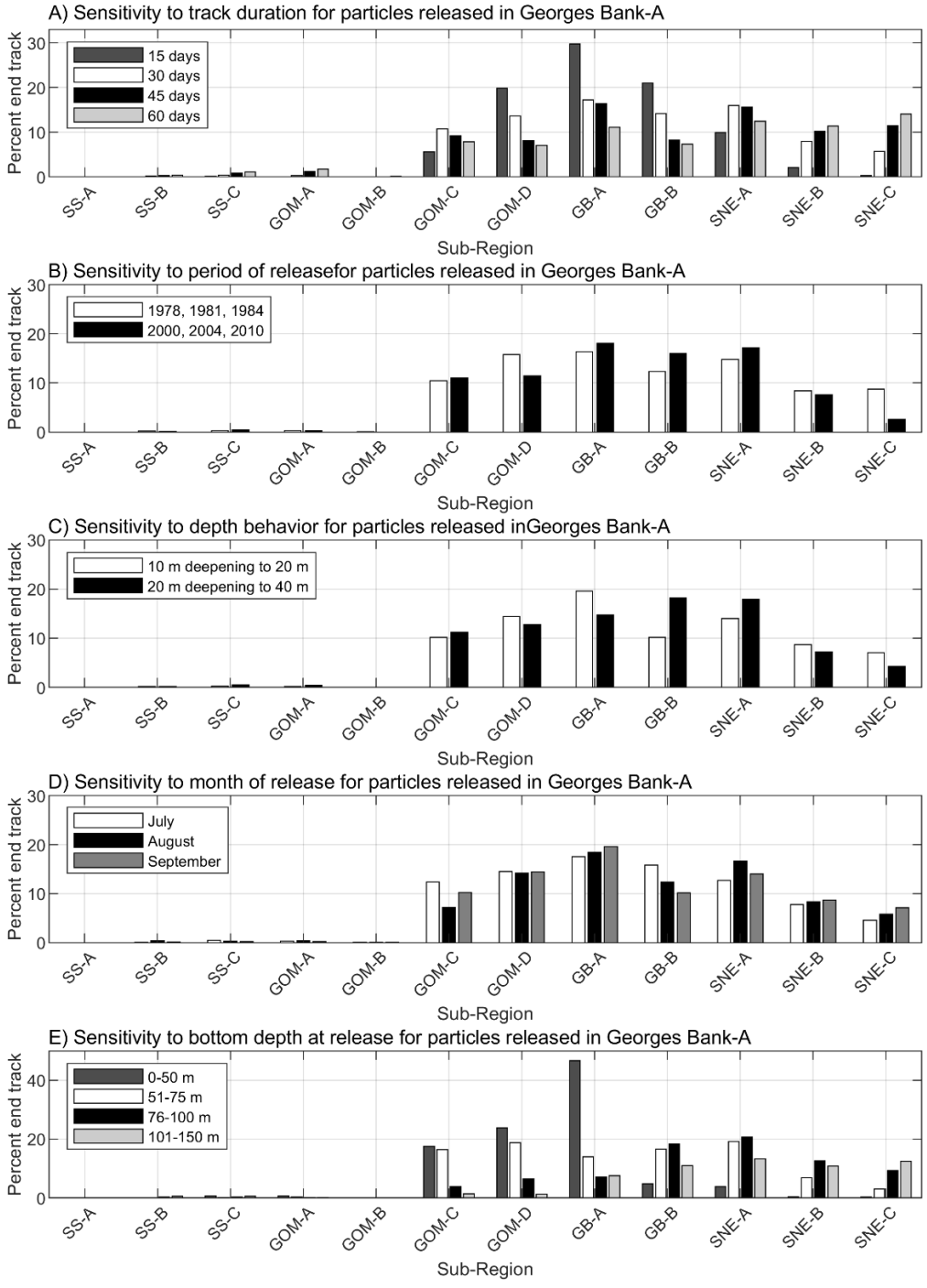

Figure 2.37. Distribution of small (≤10 cm) red hake during the fall survey on the *Bigelow*. Upper left panel shows the 2009-2012 distribution which is typical of most of the time series. Upper right panel shows the 2013-2018 distribution. Bottom left panel provides a comparison of the areas and stations of highest abundance for 2009-2012 (red shading, green dots) and 2013-2018 (blue shading and cyan dots).

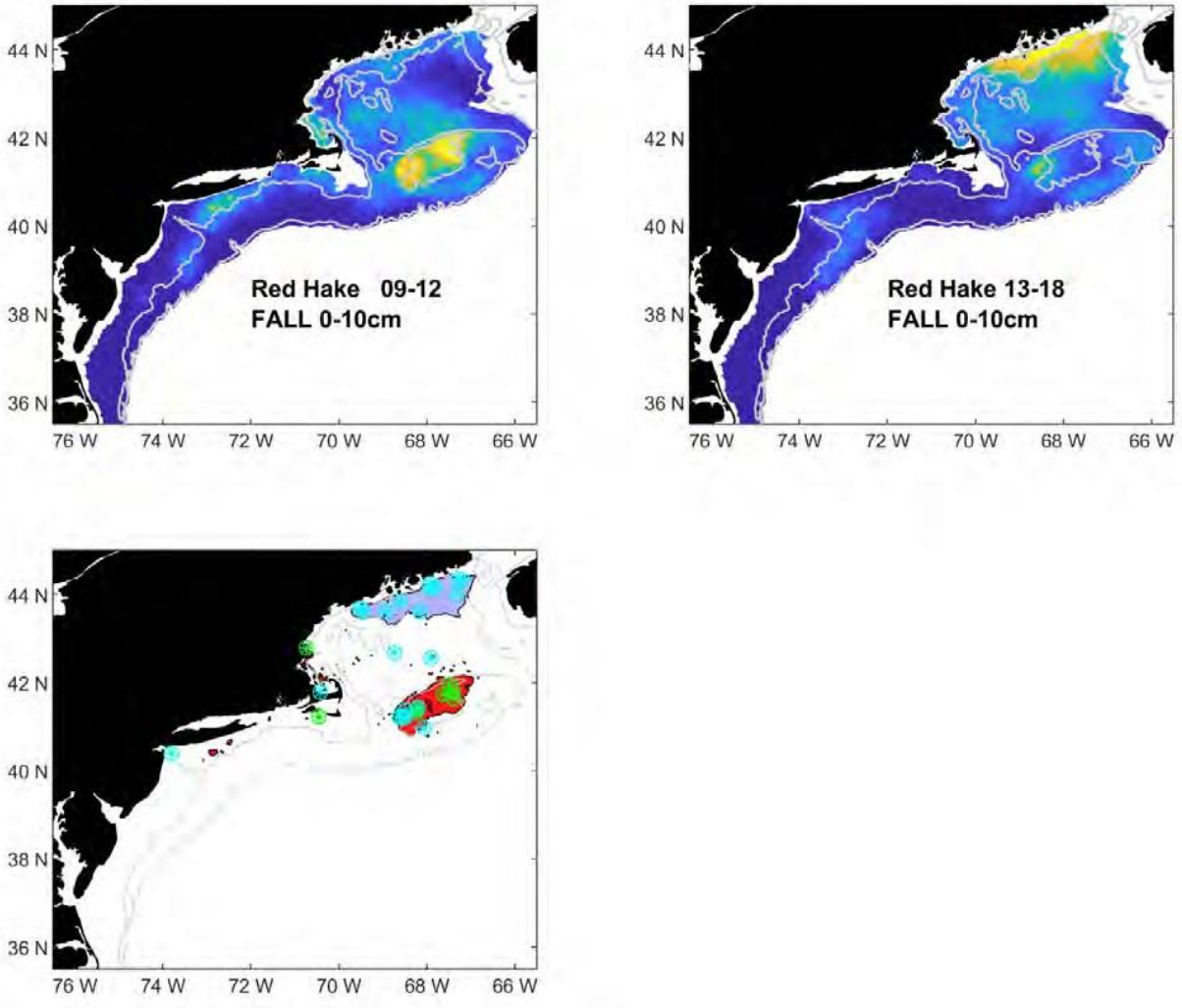

Figure 2.38. Time series of (upper panel) Age-0 red hake in Gulf of Maine-A during the NEFSC survey on the *NOAA Ship Henry Bigelow* and (lower panel) Age-1 red hake on the DFO trawl survey in the Bay of Fundy.

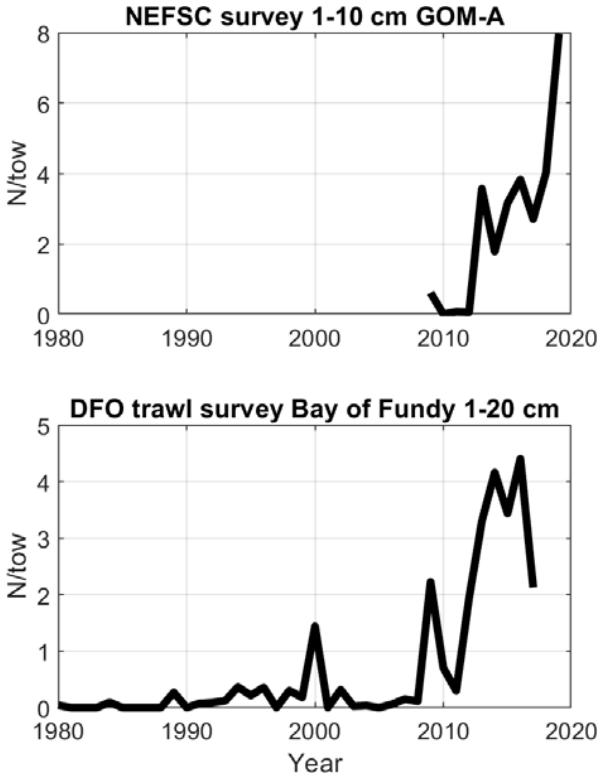

Figure 2.39. Potential migration pattern of red hake that would explain the contrast in the distribution of early life stages versus adult biomass during the spring and fall. Top right shows the distribution of mature fish from 2000-2008 in the Spring. Bottom right: By summer larval data indicates that a majority of larvae are on Georges Bank. A spawning migration by Gulf of Maine fish to Georges Bank is consistent with these patterns. Bottom left is the distribution of young-of-the-year in the fall. Top left is the distribution of Age-1 fish in the spring. An overwintering migration of juveniles from Georges Bank to the Gulf of Maine could explain this pattern.

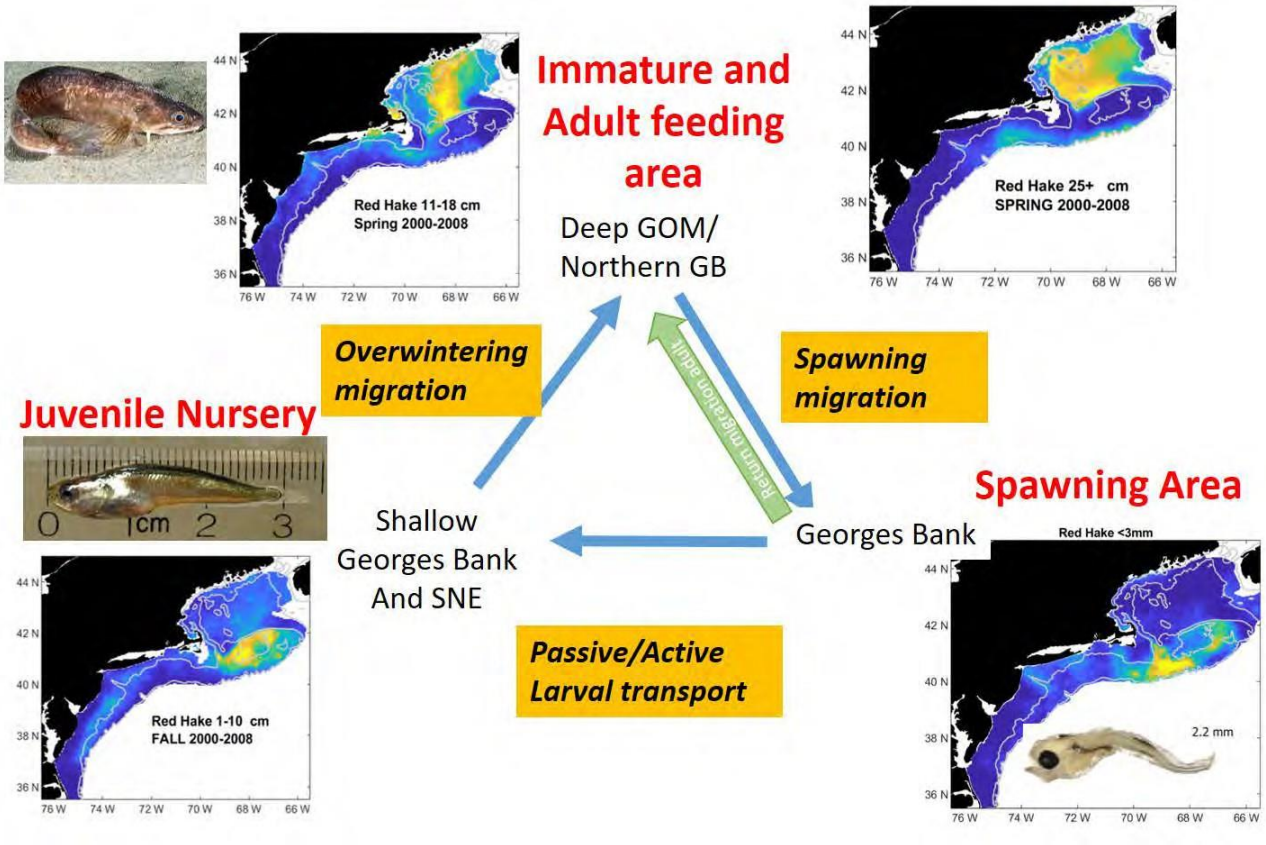

Figure 2.40. Selected AIM output plots for the One Stock run. A) The results of the randomization test with the critical value marked with a black line. B) The relationship between abundance and removals. Where the regression line crosses the log of the replacement ratio = zero is the estimated F_{msy} proxy.

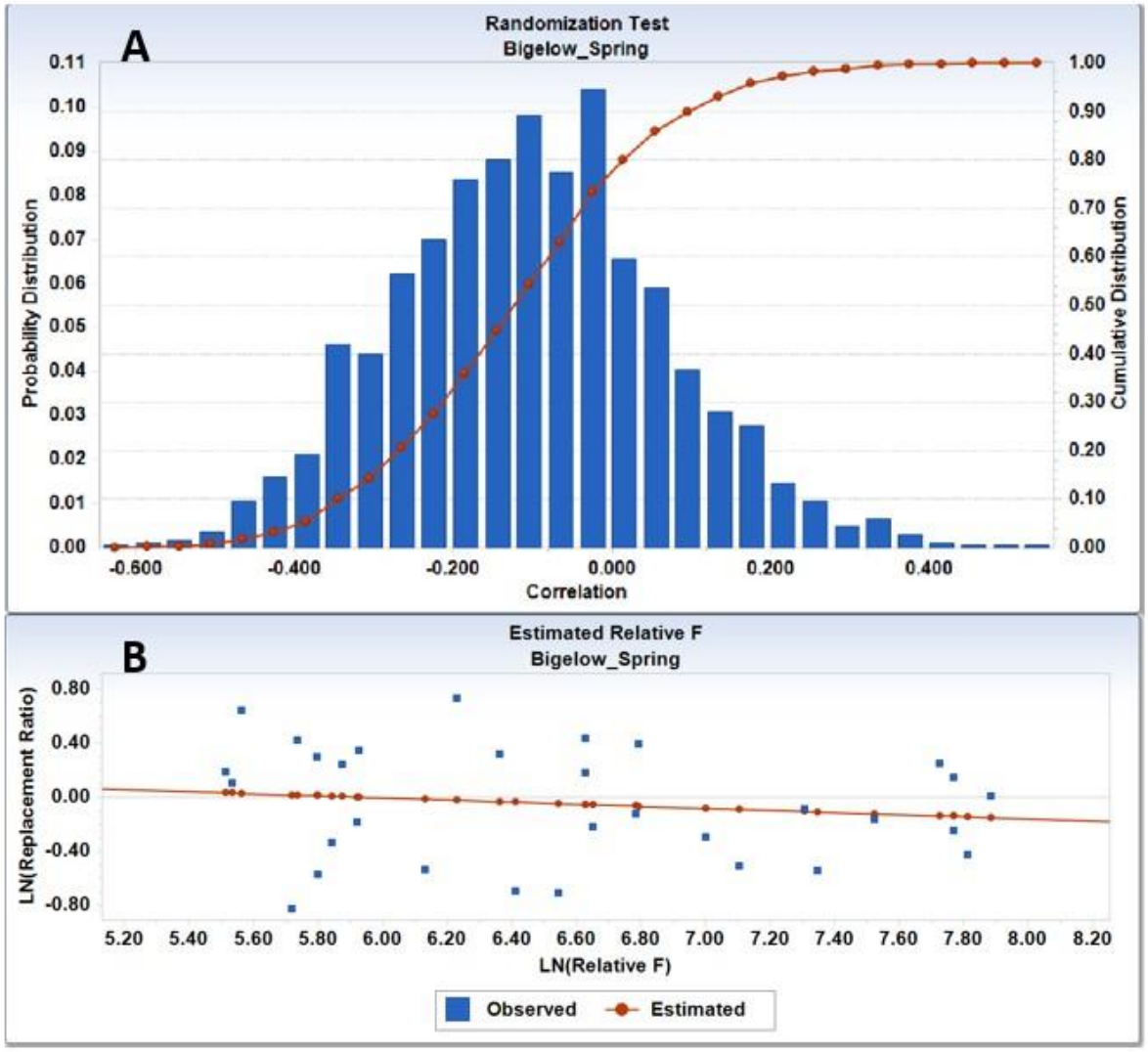

Figure 2.41. AIM output plots for the Two Stocks run, northern stock. A) The results of the randomization test with the critical value marked with a black line. B) The relationship between abundance and removals. Where the regression line crosses the log of the replacement ratio = zero is the estimated F_{msy} proxy.

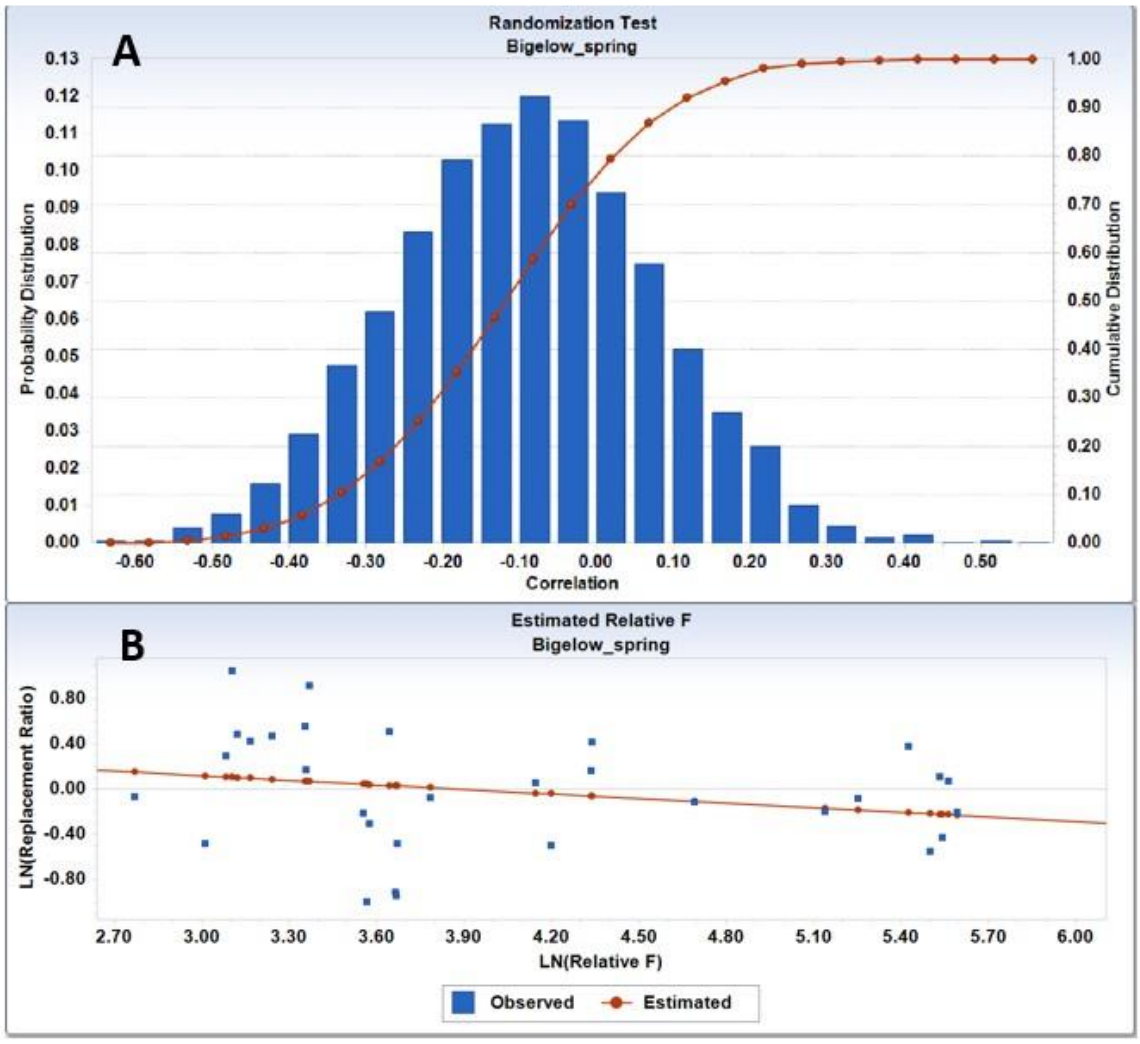

Figure 2.42. AIM output plots for the Two Stocks run, southern stock. A) The results of the randomization test with the critical value marked with a black line. B) The relationship between abundance and removals. Where the regression line crosses the log of the replacement ratio = zero is the estimated F_{msy} proxy.

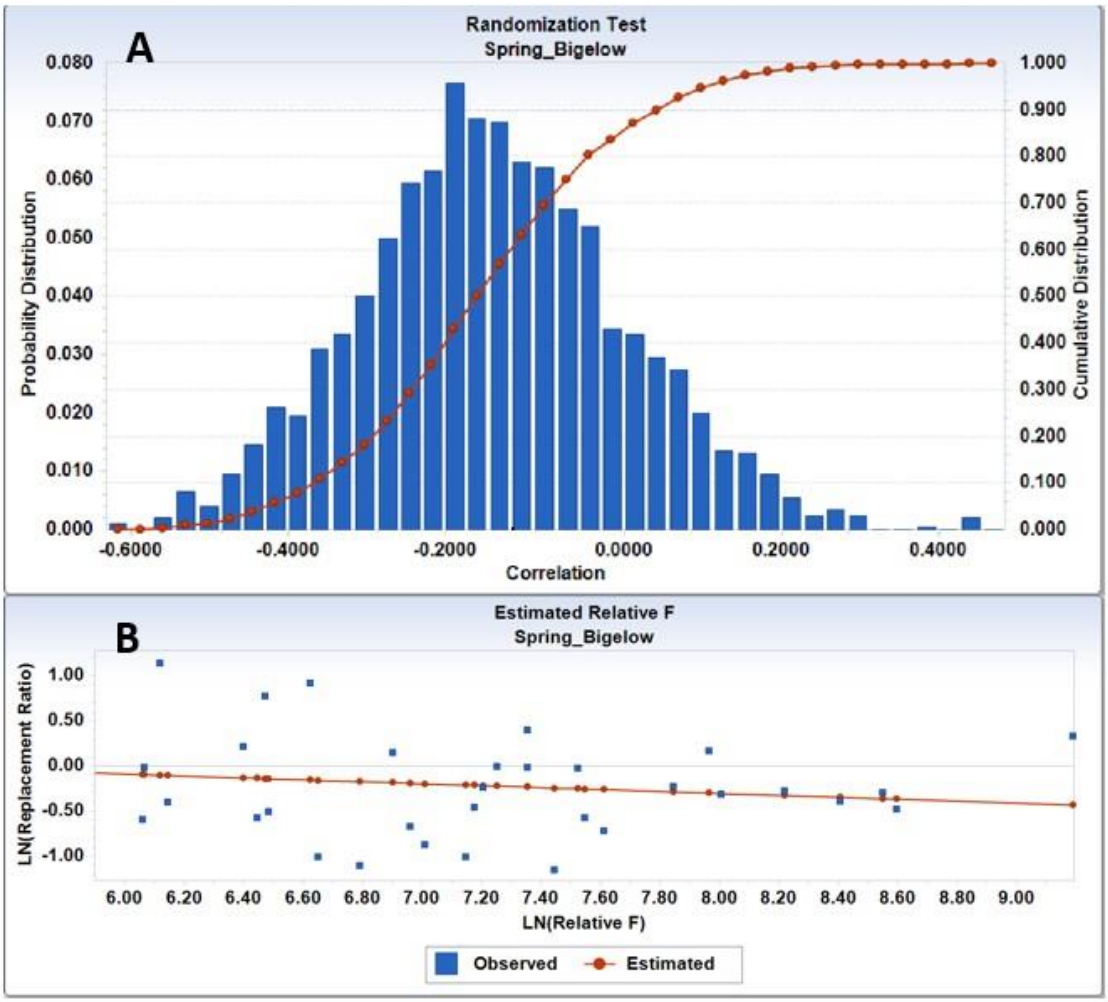

Figure 4.1 Plot of measured wingspread versus depth on the bottom trawl survey 2009-2016, and the frequency distribution of measured wingspreads.

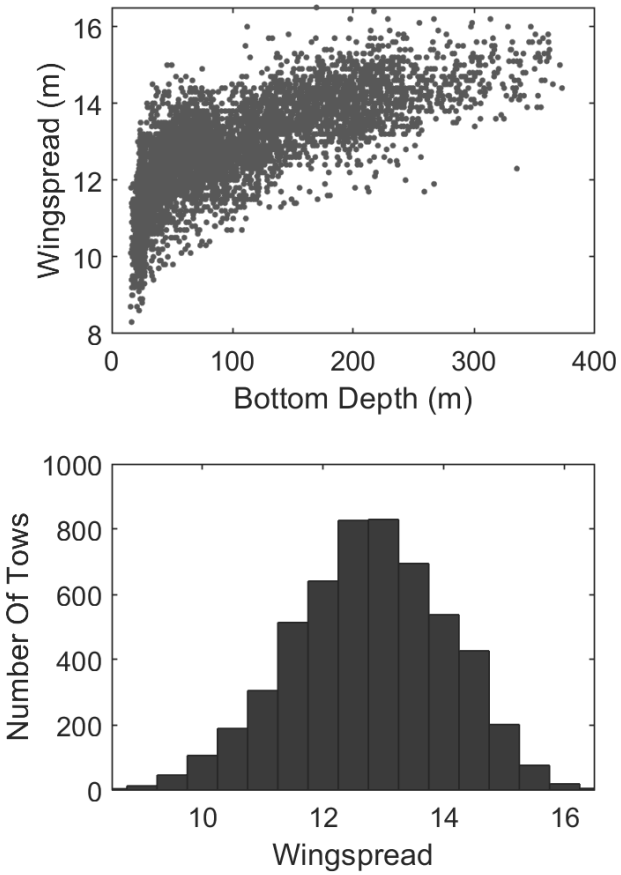

Figure 4.2. Simple diagram of a bottom trawl gear illustrating the difference between door-swept area (blue+orange) and wing swept area (orange). The use of door swept area as a measure of area swept assumes that fish are actively herding to the center of the tow path. Herding occurs when a fish that is disturbed by the bridles actively swims perpendicular to the disturbance (shown by the arrows) until positioned in front of the trawl net.

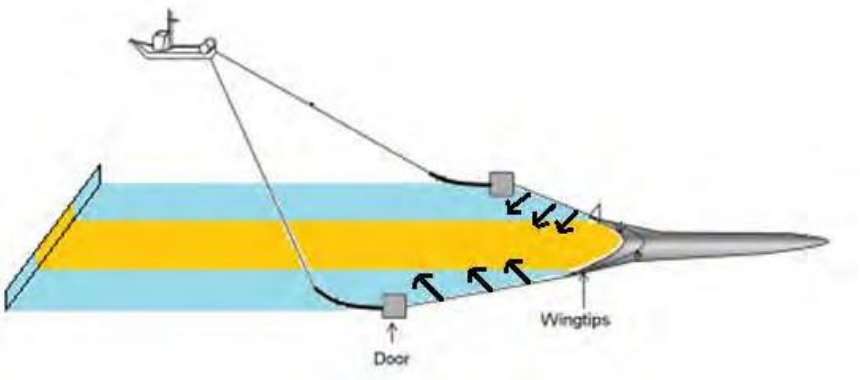

Figure 4.3. HabCam system used on the NEFSC scallop survey.

Figure 4.4. Red hake abundances in the Mid Atlantic Bight based on the HabCam 2015 survey (red) and spring (blue) and fall (green) bottom trawl surveys.

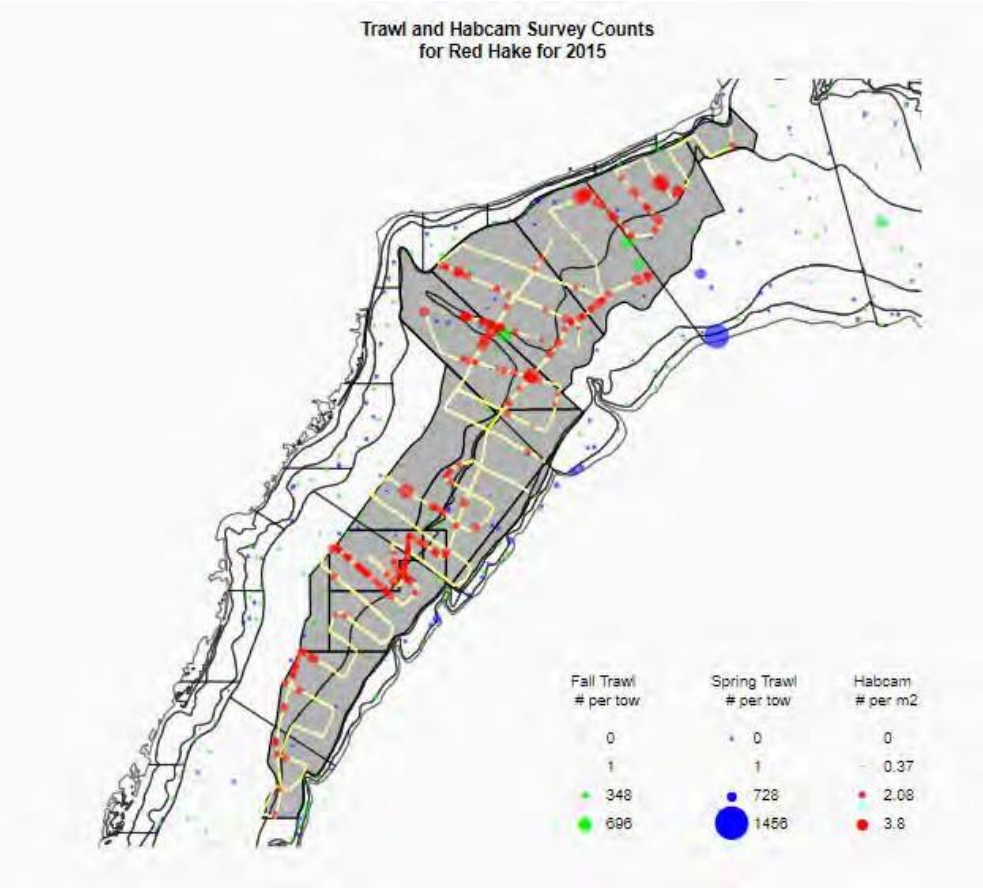

Figure 4.5. Red hake abundances on Georges Bank based on the HabCam 2015 survey (red) and spring (blue) and fall (green) bottom trawl surveys and the dredge (purple) survey.

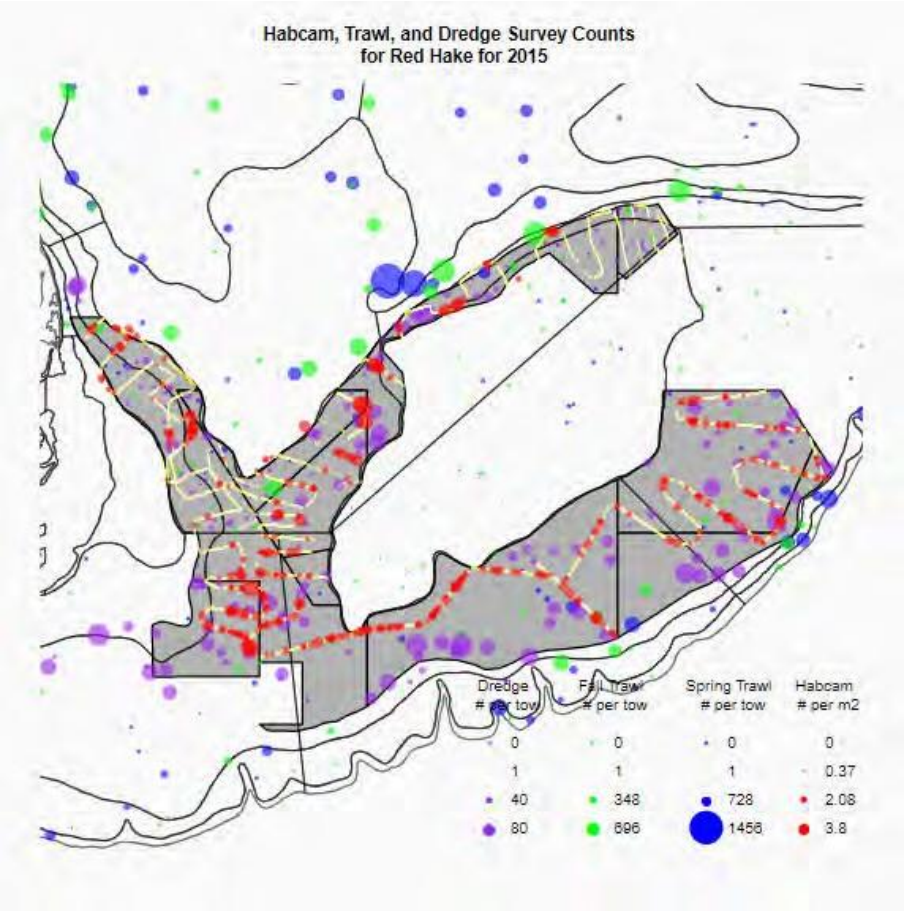

Figure 4.6. Diagram of the rockhopper sweep used on the NEFSC bottom trawl survey

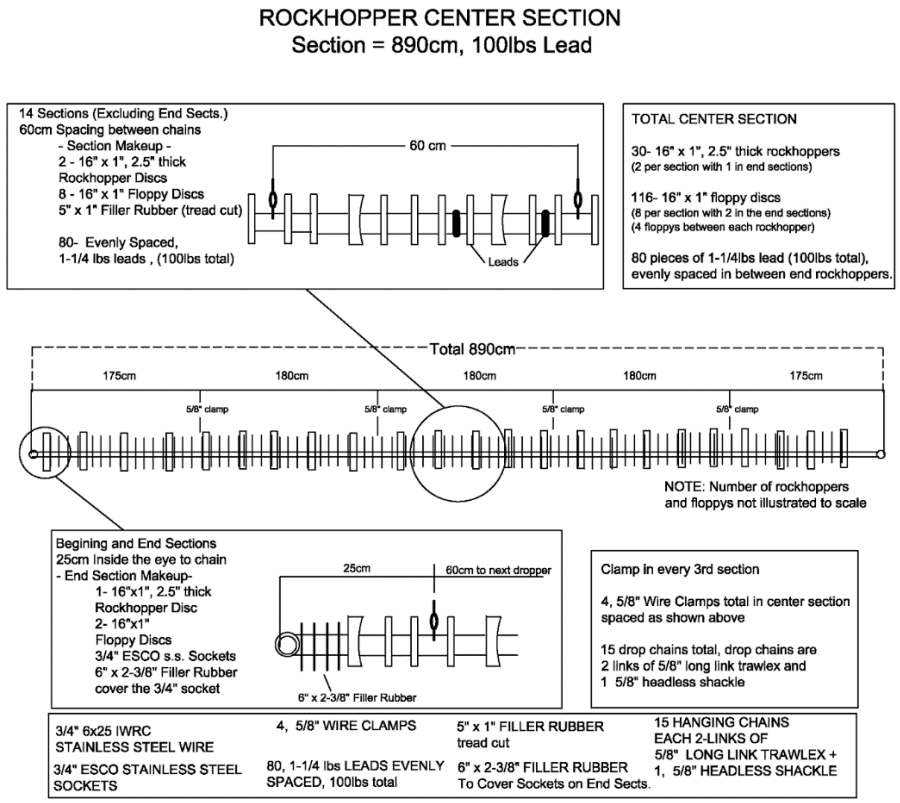

Figure 4.7. Diagram of the chain sweep used on the twin-trawl sweep efficiency study.

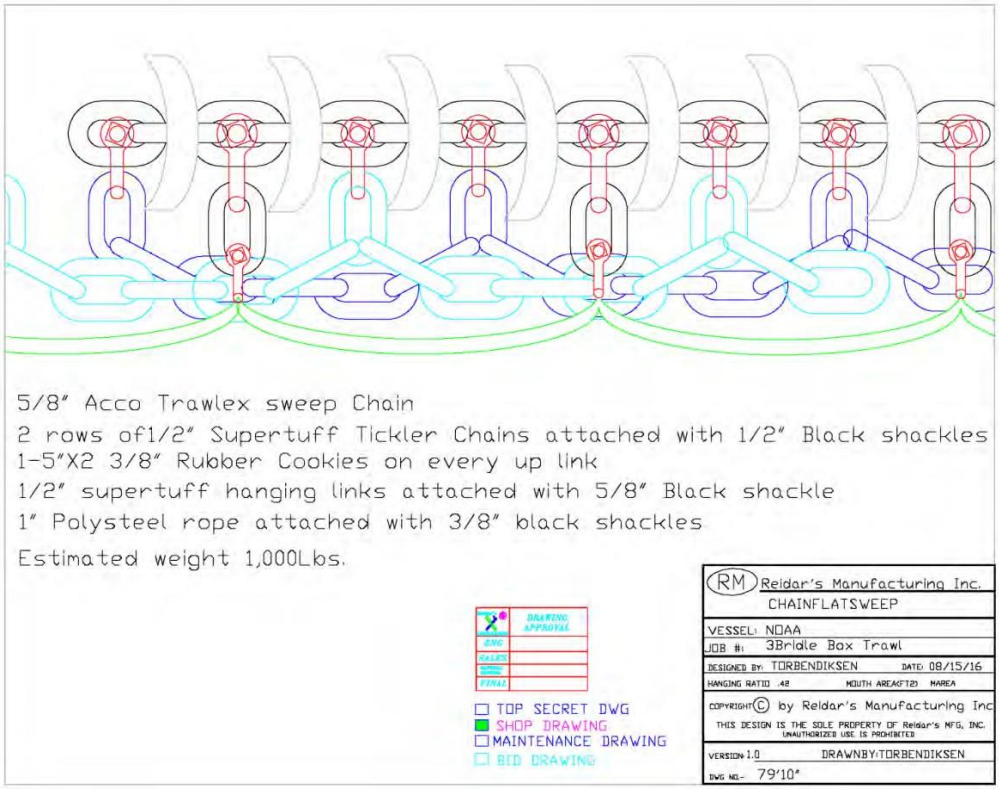

Figure 4.8. Image of the rockhopper and chain sweeps on the F/V/ Karen Elizabeth.

Figure 4.9. Locations of stations in 2017 where the *F/V Karen Elizabeth* conducted twin-trawl sets with the standard bottom trawl gear and the gear with a chain sweep instead of the rockhopper sweep

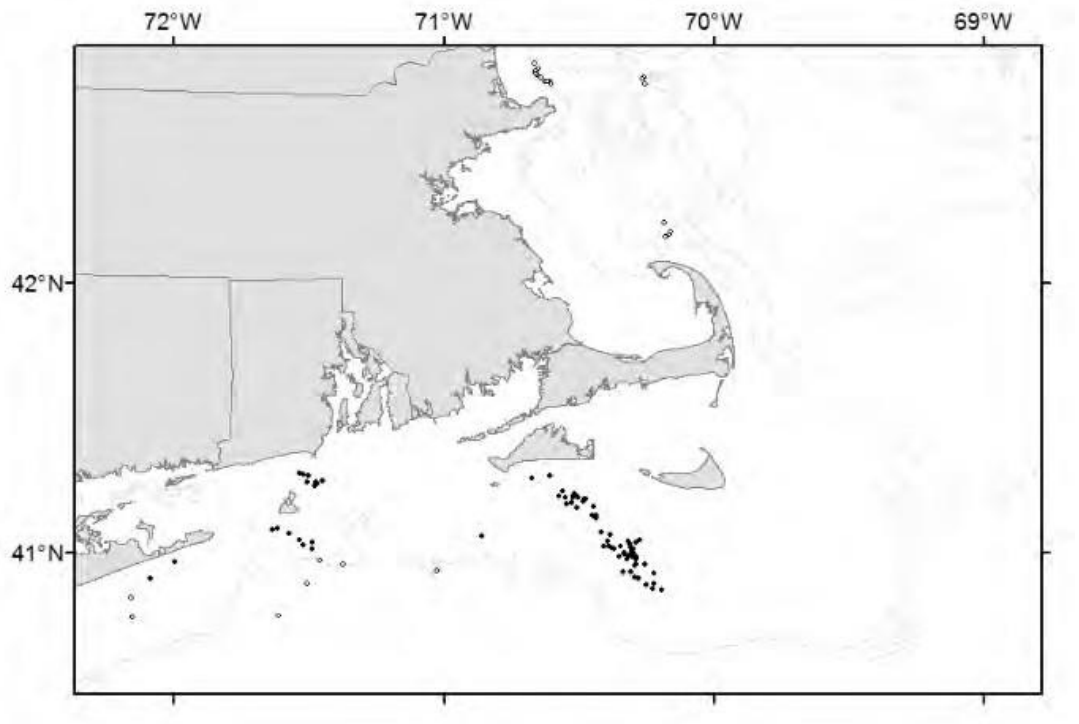

Figure 4.10. Estimated relative catch efficiency of red hake from the best model (BB9). Black and gray lines are for mean and tow-specific relative catch efficiencies, respectively. Gray polygons and dashed red lines reflect 95% confidence intervals using derived from delta method-based variance estimates and bootstrap quantiles, respectively.

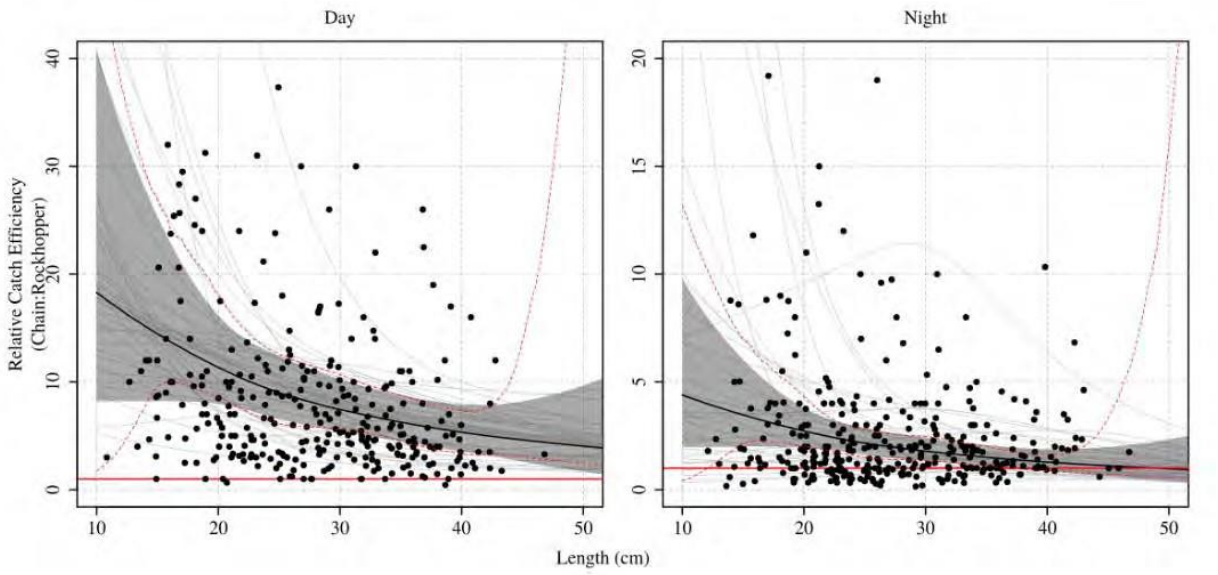

Figure 4.11. Estimated annual chain sweep-based biomass of northern red hake during the fall and spring surveys between 2009 and 2019. Estimates use relative catch efficiency from the best model (BB_9). Gray polygons reflect 95% confidence intervals derived from bootstrap quantiles.

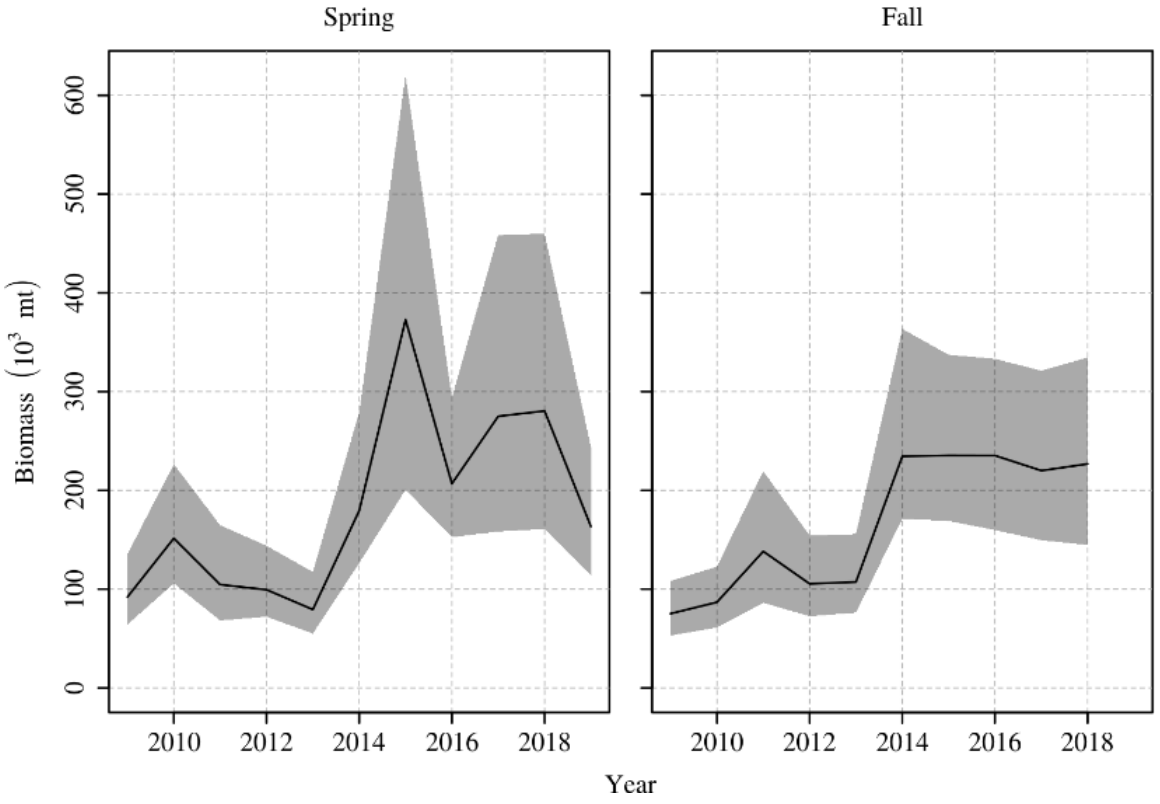

Figure 4.12. Estimated annual chain sweep-based biomass of southern red hake during the fall and spring surveys between 2009 and 2019. Estimates use relative catch efficiency from the best model (BB9). Gray polygons reflect 95% confidence intervals derived from bootstrap quantiles.

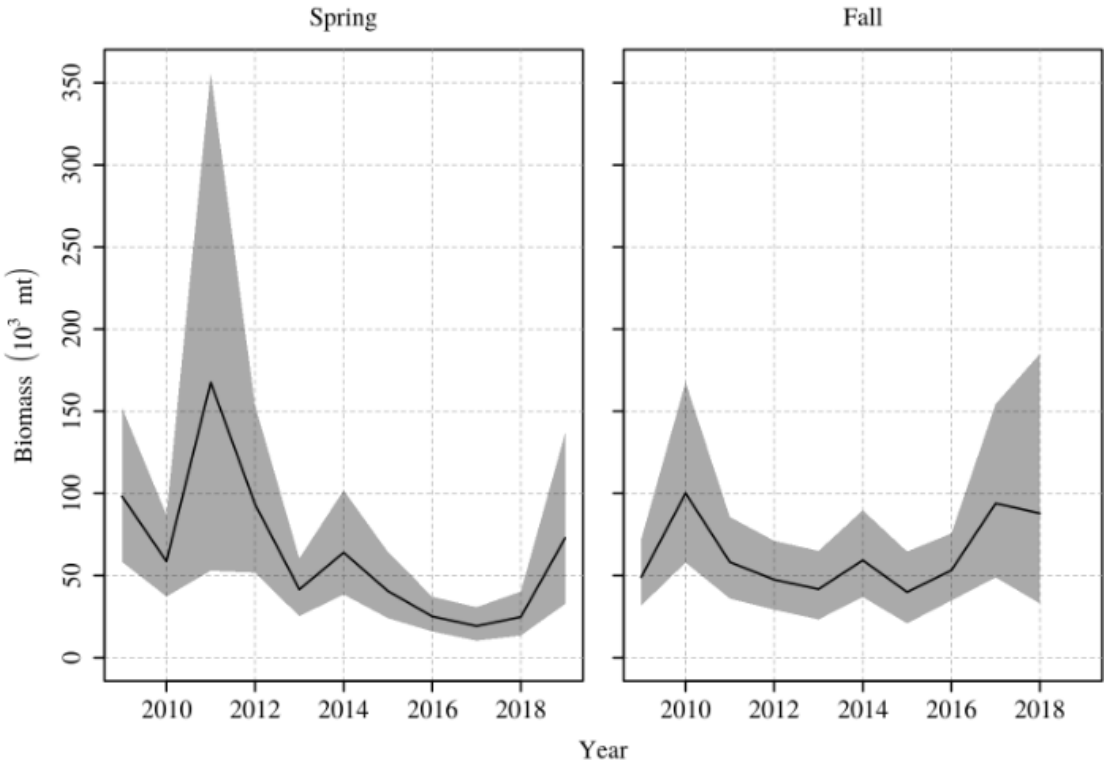

Figure 4.13. The general hypothesized relationships between catch efficiency and net wing spread for a set of species based on conversations with people familiar with this gear. Trawl efficiency is hypothesized to be optimal at the targeted wingspread and to decline at wider and narrower wingspreads.

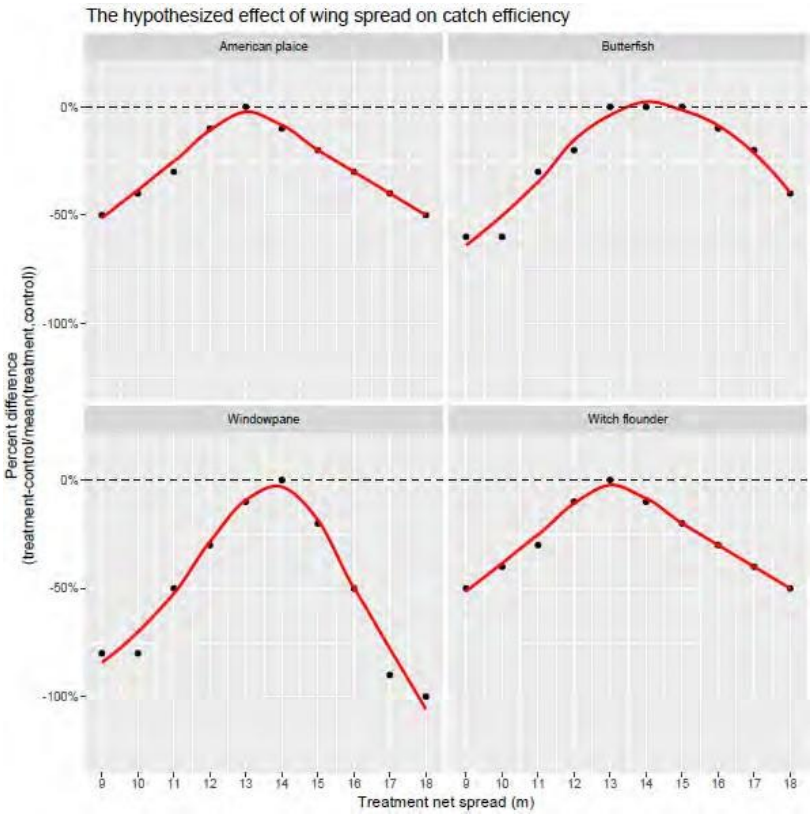

Figure 4.14: The locations of the stations sampled during the 14 day wingspread study.

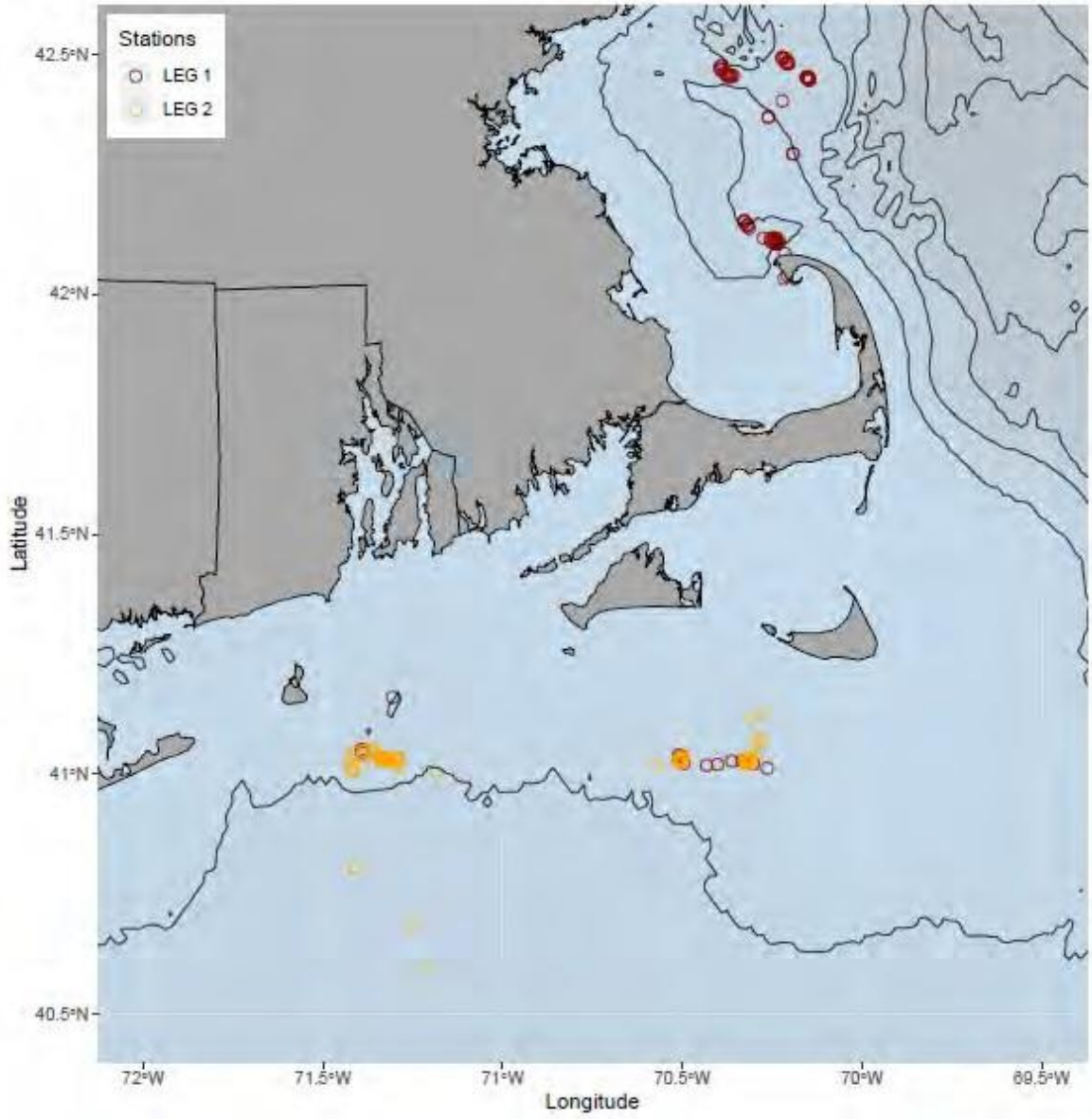

Figure 4.15: A plot showing the measured net with for each net at a given station (503). After trimming the spread data to the time when the net is on the bottom, a mean (line) is fit to each time series of widths after trimming it to a stationary period. These mean spreads of each net were inspected for each station. Additionally, assuming the control net performed within the acceptable limits (12.5 and 13.5 m), the mean value of the treatment net was used for analyses (rather than the target net width).

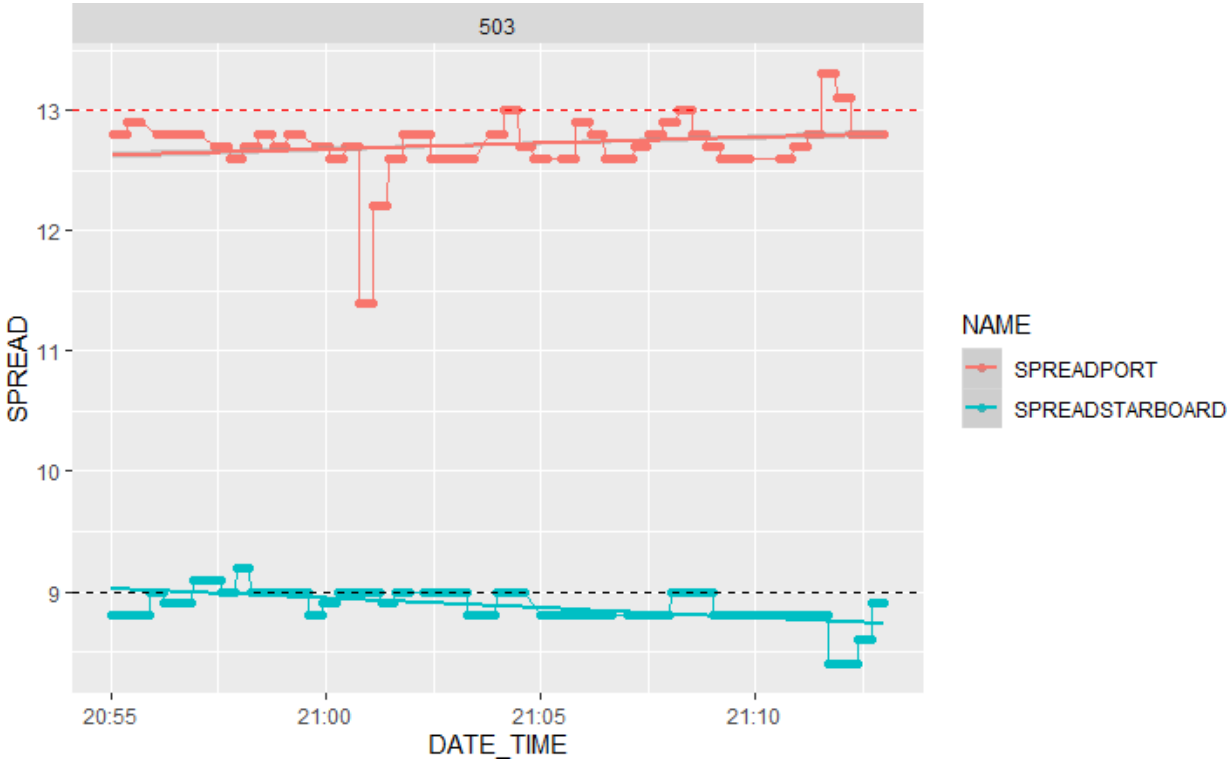

Figure 4.16. The relationship between net wingspread and a measure of catch and efficiency for red hake (percent difference in summed weight between treatment and control nets). Here, positive values suggest higher catches in the treatment net. In panel A) the data is shown without correcting for the difference in swept area between nets. In panel B) the difference in swept area between nets has been corrected for.

A)

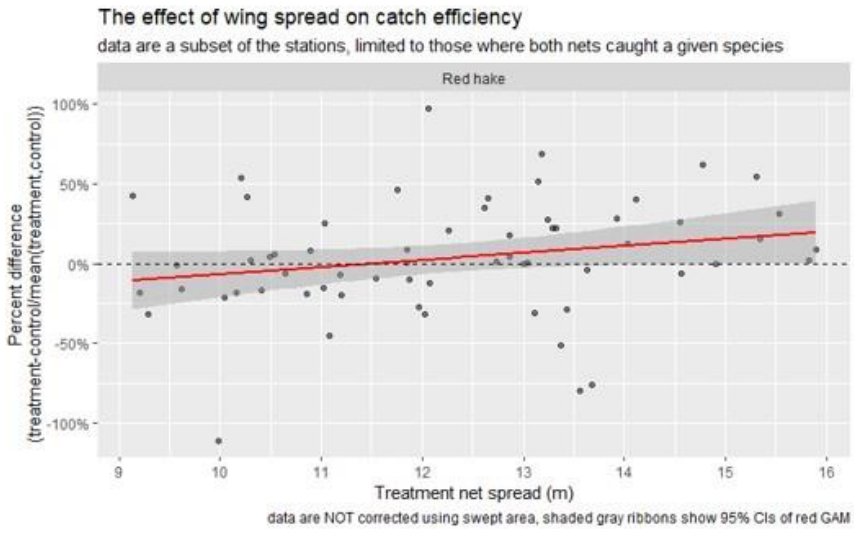

B)

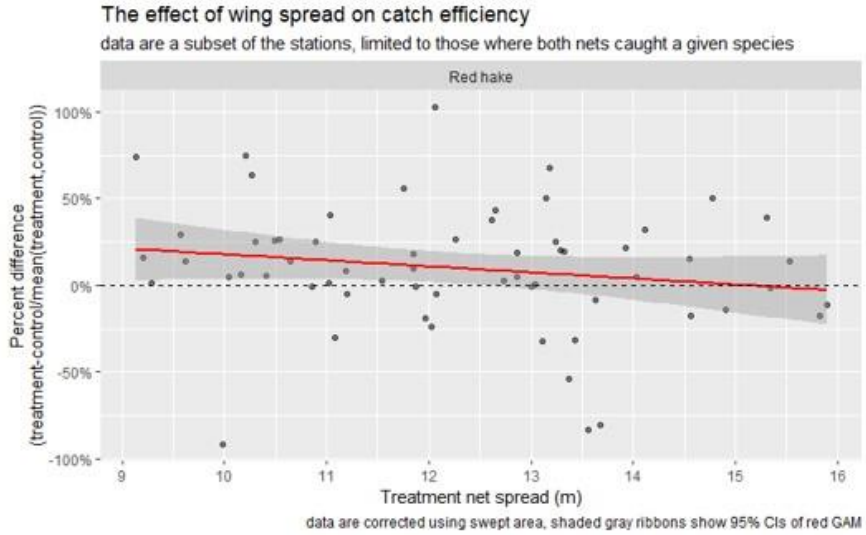

Figure 4.17. Example of model results from the length-based analyses. Specifically, we see the relationship between net wingspread and catch efficiency for different lengths of red hake from the best model with widespread effects (model number 10). This model was not the best overall model (as measured by AIC). The mean model results are shown on the left and the standard deviation of results is shown on the right. Positive values suggest higher catches in the treatment net.

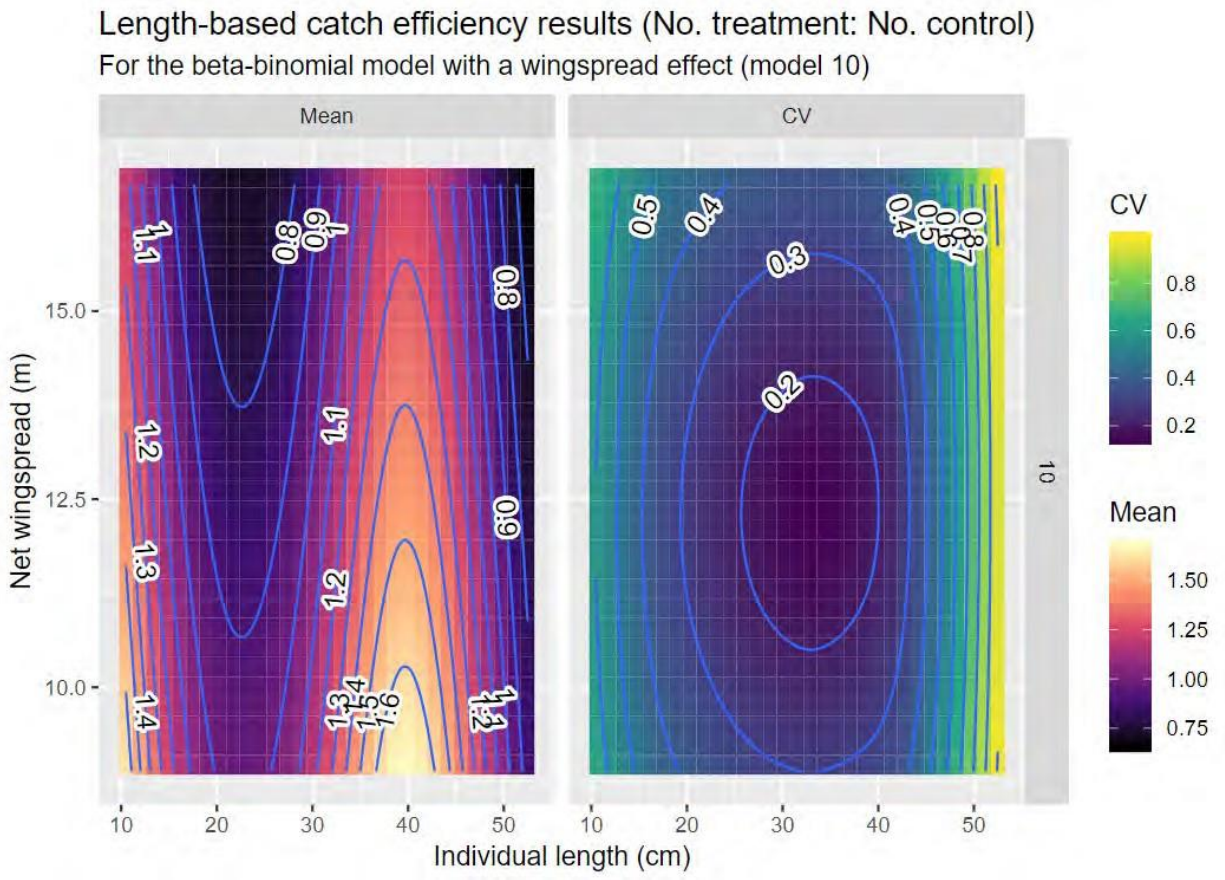

Figure 4.18. Mean number of red hake caught at each length for treatment (blue) and control (red) nets. Data are shown with numbers binned by experimental net width into three categories: > 13 m 'overspread', 13 m 'targets spreads', and < 13 m 'underspread'. Error bars represent bootstrapped standard errors. Treatment points and error bars are jittered slightly right to better visualize catches from both nets on the same plot.

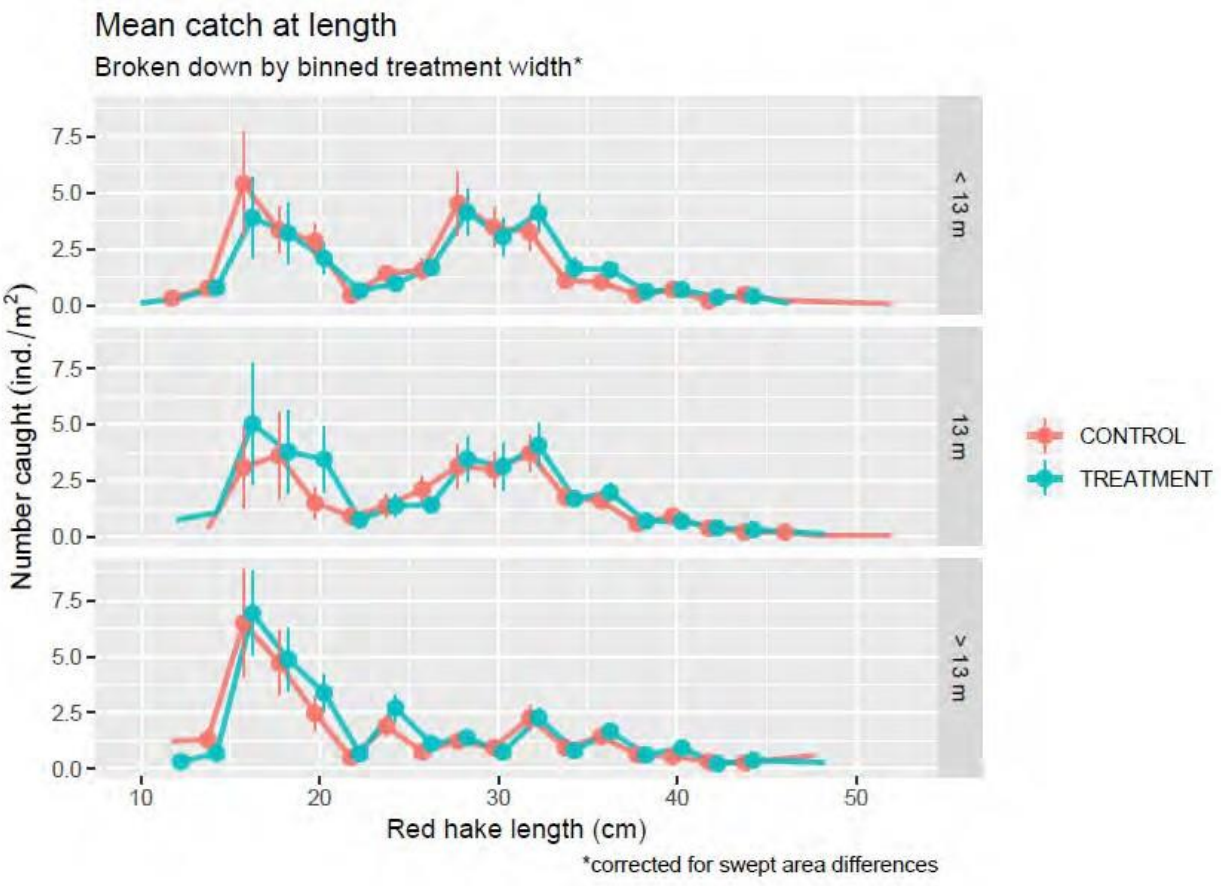

Procedures for Issuing Manuscripts in the *Northeast Fisheries Science Center Reference Document* (CRD) Series

Clearance

All manuscripts submitted for issuance as CRDs must have cleared the NEFSC's manuscript/abstract/webpage review process. If any author is not a federal employee, he/she will be required to sign an "NEFSC Release-of-Copyright Form." If your manuscript includes material from another work which has been copyrighted, then you will need to work with the NEFSC's Editorial Office to arrange for permission to use that material by securing release signatures on the "NEFSC Use-of-Copyrighted-Work Permission Form."

For more information, NEFSC authors should see the NEFSC's online publication policy manual, "Manuscript/abstract/webpage preparation, review, and dissemination: NEFSC author's guide to policy, process, and procedure," located in the Publications/Manuscript Review section of the NEFSC intranet page.

Organization

Manuscripts must have an abstract and table of contents, and (if applicable) lists of figures and tables. As much as possible, use traditional scientific manuscript organization for sections: "Introduction," "Study Area" and/or "Experimental Apparatus," "Methods," "Results," "Discussion," "Conclusions," "Acknowledgements," and "References Cited."

Style

The CRD series is obligated to conform with the style contained in the current edition of the United States Government Printing Office Style Manual. That style manual is silent on many aspects of scientific manuscripts. The CRD series relies more on the CSE Style Manual. Manuscripts should be prepared to conform with these style manuals.

The CRD series uses the American Fisheries Society's guides to names of fishes, mollusks, and decapod crustaceans, the Society for Marine Mammalogy's guide to names of marine mammals, Integrated Taxonomic Information System guidance on scientific and common names for all other species, the Biosciences Information Service's guide to serial title abbreviations, and the ISO's (International Standardization Organization) guide to statistical terms.

For in-text citation, use the name-date system. A special effort should be made to ensure that all necessary bibliographic information is included in the list of cited works. Personal communications must include date, full name, and full mailing address of the con- tact.

Preparation

Once your document has cleared the review process, the Editorial Office will contact you with publication needs – for example, revised text (if necessary) and separate digital figures and tables if they are embedded in the document. Materials may be submitted to the Editorial Office as email attachments or intranet down- loads. Text files should be in Microsoft Word, tables may be in Word or Excel, and graphics files may be in a variety of formats (JPG, GIF, Excel, PowerPoint, etc.).

Production and Distribution

The Editorial Office will perform a copyedit of the document and may request further revisions. The Editorial Office will develop the inside and outside front covers, the inside and outside back covers, and the title and bibliographic control pages of the document.

Once the CRD is ready, the Editorial Office will contact you to review it and submit corrections or changes before the document is posted online.

A number of organizations and individuals in the Northeast Region will be notified by e-mail of the availability of the document online.

Research Communications Branch
Northeast Fisheries Science Center
National Marine Fisheries Service, NOAA
166 Water St.
Woods Hole, MA 02543-1026

Publications and Reports of the Northeast Fisheries Science Center

The mission of NOAA's National Marine Fisheries Service (NMFS) is "stewardship of living marine resources for the benefit of the nation through their science-based conservation and management and promotion of the health of their environment." As the research arm of the NMFS's Northeast Region, the Northeast Fisheries Science Center (NEFSC) supports the NMFS mission by "conducting ecosystem-based research and assessments of living marine resources, with a focus on the Northeast Shelf, to promote the recovery and long-term sustainability of these resources and to generate social and economic opportunities and benefits from their use." Results of NEFSC research are largely reported in primary scientific media (*e.g.*, anonymously-peer-reviewed scientific journals). However, to assist itself in providing data, information, and advice to its constituents, the NEFSC occasionally releases its results in its own media. Currently, there are three such media:

NOAA Technical Memorandum NMFS-NE -- This series is issued irregularly. The series typically includes: data reports of long-term field or lab studies of important species or habitats; synthesis reports for important species or habitats; annual reports of overall assessment or monitoring programs; manuals describing program-wide surveying or experimental techniques; literature surveys of important species or habitat topics; proceedings and collected papers of scientific meetings; and indexed and/or annotated bibliographies. All issues receive internal scientific review and most issues receive technical and copy editing.

Northeast Fisheries Science Center Reference Document -- This series is issued irregularly. The series typically includes: data reports on field and lab studies; progress reports on experiments, monitoring, and assessments; background papers for, collected abstracts of, and/or summary reports of scientific meetings; and simple bibliographies. Issues receive internal scientific review and most issues receive copy editing.

Resource Survey Report (formerly *Fishermen's Report*) -- This information report is a regularly-issued, quick-turnaround report on the distribution and relative abundance of selected living marine resources as derived from each of the NEFSC's periodic research vessel surveys of the Northeast's continental shelf. This report undergoes internal review, but receives no technical or copy editing.

TO OBTAIN A COPY of a *NOAA Technical Memorandum NMFS-NE* or a *Northeast Fisheries Science Center Reference Document*, either contact the NEFSC Editorial Office (166 Water St., Woods Hole, MA 02543-1026; 508-495-2228) or consult the "Northeast Fisheries Science Center Publications" webpage https://www.fisheries.noaa.gov/new-england-mid-atlantic/northeast-center-reference-document-series